c-Met/HGF in Triple Negative Breast Cancer

A thesis submitted for the degree of PhD By

Patricia Gaule, BSc.

January 2015

The work in this thesis was carried out under the supervision of

Dr. Norma O' Donovan

&

Prof. John Crown

National Institute for Cellular Biotechnology

School of Biotechnology

Dublin City University

I hereby certify that this material, which I now submit for assessment on the programme of study leading to the award of PhD, is entirely my own work, that I have exercised reasonable care to ensure that the work is original, and does not to the best of my knowledge breach any law of copyright, and has not been taken from the work of others save and to the extent that such work has been cited and acknowledged within the text of my work.

Signed: _____

ID No.: _____

Date: _____

Acknowledgements

Firstly I wish to express my sincere gratitude to my supervisor Dr. Norma O' Donovan, without your constant support and guidance (in spite of all my 'negative' days), none of this would have been possible. I also want to thank Prof. John Crown for the opportunity and perpetual encouragement that allowed me to do my PhD in such a wonderful group. Thank you to Dr. Naomi Walsh for the supervision while Norma was away on maternity leave and more recently for all the wonderful advice for the future.

Special thanks to Dr. Louise Flanagan and Dr. Cecily Quinn for their help with the immunohistochemistry staining; to Prof. Joe Duffy and all his lab group for all the help with cell culture assays and protocols, and to Dr. Paul Dowling and Dr. Damian Pollard for their help with luminex assays.

I also want to thank all the members of our lab group, past and present; Thamir, Alexandra, Martina, Neil, Laura, Nicola and Alanna. Despite all the 'borrowing' of lab supplies, it's been wonderful. Special mention here to the two biggest 'borrowers', Alex and in particular Denis, whom took myself and Karen under their wing at the very beginning to teach us all they knew and were always available for a question or comment (when needed or not ☺).

I couldn't mention Karen without thanking her and Dee for a fabulous four years. It's been a series of ups and downs but both of you were always there to make the best of every situation (usually armed with a kebab and can). Wednesdays are defitinely much happier when you two are around.

I mentioned two friendships I gained above, however, that only scratches the surface. I feel privileged to have worked in such a unique environment which allowed the development of relationships that will last a lifetime. Particular mention here to the Jagerbomb twins, Erica and Sandra, never a dull moment with you guys. Also to the lunch gang, Fiona, Laura (B), Justine, Joanne and Rob.

I want to thank Prof. Martin Clynes whose leadership in the NICB encourages such a collaborative and friendly environment. Thanks to Mairead, Carol, Yvonne and

Geraldine for always ensuring the place runs like clockwork and everyone in the centre. Ye truly are a wonderful bunch of people.

I wish to thank my family for their unending support and love; Louis, Claire, Colm and the four girls (Emma, Aine, Aoife and Kate) who never fail to make me smile.

Finally there are three people to whom I'd like to dedicate this thesis;
My grandmother 'Nanny Gaule' for always shoving the car door closed when it seemed impossible.
My Mam and Dad, for showing me the shining example of what the belief in yourself and a little hard work can accomplish. Ye have never faltered in your support of me and I am eternally grateful. Thank you.

Table of Contents

Abbreviations

2D	2-Dimensional
3D	3-Dimensional
ARG	Arginine
ASN	Asparagine
ATCC	American Type Culture Collection
ATP	Adenosine Tri Phosphate
BCA	Bicinchoninic Acid
BCL-XL	B-Cell Lymphoma Extra Large
BCS	Breast Conserving Surgery
BL-1	Basal-Like 1
BL-2	Basal-Like 2
BLBC	Basal Like Breast Cancer
c-CBL	Casitas B-lineage Lymphoma
cDNA	Complementary Deoxyribonucleic acid
CI	Combination Index
CM	Conditioned Media
cPR	Complete Pathological Response
CST	Cell Signalling Technology Inc.
CT	Cycle Threshold
CYS	Cysteine
DCIS	Ductal Carcinoma In Situ
DMEM	Dulbecco's Modified Eagle Medium
DNA	Deoxyribonucleic Acid
DNTP	Deoxyribose Nucleoside Triphosphate
DPX	Di-n-Butyl Phthalate
DSMZ	Deutsch Sammlung von Mikroorganismen und Zellkulturen
ECM	Extracellular Matrix
EDTA	Ethylenediamineetraacetic Acid
EGF	Epidermal Growth Factor
EGFR	Epidermal Growth Factor Receptor
ELISA	Enzyme Linked Immnuosorbent Assay
EMT	Epithelial to Mesenchymal Transition

EMA	European Medicines Association
ER	Oestrogen Receptor
ERK	Extracellular Signal Related Kinase
FAK	Focal Adhesion Kinase
Fc	Fragment Crystallisable Region
FcgR	Fragment Crystallisable Gamma Receptor
FCS	Foetal Calf Serum
FDA	U.S. Food and Drugs Authority
FFPE	Fresh Frozen Parrafin Embedded
FISH	Fluorescent In Situ Hybridisation
GRB-2	Growth Factor Receptor Bound Protein-2
HER2+	Human Epidermal Receptor 2
HER3	Human Epidermal Receptor 3
HER4	Human Epidermal Receptor 4
HGF	Hepatocyte Growth Factor
HIF	Hypoxia Inducible Factor
HR	Hormone Receptor
HRP	Horse Radish Peroxidase
IDC	Invasive Ductal Carcinoma
IGFIR	Insulin Like Growth Factor-1 Receptor
IHC	Immunohistochemistry
IM	Immunomodulatory
IR	Insulin Receptor
ISH	In Situ Hybridisation
IU	International Units
LAR	Luminal Androgen Receptor
LHS	Left Hand Side
LN	Lymph Node
LVI	Lympho Vascular Invasion
LYS	Lysine
M	Mesenchymal
MAPK	Mitogen Activated Protein Kinase
mRNA	Messenger Ribonucleic Acid
MRS	Met Related Structure

MSL	Mesenchymal Stem Like
MSP	Macphrophage Stimulating Protein
NaCL	Sodium Chloride
NaOV	Sodium Orthovanadate
NET	NaCl, EDTA, Tris
NF-κB	Nuclear Factor Kappa-Light-Chain-Enhancer of Activated B Cells
NK1/2	N Terminal Kringle Containing Domain ½
NR	Not Reported
NRK	Normal Rat Kidney Epithelial Cells
NSCLC	Non-Small Cell Lung Cancer
NTC	No Template Control
ORR	Overall Response Rate
OS	Overall Survival
PAM	Prediction Analysis Microarrays
PBS	Phosphate Buffered Saline
PBS-T	Phosphate Buffered Saline-Tween
PDK1	Phosphoinositide Dependent Kinase-1
PDX	Patient Derived Xenograft
PFS	Progression Free Survival
PI	Protease Inhibitors
PI3K	Phosinositide-3 Kinase
PIP2	Phosphatidylinositol 4,5-Bisphosphate
PIP3	Phosphatidylinositol (3,4,5)-Trisphosphate
PKC	Protein Kinase C
PMSF	Phenylmethanesulfonyl Fluoride
PNP	P-Nitro Phenol Phosphate
PR	Progesteron Receptor
PTB	Protein Tyrosine Phosphatase
qRT-PCR	Quantitative Real-Time Polymerase Chain Reaction
RFS	Regression Free Survival
RHS	Right Hand Side
RIPA	Radioimmunoprecipitation Buffer
RNA	Ribonucleic Acid
RON	Recepteur D'origine Nantais

RPMI	Roswell Park Memorial Institute Medium
RPPA	Reverse Phase Protein Array
RT	Room Temp
RTC	Reverse Trancription Control
RTK	Receptor Tyrosine Kinase
SBSP	Spry-Domain Containing SOCs box -1
SER	Serine
SERMS	Selective Oestrogen Modulating Receptor
SF	Scatter Factor
SFM	Serum Free Medium
SH2	Src Homology 2
sMet	Soluble fragment c-Met
SOS	Son Of Sevenless
Ssp	Single Sample Predictors
SVUH	St. Vincent's University Hospital
TCPTP	T-cell Phosphatase
THR	Threonine
TKI	Tyrosine Kinase Inhibitor
TMA	Tissue Microarray
TNBC	Triple Negative Breast Cancer
TNF	Tumour Necrosis Factor
TNM	Tumour Node Metastase
tPA	Tissue Plasminogen Activator
TRIS-HCL	Tris(hydroxymethyl)aminomethane Hydochloric Acid
UHP	Ultra High Purity Water
uPA	Urinary Plasminogen Activator
UTR	Untranslated Region
VAL	Valine
VEGFR	Vascular Endothelial Growth Factor Receptor-1
WT	Wild Type
XAA	Unknown/Unspecified Amino Acid
XIAP	X-Linked Inhibitor of Apoptosis Protein
YB	Y-Box Binding Protein
ΔCT	Delta Cycle Threshold

Abstract

Triple negative breast cancer (TNBC) is a subtype of breast cancer which is negative for the oestrogen receptor, progesterone receptor and lacks over-expression of HER2. The aim of this PhD was to examine c-Met and its ligand HGF as potential targets for TNBC. Expression of c-Met was higher in TNBC relative to other subtypes of BC. c-Met expression did not show a significant association with patient outcome (DFS/OS). We evaluated 3 c-Met/HGF selective inhibitors (CpdA, PRS110 and rilotumumab) in the panel of TNBC cell lines. Only CpdA showed moderate responses in proliferation assays. Cell lines were significantly more sensitive to c-Met inhibition by either CpdA or PRS110 in clonogenic assays. 3D growth assays were all significantly less sensitive to c-Met inhibition. Co-expression of c-Met and Src/p-Src (Y418) was detected in 86.6 /38.8 % respectively. No significant association was seen between clinico- pathological variables. Combined treatment with c-Met inhibitors and HGF, EGFR or Src inhibitors enhanced response in some cell lines suggesting a potential role in specific subsets of TNBC.

A dasatinib resistant and a cetuximab resistant TN cell line (231-DasB and MDA-MB-CR) showed increased sensitivity to CpdA compared to the parental cells. The parental cell lines show synergistic inhibition of growth with combination of CpdA and dasatinib or cetuximab.

We identified 7 receptor tyrosine kinases (FGFR1, FGFR3, VEGFR1, PDGFRβ, ROS1, TIE1 and EPHA5) which are associated with poor outcome (DFS/OS). Combined expression of FGFR3, EPHA5 and ROS1 shows significantly stronger association than the RTKs as single prognostic indicators. FGFR3 was associated with histological subtype and EPHA5 was significantly associated with increased age at diagnosis.

Based on our in vitro evaluation, targeting c-Met/HGF signalling does not appear to be a promising therapeutic strategy for TNBC. We identified FGFR3 and EPHA5 as potential targets which warrant further investigation in TNBC.

Chapter 1

Introduction

1.1 Breast cancer

The normal breast is one of the few organs which undergoes continued development throughout the lifetime of a woman. This development occurs in key stages; embryonic, prepubertal, pubertal, pregnancy, lactation and involution. In the mammary gland there are two key cellular compartments; the epithelium (which lines ducts and lobules) and the surrounding supportive stroma. Various pathways and hormones regulate the different stages of development [1]. Breast cancer is one of the most common invasive cancers observed in women. It was the most frequently diagnosed (31%) and the second most common cause of cancer deaths in women resulting in 687 deaths (16.6%) between 2009 and 2011 in Ireland. Breast cancer incidence has increased at an average annual rate of 1.7% between 1994 and 2011 [2]. Breast cancer develops within the epithelia of the breast; however, interaction between epithelial cells and the mesenchymal compartment of the breast is known to be important for both the development of normal breast and in carcinogenesis. The stroma provides important growth and regulation signals e.g. parathyroid hormone related protein; which is involved in the fates of the cells of the nipple, ductal mammary epithelium and the mesenchymal portion of the breast [3, 4].

1.2 Breast cancer sub-types

Breast cancer is a highly heterogeneous disease. The heterogeneity of breast cancer often results in variable responses to treatments. Breast cancer has been sub-divided using various approaches. The tumour, node, metastasis system (TNM) takes into account size of the primary tumour, regional lymph node status and the presence of distant metastases [5]. Histological grading is based on the degree of differentiation and proliferative activity. Certain specific morphological and cytological patterns are associated with certain clinical presentations and outcomes [6]

The development of microarray technology ushered in a new era of classifying breast cancer. Four main molecular subtypes were identified composed of luminal, HER2 positive, normal like, and basal (Table 1-1). Luminal breast cancer was further classified into subtypes luminal A and luminal B. Of these subtypes only the luminal are positive for the oestrogen receptor (ER) while the basal type, HER2 positive and normal like are negative for the ER receptor [7-9].

Table 1 - 1 Receptor status and treatment options for the molecular subtypes of breast cancer (ER- Oestrogen receptor, PR-Progesterone receptor).

Subtype	Receptor Status	Treatment options based on molecular subtype
Luminal	ER +ive HER2 normal	Tamoxifen is standard of care however a range of drugs known as selective oestrogen receptor modulator (SERMS) now exist which act in mainly the same way [10].
HER2+	ER +/–ive HER2 overexpression	Herceptin (trastuzumab) [11] Pertuzumab [12] TDM1[13] Lapatinib in refractory metastatic breast cancer [14]
Normal like	ER -ive HER2 normal	Tumours are usually small and are treated with surgery and radiotherapy
Basal-like	ER –ive HER2 normal PR-ive	Cytotoxic chemotherapies

1.3 Triple negative breast cancer (TNBC)/basal-like breast cancer

In general, the mortality rate of breast cancer is falling. This is thought to predominantly to be due to early detection, screening programmes and the development of targeted and neo-adjuvant therapies. TNBC remains a disease with a poorer prognosis than other subtypes. It also lacks the expression of ER, PR and the over-expression HER2 positive receptors on the tumour cell surface. To be categorised as TNBC the American Society of Clinical Oncologists have published the following guidelines; ER/PR positivity as determined by immunoreactivity of tumour cell nuclei is <1% [15]. Due to the lack of receptor expression, currently approved targeted therapies have no beneficial effect.

TNBC accounts for 15% of all breast cancer and displays a higher incidence rate in African and African-American pre-menopausal women. Women with TNBC are significantly younger when diagnosed. Diagnosis tends to be of more locally advanced disease and with a higher occurrence of dissemination to the lymph nodes. However, unlike other types of breast cancer, no correlation with tumour size and lymph node invasion has been seen. Also, TNBC tends towards visceral metastases [16]. Mortality rates also differ dramatically when compared to other subtypes of breast cancer [17]. Dent *et al*. showed a 42.2% death rate within 5 years in TNBC compared to 28% in other breast cancer subtypes and all mortality occurring as a result of TNBC occurring within 10 years in comparison to 18 years for non-TNBC [17]. Distant recurrence was also increased in TNBC however, recurrence seems to occur within 1-4 years compared to up to 17 years for other subtypes [17].

Basal-like tumours can be characterised by expression of cytokeratin 5/6 and morphologically with increased mitotic count, stromal lymphocytic response, central tumour necrosis and a pushing border of invasion [18]. They also show high level of p53 protein as a result of mutations in TP53, and high c-Kit expression correlating with a poorer clinical prognosis [19, 19-22]. Basal-like breast cancers have also demonstrated a high level of expression of the epithelial growth factor receptor (EGFR/HER1) with levels of overexpression ranging from 18-60% and also show a higher mutation load than other subtypes. [20, 23-26].

Basal-like (BL) tumours were initially thought be derived from myoepithelial cells, however, Livasy *et al.* recorded the expression of luminal markers (cytokeratin 8/18) in basal like breast tumours with the absence of some myoepithelial markers (SMA 4/18, p63 and CD 10) [18].

Another subtype of breast cancer which presents predominantly with triple negativity is the claudin-low subtype. As the name suggests, claudin low tumours are characterised by low expression of Claudins 3, 4 and 7 and other genes involved in tight junctions and cell-cell adhesion [27]. Similarly to BL tumours they show high genomic instability and can be characterised by high expression of epithelial to mesenchymal, immune response, angiogenesis and cancer stem cell markers [28-30]. Claudin low tumours cluster with the Mesenchymal (M) and Mesenchymal stem-like subtypes of TNBC described in Table 1 - 2 [31].

TNBC and BL sub-types have been considered interchangeable to date, however, it is important to note, the groups are not mutually exclusive but do show high levels of overlap.

TNBC/basal like breast cancer (BLBC) contains a large number of tumours types who may, despite their shared triple negatively/expression of cytokeratins may in fact represent separate distinct disease entities [32]. TNBC which identifies genetically as luminal or with HER2 gene enrichment (despite low expression of HER2), show almost indistinguishable gene profiling to luminal/HER2 overexpressing tumours. TNBC tumours of basal origin show their own distinct genetic profiles. This would suggest that triple negativity is not a sufficient biomarker to classify patients in clinical trials [33]. c-Kit has shown potential as a biomarker for luminal cells and could help characterise these luminal TNBC patients [34, 35]. Lehmann *et al.* published a study of 386 TNBC from 21 publically available data sets and identified 6 groups [31]. These include 2 basal-like (BL1 and BL2), immunomodulatory (IM), mesenchymal (M), mesenchymal stem-like (MSL), luminal androgen receptor (LAR) type [31]. These subtypes are described in detail in Table 1 - 2. These subtypes were supported by a recent publication by Burnstein *et al.* which identified four subtypes including, luminal-AR, mesenchymal, basal like-immuno-suppressed, basal-like immnuo-activated. The basal-like immune-suppressed group showed the poorest prognosis in this analysis [34].

Table 1 - 2 Sub-groups within TNBC and pathways implicated in each sub-type [31]

Sub-Group	Associated with	Elevated gene expression
Basal like-1 (BL1)	Cell cycle and cell division pathways	AURKA, AURKB, CENPA, CENPF, BUB1, TTK, CCNA2, PRC1, MYC, NRAS, PLK1, BIRC5
Basal-like 2 (BL2)	Growth factor signalling	EGF, NGF, MET, Wnt/β-catenin, IGF1R signalling, EGFR, EPHA2, c-Met receptor
Immunomodulatory (IM)	Immune cell processes	TH1/TH2 pathway, NK cell pathway, B cell receptor signalling pathway, DC pathway and T cell receptor signalling, cytokine pathway, IL-12 and IL-7, NFκB, TNF, JAK/STAT signaling
Mesenchymal (M)	Cell motility, ECM receptor interaction and cell differentiation	TGFB1L1, BGN, SMAD6, SMAD7, NOTCH1, TGFB1, TGFB2, TGFB3, TGFBR2, TGFBR3, MMP2, ACTA2, SNA12, SPARC, TAGLN, TCF4, TWIST1, ZEB1, COL3A1, COL5A2, GNG11, ZEB2, FGF, IGF, PDGF, CTNNBI, DKK2, DKK3, SFRP4, TCF4, TCF7L2, FZD4, CAV1,

Sub-Group	Associated with	Elevated gene expression
Mesenchymal stem-like	Similar to M subtype with low levels of proliferation genes and enrichment of genes associated with stem cells	ABCA8, PROCP, END, ALDHA1, PER1, ABCB1, TERF2IP, BCL2, BMP2, THY1, HOXA5, HOXA10, MEIS1, MEIS2, MEOX1, MEOX2, MSX1, BMP2, ENG, ITGAV, KDR, NGFR, NT5E, PDGFRβ, THY1 AND VCAM1
Luminal androgen receptor (LAR)	Hormonally regulated pathways	DHCR24, ALCAM, FASN, FKBP5, APOD, PIP, SPDEF, CLDN8, FOXA1, KRT18, XBP1

Basal-like breast cancer demonstrates large similarity in its development to familial breast cancer caused by the mutation in the tumour suppressor gene BRCA (Table 1-3). Mutations in BRCA1 predispose women to developing breast cancer with an 80% lifetime risk associated with those harbouring the mutation [36]. Characterisation of normal and preneoplastic tissue from heterozygous BRCA1 mutant women was examined for early epithelial cell subsets. Three subsets were identified, a basal stem/progenitor group, a luminal progenitor group and mature luminal cells. The luminal progenitor group was expanded and showed enhanced clonogenic activity *in vitro* in BRCA1 cancers suggesting that BRCA cancers are derived from luminal progenitors and not basal-like stem cells as previously believed [35].

Table 1 - 3 Similarities between familial BRCA1 associated cancers and basal-like sporadic cancers [36]**. IDC = invasive ductal carcinoma, NR= not reported.**

Parameter	**BRCA1 cancers**	**Basal-like sporadic cancers**
Histological type	IDC Medullary-like	IDC Medullary/atypical Metaplastic breast cancer
Grade	High (3)	High (3)
Borders	Pushing	Pushing
Medullary/atypical medullary features	Present	Present
Proliferation rates	High	High
Brisk lymphocytic infiltrated	Present	Present
Central necrosis	Present	Present
Metaplastic elements	NR	Yes
ER	Negative	Negative
PR	Negative	Negative
HER2	Rare	Rare
EGFR	Overexpression – 60–70% Amplification – NR	Overexpression – 60–80% Amplification – 15–35%
Basal keratins	Positive	Positive
Cyclin D1 expression	Low levels	Low levels
Ploidy	Aneuploid	Aneuploid

1.4 Breast Cancer Treatment

The mainstays of treatment for breast cancer include radio- and chemo-therapy regimens. The optimal use of the radio- and/or chemo- therapies is defined in guidelines established by the U.S. Food and Drug Administration (FDA) and the European Medicines Agency (EMA) [37].

1.4.1 Chemotherapy

For early stage breast cancer chemotherapy can be administered in two ways, as an adjuvant or neo-adjuvant therapy. Adjuvant therapy is administered post primary therapy (usually surgery), whereas neo-adjuvant therapy is given prior. Neo-adjuvant therapy may be useful in cases where at initial diagnosis the tumour bulk is too large for surgical removal. In previous meta-analyses no significant difference was observed between adjuvant and neo-adjuvant therapy however recently in TNBC neo-adjuvant therapy has been associated with improved survival outcome but only in patients who achieved a complete pathological response [38, 39]. There are currently 20 approved chemotherapy drugs for the treatment of breast cancer (described in Table 1 - 4).

Table 1 - 4 Chemotherapy drugs approved for treatment of breast cancer [40]

Brand Name(s)	Chemical Name	Family Mode of Action
Abraxane	Albumin bound or nab-paclitaxel	Taxanes/Mitotic Inhibitor
Adriamycin Doxil	Doxorubicin	Anthracyclines/Inhibition of DNA and RNA synthesis Inhibition of topoisomerase II Generation of oxygen free radicals Induction of histone eviction from chromatin
Paraplatin	Carboplatin	Platinum based chemotherapy/DNA alkylating agent.

Brand Name(s)	Chemical Name	Family Mode of Action
Cytoxan Revimmune Clafen Neosar	Cyclophosphamide	Nitrogen mustard family/alkylating agent
Cerubidine DaunoXome	Daunorubicin	Anthracyclines/Inhibition of DNA and RNA synthesis Inhibition of topoisomerase II Generation of oxygen free radicals Induction of histone eviction from chromatin
Ellence	Epirubicin	Anthracyclines/Inhibition of DNA and RNA synthesis Inhibition of topoisomerase II Generation of oxygen free radicals Induction of histone eviction from chromatin
Adrucil Efudex Fluoroplex	5-fluorouracil	Antimetabolite chemotherapy/Induce cell death through interfering with DNA and RNA synthesis.
Gemzar	Gemcitibine	Antimetabolite chemotherapy/Induce cell death through interfering with DNA and RNA synthesis.
Halaven	Eribulin	Microtubule inhibitor/disruption of microtubule formation.
Ixempra	Ixabepilone	Epothilone chemotherapy/disruption of microtubule formation.

Brand Name(s)	Chemical Name	Family Mode of Action
Abitrexate Folex PFS Folex Methotrexate LPF Mexate-AQ Mexate	Methotrexate	Antimetabolite chemotherapy/Induce cell death through interfering with DNA and RNA synthesis.
Mitomycin	Mutamycin	Antitumour antibiotic chemotherapy/ DNA crosslinking
Novatrone	Mitoxantrone	Anthracyclines/Inhibition of DNA and RNA synthesis Inhibition of topoisomerase II Generation of oxygen free radicals Induction of histone eviction from chromatin
Navelbine	Vinorelbine	Vinca alkaloid chemotherapy/disruption of microtubule formation
Taxol	Paclitaxel	TaxanesMitotic Inhbitor
Taxotere	Docetaxel	TaxanesMitotic Inhbitor
Thioplex	Thiotepa	Alkylating agent chemotherapy
Oncovin Vincasar PES Vincrex	Vincristine	Vinca alkaloid chemotherapy/disruption of microtubule formation
Xeloda	Capcetibine	Antimetabolite chemotherapy/Induce cell death through interfering with DNA and RNA synthesis.

Chemotherapy is often most effective when given in combinations or regimens. Preferred regimens include a doxorubicin/cyclophosamide combination alone or followed by two weekly/weekly paclitaxel. For HER2 positive disease preferred regimens also include a HER2 targeted agent such as trastuzumab or pertuzumab and ER positive disease includes a hormone targeted therapy such tamoxifen or aromatase inhibitors [41].

1.4.2 Radiotherapy

Radiation therapy is used to prevent local recurrence from undetectable cells in patients who have undergone breast conserving surgery (BCS) or mastectomy. Radiotherapy may be administered as whole breast irradiation involving the majority of the breast tissue, chest wall irradiation which also incorporates the ipsilateral chest wall, mastectomy scar and drain sites and finally regional node irradiation. Radiotherapy post BCS/mastectomy has shown an enhanced long term survival (>15years) however no significant difference is observed in 5 year recurrence or survival [42]. Additionally, higher/additional dose radiotherapy demonstrated a significant decrease in recurrence rates at 5 years in women under 40 years of age [43].

1.5 Current treatments for TNBC and basal-like breast cancer

Currently there is no recommended systemic treatment regimen for TNBC due to the lack of a proven molecular target, leaving only cytotoxic chemotherapies. TNBC demonstrates higher sensitivity to anthracycline based neoadjuvant chemotherapy than ER positive subtypes, however, higher rates of reoccurrence and shorter periods of disease free survival are observed in TNBC. This may be due to the treatment of ER positive tumours with targeted endocrine therapies, suggesting that in cases of TNBC where a pathological complete response (pCR) is not achieved the risk of reoccurrence and earlier mortality rates are significantly higher [44]. This has also been shown with paclitaxel and doxorubicin containing chemotherapies and platinum based chemotherapy in the neo-adjuvant setting [45][46]. Overall basal-like tumours show high levels of chemosensitivity in comparison to other subtypes, however, when pCR is not achieved the prognosis for patients is significantly worse, indicating the need for the development of targeted treatments [47].

1.6 Targeted therapies

Targeted therapies are treatments that target specific molecules expressed in or on the surface of cancer cells, which are involved in carcinogenesis and/or tumour growth. Conventional chemotherapy and radiotherapy lack selectivity for tumour tissue and are highly systemically toxic [14]. Most of the molecules targeted have a function in normal cell growth and development but are aberrantly expressed to confer proliferation/growth advantages on the tumour cell. Examples of targeted therapies in breast cancer include tamoxifen for the treatment of ER positive tumours and

trastuzumab in the treatment of HER2 positive tumours. Receptor tyrosine kinases (RTKs) are attractive targets for targeted therapy because more than half of RTKs have been found to be over expressed or mutated in human hypoproliferative diseases and are therefore considered rational targets for cancer therapy [48, 49]. Targeted therapies include both small molecule inhibitors and monoclonal antibodies.

1.6.1 Small molecule inhibitors

Small molecule inhibitors are chemically synthesised compounds, which generally work by targeting intracellular signalling pathways, in particular kinases. They are usually administered as an oral treatment and are generally less specific than monoclonal antibodies. Most small molecule inhibitors are metabolized by cytochrome 450 enzymes. This can result in interactions with other medicines including antibiotics and anticoagulants. They additionally have a short half-life indicating the need for daily dosing [50, 51].

1.6.2 Monoclonal antibodies

Monoclonal antibodies were first established in 1975 by Kohler *et al.* Early antibodies had the drawback of allergic and anti-antibody responses due to their murine or chimeric nature. This was overcome by the creation and manufacture of fully humanised antibodies [51, 52].Monoclonal antibodies bind specifically to their target molecule through the fragment antigen binding (Fab) portion which recognises specific sequences in the antigen of interest [50]. Upon binding monoclonal antibodies exert their effect through a number of mechanisms including; inhibition of signal transduction, induction of apoptosis, inhibition of angiogenesis, enhancement of immune response and finally delivery of cytotoxic drugs.

Inhibition of signal transduction can occur through interaction directly with the receptor to block ligand binding or indirectly by binding and blocking interaction of the ligand, removing the activating stimulus. Cetuximab, an anti-EGFR monoclonal antibody, competitively binds to EGFR blocking ligand binding thereby inhibiting downstream signalling [53], Bevacizumab in contrast binds to the ligand (VEGF-A) of the receptor (VEGFR) inhibiting interaction and thus inhibiting downstream signalling. VEGF is implicated in tumour mediated angiogenesis and therefore bevacizumab anti-tumour effects may be attributable to anti-angiogenesis [54].

Monoclonal antibodies may also act as ligand mimics targeted at death receptors in the tumour necrosis factor (TNF) family [55]. An antibody termed anti-APO-1 targeted CD20 on B lymphocytes cell surfaces and led to rapid induction of apoptosis. Anti-APO-1 was later identified as FAS (a TNF family ligand) which led to death receptor activation [55, 56]. Enhancement of the immune response can occur through two mechanisms; complement mediated cytotoxity (CDC) and antibody dependent cytoxicity (ADCC). CDC can only be activated when IgM and IgG classes of monoclonal antibodies are utilised. The Fc portion of the antibody is capable of binding the first component of the complement cascade (C1). This triggers the complement cascade which results in the recruitment of phagocytic cells and resultant death of the antibody bound cells [57, 58]. Additionally the Fc portion of the antibody can bind an Fc gamma receptor (FcgR) on effector cells. ADCC is triggered when both Fc and Fab portion of the Ab engage both tumour cell antigen and FcgR of the effector cells. Effector cells include natural killer cells, macrophages, neutrophils and eosinophils. These effector cells then release perforins and granzymes to lyse the antibody labelled cell [57, 59, 60]. ADCC has been implicated as a critical mechanism of action of monoclonal antibodies and polymorphisms in the FcgR region of effector cells have been attributed to a reduction in activity of a number of monoclonal antibodies including trastuzumab, rituximab and cetuximab [60].

Finally, antibody drug conjugates are currently under investigation as a mechanism of selected delivery of cytotoxic drugs. Trastuzumab emtansine (TDM-1) incorporates the monoclonal antibody trastuzumab and the microtubule inhibitor DM1 [61]. Emtansine was developed in 1980s, however was deem too toxic for patient treatment. Conjugation of low concentrations to trastuzumab allow directed delivery of drug to HER2 expressing cells. TDM-1 significantly increased progression-free and overall survival in HER2 positive metastatic patients [13].

1.7 Receptor tyrosine kinases (RTKs)

RTKs are a family of cell surface receptors whose functions are diverse and many. In most instances they function as receptors for growth factors. The primary structure of a RTK was initially demonstrated through the EGFR. The RTK class of cell surface receptors now comprises 58 known members that are distributed among 20 subfamilies.

However, despite the large number of members and their diverse biological functions, most demonstrate the same core structure as described below [62].

RTKs consist of four main domains. The extra-cellular domain with responsibility for ligand binding, the intracellular tyrosine kinase domain which is responsible for activity and biological response, the transmembrane domain which connects the two and finally a regulatory domain [63, 64]. The general mechanism for activation of a RTK is as follows; a ligand will bind to the receptor which induces a transformational change through dimerisation (either hetero- or homo). This transformational change triggers autophosphorylation of tyrosine residues, causing subsequent downstream phosphorylation propagating the signal. The phosphorylated tyrosines serve as docking sites for secondary messengers, such as growth factor receptor bound protein-2 GRB2. Upon activation GRB2 binds to the cytoplasmic domain of the RTK through its Src homology 2 (SH2) region. GRB2 consists of one SH2 domain and two SH3 domains. The SH3 domains are responsible for the binding of the next protein in the cascade. SH3 domains recognise proline rich areas in other proteins such as son of sevenless (Sos). Sos is a guanine exchange factor which switches RAS from its GDP-bound inactive form to its GTP bound active form. RAS is known to activate numerous pathways including MAPK and AKT which are involved in cellular growth and regulation of transcription factors. Another downstream pathway activated by RTKs is the PI3K pathway which is also involved growth, proliferation differentiation, motility and survival [48]. RTKs are subject to both positive and negative feedback loops. Positive feedback increases the sensitivity of the system to signalling inputs by amplifying the stimulus [65].

1.8 RTKs implicated in TNBC

1.8.1 EGFR

EGFR is overexpressed in BL/TNBC with expression levels reported between 18 and 60 % [20, 66-69]. EGFR overexpression has been associated with larger tumour size and poorer progression free/overall survival, poor response to therapy and development of resistance to chemotherapeutics [68, 70-73]. TNBC cell lines show resistance to EGFR specific inhibitors and signal agent clinical trials with gefitinib and erlotinib showed limited activity [74-77] One mechanism suggested for poor activity has been through interaction with c-Met as described below in section 1.15.1.

1.8.2 c-Kit

The proto-oncogene c-Kit encodes a transmembranse receptor tyrosine kinase c-Kit. c-Kit is activated by its ligand colony stimulating factor. Its functionality in normal tissues includes haematopoiesis, melanogenesis, spermatogenesis and the development of the interstitial cells of Cajal. c-Kit is normally expressed in haematopoietic stem cells, tissue mast cells, germ cells, melanocytes, interstitial cells of Cajal and mammary gland epithelium [78]. A loss of c-Kit expression has been associated with embryonic lethality in mice and more advanced disease and poor prognosis in basal-like breast cancer [59, 60]. Imatinib is a c-Kit targeting small molecule which showed activity *in vitro* however, a phase II trial in metastatic breast cancer showed no activity of imatinib in reducing primary tumour burden [79]. Previous pre-clinical data from our laboratory supports this as imatinib showed limited effect on the proliferation of five TNBC cell lines with $IC_{50} > 20\ \mu M$ [80].

1.9 c-Met

c-Met has previously been implicated in the development of basal-like tumours in mice [81]. Expression has been documented in breast cancer in a number of studies described below (Table 1 - 3). In early gene studies Ponzo *et al.,* identified a c-Met gene signature which was significantly associated with the BLBC [82]. Despite all the evidence supporting c-Met as a potential target in TNBC/BLBC it had not been fully evaluated as a potential therapeutic target for TNBC/BLBC. Thus, the main aim of this thesis was to examine the expression and function of c-Met in TNBC and to evaluate c-Met and it's ligand hepatocyte growth factor (HGF) selective and non-selective inhibitors as a potential therapeutic option. The currently available literature about the structure/function of c-Met is discussed in detail below. Additionally, we discuss previous research on c-Met/HGF in breast cancer specifically TNBC, and the current stage of development of c-Met/HGF inhibitors.

The MET oncogene was originally identified from a chemically transformed osteosarcoma-derived cell line and was mapped to chromosome 7 between 7p11.4 and 7q22. Direct hybridisation indicated this oncogene was unrelated to other known oncogenes [83]. The MET oncogene spans more than 120 kb in length and consists of 21 exons, 20 introns and a single open reading frame of 4224 nucleotides. *In vitro* the MET oncogene is activated by chromosomal rearrangement and fusion between the unrelated TPR gene on chromosome 1 and MET oncogenes [84]. The product of the

MET oncogene is a RTK known as HGFR or c-Met [85]. Initially c-Met is translated as a 150 kDa polypeptide that is partially glycosylated to produce a 170 kDa precursor protein. Following further glycosylation the precursor is cleaved into a 50 kDa α chain (completely extracellular) and 140 kDa β-chain [86]. The large extracellular domain is cysteine rich, a characteristic typical of ligand binding domains and residues are dispersed throughout the extracellular domain (ECD) [85, 87].

The mature c-Met protein is post-translationally cleaved at the amino acid sequence Arg-Lys-Lys-Arg-Ser, dividing the receptor into α (25 kDa) and β (165 kDa) subunits. The α-subunit (N terminal peptide) then associates with the membrane bound β subunit via disulphide bonds similar to that of the human insulin receptor [88]. Homology exists between c-Met and the semaphorins confined to the N-terminal cysteine rich domain [87]. Semaphorins play a role in axon guidance and are also thought to play a role in regulating developmental processes including morphogenesis and cell migration. The conserved domain of c-Met called the sema domain consists of approximately 500 amino acids. Semaphorins have been shown to be responsible for biological activity and receptor specificity [88, 89].

c-Met is the prototypic member and the most characterised of a family of Met receptors consisting of c-Met, and recepteur d'origine nantais (RON). RON's ligand, macrophage stimulating protein (MSP), is also involved in cell scattering. c-Met and RON share a region of homology referred to as the Met related structure (MRS) which maps the conserved nature of the positions of cysteine residues within the receptors [90-94].

1.10 c-Met signalling pathway

c-Met activation occurs when its ligand HGF binds to the receptor resulting in the autophosphorylation of tyrosine residues on the intracellular region of the β chain. Tyrosines are the only residues phosphorylated to any detectable level and the activation process seems to require ATP as phosphate donors for phosphorylation to occur. The initial sites for autophosphorylation are at Y1234 and Y1235, within the activation loop of the tyrosine kinase domain. This then triggers the phosphorylation of Y1349 and Y1356 located in a cluster of amino acids in the C-terminal of c-Met activating the multifunctional docking site [86, 95]. c-Met then interacts with a number of Src

Homology 2 (SH2) containing signalling molecules. These include (PI3K), phospholipase Cγ, pp60$^{c\text{-}src}$ and GRB-2-Sos complex. The SH2 domains are responsible for the interaction of the cytoplasmic mediators with the phosphotyrosine residues on the tyrosine kinase receptor.

In c-Met the diverse biological events seen are almost exclusively thought to be due to an interaction of these SH2 containing molecules with a single multifunctional docking site made of a tandemly arranged degenerate sequence [96]. Met can also be constitutively activated in cancer through somatic mutations in the kinase domain and chromosomal translocations [97, 98]. Y1349 and Y1356 also bind N- and C- terminal SH2 domains in PLC-γ, pp60$^{c\text{-}Scr}$ · Activation of either Y1349 or Y1356 is sufficient to facilitate binding however, binding affinity is much stronger when both Y1349 and Y1356 are involved (Figure 1 - 1) [99] .

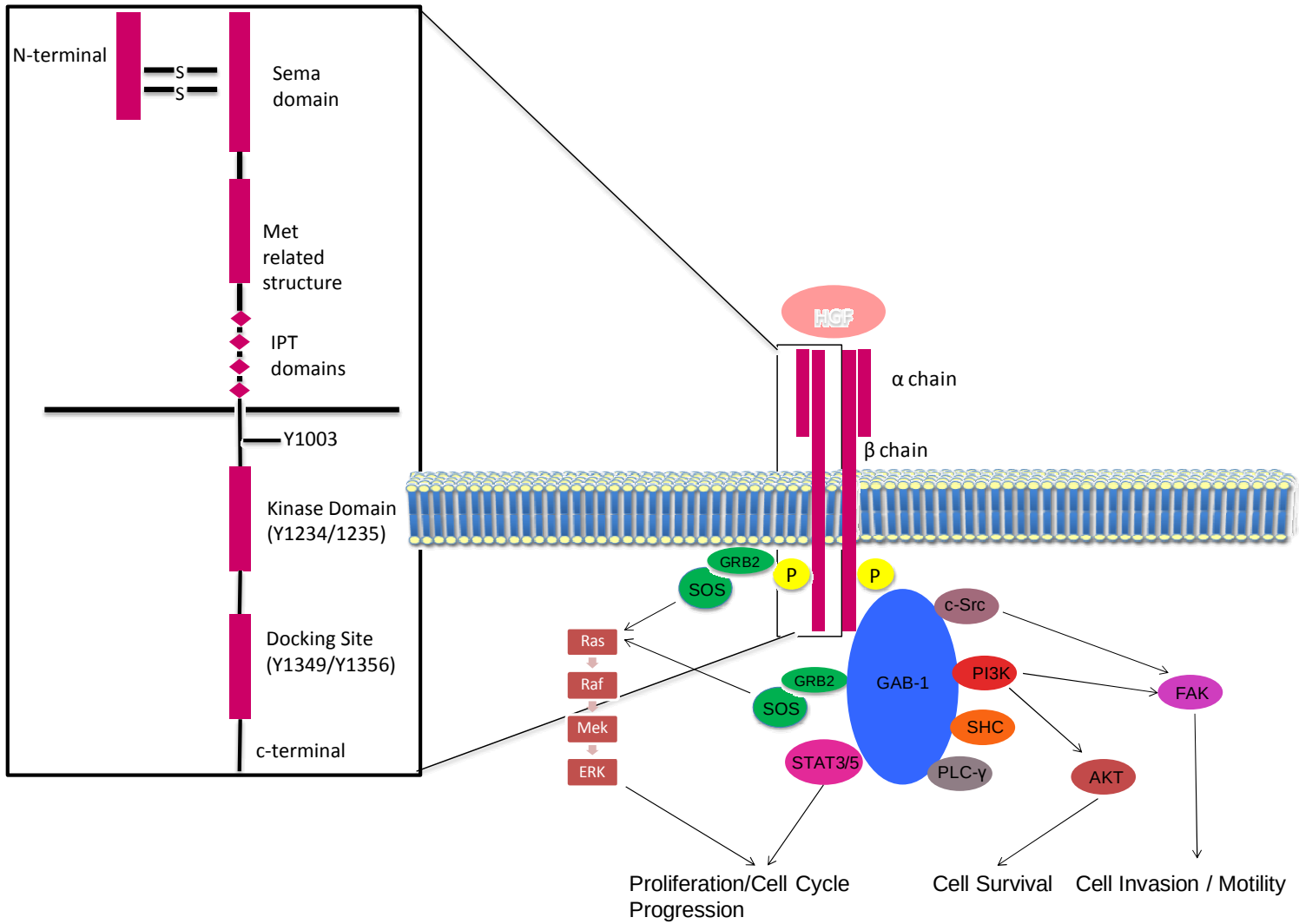

Figure 1 - 1 Schematic structure of the c-Met receptor and downstream signalling pathway [100].

1.11 Hepatocyte growth factor (HGF)

Hepatocyte growth factor/scatter factor (SF) is the only known ligand to bind to c-Met. HGF/SF is so called because they were initially identified as individual molecules, each with its own biological activity [101, 102]. Through analysis of numerous parameters e.g. growth, motility, binding affinities etc. the ligands were shown to be indistinguishable [101, 102]. Hepatocyte growth factor was identified as a hepatotrophic factor playing a role in the regeneration of hepatocytes in rats [103]. Scatter factor was identified as a growth factor responsible for movement and positioning of cells released from fibroblast cells acting only on the epithelial cells. HGF is similar in sequence to that of some proteases involved in fibrinolysis and blood coagulation. HGF is made up of two polypeptide chains; an α-chain of molecular weight 69 kDa and a β-chain of molecular weight 34kDa, linked covalently via a disulphide bond to form a heterodimeric molecule (Figure 1 - 2) [104].

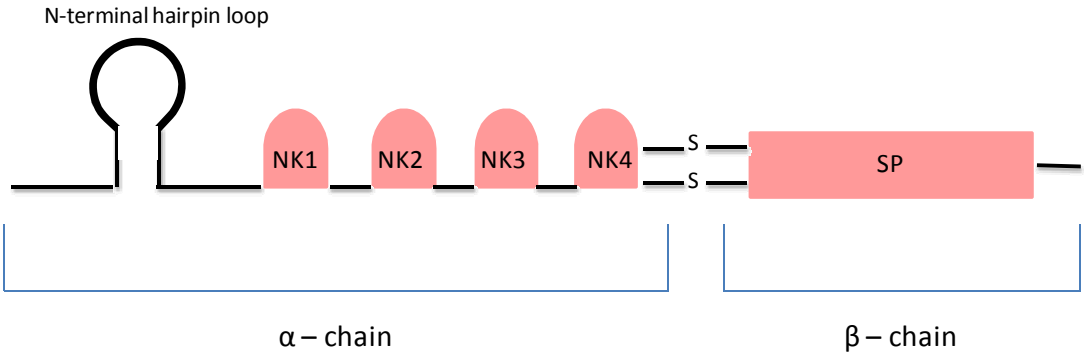

Figure 1 - 2 Schematic structure of HGF [100]**.**

The gene for HGF is located on chromosome 7, is approximately 70 kbp in length and consists of 18 exons and 17 introns. Nucleotide sequencing predicted the translation of a 404 residue protein and an untranslated 3' sequence. HGF is sequenced from a single open reading frame to produce a 728 amino acid polypeptide which includes both an α and a β chain. The chains are cleaved by a trypsin like protease e.g. urokinase/tissue plasminogen activator) (uPA/tPA) at an Arg-Val site. Factor XIIa of the blood coagulation system is also known to be able to activate HGF *in vitro* via a cleavage reaction [105-108]. Cleavage is essential for biological activity [109].

Of the first 54 amino acids, the first 29 are hydrophobic typical of a signalling sequence while the rest constitute the pro-sequence. The pro-HGF molecule shows approximately

40% homology to plasminogen with its α chain containing 4 kringle structures and plasminogen containing 5 kringle structures. These kringle structures are thought to play a role in protein-protein interaction although there full biological role is as yet unknown. The β chain also shows homology to plasminogen in its serine protease domain but histidine and serine residues in the active site in plasminogen are replaced by glutamine and tyrosine in HGF indicating HGF has no serine protease activity. In the mature molecule homology is also seen with plasmin in the formation of an interchain bridge at Cys 604 in the β chain and Cys 487 in the α chain [105]. Each chain contains two Asn-Xaa-Thr/Ser sequences, potential sites for N-linked glycosylation; these are at residues 240-242 and 348-350 of the α chain and at residues 74-76 and 161-163 of the β chain [103].

HGF is unique by virtue of its binding of the c-Met receptor as the only kringle containing protein known to bind to a transmembrane receptor. It has been shown that the α chain N-terminal region and the first kringle domain is sufficient to produce this activity [105, 110]. While the β chain is not exclusively necessary for receptor binding, certain residues (Y673 and V692) are essential for structure, regulation and activity of HGF [105]. Amino acids 28-210 comprise the first kringle domain. HGF contains two natural splice elements. The first N-terminal Kringle domain NK1 consists of two globular subunits; the N terminal and the first kringle (K) domain connected by a short linker (Lys 122-ASN 127). The N terminal consists of three main elements, a 5 strand β-pleated sheet, a 2 strand β-pleated sheet and an α helix region. In contrast the K domain consists of 3 disulphide bridges and a 2 strand anti-parallel β-pleated sheet. It is thought that binding of the NK1 domain is possibly stabilised by interaction with heparin [111, 112]. 10 residues cluster within the NK1 domain, which are known to play a role in receptor binding and activation [113]. The second splice site is known as the NK2 domain and consists of the N terminal and the first 2 kringle domains. NK2 is a c-Met antagonist and is able to bind to the Met receptor and induce cell motility but not mitogenesis. Binding of NK2 to c-Met does not facilitate dimerisation of c-Met due to NK2 monomeric nature. This is potentially the reason for NK2 c-Met antagonism. [110, 114].

1.12 Major signalling pathways downstream of c-Met

1.12.1 PI3K-Akt axis

Phosphatidylinositol-3 kinase (PI3K) can bind directly to the phosphorylation sites at Y1349 and Y1356 of c-Met. PI3K binds to these two docking sites as it contains two SH2 domains however the C-terminal SH2 presents with a higher affinity for binding to c-Met. The N-terminal SH2 domain's affinity may be affected by the phosphorylation status of the C-terminal SH2 domain. Indirect activation of PI3K can also occur through binding of Ras. PI3K phosphorylates phosphatidylinositol-4-5-bisphosphate (PIP2) to phosphatidylinositol-3-4-5-trisphosphate (PIP3) [115]. Akt binds to PIP3 resulting in translocation to the cell membrane where it is phosphorylated by phosphoinositide-dependent kinase-1 (PDK1) at Thr308. Full activation of Akt requires a second phosphorylation at Ser473. Activated Akt is then released into cytosol where it interacts with multiple effector proteins [116]. In ovarian cancer treatment of cell lines with c-Met inhibitor PHA665752 resulted in dephosphorylation of Akt and subsequent downregulation of anti-apoptotic proteins XIAP and BCL-XL [117].

1.12.2 MAPK cascades

c-Met can also activate Ras through the GRB-2-Sos complex. GRB-2-Sos can interact directly or can be associated through SHC adapter proteins to c-Met [96]. GRB-2-Sos only requires to Y1356 [99]. This leads to activation of the family of mitogen activated protein kinase (MAPK)/extracellular signal regulated (ERK) cascades. HGF increases levels of p-ERK in gastric cancer and inhibition of c-Met using inhibitor SU11274 demonstrated activation of ERK leading to decreased SU11274 induced autophagy through interaction with p53 and BCL-2 [118].

1.12.3 STAT3 pathway

Stat3 associates with phosphorylated c-Met through SH2 domains (Figure 1 - 3). Resultant phosphorylation of STAT3 leads to the formation of STAT3 homodimers. STAT3 homodimers translocate to the nucleus where they function as transcriptional controls [119]. It has been reported that c-Met signal specific control of STAT3 requires internalisation of c-Met receptor and trafficking to the peri-nuclear compartment [120]. STAT3 can also be activated through Src family kinases and it is these different

methods of activation of STAT3 which determine the effects exerted on transcription of proteins [121].

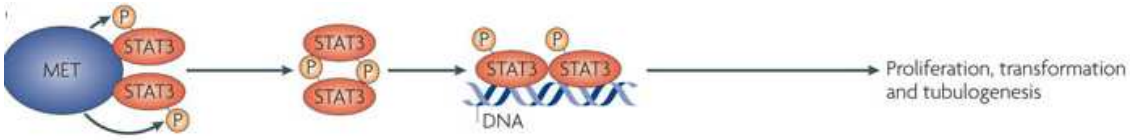

Figure 1 - 3 Interaction of STAT3 and c-Met [122].

1.13 Regulation of c-Met

Regulation of c-Met activity is controlled in a number of ways. It can undergo degradation post stimulation with HGF. The receptor is internalised and degraded via an ubiquitin-proteosome labelling system. This pathway is dependent on kinase activity of the receptor. It has been suggested that activation of the receptor through phosphorylation and dimerisation unmasks the ubiquitin recognition sequences [123]. A dileucine enriched motif has been identified which indicates the presence of a selective endocytic assembly for c-Met. Ambiguity exists over whether endocytic internalisation of c-Met results in downregulation of signalling or functions to enhance signal transduction. It is probable that both scenarios exist however more research is needed to confirm [124]. Ubiquitination of c-Met is mediated by c-Casitas B-lineage Lymphoma protein (c-CBL) binding on the juxtamembrane domain of the c-Met receptor. The c-CBL protein requires an intact tyrosine kinase binding domain and phosphorylation at Y1003. In cells which express mutant Y1003, (Figure 1 – 1) c-Met may still be internalised, however the receptor is not trafficked into degradation pathways [125, 126].

Phosphatases are biological molecules which dephosphorylate residues therefore deactivating them. Phosphatases have been implicated in the negative regulatory element of c-Met and the following target the main phosphorylation sites Y1234 and Y1235; protein-tyrosine-phosphatase (PTB) 1B as well as T-cell phosphatase (TCPTP). PTB-1B is a non-receptor tyrosine phosphatase and possesses a phosphatase catalytic domain as well as a proline rich domain. PTB-1B has been shown to interact with multiple RTKs. TCPTP is closely related and structurally similar to PTB-1B but possess different specificities. PTP-1B and TCPTP both co-localise with c-Met after HGF induced activation and dephosphorylate the major autophosphorylation site [127].

Finally, dorsal ruffles are apical protrusions produced in response to growth factors. Dorsal ruffles form only transiently in response to growth factor activation and in the case of c-Met signalling are enriched in Gab1 (a Met substrate) thereby providing a prolonged localised plasma membrane signalling microdomain. Enriched Gab1 dorsal ruffle domains enhance c-Met degradation indicating that dorsal ruffles not only create a microdomain for downstream signalling but also create a pathway for internalisation of

the receptor and targeting for degradation. Data suggests that this method of degradation works independently of ubiquitination and occurs when the dorsal ruffle collapses causing bulk internalisation and subsequent entry into the canonical degradation pathway [128].

1.14 Role of HGF and c-Met signalling in normal development

The HGF and c-Met signalling pathway is involved in numerous developmental events. HGF was initially identified as a growth factor for hepatocytes playing a role in the development and regeneration of the liver [101]. HGF is involved in embryogenesis, demonstrated by the embryonic lethality of offspring of homozygous HGF null mice from heterozygous parental mice [129]. Abnormality of the placenta in mutant mice was seen demonstrating a role for HGF in placenta formation. The placentas displayed abnormal labyrinth regions (areas of fine embryonic vessels surrounded by trophoblast epithelial cells bathed in maternal blood) with a decreased number of trophoblast cells resulting in markedly decreased size of the region. C-Met expression was documented on the trophoblast cells suggesting that interaction with HGF is essential for normal foetal development. This hypothesis is also supported by the presence of c-Met mRNA transcripts in a wide variety of foetal tissue with highest concentrations occurring in the liver and spleen [129-131]. In foetal development HGF is also required for the normal development of limbs and that of a normal diaphragm [132]. HGF is also known to play a role in wound and tissue healing. In response to injury of the liver and kidney the rate of pro-HGF conversion to its active form is up-regulated. While conversion rates only increase in the injured organs, synthesis of pro-HGF in other tissues increases indicating a paracrine method of action for HGF on c-Met, however, wound healing is one of the few instances in non-pathogenic states where autocrine signalling and activation can occur [108, 133]. HGF also plays a role in normal mammary gland development where over-expression results in increased size and number of the ductal end bud (growth regulatory control point) as well as hyperplastic branching morphogenesis during pubertal development. Throughout mammary gland development a serine protease matriptase is known to act as an activator for HGF by cleaving the pro form into its biologically active state [134, 135] In normal breast tissue expression of c-Met is predominately located in the ductal cells with little expression demonstrated in normal stromal cells [136-138].

1.15 c-Met/HGF in cancer

c-Met/HGF signalling mediates a diverse range of biological events. c-Met/HGF activation can occur through a number of mechanisms; over expression, paracrine/autocrine loops and amplification/mutation. Tumours of epithelial origin show aberrant signalling predominantly through over expression and/or a paracrine relationship with HGF [138-140]. Mutations have been detected in papillary renal cell carcinomas and head and neck squamous cell carcinomas [98, 141] while tumours of haemopoietic origin, neurological tumours, gastric cancers and lung cancer cell lines have shown autocrine activation of c-Met [142-144]. In tumour development, particularly that of carcinomas, there is often a correlation between the differentiation stage of the tumour cells and their ability to invade and metastasise, i.e. a highly differentiated tumour cell will show poor invasive characteristics and vice versa. Early studies found carcinoma cell lines which were poorly differentiated mediated a much stronger response to invasion following stimulation by HGF in comparison to that of cell lines with better differentiation and of normal epithelial tissue [145]. This observation suggests that HGF and c-Met signalling can be implicated in increased tumorigenesis, invasiveness and metastatic ability in human cells. This increase may be due to the activation of the uPa proteolysis network resulting in the establishment of a proteolytically active cell surface facilitating cell invasion via degradation of the extracellular matrix (ECM) [146]. HGF/c-Met signalling significantly increases the protein levels of both uPa and its receptor in sarcoma cells [146].

The c-Met axis is also involved in the development of lymphatic vessels in the embryonic stage, during cutaneous tissue repair and during the establishment of metastasises. This role has been demonstrated both *in vitro* and *in vivo*. HGF stimulation of lymphangiogenesis does not require VEGFR-3 signalling unlike that of other stimulating factors and facilitates lymphangiogenesis through interaction with integrin alpha 9. HGF not only plays a role in formation but also in the function of lymphatic vessels as when the c-Met receptor is blocked lymph vessels cannot respond via enlargement during inflammatory events [147].

1.15.1 c-Met/HGF in breast cancer

Overexpression of c-Met has been documented in numerous clinical studies in breast cancer. The main findings of these studies are summarised in Table 1 - 3. The expression and phosphorylation of c-Met across the human breast cancer subtypes using

microarrays was examined and c-Met was detected to be significantly associated with ER and HER2 negativity [148]. Overall, overexpression of c-Met is associated with a poorer prognosis for patients. Overexpression levels of c-Met according to the studies described in Table 1 - 3 and range from 36 to 100% however this overexpression does not seem to be linked to MET amplification in breast cancers. Carracedo *et al.*, carried out FISH on 155 ductal infiltrating carcinomas and lobular carcinomas but observed no amplification of c-Met [149]. Additionally genome wide screening for focal amplifications in 56 TNBC did not show any significant alterations in the copy number for the MET locus [150]. MET amplification has been reported in 4.7% (3/63) of invasive breast cancer tumours however, study numbers are low and do not achieve any statistical significance in survival although associations between high grade histology and increased tumour burden were reported [151]. As mentioned above the kinase activity of c-Met is activated by phosphorylation. To our knowledge only one study has examined levels of phospho-Met in tumour tissue. High levels of phosphorylation were seen in 123/257 fine needle aspirates from breast tumours (47.8%) and this was significantly associated with relapse free survival (RFS) and overall survival (OS) however, no significant difference was seen across hormone receptor (HR) positive, HER2 or triple-negative subtypes [152].

Lengyel *et al.* and Bevigilia *et al.* both showed increased expression of c-Met in lymph nodes and metastatic disease during the progression of disease (Table 1-4) suggesting c-Met inhibition may be a potential treatment option for metastatic disease [153, 154]. Metastatic breast cancer shows high levels of metastases to the bone, with almost 80% of metastatic disease developing bone disease [155]. The c-Met axis has been implicated in the development of bone metastases through regulation of the β catenin pathway [154, 156]. *In vivo* treatment of xenograft models with c-Met specific inhibitor ARQ197, prior to the establishment of bone metastases resulted in reduction of metastases in both size and number, and prolonged overall survival of mice. It may be important to note the lack of efficacy of ARQ197 in this study in reducing primary tumour burden and that of already established metastases [81].The role of c-Met in metastases may be mediated through Spry-domain containing SOCs box -1 (SPSB-1). In HER2 amplified tumours recurrence and metastases is dependent on up-regulation of SPSB-1. HER2 amplified tumours may become HER2 low post treatment with a specific HER2 inhibitor e.g. lapatinib. Cells which show HER2 down-regulation show an up-regulation of SPSB-1 which enables the cell to avoid apoptosis. c-Met binds to

PSB-1 and increased c-Met phosphorylation was observed in HER2 positive cells (BT474) following lapatinib treatment. The authors show that SPSB-1 mediated inhibition of apoptosis is c-Met dependent [157]. c-Met also mediates inhibition of apoptosis through downregulation of p53. In non-small cell lung cancer (NSCLC) cell lines treatment with c-Met inhibitor SU-11274 caused an increase in the amount of p53 protein and subsequent sensitivity to apoptosis induction [158].

High levels of HGF in primary breast tumours have been shown to be a strong predictor of recurrence and survival in breast cancer [140, 159, 160].Expression levels are variable ranging from 43.6% to 66% [138, 161, 162]. HGF is thought to be primarily derived from the stromal cells however; HGF has been detected at significantly higher levels in invasive breast carcinomas than in non-invasive areas [160]. HGF mRNA has been detected in adipocytes, endothelial cells and stromal fibroblasts which lacked c-Met mRNA. However, in areas of strong expression of c-Met mRNA high levels of HGF mRNA were also detected, suggesting the presence of an autocrine loop [140].

Co-expression of c-Met and HGF in breast tumours has been associated with a poorer prognosis [153, 161]. In one cohort of Japanese women, 88.8% of samples which showed c-Met expression at the leading edge of the tumour showed co-expression of HGF in a front accentuation pattern. This front accentuation pattern was associated with lymph node involvement, grade and increased KI-67 index [161].

Serum levels of HGF are significantly higher in the following instances; ER negativity, poorly differentiated tumours, more advanced primary staging, patients with distant metastases, and patients with reoccurrence [163, 164].

In vitro studies demonstrated that HGF confers resistance to apoptosis by certain DNA damaging events caused by adriamycin in some cell lines. Thus, it is possible that HGF confers resistance to cell death induction by conventional cytotoxic treatments. This study included the breast carcinoma cell line MDA-MB-453 and EMT6 mouse mammary tumour cells, however, no protection was conferred on a TNBC line examined, MDA-MB-231 [165].

Huang *et al.,* showed that HGF treatment enhanced lung and liver metastasis in a xenograft model of triple negative breast cancer, by inducing expression of the chemokine receptor CXCR4 on the tumour cell [166].

Table 1 - 3 Summary of c-Met studies in breast tumours.

Reference	Tissue type	Method	% Positivity for c-Met expression	Clinical Associations
Tuck *et al.* [140]	(IDC) DCIS	ISH, IHC	168/168 (100%)	Heterogeneous expression in both benign and malignant tissue. Strong positivity at leading edge of tumour
Lindemann *et al.* [138]	DCIS	IHC, IF	39/39 (100%)	Differential expression between DCIS lesion and normal mammary epithelium Significant correlation between tumour grade and high expression
Raghav *et al.* [152]	FNA from invasive breast carcinoma	RPPA	181/257 (70.4%)	No significant differences in expression observed between subtypes High expression significantly associated with decreased RFS and OS in HR
Carracedo *et al.* [149]	Invasive breast tumours	FISH, IHC	65/168 (38.7%)	Expression was significantly associated with PR negativity
Beviglia *et al.* [154]	Biopsy specimens from human breast carcinomas	IHC	6/6 (100%)	Similar levels in adjacent normal tissue and tumour tissue. Levels were maintained in metastatic lesions and up-regulated in 50% (3/6)

Reference	Tissue type	Method	% Positivity for c-Met expression	Clinical Associations
Edakuni *et al.* [161]	IDC	ISH, IHC	64/88 (72.7%)	Co-expression of c-Met and HGF in the leading edge of the tumour and associated with decreased OS, high tumour grade and high KI-67 index
Garcia *et al.* [167][168]	TMA from breast carcinomas	IHC	330/916 (36.0%)	Overexpression associated with poor survival
Lengyel *et al.* [153]	Breast cancers with ≥3 positive auxiliary nodes	IHC	29/40 (72.5%)	Decrease in DFS Higher expression in lymph nodes than primary tumours
Kang *et al.* [162]	TMAs from node negative breast carcinomas	IHC	165/330 (50%)	Overexpression is associated with more aggressive tumours Cytoplasmic domain stronger predictor of outcome
Ho-Yen *et al.* [169]	TMAs from primary invasive breast carcinoma	IHC	1274	Overexpression is associated with poorer overall survival Associated with HER2 status

1.16 c-Met in TNBC/Basal-like breast cancer

Through genome wide profiling, c-Met was shown to represent a differential marker in the basal-like subtype of breast cancer cell lines. The classification was carried using established markers of basal-like breast cancer (BLBC) however, c-Met among other RTKs (EGFR, c-Kit) emerged as a new marker shown to be differentially up-regulated relative to the luminal subtype [170, 171]. We described earlier the gene expression analysis which sub-divided TNBC into 6 subtypes (Table 1 - 2). Only one subtype showed elevated gene expression for c-Met. This is the BL2 subtype which also shows enriched gene ontologies for EGF, NGF, MET, Wnt/β-catenin, IGF1R signalling, EGFR and EPHA2. The authors also showed a high KI-67 index [31]. On tissue microarrays of 1274 invasive breast cancers, c-Met was significantly associated with BLBC with an inverse correlation to tumour size. Given that in general BLBC tumours tend to present as larger tumours, the authors postulate that c-Met may therefore be playing a more predominant role in TNBC tumours of smaller size [169]. Expression of c-Met has also demonstrated trends towards poor survival in two studies in BLBC however, this did not reach statistical significance [152, 169]. Another study evaluated c-Met in conjunction with loss of PTEN and expression of cytokeratins 5/6. In this study a cohort of 97 patients with TNBC disease were evaluated for the above markers using immunohistochemistry. Expression of c-Met alone did not achieve statistical significance as a prognostic marker of recurrence, however, c-Met was associated with T1-2 tumours and tumours of a higher grade in TNBC. c-Met expression also correlated significantly with the number of metastatic lymph nodes and with increased risk of recurrence and death. Collectively, these markers were associated with an increased risk of recurrence and death in patients with TNBC overall. [172]. These studies support the hypothesis that c-Met is a useful indicator of poor prognosis specific to BLBC/TNBC, however, may not function as a single prognostic indicator in survival studies.

c-Met has been implicated in the early progression and development of BLBC in a number of mouse models [82, 148]. In a study carried out by Ponzo *et al.* expression of c-Met in BLBC correlated with tumours which developed clustered into two types, ‘solid and mixed phenotype (consisting of papillary, scirrhous, adenosquamous, and spindle cell pathologies)’. The mixed pathology tumours showed an enrichment of gene ontologies related to WNT and EMT pathway, while solid tumours showed over expression of genes related to apoptosis, cell adhesion, and small GTPase signal

transduction. Additionally the mixed pathology group of tumours clustered with p53 mutated tumours and when using hierarchical clustering in 172 human breast cancers the mixed pathology tumours show the highest correlation with BLBCs. This MET signature was expressed at a significantly higher level in BLBCs [82]. Further strength is added to the conjecture that activated c-Met may function as an inducer of basal-like tumours through the generation of a mouse model with mutationally activated c-Met to induce tumours [148]. Additionally loss of TP53 in combination with the expression of a mutationally activated c-Met resulted in increased tumour aggressiveness and correlated significantly with hormone receptor negativity as well as poorer prognosis. These tumours showed predominantly a spindeloid morphology and when examined cluster with the claudin low category of TNBC. Inhibition of c-Met resulted in a marked change in morphology and reduced metastatic burden as well as restoring cell-cell junctions and rescuing claudin1 expression [173].

BLBC is suspected to derive from luminal progenitors despite the expression of basal markers at later stages. These luminal progenitors have been shown in mouse models to express high levels of c-Met. Constitutive activation of c-Met results in a preferential differentiation of these progenitors into the basal lineage suggesting a major role for c-Met signalling in the initial development of BLBC [174]. Additionally, *in vitro* dramatic upregulation of HGF secretion was seen from fibroblasts co-cultured with normal mammary epithelial cells representing the atypical ductal hyperplasia stage to replicate epithelial-stromal interactions occurring in development of malignant lesions. The upregulation of HGF alone was not capable of creating the basal-like phenotype, however, in cells representative of the DCIS phenotype, upregulation of expression of c-Met was also observed and stimulated changes in cell morphology indicative of a more invasive phenotype similar to that of BLBC. These changes were reversed by blocking the HGF signal using an antibody, confirming the role of HGF/c-Met in development and progression [175].

This study also confirms the crucial importance of stromal cell interaction in relation to c-Met/HGF activity. Furthermore, Sung *et al.* also demonstrated downregulation of HGF production in a 2D culture model of human mammary fibroblast cells (HMF) when compared to a 3D matrix. The HMFs cultured in the 3D model advanced the progression of MCF10-DCIS cells to a more invasive phenotype agreeing with the results of the study above that HGF secretion by the fibroblasts is important in progression from DCIS to IDC [176]. Both of these studies also highlight the role of

activated c-Met (primarily through paracrine binding of HGF) in the development and progression of BLBC.

In a cohort of 930 breast carcinomas, high c-Met expression was associated with highly invasive malignancies and a negative outcome. Where expression of c-Met was observed there was co-expression of other basal markers [168].

Finally in a limited cohort of primary and metastatic breast cancers, c-Met expression was seen exclusively in basal-like primary tumours with variable expression shown in the metastatic sites of these tumours. Within this study only four tumours were classified as TNBC/BLBC, however, tumour tissue from a minimum of 6 metastatic sites was collected and examined for c-Met. Expression of c-Met in the metastases was never lower than the primary tumour but two patients showed higher grade staining in some of the metastatic tumours. These sites included pericardium in one patient and auxiliary lymph node, omentum and diaphragm in the other [177]. The maintenance of staining between primary sites and metastatic sites was also noted in an earlier study, however, this also had very limited sample numbers (n=6) [154].

Greater than 70% of primary BLBC express transcription/translation factor Y-box binding protein (YB-1). YB-1 has been found in TNBC cell lines and silencing has been shown to decrease cell proliferation. In co-immunopreciptation YB-1 and c-Met were found to be associated with YB-1 binding to the MET promotor and stimulating transcription. Mutant YB-1 overactive cell lines showed increased c-Met expression and silencing of YB-1 or MET resulted in decreased anchorage independent growth [69, 178].

1.17 Crosstalk with other tyrosine kinases

Crosstalk between different families of receptors occurs in a number of cancers. c-Met communicates directly with a number of receptors including EGFR, Src HER2, HER3, death receptor Fas, Ron, α6β4 integrin, CD44 and semaphoring receptor plexin B1.

1.17.1 EGFR

Crosstalk between EGFR and c-Met is probably the best characterised interaction of c-Met with other receptors. EGFR TKIs have demonstrated efficacy as a treatment option in lung and pancreatic cancers but no significant response has been seen in breast cancer. In lung cancers with developed resistance to EGFR inhibitors, c-Met amplification/HGF activation of c-Met has been implicated as a potential mechanism of

resistance [179, 180]. In human breast cancers EGFR over-expression alone is unable to cause tumour formation and necessitates an interaction with c-Met [181]. Communication between c-Met and EGFR can be mediated through the RAS/MAPK signalling pathway and c-Met/EGFR interaction can stimulate similar cellular responses including growth and motility [182, 183]. EGFR is also capable of stimulating a delayed activation of c-Met through c-Src activation. EGF treatment of a NSCLC cell line resulted in a biphasic activation of c-Src with peaks in phosphorylation at 2 hours and 8 hours post treatment corresponding to delayed activation of c-Met via EGFR. Inhibition of c-Met with PF2341066 inhibited the phosphorylation of c-Met with no effect on Src phosphorylation levels. Conversely inhibition of c-Src via dasatinib or PP2 resulted in a decrease in phosphorylation of c-Met, however, had no effect on c-Met autophosphorylation [184]. The combination of a c-Met inhibitor (PHA-6657562) and EGFR inhibitor (erlotinib) showed synergistic growth inhibition in the TNBC cell line MDA-MB-468 [185]. *In vitro* cell lines treated with the EGFR inhibitor gefitinib showed significantly reduced HGF induced motility and cell scattering in a breast cancer cell line [186]. Activation of c-Met by stromally derived HGF also contributes to the resistance of TNBC cell lines to EGFR inhibitor gefitinib [187]. Direct interaction of c-Met and EGFR has been shown and the potential benefits of combined targeting of c-Met and EGFR have been shown in numerous preclinical studies in a variety of cancer types including breast cancer [181, 188-190].

1.17.2 Src

Src family kinases are non-membrane bound tyrosine kinases consisting of nine members. Src, Yes, Fyn and FGR belong to the Src A family subtype. Lck, Hck, Blk and Lyn belong to Src B family subtype. Frk is in its own subfamily [191]. Pre-clinical studies have shown preferential sensitivity to Src inhibition in TNBC than other breast cancer subtypes and in head and neck cancers [80, 192-194]. Combined targeting of c-Met and Src in TNBC cell lines can augment response in cell lines compared to either inhibitor alone [195, 196].

1.17.3 HER2

Direct interaction of c-Met and HER2 has never been documented, however, HGF activation of c-Met has shown the ability to ‘rescue’ gastric, lung and breast cell lines from lapatinib induced apoptosis through reactivation of MAPK and PI3K downstream signalling [179, 197-199]. Co-expression has been associated with innate resistance to

HER2 targeted therapies and synergistic inhibition of cell growth can be achieved by dual targeting of c-Met and HER2 in HER2 amplified breast cell lines [199, 200]. Additionally, HGF activation of c-Met enhances the invasive malignant phenotype in HER2 over-expressing cells [201]. Activation of c-Met has also been suggested to contribute to trastuzumab resistance in HER2 over-expressing breast cancer through inhibition of p27 induction. A subset of HER2 over-expressing cells also upregulate production of c-Met in response to trastuzumab treatment and high copy number correlates with poorer outcome [202, 203].

1.17.4 HER3

Interaction between c-Met and HER3 has also been recognised as a method of resistance to gefitinib in lung cancer. Met amplification stimulates the HER3 dependent phosphorylation of the PI3K pathway [179].

1.17.5 α6β4 integrin

α4β6 can form direct complexes with c-Met resulting in enhanced invasiveness in carcinoma cells. Upon association tyrosine phosphorylation occurs on the β6 transmembrane domain stimulating signalling through P13K. FAK is a well-established protein kinase involved in integrin mediated cell motility. Downstream FAK is activated via c-Met stimulated c-Src. FAK also can interact directly with c-Met when c-Met is constitutively active or over-expressed [204-206].

1.17.6 CD44

HGF induces a time dependent association of c-Met with CD44v10 and regulates HGF induced endothelial cell barrier enhancement. Up-regulation of c-Met and CD44 have been implicated in tumour cell growth and metastases through prolonged signalling from c-Met through MAPK pathways [207, 208].

1.17.7 HIF1α

Most solid tumours possess an area of hypoxia where inadequate tissue vasculature results in low oxygen levels. The hypoxic environment is involved in mediating a number of steps including epithelial-mesenchymal transition and can regulate a number of growth factors including HGF. Hypoxia not only increases levels of c-Met RNA in tumours but also sensitises tumour cells to HGF stimulation [209]. Hypoxia inducible factors (HIFs) mediate transcriptional responses to low oxygen levels. HIF1α is stabilised through interaction with ROS1 which in turn leads to increased

expression/activation of c-Met in melanoma cells [210]. Nuclear factor kappa-light-chain-enhancer of activated B cells (NF-κB) has also been implicated in regulating HIF-1α induced by HGF leading to transactivation, however, in a TNBC cell line this HIF-1α transactivation was undetectable and HGF caused a temporary downregulation of HIF-1α [211].

1.18 Preclinical studies on c-Met in TNBC

Although only a limited number of studies have focused specifically on c-Met/HGF as a therapeutic target in basal-like/TNBC, a number of early studies of c-Met/HGF in breast cancer included cell lines which we now know to be BLBC/TNBC. A panel of breast cancer cell lines was tested for responsiveness to HGF in invasive and migratory properties. The cell lines BT20 and MDA-MB-231 both showed the strongest responses to HGF treatment in a dose dependent manner [154]. c-Met has been shown to be expressed at higher levels in TNBC cell lines relative to that of other subtypes [185].

Combinations of protein kinase C α and c-Met inhibitors showed synergism in TNBC cell lines [212]. Co-targeting of c-Met with Src inhibitors (dasatinib) showed significant decreases in proliferation in cell lines relative to either single agent and no significant response was seen in non-TNBC cell lines tested [195] . Cell lines which show resistance to EGFR inhibition display constitutive c-Met activation independent of HGF. Co-immunoprecipatation experiments demonstrated that this was through a physical association between c-Met and EGFR. Src also was associated with EGFR and c-Met in these cell lines. Inhibition of c-Src resulted in a decrease in phosphorylation of EGFR and reduced proliferation and knockdown of Src resulted in moderate sensitisation to the EGFR inhibitor gefitinib. Inhibition of EGFR did not result in a decrease in activation of Src suggesting a secondary method. In cells treated with gefitinib (an EGFR inhibitor) levels of c-Met phosphorylation increased maintaining Src phosphorylation. c-Met activation exerted no effect on levels of EGFR activation alone, however, dual inhibition resulted in a decrease in Src phosphorylation and proliferation of the cell lines. This indicates activated c-Met results in EGFR inhibitor resistance. Further proof of this is the de-sensitisation of sensitive TNBC cell lines to EGFR inhibition via the introduction of HGF (recombinant or fibroblast conditioned media) to culture. This resulted in a significant decrease in sensitivity to gefitinib in proliferation and clonogenic survival assays [181, 187, 213].

Radiotherapy is one of the conventional treatments used to treat localised breast cancers. When a TNBC cell line (MDA-MB-231) was irradiated with a therapeutic dose of ionising radiation (IR), overexpression of c-Met was induced through upregulation of MET promoter sequence which increased transcription levels of the protein. Post-irradiation the cells were treated with a selective c-Met inhibitor which increased apoptosis in the cell lines. Furthermore when the cells were treated with a sub-optimal

dose of IR in combination with the c-Met inhibitor, apoptosis was significantly increased compared to IR alone, both *in vitro* and *in vivo* [214]. Treatment with histone deacetaylase inhibitor (HDAC) sodium butyrate results in resistance to apoptosis. In TNBC cell-line MDA-MB-231 this resistance was mediated via c-Met expression.This was confirmed by an increase in the levels of apoptosis in response to sodium butyrate post c-Met knockdown. These c-Met expressing resistant cells share similar characteristics to cancer stem cells and had a much greater ability to initiate tumour formation in Severe Combined Immunodeficiency (SCID) mice [215].

1.19 c-Met as a therapeutic target in TNBC

c-Met is a potential druggable target to treat TNBC. The c-Met/HGF inhibitors currently in preclinical/clinical development are listed in Table 1 - 4. In the stratification of TNBC into 6 subtypes, c-Met was only associated with the BL2 subtype which may impact the success of c-Met inhibition if tested in other subtypes of TNBC in clinical trials [31, 169]. Two trials are underway with c-Met inhibitors in TNBC, tivantinib in patients with recurrent or metastatic TNBC and cabozantinib in metastatic TNBC. Results of a single agent phase II trial of tivantinib in metastatic breast cancer showed partial resolution of metastatic lesions and cabozantinib exhibited clinical activity in patients regardless of receptor status and prior treatment [216, 217]. Some controversy exists over tivantinib and whether it is a true c-Met inhibitor. It was initially identified as a non-ATP competitive, selective, c-Met inhibitor with a Ki of ~ 335nM however, Katayama *et al.* showed that tivantinib in addition to inhibiting c-Met caused microtubule disruption and therefore its activity could not be solely attributed to c-Met inhibition [218, 219].

Table 1 - 4 c-Met/HGF inhibitors and stage of development.

Compound	**Mode of Action**	**Phase of Development** [220]	**Indication** [220]
Rilotumumab *Amgen Inc.*	HGF monoclonal antibody	Phase III	Advanced Gastric and or Gastroeosphageal cancer
AMG458 *Amgen Inc.*	c-Met selective TKI	Pre-clinical	
AMG208 *Amgen Inc.*	c-Met selective TKI	Phase I	Patients with Advanced Solid Tumours
AMG337 *Amgen Inc.*	c-Met selective TKI	Phase II	MET Amplified Gastric/Oesophageal Adenocarcinoma or Other Solid Tumours
MetMAb *Genentech Inc.*	c-Met monoclonal antibody	Phase III	NSCLC
Ficlazutumab *Aveo Pharmaceutical Inc.*	HGF monoclonal antibody	Phase II	NSCLC
MK2461 *Merck Sharp & Dohme*	Multi-targeted TKI	Phase II	Advanced Cancer
MK-8033 *Merck Sharp & Dohme*	c-Met selective TKI	Phase I	Advanced Solid Tumours

Compound	**Mode of Action**	**Phase of Development** [220]	**Indication** [220]
INC280 *Novartis Pharmaceuticals*	c-Met selective TKI	Phase II	c-Met dependent advanced solid tumours
PF-04217903 *Pfizer*	c-Met selective TKI	Phase I	Advanced Cancer
BMS817378 *Bristol-Myers Squibb*	Dual c-Met/VEGFR2 inhibitor	Pre-clinical	n/a
Cabozantinib *Exelixis Inc.*	Dual c-Met/VEGFR2 inhibitor	Phase III	Advanced Medullary Thyroid
LY2801653 *Eli Lilly & Co*	Multi-kinase inhibitor	Phase I	Advanced Cancer
PRS-110 *Pieris Ag. Inc.*	c-Met anticalin	Pre-clinical	n/a
Foretinib *GlaxoSmithKline*	Dual c-Met/VEGFR2 inhibitor	Phase II	Squamous Cell Cancer of the Head and Neck
LY2875358 *Eli Lilly & Co*	c-Met monoclonal antibody	Phase II	Met Positive Gastric Cancer

1.20 Non-selective c-Met small molecule inhibitors

1.20.1 Crizotinib (PF-2341066)

PF-2341066, developed by Pfizer, is also an oral, ATP-competitive, small-molecule dual inhibitor of c-Met and ALK with IC_{50} values of 4 nM and 25 nM respectively. It is considered highly selective for the c-Met receptor and was found to be able to select out the c-Met receptor in a panel of 120 tyrosine and serine-threonine kinases. It potently inhibits c-Met phosphorylation and c-Met–dependent proliferation, migration, or invasion of human tumour cells via inhibiting HGF-stimulated or constitutive total tyrosine phosphorylation of c-Met. In xenograft mouse models, PF-2341066 displayed similar inhibitory activities as those observed in cellular studies. It has also been demonstrated that PF-2341066 is less potent against the Y1230C and Y1235D mutant variants of c-Met located near the kinase domain activation loop. This indicates that PF-2341066 activity is dependent on the location of the mutation in the active site [221]. There have been numerous clinical trials involving PF-2341066 however, most have focused on crizotinib as an ALK inhibitor in NSCLC [220].

1.21 Other non-selective c-Met small molecule inhibitors

XL880/GSK1363089 is a non-selective small-molecule kinase inhibitor that targets members of the HGF and VEGF receptor tyrosine kinase families. However, while the main targets are the two families mentioned previously, it exhibits additional inhibitory activity toward c-KIT, Flt-3, platelet-derived growth factor receptor (PDGFR) β, and Tie-2. Binding of XL-880 to c-Met and VEGF receptor 2 is characterized by very slow dissociation from its target, which is verified using X-ray crystallography data showing that the inhibitor is deeply bound in the c-Met receptor active site cleft. It inhibits, in cellular models, HGF-induced c-Met phosphorylation and VEGF-induced ERK phosphorylation and prevents both HGF-induced responses of tumour cells and HGF/VEGF-induced responses of endothelial cells. Although it was optimised for inhibition of Met, XL880/ GSK1363089 also displays potency toward Ron, and other VEGF receptors [222, 223]

MP470 developed by Supergen is another non-selective kinase inhibitor which effectively inhibits PDGFR, c-Kit and c-Met. When compared to the activity of

erlotinib or imatinib, MP470 inhibits cell proliferation, induces cell growth arrest and promotes apoptosis in prostate LNCaP cancer cells. When combined with erlotinib it resulted in the destruction of the HER family/PI3K/Akt pathway with associated tumour growth inhibition in an LNCaP mouse xenograft model [224].

GCD265 (Methylgene) is a potent and orally active inhibitor of c-Met, RON, VEGFR1/2/3 and TIE-2. A phase I trial with dose escalation is ongoing in patients with advanced malignancies.

BMS-777607 (BMS) is another potent and orally bio-available inhibitor of c-Met, RON, AXL and TYRO3. It is slightly less active against several other kinases.

MK2461 (Merck) is an orally active inhibitor of c-Met as well as FLT1/3/4, FGFR, VEGFR2 and TRKA/B. A phase I trial in advanced patients was recently completed but the final results have not been disclosed [222].

AMG 208 is a small-molecule inhibitor of c-Met. It is selective for both c-Met and RON. c-Met inhibitor AMG 208 inhibits the ligand-dependent and ligand-independent activation of c-Met, inhibiting its tyrosine kinase activity, which may result in cell growth inhibition in tumours that over express c-Met [225].

1.22 PRS110

Anticalins are engineered lipocalins, endogenous low-molecular weight human proteins typically found in blood plasma and other body fluids that naturally bind, store and transport a wide spectrum of molecules. PRS110 is an anticalin antagonist of c-Met which functions in both ligand dependent and independent systems. It binds specifically to c-Met and blocks HGF interaction with the receptor without inducing agonism of the receptor a side effect of other bivalent monoclonal antibodies [226, 227]. PRS110 is highly selective for c-Met with an IC_{50} of 3.2 ± 0.4 nM and binds to the extracellular domain of c-Met. Upon bind to c-Met PRS110 is internalised and trafficking to endosomal compartments. PRS110 has also shown efficacy in inhibiting *in vivo* growth in a U87-MG and Caki-1 xenograft models [228] .

1.23 Monoclonal antibodies in targeting HGF/c-Met

1.23.1 AMG102 (Rilotumumab)

AMG102 is a humanised IgG2 directed against HGF and capable of preventing HGF binding to c-Met and subsequent c-Met activation [229]. Phase I trials of AMG102 have indicated it is well tolerated for the treatment of solid tumours and these encouraging results have led to further clinical trials including in conjunction with anti-angiogenesis agents (which demonstrated a similar patient tolerance to treatment with the inhibitor alone and an acceptable safety profile) [225]. AMG102 has also undergone phase II trials in patients with recurrent glioblastoma multiforme [230]. When it was tested in combination with temozolomide and docetaxel in U-87 Mg xenografts, the combined inhibitory effect on tumour cell growth was significantly increased when compared to either agent alone. It is thought that temozolomide and docetaxel work through induction of caspase 3/7 activity and this is enhanced through the presence of AMG102 [231]. Amgen Inc. has recently identified c-Met protein expression as a biomarker to response of AMG102 in gastric cancer and are currently pursuing a phase III clinical trial in gastric cancer [229, 232].

Onartuzumab (MetMAb^{TM}, Roche) is a recombinant humanised monovalent monoclonal antibody which targets the extracellular domain of c-Met The unique monovalent design of onartuzumab inhibits HGF binding, while avoiding agonistic activity, which has been reported with traditional bivalent antibodies [33, 233]. In a phase II trial in NSCLC, patients with c-Met positive tumours receiving onartuzumab plus erlotinib had a significant improvement in progression-free survival and overall survival compared to treatment with erlotinib alone [234].

On the basis of the positive findings in the above study, a phase III trial in confirmed c-Met-positive NSCLC was launched [234]. However, the phase III trial has recently been halted, based on the recommendations of the independent data monitoring committee, due to a lack of clinically meaningful efficacy [235]. Onartuzumab is also currently being tested in combination with chemotherapy in a phase III trial in patients with HER2 negative, c-Met positive gastric cancer [220].

TAK-701 is another humanised monoclonal anti-HGF antibody which binds and inhibits HGF/c-Met driven proliferation. Phase I studies carried out have shown it is well tolerated and safety and pharmacokinetic profiles are of acceptable levels [236].

1.24 Compounds evaluated in TNBC in this thesis

We evaluated five c-Met inhibitors in this thesis. They included rilotumumab (HGF monoclonal antibody), CpdA (a c-Met selective inhibitor) and PRS110 (a c-Met selective anticalin) which were all obtained through industry partnerships. Additionally we evaluated two non-selective c-Met inhibitors, crizotinib and BMS-777607. Crizotinib inhibits both c-Met and ALK although. ALK has been indicated as a potential oncogenic driver in TNBC and as such was deemed a target to evaluate in addition to c-Met [237]. BMS-777607 was selected for further evaluation due to its dual inhibitory effects on RON. c-Met and RON interaction have been documented in a number of cancer types including lung, pancreatic and breast [238].

1.25 Survival analysis in cancer

TNBC/BLBC is heterogeneous disease which can by sub-typed into a number of distinct tumour types [31, 34]. The confirmed presence of these subtypes and the highly proliferative adaptability of TNBC/BLBC affirm the view that meaningful treatment of TNBC/BLBC may not be achieved through targeting a single protein. EGFR, for example, is overexpressed in TNBC, however, tumours are insensitive to EGFR inhibitors. Many publications have suggested the reasoning behind this is interaction with other RTKs. For these reasons we examined the 58 known RTK's and their influence on progression and survival. Dr. Stephen Madden analysed the survival curve using a database of his own creation BreastMark. BreastMark combines gene expression data from 21 DNA microarray experiments and detailed clinical data to correlate survival/outcome with gene expression levels [239].

Survival data in cancer studies focuses on the start time (e.g. treatment with targeted agent) to the time of the event of interest. These events include overall survival and progression-free survival i.e. time to reoccurrence and it is these events that help to monitor the response to certain situations Since survival data is rarely normally distributed but skewed consisting of many early events and relatively few late events it necessitates a form of statistical analysis known as survival analysis. A key point for survival analysis is to define a closing date of follow-up as it is impractical to follow every patient infinitely. Another variable in survival analysis is the loss of subjects prior to completion of the study i.e. those who withdraw/drop out and those who survive beyond closing date. This is known as censoring. Both right and left censoring exists. Right censoring involves the estimating the time to occurrence of the event because the patient did not experience the event during follow-up. This is the more common censoring that occurs in survival data. Left censoring occurs when the time of the event is unknown i.e. development of a metastatic lesion diagnosed 3 months post-surgery. While the event will be recorded at 3 months, it may have developed at any point in the 3 month window [240, 241]. Survival data is generally described as two probabilities survival [S(t)] and hazard [h(t)].The survival probability, S(t), is the 'probability that an individual survives from the time of origin to a specified future time'. The hazard probability, h(t), is the 'probability that an individual who is under observation at a time t has an event at that time'. The survival probability can be estimated using the Kaplan

Meier (product limit) Method. The Kaplan Meier survival curve plots the survival probability against time [241].

Gene expression profiling has been used to segregate breast cancer into subtypes [7]. Within these subtypes notable differences can be observed in survival analysis. Two methods to identify patients within the subtypes include prediction analysis microarrays (PAM) and single sample predictors (SSP). In this study we used PAM50, SSP 2003 and SSP 2006. In order to create the classifiers an 'intrinsic' gene list was identified which consisted of genes which showed the least variation from successive tumour samplings. Profiles (known as centroids) consisting of the average expression for each of the genes where then used to predict class of the tumours [8, 242]. While every classifier identifies molecular subtypes with similar survival not every patient is reliably assigned to the same molecular subtype. In the basal-like subtype however, the greatest degree of agreement was shown ($\kappa>0.812$ where κ = Cohen's coefficient) regardless of the SSP used [242].

1.26 Study Aims

The aims of this study were as follows:

- To investigate the expression of c-Met/HGF expression in TNBC as a potential prognostic or predictive biomarker for progression/survival
- To examine the expression of c-Met in conjunction with EGFR and Src in TNBC
- To pre-clinically evaluate selective and non-selective c-Met/HGF inhibitors in TNBC cell lines
- To pre-clinically evaluate selective c-Met inhibitors in combination with EGFR and Src inhibitors
- To examine the role of c-Met/HGF in TNBC cell line models of acquired resistance
- To identify novel RTKs implicated in TNBC as potential future targets

Chapter 2

Materials and methods

2.1 Cell lines, cell culture and reagents

Sixteen human breast cancer cell lines were used in this study including nine TNBC (BT20, HCC1937, HCC1143, MDA-MB-468, MDA-MB-231, CAL-120, CAL-85-1, HDQ-P1 and BT549) two drug resistant variants (231-DasB and MDA-MB-468CR) and seven non-TNBC cell lines (SKBR3, MDA-MB-453, BT474, HCC1419, CAMA-1 and MCF-7). The cell lines, BT20, HCC1937, HCC1143 MDA-MB-231, MDA-MB-468, HCC1419, BT474, SKBR3, CAMA-1, MCF-7 and T47D were obtained from the American Type Culture Collection (ATCC). MDA-MB-453 cell line was obtained from the University of California, Los Angeles, USA. CAL-120, CAL-85-1 and HDQ-P1 were obtained from Leibniz-Institut Deutsche von Mikroorganismem und Zellkulturen GmbH (DSMZ). The BT549 cell line was obtained from Dr. Bo Li in University College Dublin, Belfield, Dublin 4. The 231-DasB was developed by Dr. Brendan Corkery in Dublin City University. The MDA-MB-468CR was obtained from Dr. Ashwag Albukhari in the University of Oxford. The most common mutations observed in the panel of TNBC cell lines are described in Table 2 – 1. The growth conditions for each cell line are described in Table 2 – 2. All cell lines were routinely tested for the presence of mycoplasma as follows. Cell culture supernatant was collected from each cell line a minimum of 3 passages post thawing and 24 hours post media change. The supernatant was added to normal rat kidney epithelial cells (NRKs) cultured on glass coverslips to 70% confluence in technical duplicate. The supernatent and NRKs were incubated for 4 days at 37ºC with 5% CO_2. Supernatent and NRK media was removed and NRKs were fixed in Carnoy's Fixative (1:3 glacial acetic acid:methanol) for 20 mins on ice and allowed to airdry. After fixation NRKs were stained with Hoechst 33258 (Sigma Cat. No. B2883) for 10mins. Each coverslip is washed twice with ultra high purity water (UHP) and read on a fluorescent microscope at an excitation wavelength of 400nm.

Drug compounds used in this study are described in Table 2 –3. Compound A (CpdA) and rilotumumab were obtained from Amgen Inc. Neratinib and saracatinib were purchased from Sequoia Research Products Ltd. PRS110 as well as a negative control for PRS110 (TLPC144-PEG40), were obtained from Pieris AG. BMS777607 was

purchased from Selleck Chemicals. HGF (294-HG-025) and epidermal growth factor (EGF) (236-EG-01M) were purchased from R&D systems Inc.

Table 2 - 1 Common genetic alterations in the TNBC cell line panel used in this study (WT- wild type, AMP – amplified and Mut – mutant) [243, 244].

	BT20	HCC1937	HCC1143	MDA-MB-468	MDA-MB-231	CAL-120	CAL-85-1	HDQ-P1	BT549
P53 mutation	Mut	WT	Mut	WT	Mut	Mut	Mut	WT	WT
EGFR	AMP		AMP	AMP			AMP		
RAS/RAF mutation	WT	WT	WT	WT	KRAS	WT	WT	WT	WT
PI3K mutation	WT	WT	WT	WT	WT	WT	WT	WT	WT
PTEN status	WT	Null	WT	Null	WT	WT	WT	WT	Null
BRCA status		Mut							

Table 2 - 2 Growth media, foetal calf serum (FCS) and supplements for each of the cell lines used in this study (TNBC-triple negative breast cancer, UC- unclassified, BL1- basal-like 1, BL2- basal-like 2, MSL- mesenchymal stem-like, M- mesenchymal [31]**) IU-international units, HER2- HER2 amplified.**

Cell line	**Cell line classification**	**Media**	**FCS**	**Supplements**
BT20	TNBC (UC)	DMEM:HAMS F12	10%	None
HCC1937	TNBC (BL1)	RPMI1640	10%	None
HCC1143	TNBC (BL1)	RPMI 1640	10%	None
MDA-MB-468	TNBC (BL1)	RPMI 1640	10%	None
MDA-MB-231	TNBC (MSL)	RPMI 1640	10%	None
CAL-120	TNBC (M)	DMEM	10%	None
CAL-85-1	TNBC (BL2)	DMEM	10%	1mM Sodium Pyruvate 2mM L- Glutamine
HDQ-P1	TNBC (BL2)	DMEM	10%	None
BT549	TNBC (M)	RRMI 1640	10%	0.023 IU Insulin
231-DasB	TNBC (M)	RPMI 1640	10%	None
MDA-MB-468CR	TNBC (BL1)	DMEM	10%	10 µg Cetuximab
T47D	Luminal	RPMI 1640	10%	None
MDA-MB-453	HER2	RPMI 1640	10%	None
HCC1419	HER2	RPMI 1640	10%	None
MCF-7	Luminal	RPMI 1640	10%	None
SKBR3	HER2	RPMI 1640	10%	None
CAMA-1	Luminal	RPMI 1640	10%	None
BT474	HER2	RPMI 1640	10%	None

Table 2 - 3 Details of targeted therapies used in this study.

Compound (source)	Class	Molecular target	Stock solution	Long-term storage	Short-term storage
Compound A (Amgen Inc.)	Tyrosine kinase inhibitor (TKI)	c-Met	10 mM in DMSO	-80 ˚C	Ambient temperature for ≤ 7 days
Rilotumumab (Amgen Inc.)	Monoclonal antibody (mAb)	HGF	30 mg/mL	-80 ˚C	4-8˚C for ≤ 7 days
PRS110 (Pieris Ag.)	Anticalin	c-Met	7160 mg/mL	-20 ˚C	4-8˚C for ≤ 14 days
Neratinib (Sequoia Research Products Ltd.)	TKI	erbB family	1 mM in DMSO	-20˚C	Ambient temperature for ≤ 7 days
Saracatinib (Sequoia Research Products Ltd.)	TKI	Src/Abl	10 mM in DMSO	-20 ˚C	Ambient temperature for ≤ 7 days
Dasatinib (Sequoia Research Products Ltd.)	TKI	Src, BCR/Abl, c-Kit, PDGFRα/β, EPH-A/B receptors	1 mM in DMSO	-20 ºC	Ambient temperature for ≤ 7 days
BMS 777607 (Selleck Chemicals)	TKI	Met/Axl/Ron	10 mM in DMSO	-80 ºC	Ambient temperature for ≤ 10 days

2.2 Protein extraction/preparation of cell lysates

Cells were grown in duplicate wells in 6-well plates or in 90 mm cell culture petri dishes and whole cell lysates were prepared as follows: cells were washed twice with cold phosphate buffered saline solution (PBS) and 150 µL/well or 350 µL/dish radioimmunoprecipitation assay buffer (RIPA) ((Sigma, R0278) 5 mM tris(hydroxymethyl)aminomethane-hydrochloric acid (Tris-HCl) pH 7.4, 1% NP-40, 0.1% SDS, 150 mM NaCl, 1% Triton x-100) containing 1x Protease Inhibitor cocktail (PI) (Calbiochem, 539131), 2 mM phenylmethanesulfonylfluoride (PMSF) (Sigma, P7626), and 1 mM sodium orthovanadate (NaOv) (Sigma, 6508), was added and cells were incubated on ice for 20 minutes. Cells were scraped into lysis buffer. The lysis buffer was collected and centrifuged at 16,200 x g for 10 minutes at 4 ^{o}C. The pellets were discarded and the supernatants collected and stored at -80^{o}C. Protein quantification was performed using the BCA (bicinchoninic acid) quantitation kit (Pierce, 23227).

2.3 Immunoblotting

Protein (30 or 50 µg) was electrophoretically resolved on 4-12% (Life Technologies NP0322BOX) or 7.5% (Lonza 59501) denaturing polyacrylamide gels. The resolved proteins were then transferred to nitrocellulose membranes (Invitrogen, IB3010-01) using the iBlot transfer system (Invitrogen, IB1001). Protein transfer was visually confirmed using Ponceau S staining (Sigma, P7170). Membranes were blocked with skimmed-milk powder (Bio-Rad, 170-6404) in PBS-tween (Sigma, P1379) (0.1%) or 1x NET buffer (0.5 M NaCl, 0.05 M EDTA, 0.1 M Tris pH 7.8), and incubated overnight at 4 ^{o}C with primary antibodies. The blotting conditions for each antibody used in this study are described in Table 2 - 4. Proteins were visualised using horse-radish peroxidise conjugated (HRP) anti-rabbit or anti-mouse as appropriate and ECL prime reagent (GE Healthcare, RPN2232) or Luminol (Fannin Ltd. SC-2048). Membranes were washed with 0.1 % PBS-tween or 1x NET buffer 3 times for 10 minutes each, both prior to and following incubation with secondary antibodies. Densitometry was performed using Epson Perfection Scanner (version 3.03A) on biological triplicate immunoblots with ImageJ software (available at http://imagej.nih.gov/ij/download.html). Results were normalised using α-tubulin.

Table 2 - 4 Details of antibodies and blotting conditions, for all antibodies used in the study; PBS-T = PBS-Tween, CST = Cell Signalling Technology.

Antibody	Phospho-site	Dilution	Blotting conditions	Secondary	+ ve control	company	Cat no.
anti-rabbit secondary		1:1000	2.5 % milk / 0.1 % PBS-T/1x NET			Sigma	A6154
anti-mouse secondary		1:1000	2.5 % milk / 0.1 % PBS-T/1x NET			Sigma	A6782
α-tubulin		1:1000	2.5 % milk / 0.1 % PBS-T/1x NET	Mouse		Sigma	T6199
anti-c-Met		1:1000	2.5 % milk / 0.1 % PBS-T/1x NET	Mouse	A549	CST	#25H2
anti-phospho-c-Met	Y1234/1235	1:1000	2.5 % milk / 0.1 % PBS-T/1x NET	Rabbit	A549 + 50 ng/mL HGF	CST	#3077s
anti-c-Src		1:1000	2.5 % milk / 0.1 % PBS-T/1x NET	Rabbit	MCF-7	CST	#2108s
Anti-phospho-Src	Y418	1:500	1x NET	Rabbit	MCF-7	Merck Millipore	05-677

2.4 Proliferation assays

2.4.1 Acid phosphatase

Cells were seeded into 96-well plates at a density of 3000-5000 cells/well (Table 2 - 5). After 24 hours, cells were treated with the appropriate media supplemented with 10 % FCS with or without serial dilutions of Compound A, AMG102, PRS110, neratinib, saracatinib, dasatinib or BMS777607. Proliferation was measured after five days using the acid phosphatase assay. For the acid phosphatase assay, media was removed and each well rinsed with PBS, 100 μL of acid phosphatase substrate (10 mM p-nitrophenol phosphate (PNP) (Sigma, 1040) in 0.1 M sodium acetate (Sigma, S2899), 0.1% triton X-100 (BDH, 9002-93-1), pH 5.5) was then added to each well followed by incubation at 37^{o}C for 60 minutes, at which time 50 μL of 1 M NaOH (Sigma, S5881) was added to each well and the absorbance was read at 405 nm with 620 nm as a reference, on Biotek plate reader using KC4 software. Proliferation was calculated relative to vehicle/untreated controls. Each assay was carried out in biological triplicate.

Table 2 - 5 The number of cells seeded per well in 96 well plate for proliferation assays for each TNBC cell line.

Cell Line	Cells seeded/well
BT20	3000
HCC1937	3000
HCC1143	3000
MDA-MB-468	3000
MDA-MB-231	3000
CAL-120	5000
CAL-85-1	3000
HDQ-P1	5000
BT549	3000

2.4.2 Combination assays

Cells were seeded into 96 well plates as described above in Table 2 - 5. Cells were then treated with or without appropriate concentrations of single agents or in combination described in Table 2 – 6. Proliferation was measured after five days as described in 2.4.1.

Table 2 - 6 Concentrations of drugs used in combination assays.

	HCC1937	BT20	HCC1143	MDA-MB-468	MDA-MB-231	CAL-120	CAL-85-1	HDQ-P1	BT549
Compound A	2 µM	2 µM	2 µM	2 µM	2 µM	2 µM	2 µM	2 µM	2 µM
AMG102	10 µg/mL	10 µg/mL	10 µg/mL	10 µg/mL	10 µg/mL	10 µg/mL	10 µg/mL	10 µg/mL	10 µg/mL
PRS110	1 µg/mL	1 µg/mL	1 µg/mL	1 µg/mL	1 µg/mL	1 µg/mL	1 µg/mL	1 µg/mL	1 µg/mL
Neratinib	0.15 µM	0.17 µM	1.18 µM	0.05 µM	0.4 µM	16 µM	4 nM	4 nM	1 µM
Saracatinib	0.7 µM	1.56 µM	1.21 µM	1.34 µM	0.4 µM	1µM	0.7 µM	0.3 µM	2 µM

2.4.3 HGF/EGF stimulation of proliferation

Cells were seeded at a density of 2.5 x 10^4 cells/well in 24-well plates. The cells were allowed to attach overnight and then washed 3 times with PBS. Cells were then grown for a further 24 hours in serum-free media after which they were treated with either 50 ng/mL HGF (294-HG-025), 10 nM EGF (236-EG-01M) or combined HGF and EGF treatment. Following either 48 or 72 hours of treatment, the media was removed from the cells and 100 µL of trypsin was added to each well. Once the cells had detached, 100 µL of media containing 10 % FCS was added to each well. In a round-bottom 96-well plate, 100 µL of cell suspension was added to 100 µL of Guava ViaCount reagent (Millipore, 4000-041). Cell counts were performed using the Guava EasyCyte ((version 5.3), (Millipore)) in triplicate and proliferation was calculated relative to serum starved controls.

2.5 Invasion assays

Invasion assays were performed using the method previously described [245]. 24-well invasion inserts (BD Biosciences 734-0036) were coated with 100 µL Matrigel™ (BD Biosciences 354234, diluted to 1 µg/µL in serum free DMEM) and left overnight at 4 °C. The following day, the plates were incubated at 37 °C for one hour. Excess Matrigel™ was removed. 5 x 10^4- 1 x 10^6 cells in 100 µL medium containing 5 % FCS were added to Matrigel™-coated inserts (Table 2 - 7). 500 µL of medium containing 10% FCS was added to each well beneath the insert. Cells were incubated for 6 hours at 37 °C before treatment, to allow cells to attach. Following treatment (100 µL 10 % foetal calf serum (FCS)-medium or drug containing (1 µM CpdA, 10 µg/mL PRS110, 1 µM neratinib or 1 µM saracatinib, 100 nM dasatinib), cells were further incubated for 18 hours. Cells were stained with 0.1 % crystal violet and the number of invading cells was estimated by counting 14 fields of view at 200 X magnification. The percentage invasion was calculated as follows; average number of cells counted/average number of cells in control well x 100. Each assay was performed in biological triplicate.

Table 2 - 7 Cells seeded per 100 µL in matrigel coated transwell inserts.

Cell Line	Cells per 100 µL
BT20	1×10^5
HCC1937	1×10^5
HCC1143	1×10^5
MDA-MB-468	1×10^5
MDA-MB-231	5×10^4
CAL-120	1×10^5
CAL-85-1	1×10^5
HDQ-P1	1×10^5
BT549	5×10^4

2.6 Migration assays

Migration assays were carried out as previously described [246]. Cells were seeded into 12 well plates and allowed to reach 100% confluence. At this point media was removed and cells were incubated with PBS for 15 mins. PBS was removed and plates were marked with a horizontal line through the well on the underside of the plate to create a reference point. A scratch was created using a P200 pipette tip perpendicular to the horizontal line on the plate. Cells were washed once with PBS. SFM was added with/without drug (1 µM CpdA, 10 µg/mL PRS110, 1 µM neratinib or 1 µM saracatinib) to cells and incubated for up to 48 hrs or until closure of wound occurred. Wound closure was examined photographically at 0, 24 and 48 hrs with duplicate photos of each well (above and below reference point). The images were analysed using Tscratch software (freely available at http://www.cselab.ethz.ch/index.php?&option=com_content&view=article&id=363). The percentage wound closure at 24/48 hrs was calculated relative to wound area at T0. Each assay was performed in biological triplicate.

2.7 Clonogenic assays

Cells were seeded at 1000-3000 cells/well in 6 well plate in duplicate and left to attach overnight. Media was removed and cells were treated with appropriate concentration of drug (Table 2 - 8). Cells were left to form colonies for 10-21 days. Media was replaced on all cells every 7 days following initial treatment. After treatment wells were washed

gently with PBS and fixed in cold Methacare (75% v/v methanol, 25% v/v acetic acid) for 30 minutes. Methacare fixative was removed and fixed colonies were washed once with PBS. The colonies were then stained using 1% Crystal Violet for 30 minutes and analysed for colony area and intensity using colony area plug-in in ImageJ software (available at http://imagej.nih.gov/ij/download.html). Each assay was performed in biological triplicate.

Table 2 - 8 Conditions of cell lines and drug concentrations used in clonogenic assays.

Cell line	Cells/well	Incubation period (days)	Cpd A (μM)	PRS110 (μg/mL)	neratinib (μM)	Saracatinib (μM)
HCC1937	3000	14	1	1	0.03	0.25
HCC1143	3000	14	1	1	0.2	0.03
MDA-MB-468	1000	14	1	1	0.02	0.75
MDA-MB-231	500	10	1	1	1.5	0.2
HDQ-P1	3000	21	1	1	0.001	0.2

2.8 3D growth assays

96 well plates were coated with 50 μL polyhema (Sigma Aldrich S3932 5 mg/mL in 96% ethanol) and baked at 50ºC for two days. Plates are stored at room temperature (RT) until required, for up to 6 months. Cells were seeded at a density of 1500-3000 cells/well in 10% FCS with 2-4% Matrigel™ (Table 2 - 9), and incubated overnight at 37ºC. 30 μL of 10% FCS with/without serial dilutions of CpdA and PRS110 starting at 10 μM and 10 μg/mL respectively, were added to the wells and incubated at 37 ºC for a further 5-7 days. 12 μL of PrestoBlue® Cell Viability reagent (10% of final volume) was added to the wells and incubated at 37 ºC for 4-8hrs and fluorescently measured at 535/590 excitation/emission wavelength on Biotek plate reader using KC4 software. A blank consisting of media and 2-4% Matrigel™ as appropriate was used to eliminate

background. Percentage viability was calculated relative to untreated control. Each assay was performed in biological triplicate.

Table 2 - 9 Cell line specific conditions used for 3D growth assays

Cell line	Cells/well	Matrigel concentration	Days incubated	Presto Blue (hrs)
BT20	1500	2%	7	4
HCC1937	3000	4%`	5	4
HCC1143	3000	4%	5	4
MDA-MB-468	3000	2%	5	4
MDA-MB-231	3000	4%	5	2
HDQ-P1	3000	4%	5	8
BT549	1500	2%	5	6

2.9 Conditioned media

2.9.1 Collection of conditioned media

Cell lines were cultured to 70-80% confluence in 90 mm tissue culture petri dishes. Cells were washed with PBS three times. Serum free (SFM) media was then added to the dishes and cells were cultured for a further 24 or 48 hours. Media was centrifuged at 900rpm for 5mins to remove debri, collected and stored at -80˚C.

2.9.2 HGF enzyme linked immunosorbent assay (ELISA)

Conditioned media was analysed for the presence of HGF using the Human HGF Quantikine ELISA kit (DHG00, R&D systems Inc.) as per manufacturer's instructions. The procedure is described briefly below in Figure 2- 1.

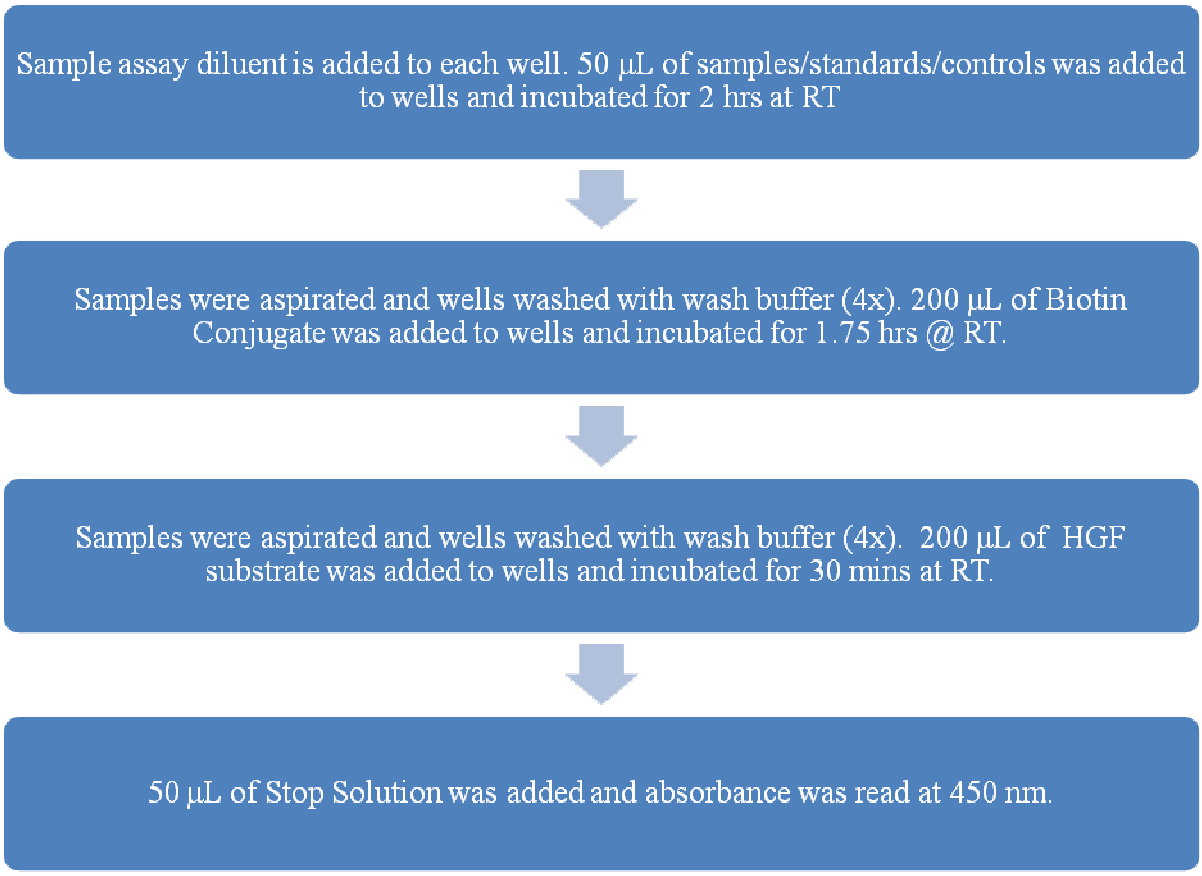

Figure 2- 1 Schematic diagram of the human HGF Quantikine ELISA procedure.

2.9.3 Soluble Met (sMet) ELISA

Conditioned media was analysed for the presence of sMet using the c-Met (soluble) Human Elisa Kit (Invitrogen KHO2031) as per manufacturer's instructions described in Figure 2- 2.

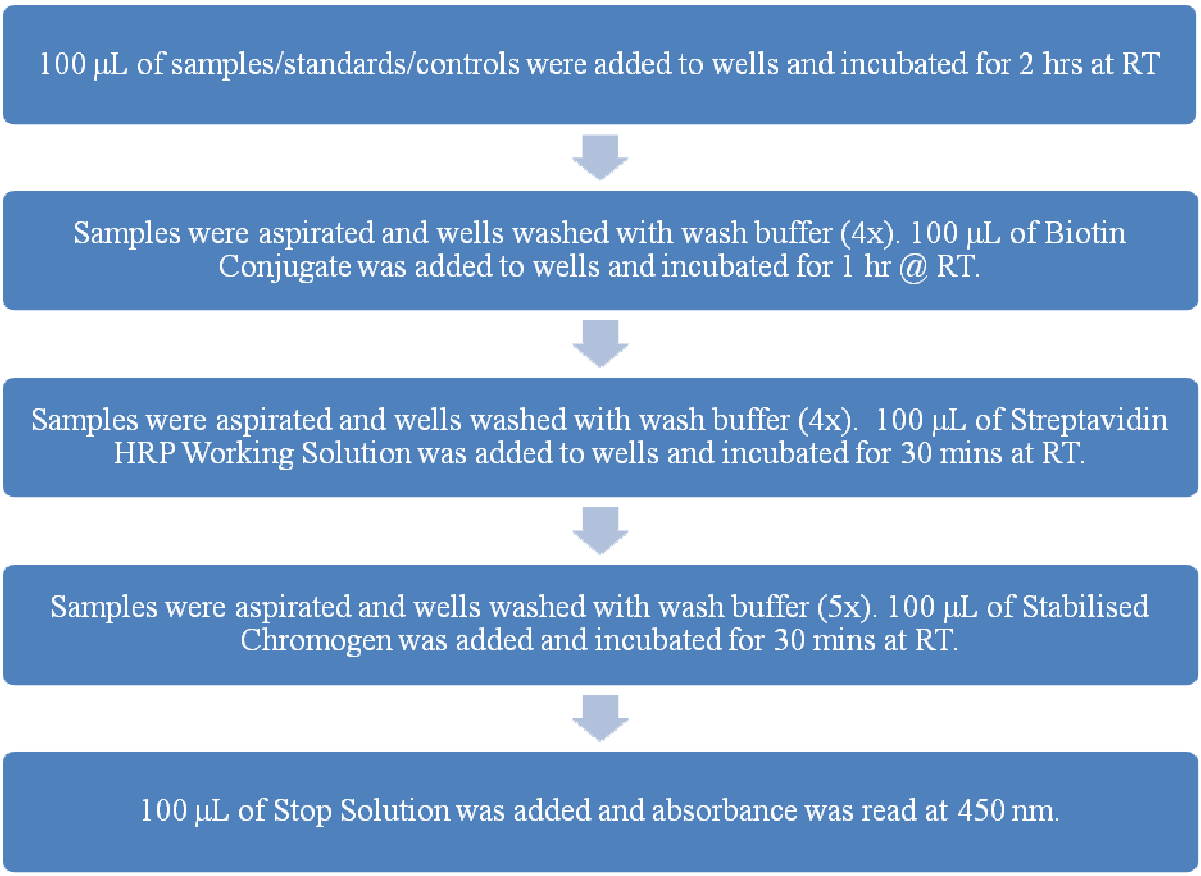

Figure 2- 2 Schematic diagram of the c-Met (soluble) human ELISA procedure.

2.10 Magpix® Magnetic Bead assays

Magnetic bead assays were performed on the Luminex® MagPix ® System (Merck Millipore (80-073) using Milliplex Map Phospho Mitogenesis RTK Magnetic Bead 7-Plex Kit (Merck Millipore 48-672 Mag) and Milliplex Map phospho Human Src Family Kinase Magnetic Bead 8-Plex kit (Merck Millipore 48-650Mag). Samples were prepared as in 2.2 . Protein (1- 10 µg) was diluted in appropriate volume of assay buffer (final volume 25 µL/well) and the assay was performed as per manufacturer's instructions as described below in Figure 2- 3.

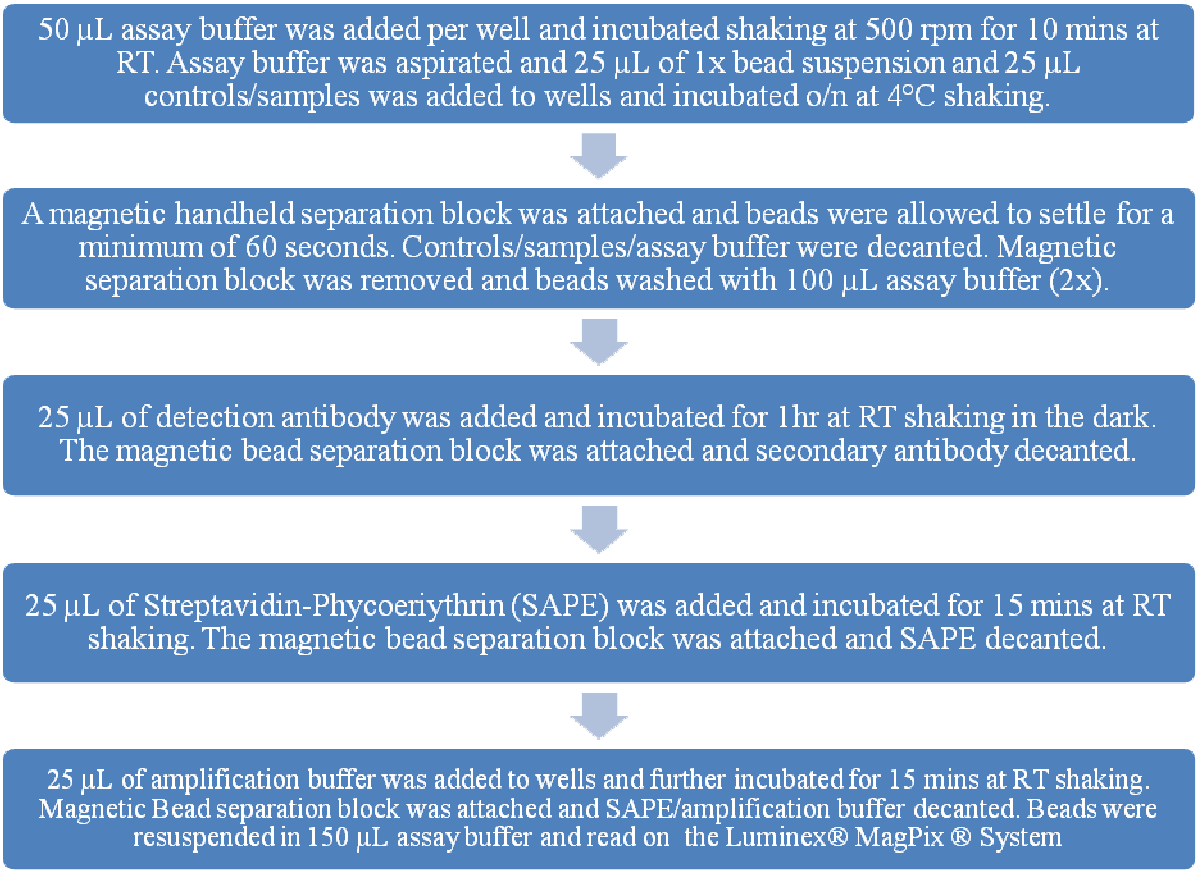

Figure 2- 3 Schematic diagram of the magnetic bead assays.

2.11 Immunohistochemistry (IHC)

Automated immunohistochemistry was performed using the DAKO Autostainer system. Antibodies against c-Met, EPHA5 and FGFR3 were used (Santa Cruz SC-161, SC-927, SC-123). The c-Met antibody was optimised using renal papillary carcinoma and triple negative breast carcinoma slides. EPHA5 and FGFR3 antibodies were optimised using triple negative breast carcinoma slides. The breast carcinoma slides are used as positive controls for IHC experiments. These slides were also used as negative controls as follows; a blocking peptide was added to antibody in a 10:1 (c-Met antibody) or 4:1 (FGFR3, EPHA5 antibodies) blocking peptide: antibody ratio a minimum of 30 minutes prior to staining.

Antigen retrieval and dewaxing was performed using automated Dako PT Link in Target Retrieval Solution pH6 (Dako S1699) for c-Met and pH9 for EPHA5 and FGFR3. Slides was placed in Dako PT link at 65 ˚C and heated to 97 ˚C and maintained at 97 ˚C for 20 minutes. The slides were cooled to 65 ˚C and removed. After de-paraffinisation, the slides were placed in the DAKO Autostainer, which performed the programmed application of reagents in order as listed in Table 2 - 10 Antibody concentrations are described in (Table 2 - 11). Washes were performed, with DAKO wash buffer, before and after the application of the each reagent, except in the case of the Real HP Block, where a blow step was performed. Slides were subsequently dehydrated in grading alcohols 70 %, 90 %, and 100 %, cleared in xylenes (2 x 3 minutes each) and mounted in Di(nbutyl) Phthalate in Xylene (DPX) (Sigma).

Tissue microarray (TMA) obtained from St. Vincent's University Hospital (SVUH) slides consisting of four cores from each case with a total of 89 TNBC cases were scored by two independent observers and was evaluated as follows [193]. Intensity was graded 0 (no staining), 1+ (weak staining) 2+ (moderate staining), 3+ (strong staining), % cells staining were graded as 0 (no staining) 1 (0-25% staining), 2 (26-50% staining), 3 (51-75%) and 4 (> 75%), and cores were marked positive/negative for membrane or nuclear staining.

Table 2 - 10 Programmed steps for immunostaining procedure for IHC staining using DAKO Autostainer system.

Reagent	Time (mins)
Real HP Block (DAKO)	10
Antibody	30
Real EnVision (DAKO)	30
Real DAB (DAKO)	5
Haematoxylin	5

Table 2 - 11 Antibody concentrations used in IHC of TMAs.

Antibody	Concentration
c-Met	1/200
EPHA5	1/100
FGFR3	1/100

2.12 Quantitative real time-polymerase chain reaction (qRT-PCR)

2.12.1 RNA extraction

RNA was extracted using the mirVana™ miRNA Isolation Kit (Ambion, AM1560) and carried out according to manufacturer's instructions. Briefly, cells were grown to 70-80% confluency, trypsinised and centrifuged at 160 x g (900 rpm) for 3 minutes. Cell pellets were then washed with PBS centrifuged as before, and placed on ice. Cells were lysed in 300 µL of lysis buffer, vortexed and 30 µL of RNA homogenate was added to the lysate and incubated on ice for 10 mins. A volume of acid:phenol chloroform equal to the volume of lysis buffer was then added, vortexed for 30-60 secs and centrifuged for 5 mins at room temperature. The top aqueous layer was then removed (volume noted) and 1.25 volumes of room temperature ethanol (100%) was added, the mix was added to a filter cartridge, centrifuged for 15 sec at 12400 x g and the flow through was discarded. Wash solution 1 was added (700 µL) and centrifuged as before followed by two additions of wash solution 2/3 (500 µL) and centrifuged as before with flow through discarded each time. The filter cartridge was centrifuged for 1 min to remove residual ethanol and placed in a fresh collection tube. Pre-heated (95°C) nuclease free water (100 µL) was applied to the filter cartridge and incubated for 1 min at room temperature. The filter cartridge was centrifuged at 12400 x g for 20-30 sec to elute RNA. RNA extracts were stored at -80°C. The concentration of total RNA in extracted samples was determined using the Nano-Drop Spectrophotometer (Thermo Scientific).

2.12.2 Reverse transcription (RT)

Stock solutions of 2 µg in 10 µL were made by diluting RNA-extracts with RNase free water (Ambion, 9932). Using a high capacity cDNA Reverse Transcription Kit (Applied Biosystems, 4368814), a 2X master mix solution was prepared as per Table 2 - 12. For each reaction 10 µL of RNA sample and 10 µL of master mix were combined in PCR tubes, briefly centrifuged to spin down contents and loaded into the thermo-cycler (G-STORM) and the reverse transcription run as per Table 2 - 13. The samples were then stored at 4 °C until required. A non-target control (NTC) which was prepared without the RNA template, and a minus reverse transcriptase control (-RTC) which was prepared without the reverse transcriptase enzyme.

Table 2 - 12 Components of master mix for RT reaction.

Component	Volume / Reaction (µL)
10X RT buffer	2.0
25X dNTP Mix (100 mM)	0.8
MultiScribe ^{TM} Reverse transcriptase	1.0
RNase-free water	4.2
10X RT random primers	2.0
Total per reaction	**10.0**

Table 2 - 13 Thermo-cycler steps, indicating the temperature and duration, for RT-PCR experiment.

Step	Temperature (°C)	Time (minutes)
1	25	10
2	37	120
3	85	5
4	4	Hold

2.12.3 Quantitative real-time polymerase chain reaction (qRT-PCR)

Using cDNA obtained from the RT step, qRT-PCR for the following assays was performed; HGF (Applied Biosystems Hs00300159-m1), EPHA5 (Applied Biosystems Hs00300724m1), FGFR3 (Applied Biosystems Hs00179829-m1) and ROS1 (Applied Biosystems Hs001772288-m1) with GADPH (Applied Biosystems, HS02758991_g1) as an endogenous control. Briefly, the cDNA samples were diluted in 30 µL of RNase-free water (Ambion, 9932) and 1 µL of this stock was added to a 96-well PCR reaction plate (Applied Biosystems, 4346906), and combined with 19 µL of assay master mix. The assay master mix consisted of 10 µL of Taqman Universal PCR Master Mix (Applied Biosystems, 4364340), 8 µL of RNase-free water (Ambion, 9932) and 1 µL of the specific assay (primer set), per reaction. The PCR plate was then sealed using Optical Adhesive film strips (Applied Biosystems, 4360954). The qrt-PCR reaction was performed on the ABI7900HT fast system using Sequence Detection System (SDS) automated controller software (version 2.2) (Applied Biosystems). The procedure for qRT-PCR was 10 minutes at 95 °C followed by 40 cycles of 15 seconds at 95 °C, and then 1 minute at 60 °C. Once complete the cycle threshold (Ct) values were exported to

Excel and relative RNA expression levels calculated using the DeltaCt method (ΔCt) where ΔCt was the Ct value of the sample minus the Ct value of the endogenous control. The ΔΔCt values were calculated as the ΔCt of the test sample minus the ΔCt of the calibration sample. The relative quantity ratios (RQ) of each sample were calculated using the equation:

$RQ = 2^{(-\Delta\Delta Ct)} = 2^{\Delta Ct}test\text{-}^{\Delta Ct}control = 2^{(Ct,X-Ct,R)}control^{-(Ct,X-Ct,R)}test$[247]

Where, Ct,X is the cycle threshold of the gene of interest and Ct,R is the cycle threshold of the endogenous reference gene.

2.13 RTK survival analysis

BreastMark is web based searchable database (available at http://glados.ucd.ie/BreastMark/) to allow determination of the association between individual genes and disease progression and survival for breast cancer. The underlying algorithm combines gene expression data from multiple microarray experiments and detailed clinical data to correlate outcome with gene expression levels. This algorithm integrates gene expression and survival data from 21 datasets on 10 different microarray platforms corresponding to 20,017 gene sequences across 3,519 samples [239]. BreastMark was designed by Dr. Stephen Madden (DCU) who carried out the survival analysis detailed in this thesis.

Kaplan Meier curves were generated for each receptor tyrosine kinase (RTK) and manually examined. RTKs were selected based on a statistically significant ($p < 0.05$) association between disease free or overall survival and gene expression. Groups were stratified using the median and 25^{th} and 75^{th}. Each level of stratification was examined. For RTKs to be considered for further evaluation we applied a cut off of reaching statistical significance in 2/3 breast cancer classifiers used, (PAM50, ssp 2003, ssp 2006).

2.14 Ephrin-A4 and FGF9 treatments

MDA-MB-231, T47D and BT20 cell lines were seeded at a density of 2.5 $x10^4$ cells/well in a 6 well plate and left to attach overnight. After 24 hours media was removed and cells washed 3 times with serum free medium. After the final wash, 2 mL of SFM was added to each well and incubated overnight. The following day SFM media was removed and 10% FCS media or 2% FCS media with/without Ephrin-A4 (1 μg/mL) or FGF9 (20 ng/mL) with heparan sulphate (2 μg/mL) was added. The cell

lines were allowed proliferate for a further 72 hours and proliferation was measured using the acid phosphatase assay described in section 2.4.1.

2.15 Statistical analysis

P values were calculated (unless otherwise stated) using the student's t-test (two tailed with unequal variance). Analysis was performed on biological triplicates. $P<0.05$ was considered significant.

2.15.1 IC_{50} determination

IC_{50} were calculated using dose effect analyser Calcusyn (Version 1.1) and are representative of three independent biological experiments.

2.15.2 Calculation of combination index (CI) values

For fixed-ratio assays, combination indices (CI) at the ED50 (effective dose of combination that inhibits 50% of growth) were determined using the Chou and Talalay equation, on CalcuSyn software (Biosoft). The combination index equation is based on the multiple drug-effect equation of Chou-Talalay derived from enzyme kinetic models. The equation determines only the additive effect rather than synergism or antagonism. Synergism is defined as a more than expected additive effect, and antagonism as a less than expected additive effect. Determination of synergy/antagonism used in our work was based on the recommended descriptions as shown in Table 2 - 14. As recommended by Chou et al., the prerequisites for CI calculations included a dose-effect curve, at least three data points for each single drug, but any number of points for a combination, and a constant combination ratio design [248].

Table 2 - 14 Range of combinations index values which determine synergism or antagonism in drug combination studies analysed with the Combination Index Method

Range of CI	Symbol	Description
<0.10	+++++	Very strong synergism
0.10-0.30	++++	Strong synergism
0.31-0.70	+++	Synergism
0.71- 0.85	++	Moderate synergism
0.86-0.9	+	Slight synergism
0.91- 1.10	±	Nearly additive
1.11-1.20	_	Slight antagonism
1.21-1.45	_ _	Moderate antagonism
1.45-3.30	_ _ _	Antagonism
3.30- 10.00	_ _ _ _	Strong antagonism
>10.00	_ _ _ _ _	Very strong antagonism

2.15.3 Statistical calculations for immunohistochemistry

Fisher's exact test was used to calculate p values for 2x2 table contingency. Chi-square test was used to calculate p values for non-parametric data greater than 2x2. The Bonferroni test was used to adjust p values for multiple testing. The Bonferroni test was determined as the product of the p value and the number of tests performed on the data set.

2.15.4 Correlation co-efficient calculation

Correlation co-efficients were calculated using Spearman Rank test with two-tailed P value.

Chapter 3

c-Met/HGF expression in TNBC

3.1 Introduction

c-Met and phosphorylated c-Met have been found at higher levels in basal compared to luminal cell cancer cell lines [173]. Furthermore, in both breast cancer cell lines and breast cancer specimens, overexpression of c-Met was associated with the basal subtype [170, 171, 249].

Expression of c-Met corresponds significantly with the development of basal mammary tumours in mice and high levels of c-Met and p-Met are expressed across all breast cancer subtypes [82, 148, 152]. Two studies have shown that expression of c-Met in mice induced basal-like breast carcinomas [148, 159]. c-Met overexpression has been associated decreased survival and poor outcomes [250].

HGF is the only known ligand for c-Met and is present mainly in stromal cells such as adipocytes, endothelial cells and fibroblasts [185]. The most likely mechanism of c-Met activation in breast cancer is via HGF acting in a paracrine manner to activate c-Met. Increased levels of HGF in primary breast tumours have been shown to be a strong predictor of a shortened recurrence-free interval and decreased survival [103, 140, 169].

While specific molecular targets are available for HER2 and ER positive subtypes, no target has as yet been proven for the TNBC/basal-like subtype. We investigated the potential role of the c-Met/HGF axis as a target by examining expression in both TNBC cell lines and in tumour samples.

3.2 c-Met expression in TNBC

3.2.1 c-Met, phosphorylated Met and soluble Met in TNBC cell lines

We assessed a panel of triple negative breast cancer cell lines for the expression and phosphorylation of c-Met by western blotting (Figure 3 - 1). Total c-Met was detected in all nine of the cell lines tested. CAL-85-1 and MDA-MB-231 showed the highest levels of total c-Met and c-Met expression was significantly associated with TNBC cell lines. p-Met (Y1234/Y1235) was detectable in 4/9 cell lines (BT20, HCC1937, HCC1143 and CAL-85-1). Three of the cell lines positive for p-Met are the Basal A subtype (BT20, HCC1937, HCC1143), however the CAL-85-1 cell line basal subtype is unknown. This suggests an association between Basal A subtype and activation of c-Met however this does not achieve statistical significance ($p=0.4$). According to the Lehman subtypes [31], of the four showing activation of p-Met, 2 are BL-1 subtype

(HCC1937, HCC1143), the CAL-85-1 are BL-2 subtype and the BT20 are unclassified. This again suggests an association with the BL subtype. The CAL-85-1 cell line has the highest level of p-Met however, when related to total Met levels the HCC1937 have the highest level of phosphorylation of c-Met. In a panel of non-TNBC cell lines consisting of both ER positive and HER2 positive cell lines, we see low levels of expression of c-Met in only 3/7 cell lines with no detectable levels of p-Met (Figure 3 - 1). Using a magnetic bead assay for seven phosphorylated RTKs we examined the levels of phosphorylation in the panel of TNBC cell lines. The phosphorylated RTKs included are p-Met (pan-Tyr), p-EGFR (pan-Tyr), p-HER2 (pan-Tyr), p-IGF1R (pan-Tyr), p-IR (pan-Tyr), p-HER3 (pan-Tyr) and p-HER4 (pan Tyr). The levels of p-Met are similar across the panel of cell lines, in contrast to the western blot of Y1234/Y1235 (Figure 3 - 2). Levels of p-EGFR varied significantly across the panel of cell with MDA-MB-468 and HDQ-P1 showing the highest levels of p-EGFR (Figure 3 - 2). This assay was also used to assess phosphorylation in powdered tumour samples discussed in *Section 3.2.2*.

Soluble Met (sMet) is a soluble cleaved form of the extracellular domain of mature c-Met. It is easily measurable in serum and plasma and cell culture supernatant. We measured sMet in conditioned media from the panel of TNBC cell lines. The CAL-85-1 cell line showed the highest level of sMet (77.1 ± 3.5 ng/mL). The BT549 showed the lowest level of sMet with 6.9 ± 2.9 ng/mL sMet. No significant correlation between c-Met levels, phosphorylation of c-Met and sMet levels was observed (p= 0.6 and 0.5 respectively) Figure 3 - 3.

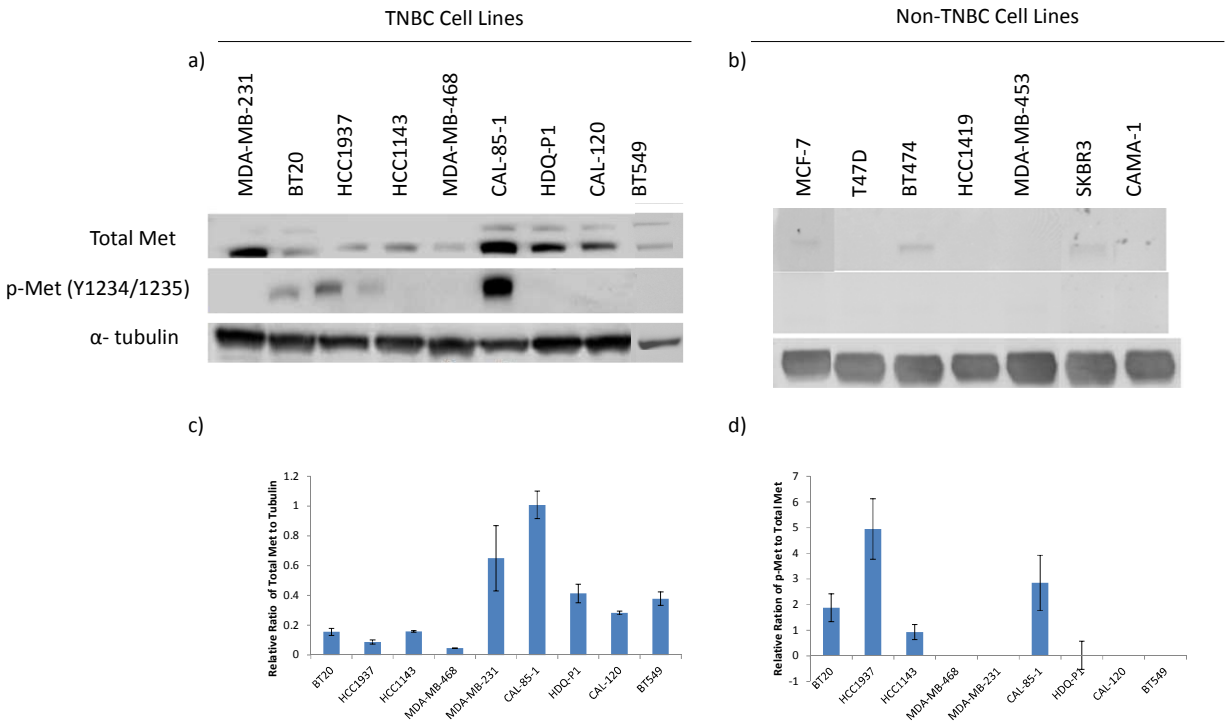

Figure 3 - 1 Western Blot analysis of c-Met and p-Met (Y1234/Y1235) in a panel of a) TNBC cell lines and b) TNBC cell lines. α-tubulin was used as a loading control c) Densitometric analysis of western blots of total c-Met normalised to α-tubulin. d) p-Met levels initially normalised to α-tubulin and then normalised to values described in c). Error bars represent the standard deviation of triplicate independent experiments.

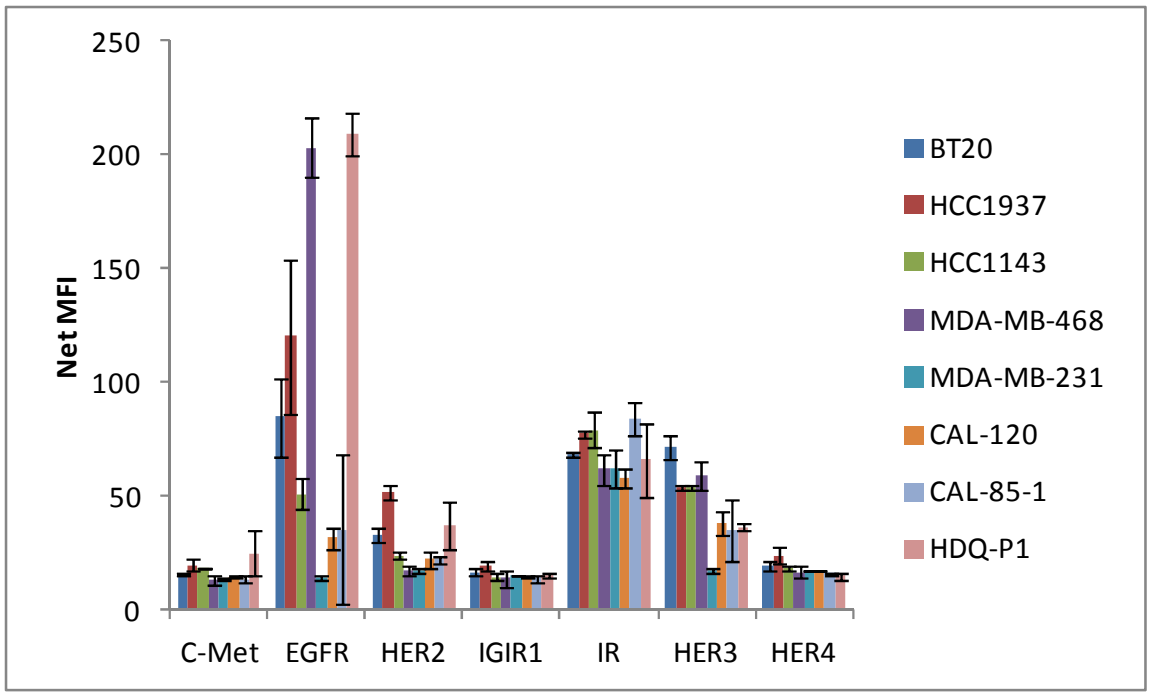

Figure 3 - 2 Levels of phosphorylated RTKs in 10 µg protein as determined by Magpix® magnetic bead assays. Error bars are standard error of biological duplicates.

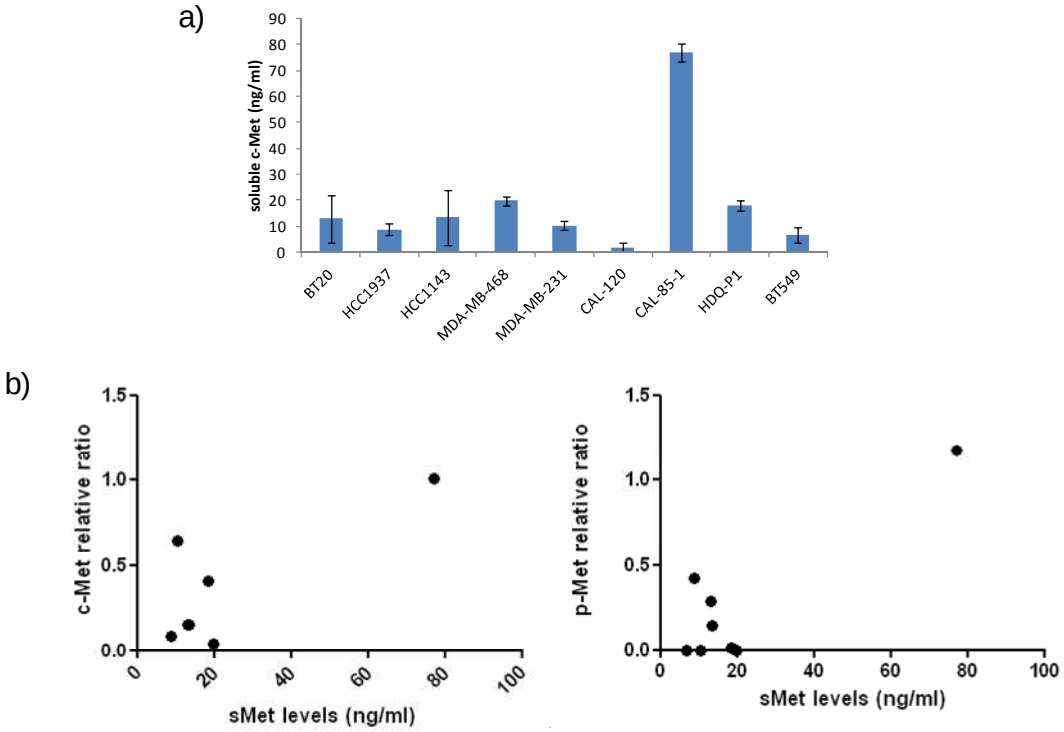

Figure 3 - 3 a) Levels of sMet measured by ELISA in panel of TNBC cell lines. b) XY scatter plot of sMet levels vs. c-Met (LHS) and p-Met (RHS) as calculated in Figure 3 - 1. Error bars are indicative of independent biological triplicates.

3.2.2 c-Met and phosphorylated Met expression in TNBC tumour samples

We examined 89 cases of TNBC and 100 non-TNBC for expression of c-Met. 83 and 93 cases respectively were suitable for evaluation. However 20 and 26 cases of those were missing at least one core per case due to lack of tumour tissue/lifting of cores. Staining for c-Met was graded according to % positivity (0-10%, 11-25%, 26%-50%, 51-75% and >75%) and intensity (neg, 1+ weak, 2+ moderate and 3+ strong). Representative images are shown in Figure 3 - 1. The patient characteristics are described in Table 3 - 1. The patients were predominantly older (>50) with ductal histology. The TNBC were mainly advanced grade (grade 3 (85% TNBC vs 25% non-TNBC) as expected. Size, lymph node and LVI status showed no significant differences between the TNBC and non-TNBC (Table 3 - 1) [193]. Median follow up for the patients in this study was 39 months.

The staining observed for c-Met was granular cytoplasmic staining. Weak nuclear staining in <10% of cells was observed in a single case in both the TNBC and non-TNBC TMAs. No specific membrane staining was present. 44/83 (53.0%) and 25/93

(26.8%) showed positive staining for c-Met in TNBC and non-TNBC cases respectively. There was a significant association between c-Met expression and TNBC subtype (p=0.004) (Table 3 - 2). No significant association was seen between any patient prognostic indicators (age, grade, histological subtype, size, lymph node status (LN), lymphovascular invasion (LVI)) and c-Met expression in this cohort of patients in the TNBC or non TNBC tumours when stained for c-Met (Table 3 – 3, Table 3 – 4, Table 3 -5, Table 3 - 6). For survival studies c-Met was dichotomised into high/low groups using 50% (median) positive staining as a cut-off point. No significant association with recurrence or survival was noted between the two groups (p= 0.95 and p= 0.52, HR = 1.03, 1.43 respectively) (Figure 3 - 2).

EGFR, c-Met and c-Src crosstalk are well documented in the literature [181, 185, 195, 251, 252]. Previous work by Dr. Siun Walsh (UCD) involved the staining of the TNBC tumours for EGFR, total c-Src and phospho-Src (p-Src, Y418). Using these results we examined whether co-positivity of c-Met and these proteins is significantly associated with patient prognostic indicators and recurrence/survival in this cohort of patients.

Only six of the TNBC tumours showed EGFR positivity, 3 of these tumours showed dual positive staining for EGFR and c-Met. All three tumours were in patients over 50 years of age with ductal carcinomas and negative for LVI invasion. Two of the patients had tumours >2cm with lymph node invasion (Table 3 - 7).

Using a cut-off of 50%, 15/18 (83.3%) of c-Met positive TNBC cases showed specific staining for both c-Met and total Src. No significant association was seen with any of the patient prognostic indicators (Table 3 - 8). No significant differences in recurrence or survival were observed for c-Met positivity combined with c-Src (p= 0.84, 0.25 HR = 0.89 and 0.55 respectively) (Figure 3 - 3).

Of the 18 tumours positive for c-Src and c-Met, 7 (38.8 %) showed positive staining for phospho Src (Y418) using a cut-off of > 50%. One other patient showed positive staining for p-Src without positive total Src staining. No significant association between co-positivity and prognostic indicators was seen (Table 3 - 9). Kaplan Meier curves of tumours with high p-Src and high c-Met expression showed no significant differences between the groups in either recurrence or survival (p= 0.74, 0.59 HR = 0.79 and 0.64 respectively) (Figure 3 - 4).

Finally we compared the percentage of KI-67 positively stained cells with the percentage positivity of c-Met in the TNBC cohort of patients. Scores were grouped into five groups (1-10%,11-25%, 26-50%, 50-75% and > 75%) and given an arbitrary

value of 1-5 (where 1= 1-10% and 5= >75%) based on the % positive cells for c-Met or KI-67. Scores were given a 0 value for no specific staining. Using the Chi Square test c-Met and KI-67 showed a weak association trending toward statistical significance with $p = 0.051$ indicating that higher c-Met percentage positivity is associated with a higher KI-67 percentage positivity.

We assessed the phosphorylation of 9 tumours using powdered tumour lysates which included three paired adjacent normal tissues. In 8/9 tumours we detected phosphorylation of c-Met and in 2/3 paired samples, p-Met was higher in the normal tissue than the tumour tissue. c-Met seems to have the lowest levels of phosphorylation of all the RTKs with the insulin receptor demonstrating higher levels than the others (Figure 3 - 5).

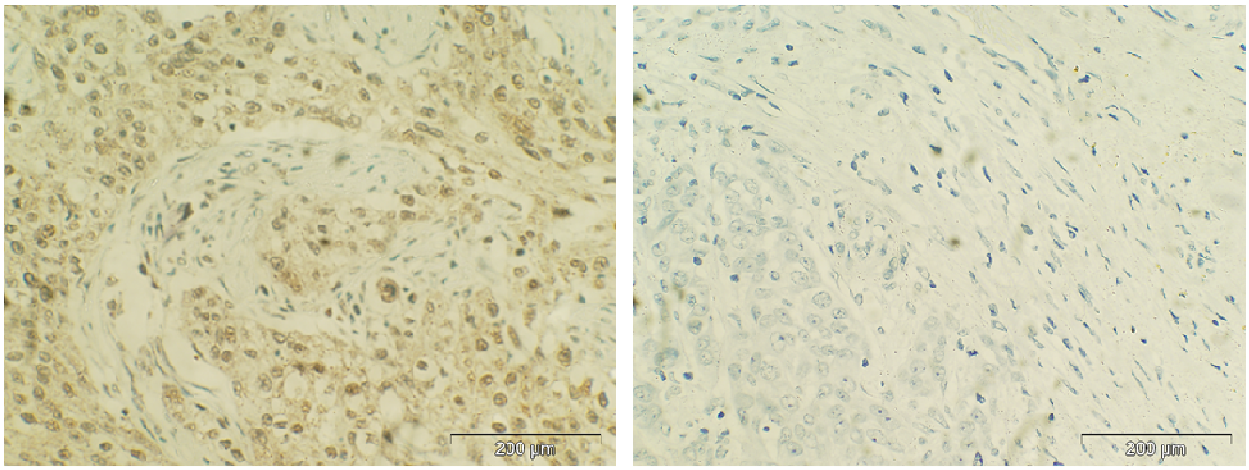

Figure 3 - 1 Representative Images of c-Met IHC staining. c-Met positive control (TNBC) (LHS) , c-Met negative control (Ab + blocking peptide) (RHS)

Table 3 - 1 Patient and tumour characteristics in TNBC and non-TNBC TMAs.

	Triple negative		Non-triple negative	
	n	**%**	**N**	**%**
Patient age at diagnosis				
< 50	35	39.3	23	23
> 50	54	60.7	77	77
Grade				
Grade 1/2	12	13.5	61	61
Grade 3	76	85.4	25	25
Unknown	0	0.0	14	14
Histological subtype				
Ductal	83	93.3	70	69
Lobular	5	5.6	26	24
Other	0	0.0	1	1
Unknown	1	1.1	3	3
Size				
<2cm	48	53.9	51	51
>2cm	39	43.8	49	49
Unknown	2	2.2	0	0
LN Status				
Negative	50	56.2	56	56
Positive	37	41.6	40	40
Unknown	2	2.2	3	3
LVI				
Negative	44	49.4	37	37
Positive	44	49.4	60	60
Unknown	1	1.1	3	3

Table 3 - 2 c-Met positivity in TNBC and non-TNBC tumour samples. P value was calculated using Fishers Exact Test and adjusted using Bonferroni Correction.

	Pos	**Neg**	**P value**	**P adj**
TNBC	44	39		
Non-TNBC	25	68	**0.0006**	**0.0042**

Table 3 - 3 Cytoplasmic c-Met positivity in TNBC TMA and patient prognostic indicators. P values were calculated using Chi square test.

	Neg	0-10%	10-25%	26-50%	51-75%	>75%	P
Patient age at diagnosis							
< 50	15	2	4	2	6	1	
> 50	24	2	6	8	11	2	0.8973
Grade							
Grade1/2	3	1	1	0	1	1	
Grade 3	37	3	11	9	14	2	0.4452
Unknown	0	0	0	1	0	0	
Histological subtype							
Ductal	38	4	11	10	12	3	
Lobular	1	0	0	0	3	0	0.0985
Other	0	0	1	0	0	0	
Size							
<2cm	20	1	6	3	9	2	
>2cm	19	3	5	7	6	1	0.6008
Unknown	0	0	0	1	0	0	
LN Status							
Negative	16	1	7	4	9	2	
Positive	23	3	4	6	6	1	0.5178
Unknown	0	0	0	1	0	0	
LVI							
Negative	17	1	6	6	11	3	
Positive	22	3	5	4	4	0	0.2011
Unknown	0	0	0	1	0	0	

Table 3 - 4 Cytoplasmic c-Met intensity in TNBC TMA and patient prognostic indicators. P values were calculated using Chi square test.

	Neg	1+	2+	3+	P value
Patient age at diagnosis					
< 50	15	12	4	0	
> 50	24	14	13	1	0.4767
Grade					
Grade ½	3	3	1	0	0.875
Grade 3	36	22	16	1	
Unknown	0	1	0	0	
Histological subtype					
Ductal	38	24	15	1	0.5163
Lobular	1	1	2	0	
Other	0	1	0	0	
Size					
<2cm	20	13	6	0	0.5036
>2cm	19	12	11	1	
Unknown	0	1	0	0	
LN Status					
Negative	16	14	7	0	0.4959
Positive	23	11	10	1	
Unknown	0	1	0	0	
LVI					
Negative	17	17	10	0	0.2352
Positive	22	8	7	1	
Unknown	0	1	0	0	

Table 3 - 5 Cytoplasmic c-Met positivity in non-TNBC TMA and patient prognostic indicators. P values were calculated using Chi square test.

	Neg	0-10%	10-25%	>50%	P value
Patient age at diagnosis					
< 50	19	2	0	0	
> 50	49	12	9	2	0.181
Grade					
Grade 1/2	40	8	7	2	
Grade 3	17	3	2	0	0.8415
Unknown	11	3	0	0	
Histological subtype					
Ductal	48	10	7	1	
Lobular	17	3	2	0	0.9314
Other	1	0	0	1	
Unknown	2	1	0	0	
Size					
<2cm	31	6	5	2	
>2cm	37	8	4		0.4462
LN Status					
Negative	37	7	5	2	
Positive	29	6	4	0	0.6626
Unknown	2	1	0	0	
LVI					
Negative	25	2	4	2	
Positive	41	11	5	0	0.0994
Unknown	2	1	0	0	

Table 3 - 6 Cytoplasmic c-Met intensity in non-TNBC TMA and patient prognostic indicators. P values were calculated using Chi square test.

	0	1+	2+	P value
Patient age at diagnosis				
< 50	19	2	1	
> 50	49	16	6	0.2725
Grade				
Grade 1/2	40	11	6	
Grade 3	17	4	1	0.6739
Unknown	11	3	0	
Histological subtype				
Ductal	48	13	5	
Lobular	17	4	1	0.8659
Other	1	0	1	
Unknown	2	1	0	
Size				
<2cm	31	7	5	
>2cm	37	11	2	0.3346
LN Status				
Negative	37	10	3	
Positive	29	8	3	0.9599
Unknown	2	1	0	
LVI				
Negative	25	5	3	
Positive	41	11	5	0.8841
Unknown	2	1		

a)

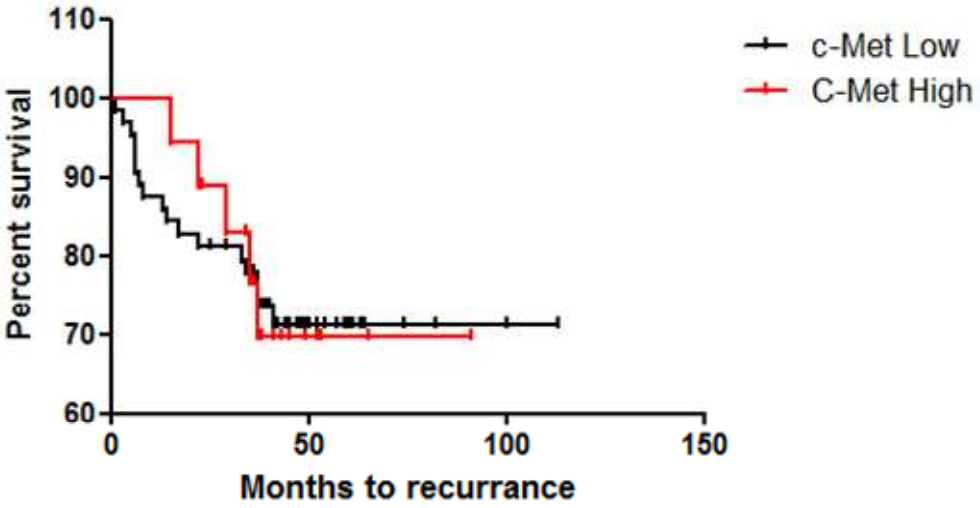

b)

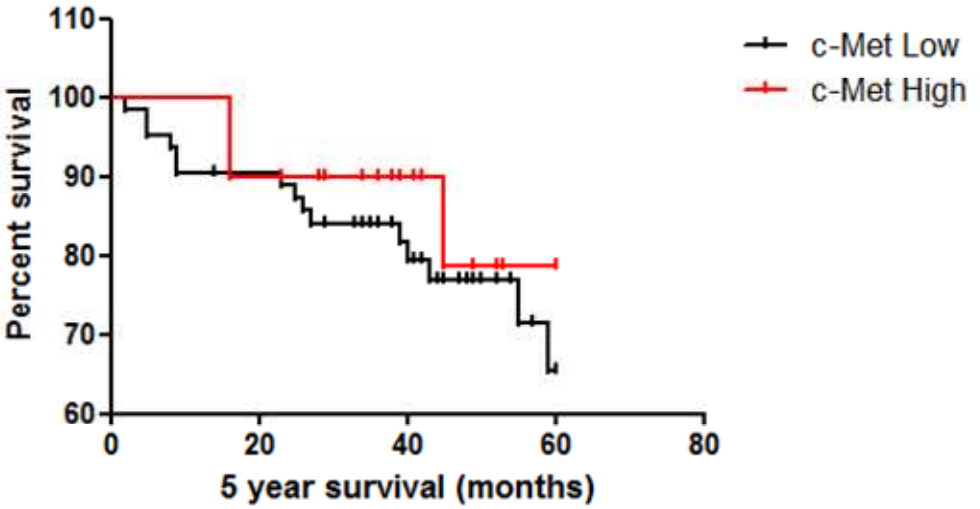

Figure 3 - 2 Kaplan Meier curve based on a) 5 year recurrence of TNBC patients divided into c-Met high (red) and c-Met low (black) groups b) 5 year survival of TNBC patients divided into c-Met high (red) and c-Met low (black) groups, where high/low = >50/<50 % of positively stained cells in tumour (n=83).

Table 3 - 7 TNBC tumours positive for both EGFR and c-Met as determined by immunohistochemistry.

Age	Grade	Subtype	Size	LN Status	LVI	5 year recurrence	5 year survival
>50	2	Ductal	<2cm	-	-	No	Yes
>50	3	Ductal	>2cm	+	-	Yes	Yes
>50	3	Ductal	>2cm	+	-	No	Yes

Table 3 - 8 Tumours samples positive for c-Met and Total c-Src in TNBC tumours. P values were calculated using Chi Square test and adjusted using Bonferroni Correction.

	Positive	P value
Patient Age at Diagnosis		
< 50	6/24	
> 50	9/42	0.7764
Grade		
Grade 1/2	3/8	
Grade 3	12/58	0.4184
Histological Subtype		
Ductal	14/63	
Lobular	1/2	0.4684
Unknown	0/1	
Size		
<2cm	9/31	
>2cm	6/33	0.5679
Unknown	0/2	
LN Status		
Negative	10/35	
Positive	5/29	0.5639
Unknown	0/2	
LVI Status		
Negative	10/31	
Positive	5/31	0.2543
Unknown	0/1	

Table 3 - 9 Tumours samples positive for c-Met and phospho-Src (Y418) in TNBC tumours. P values were calculated using Fishers Exact Test.

	Positive/negative	P value
Patient age at diagnosis		
< 50	3/27	
> 50	5/46	1.0
Grade		
Grade 1/2	3/8	
Grade 3	6/65	0.0725
Histological subtype		
Ductal	7/70	
Lobular	1/2	0.2741
Other	0/1	
Size		
<2cm	6/34	
>2cm	2/37	0.2633
Unknown	0/2	
LN Status		
Negative	5/40	
Positive	3/31	1.0
Unknown	0/2	
LVI		
Negative	4/37	
Positive	4/35	1.0

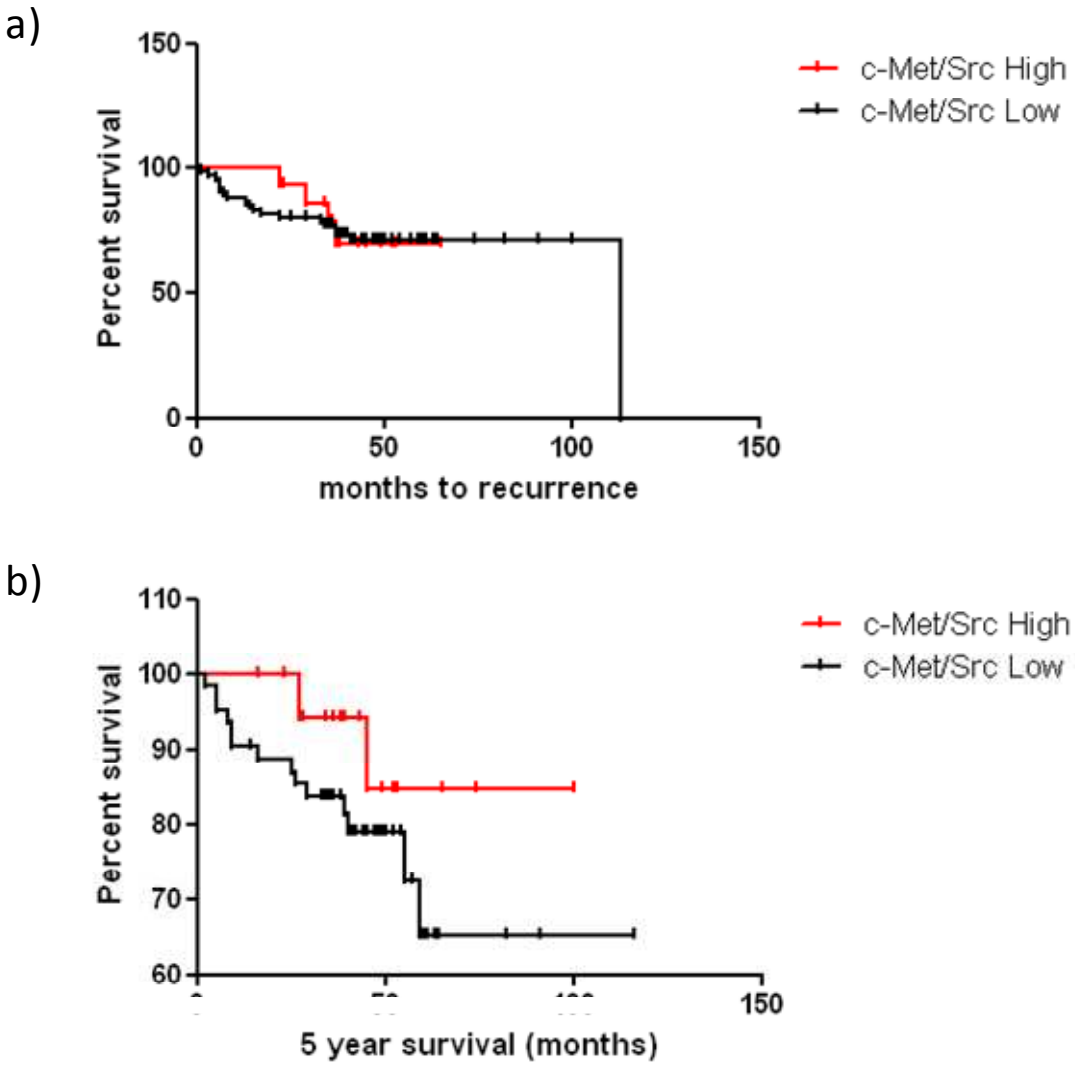

Figure 3 - 3 Kaplan Meier curve based on a) 5 year recurrence and b) 5 year survival of TNBC patients divided into c-Met high/low and c-Src high low, where c-Met high/low = >50/<50 % of positively stained cells in tumour and c-Src high/low = >50%/<50% of positively stained cells in tumour (n=81).

a)

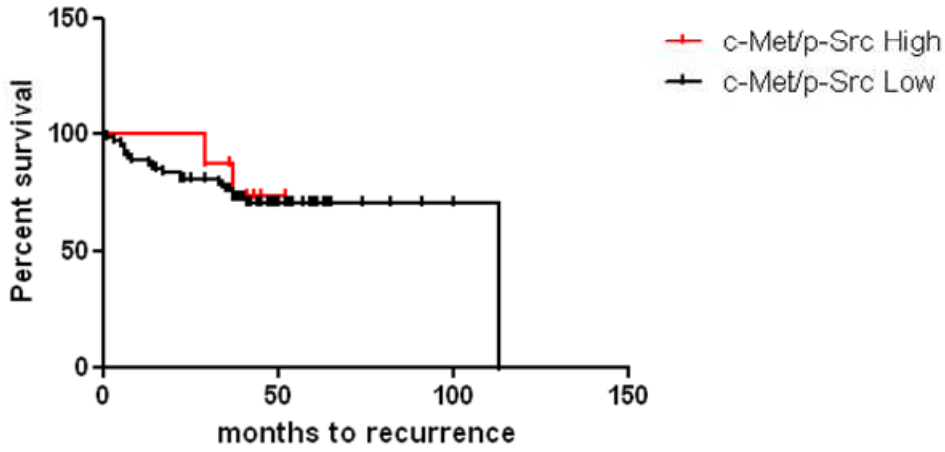

b)

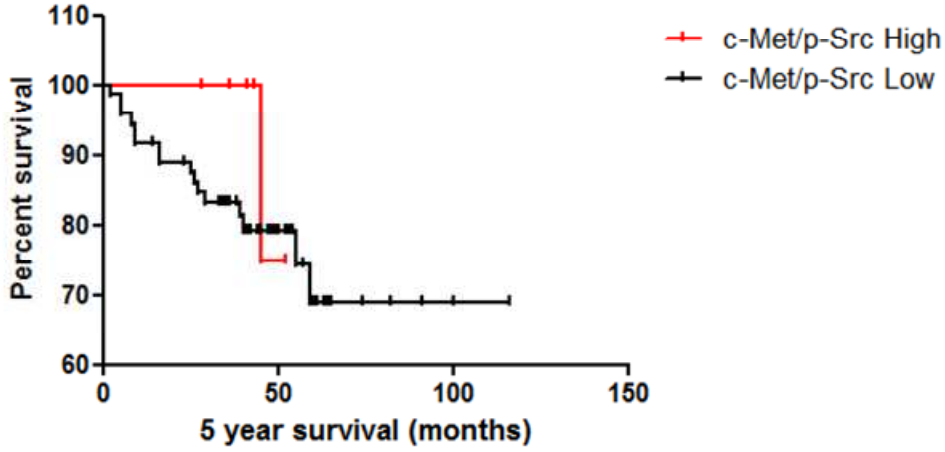

Figure 3 - 4 Kaplan Meier curve based on a) 5 year recurrence and b) 5 year survival of TNBC patients divided into c-Met high/low and p-Src high low, where c-Met high/low = >50/<50 % of positively stained cells in tumour and p-Src high/low = >50%/<50% of positively stained cells in tumour (n=81).

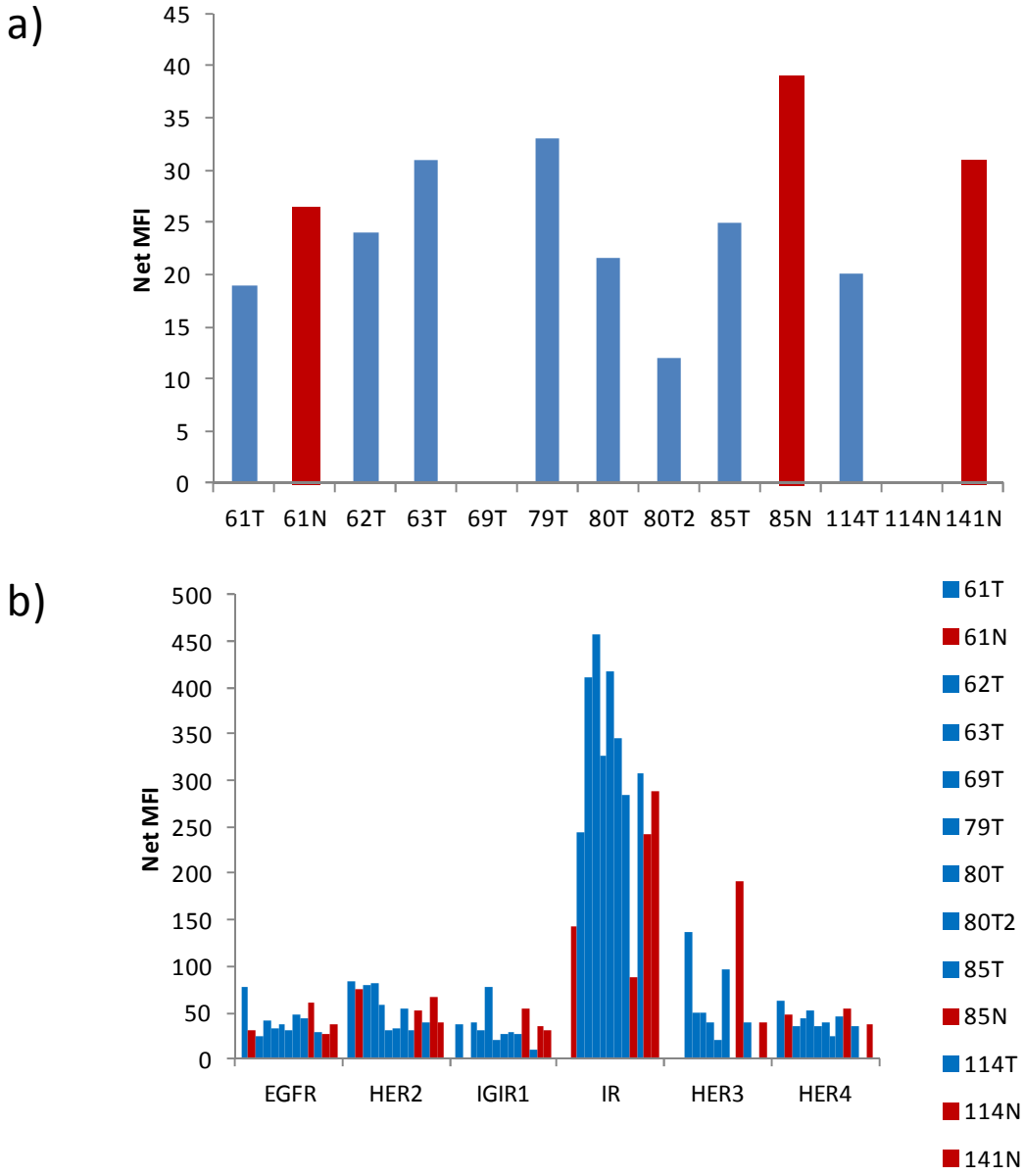

Figure 3 - 5 Levels of phosphorylated a) c-Met and b) phosphorylated RTKs in 10 µg protein from powdered tumour (blue) and normal (red) samples as determined by Magpix® magnetic bead assays. Samples were tested in single replicates.

3.3 Role of HGF in TNBC

3.3.1 HGF expression in TNBC cell lines

We examined TNBC cell lines for HGF expression using two methods, a HGF ELISA to detect the mature molecule in conditioned media, and qRT-PCR to detect HGF mRNA. U87-MG-luc2 glioma cell line was used as a positive control for both experiments. Two cell lines (p-Met positive HCC1937 and p-Met negative MDA-MB-

231) were assayed for secretion of HGF into 6 mL conditioned medium. No HGF was detectable in either cell line (Table 3 – 10). A calibration curve was generated using the log absorbance of a set of standards provided with the ELISA ranging from 0.125 to 8 ng/mL (Figure 3 - 6). Using qRT-PCR we determined mRNA expression levels of HGF in 13 TNBC cell lines. No HGF mRNA was detected in any of the TNBC cell lines, whereas HGF mRNA was detected at high levels in U87-MG-luc2 cells, with a Ct value of 18.58 compared to >40 for the TNBC cell lines (Figure 3 – 10).

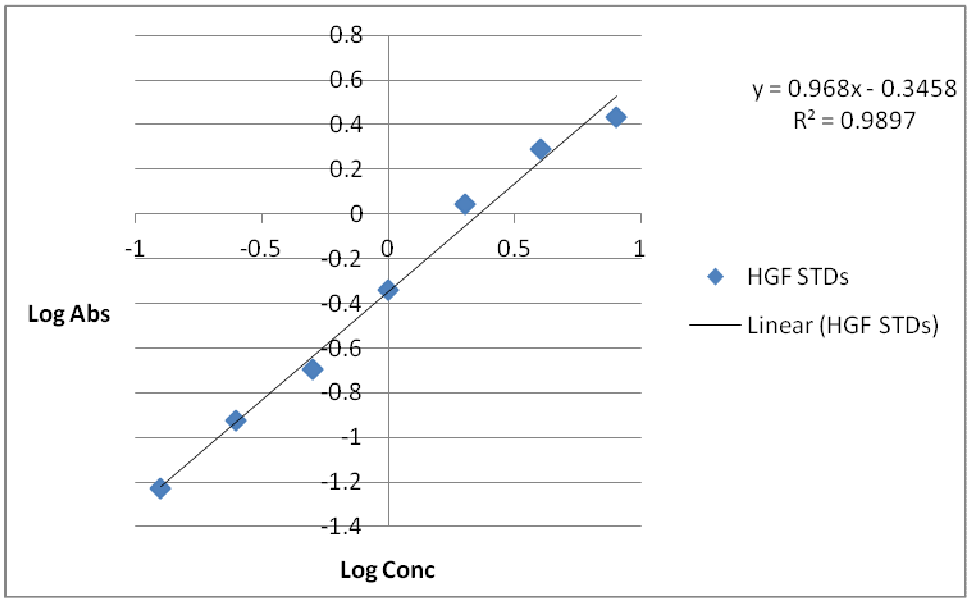

Figure 3 - 6 Calibration curve of ELISA plotting log absorbance vs. log HGF concentration.

Table 3 - 10 Concentrations of positive controls and samples tested for HGF by ELISA. *ND - Not detected

Sample	Absorbance	Concentration (ng/mL)
U87-MG-Luc2	0.261	0.91
HCC 1937	0.089	ND*
MDA-MB-231	0.071	ND*

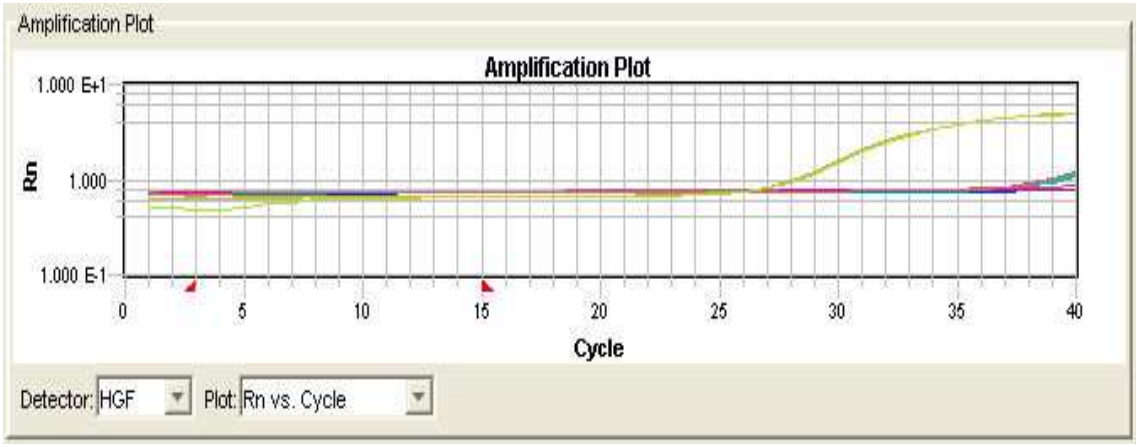

Figure 3 - 7 Amplification plot for HGF mRNA in TNBC cell lines and U-87-MG-luc2 glioma cell line (shown in green) showing reaction vs cycle number.

3.3.2 HGF stimulation of proliferation

Expression and phosphorylation of c-Met has been shown in both TNBC cell lines and TNBC tumours however no HGF was detected. We treated five cell lines (2 positive for phosphorylation and 3 negative) with saturating concentrations of HGF (50 ng/mL) and EGF (10 nM) to stimulate growth. HGF treatment caused a significant increase in proliferation in 2/5 cell lines, HCC1937 and BT20 ($p= 0.026$ and 0.049 respectively). EGF treatment caused a significant increase in proliferation in HCC1937 ($p = 0.007$). No significant increase was seen in response to combination treatment with both HGF and EGF (Figure 3 - 8).

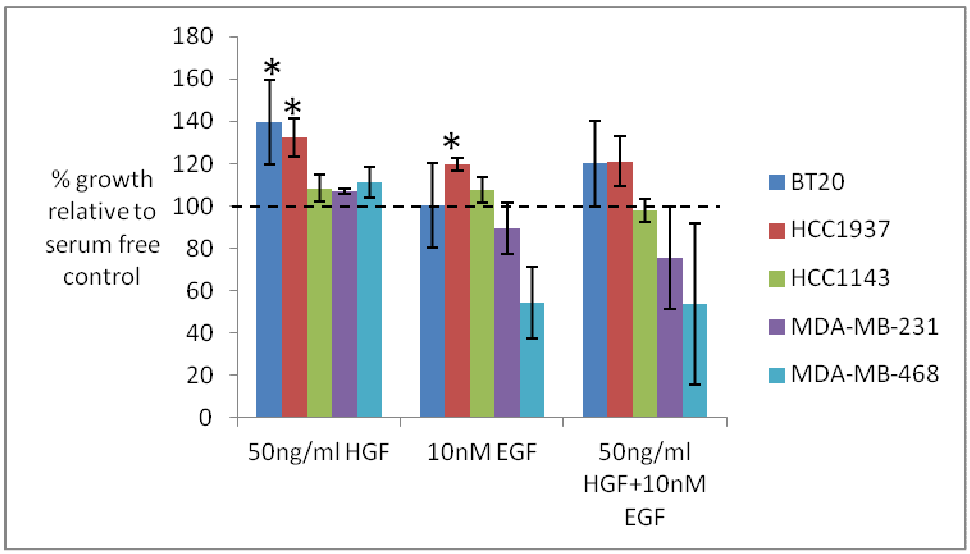

Figure 3 - 8 Proliferation assay showing % growth relative to serum free control 48 hrs post treatment with HGF (50 ng/mL), EGF (10 nM) alone or in combination.

3.4 Summary

c-Met expression was detected in all nine TNBC cell lines tested and phosphorylation (Y1234/Y1235) was detectable in 4/9 cell lines in contrast to non-TNBC cell lines where total c-Met was detectable in 3/7 cell lines with no detectable levels of phosphorylation. Examination of pan-Tyr phosphorylation of six RTKs in the panel of TNBC did not reveal significant differences between the cell lines. Soluble Met was detectable in all TNBC cell lines with CAL-85-1 cells showing the highest levels. There was no significant correlation between the expression of c-Met or p-Met and levels of sMet. c-Met was detected more frequently in TNBC than non-TNBC tumours with 44/83 (53.0%) of TNBC tumours positive for c-Met. However no significant association was seen between expression and patient prognostic indicators. No significant association between c-Met expression and recurrence or survival was seen. Expression of c-Met was examined in conjunction EGFR, c-Src and activated c-Src. Levels of EGFR positive tumours were too low for statistical analysis but 3/6 tumours positive for EGFR also show c-Met expression. 83.3% of c-Met expressers also show expression of total Src with 38.8% of these patients showing phosphorylation of c-Src at Y418. No significant association between co-expression of c-Met, Src and phospho-Src and the prognostic indicators was determined.

In nine TN tumours assessed for phosphorylation, 8/9 tumours show phosphorylation of c-Met however, phosphorylation of c-Met was detected at higher levels in 2/3 normal

tissues with paired samples. Interestingly, the insulin receptor showed notably higher levels of phosphorylation than other receptors in all of the tumours tested.

HGF is undetectable in the TNBC cells however the presence of HGF stimulates the growth of 2/5 cell lines tested from the TNBC cell line panel.

Chapter 4

Preclinical evaluation of CpdA and rilotumumab in TNBC cell lines

4.1 Introduction

TNBC currently lacks a validated molecular target for treatment and is managed via cytotoxic chemotherapies (anthracycline and taxane based). c-Met has been implicated in the development of basal-like/TNBC breast cancer and is frequently over expressed in these tumours, however c-Met signalling has not been extensively evaluated as a target for treating TNBC [152, 161, 162, 167-169, 185]. We evaluated a c-Met selective inhibitor (CpdA) and a HGF monoclonal antibody (rilotumumab) in TNBC cell lines. Kim *et al.* have recently reported that PHA-665752 (selective c-Met inhibitor) inhibits growth in 6 of nine TNBC cell lines, additionally c-Met has been implicated in resistance to EGFR TKIs in NSCLC mediated by interaction and activation of Src [180]. An enhancement of response to EGFR inhibitors via c-Src inhibition has been observed previously in two breast cancer cell lines (HER2 positive and TNBC) [213]. We evaluated the combination of c-Met and HGF inhibition, and c-Met and EGFR/Src inhibition using the pan-erbB inhibitor neratinib and Src inhibitor saracatinib. Neratinib is currently in phase II clinical trials in combination with temsirolomous in metastatic HER2 positive or TNBC. Saracatinib is currently in phase II trials for recurrent osteosarcoma [220]. A trial of saracatinib in metastatic hormone receptor negative breast cancer was discontinued due to lack of efficacy as a single agent [253].

4.2 Sensitivity of TNBC cell lines in 2D growth assays

4.2.1 Proliferation assays

CpdA inhibited 2D growth in all of the TNBC cell lines tested. In only six of nine cell lines an IC_{50} value was achieved when tested with CpdA at concentrations up to 10 µM. MDA-MB-231 was the most sensitive cell line with an IC_{50} of 2.5 ± 0.3 µM (Figure 4 - 1). Rilotumumab did not significantly inhibit the growth of any of the TNBC cell lines. Maximum growth inhibition achieved at 10µg/mL was approximately 8.2 ± 1.9% in the HCC1143 cell line (Figure 4 - 2). The TNBC cell lines all showed sensitivity to neratinib. CAL-85-1 and HDQ-P1 were the most sensitive cell lines with IC_{50} < 100 nM. The BT549 cell line were the least sensitive with an IC_{50} of 6.6 ± 0.5 µM (Figure 4 - 3). An IC_{50} was achieved in seven of nine TNBC cell lines when treated with saracatinib at concentrations up to 10 µM. The HDQ-P1 cell line displayed the most

sensitivity with an IC50 of 0.3 ± 0.1 µM. The least sensitive cell line was BT20 which had an IC_{50} of 1.7 ± 0.3 µM (Figure 4 – 4). The IC_{50} for each cell line is described in Table 4 - 1.

The combination of CpdA and rilotumumab at fixed concentrations of 2 µM and 10 µg/mL respectively, resulted in significantly decreased growth in 3/8 cell lines; HCC1937, MDA-MB-231 and MDA-MB-468 (p= 0.02, p= 0.03, p= 0.009 relative to CpdA as single agent respectively as shown in Figure 4 - 5. Combinations of CpdA (2 µM) and neratinib (IC_{50} concentrations-Table 4 - 1) resulted in significantly decreased growth in the MDA-MB-468 cell line only (p = 0.003 relative to neratinib effect) compared to Cpd A and neratinib as single agents respectively) (Figure 4 - 6). Combinations of Cpd A (2 µM) and saracatinib (IC50 concentrations-Table 4 - 1) resulted in significantly decreased growth in four of nine cell lines, HCC1937, MDA-MB-468, MDA-MB-231 and HDQ-P1 (p=0.023 p= 0.003, p= 0.00033, p= 0.0003 relative to saracatinib effect (Figure 4 - 7).

Table 4 - 1 Sensitivity of TNBC cell lines to CpdA, neratinib and saracatinib in 2D proliferation assays. IC_{50} is the concentration required to inhibit growth by 50%. % growth at 10 µg/mL is relative to untreated vehicle control ± standard deviation of independent biological triplicates. UC-unclassified, BL1/2- basal-like 1/2, M-mesenchymal, MSL-mesenchymal stem-like.

Cell Line	TNBC subtype	IC_{50} (µM) CpdA	%Growth at 10 µM CpdA	IC_{50} (µM) neratinib	IC_{50} (µM) saracatinib
BT20	UC	>10	73.7 ± 4.9	0.4 ± 0.04	1.7 ± 0.2
HCC1937	BL1	4.1 ± 0.5	11.4 ± 1.8	0.2 ± 0.02	0.8 ± 0.1
HCC1143	BL1	>10	89.9 ± 8.5	0.6 ± 0.09	1.1 ± 0.2
MDA-MB-468	BL1	3.1 ± 0.4	11.6 ± 1.8	0.05 ± 0.01	1.3 ± 0.3
MDA-MB-231	MSL	2.5 ± 0.3	9.0 ± 2.2	2.8 ± 0.2	0.5 ± 0.1
CAL-120	M	3.8 ± 0.3	37.4 ± 9.5	1.6 ± 0.2	>10
CAL-85-1	BL2	>10	86.2 ± 3.8	<0.03	0.7 ± 0.1
HDQ-P1	BL2	5.1 ± 0.4	36.7 ± 3.6	<0.03	0.3 ± 0.05
BT549	M	>10	41. 3 ± 4.3	6.6 ± 0.5	>10

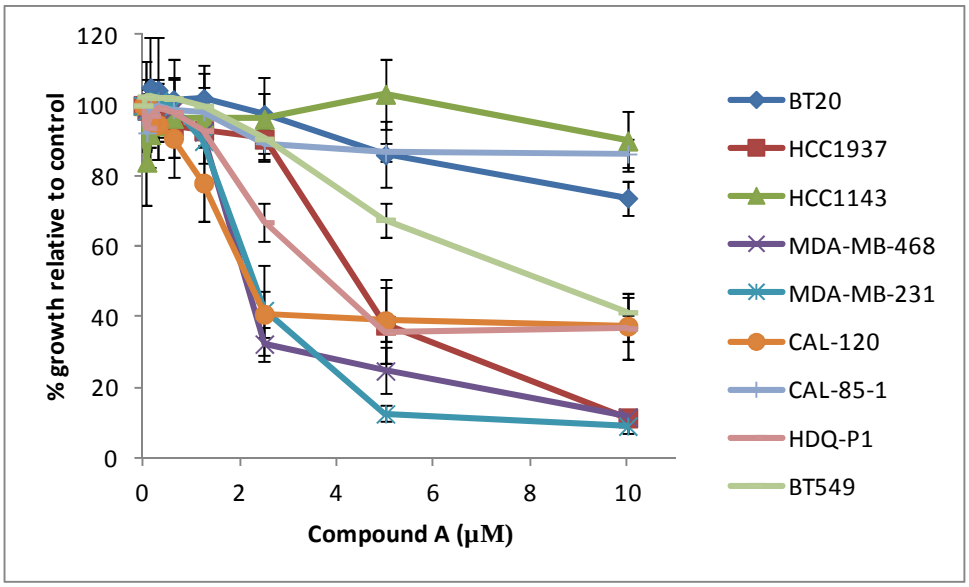

Figure 4 - 1 Proliferation assays of TNBC cell lines treated with CpdA at serially decreasing concentrations from 10 µM relative to vehicle control in 2D proliferation. Error bars represent the standard deviation of three independent biological triplicates.

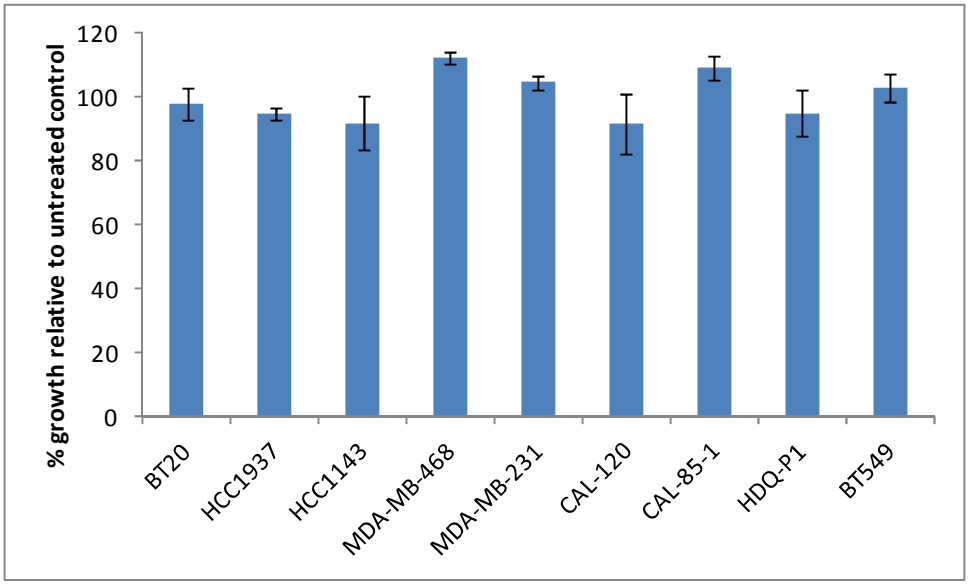

Figure 4 - 2 Proliferation assays in TNBC cell lines treated with 10 µg/mL rilotumumab. % growth is relative to untreated control. Error bars represent the standard deviation of triplicate independent experiments.

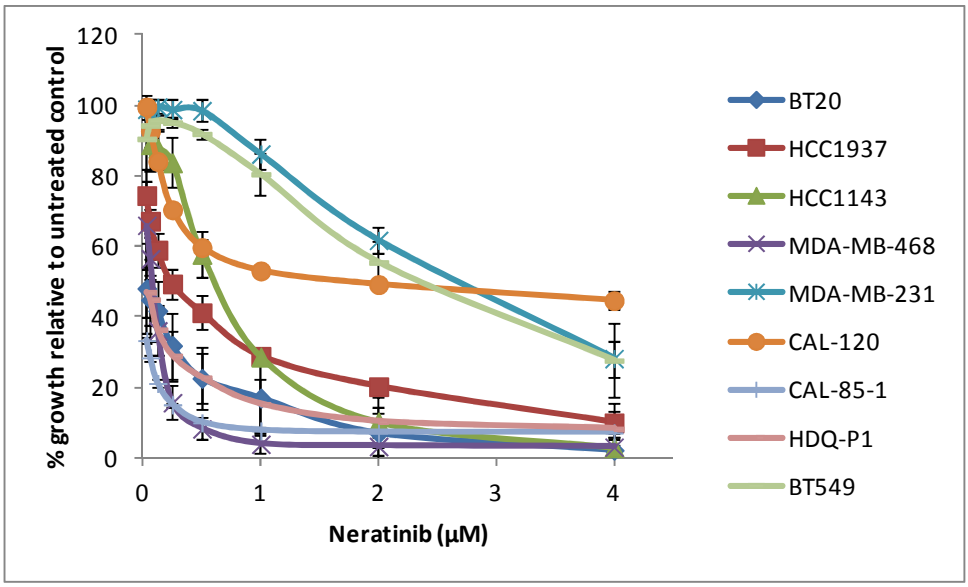

Figure 4 - 3 Proliferation assays in TNBC cells treated with neratinib at serially decreasing concentrations from 10 µM. Error bars represent standard deviations of triplicate independent experiments.

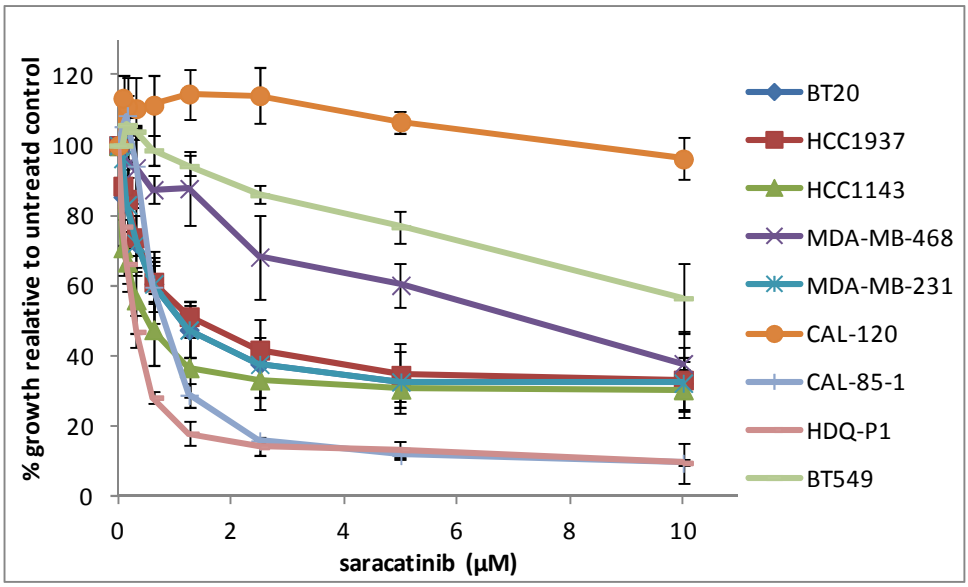

Figure 4 - 4 Proliferation assays in TNBC cells treated with saracatinib at serially decreasing concentrations from 10 µM. Error bars represent standard deviations of triplicate independent experiments.

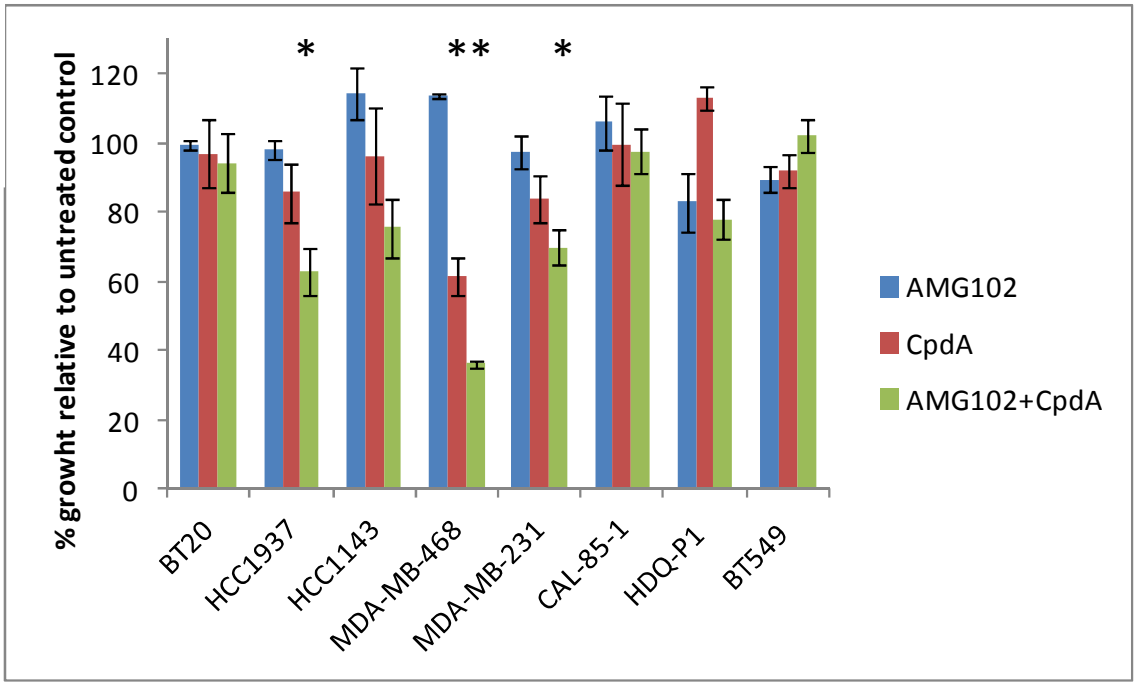

Figure 4 - 5 % growth relative to untreated control of cell lines of rilotumumab (AMG102-10 µg/mL) and CpdA (2 µM) Error bars represent the standard deviation of triplicate independent experiments.* = p<0.05, ** = p< 0.01 relative to CpdA as single agent

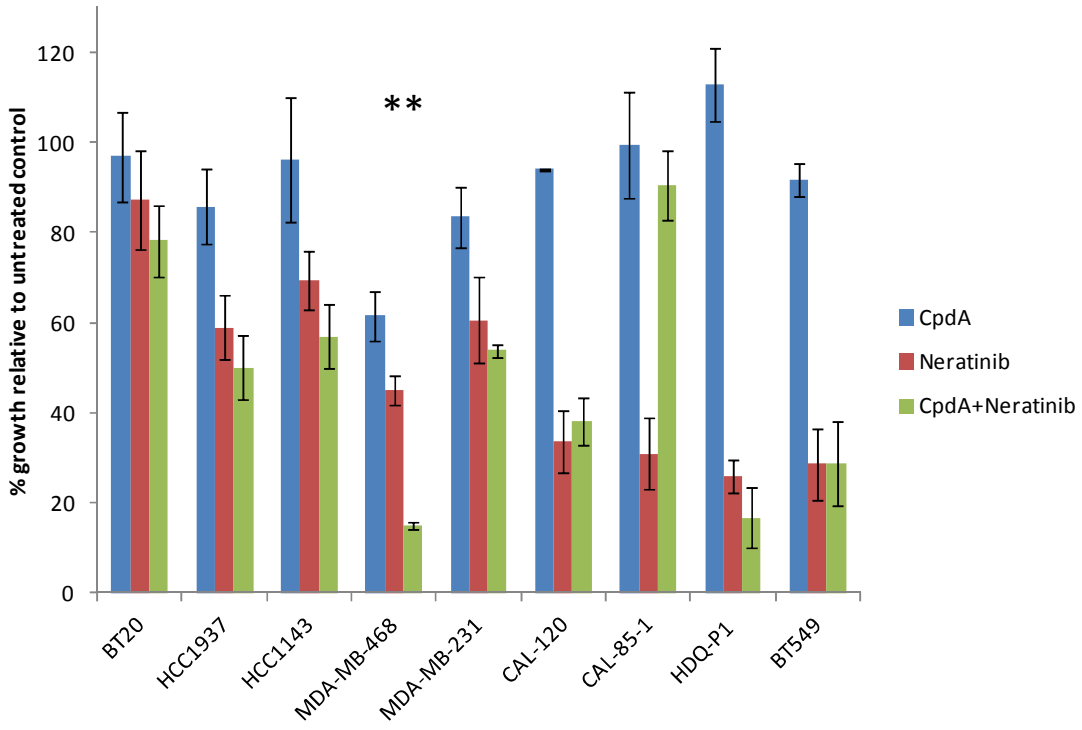

Figure 4 - 6 Proliferation assays in TNBC cells treated with CpdA (2 μM) and neratinib at respective IC_{50} concentrations. Error bars represent the standard deviation of triplicate independent experiments. ** = p<0.01 relative to CpdA as a single agent.

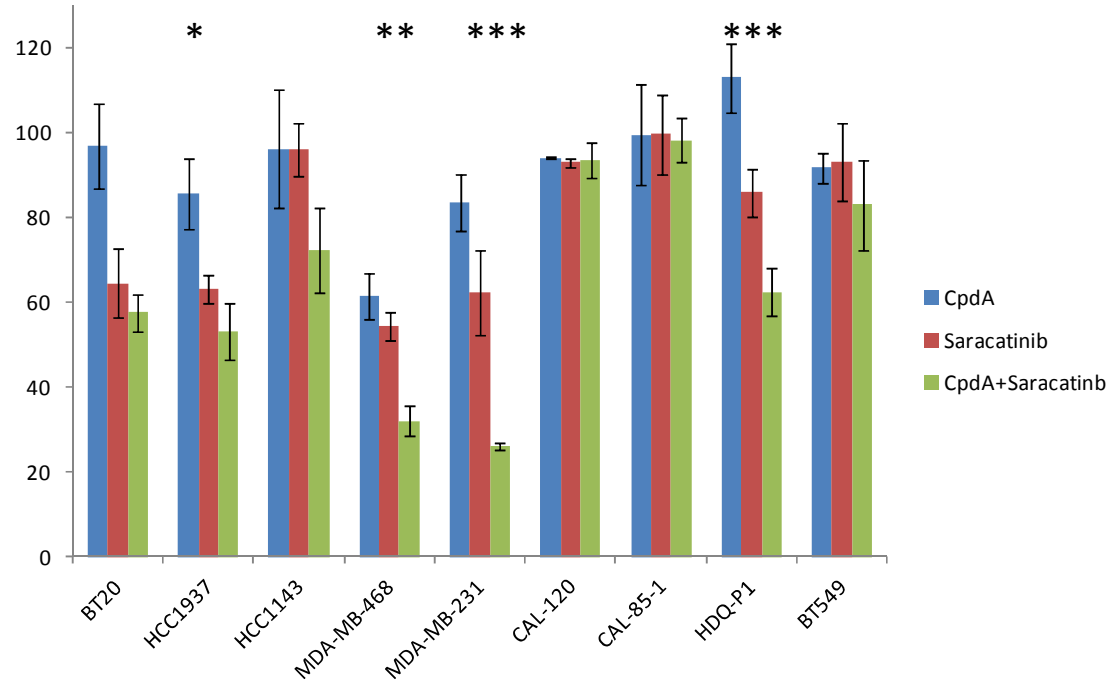

Figure 4 - 7 Proliferation assays in TNBC cells treated with CpdA (2 µM) and saracatinib at respective IC_{50} concentrations. Error bars represent the standard deviation of triplicate independent experiments. * = p<0.05, **= p<0.01 and ***= p<0.001 relative to CpdA as a single agent.

4.2.2 Clonogenic Assays

2D clonogenic assays or colony formation assays are *in vitro* cell survival assays which measure a single cells ability to reproduce. Classically they have been used to measure response to IR however they may be additionally used to evaluate cytotoxic agents as we present here. Commonly the clonogenic assays are manually counted and colony forming efficacy calculated based on the number of colonies and number of cells seeded. Only a limited number of cells should possess the ability to form colonies. The data presented in this thesis uses % area covered and average intensity of the colonies as a measurement as determined by the automated software Image J (see Section 2.7).

We assessed five cell lines for response to CpdA, neratinib and saracatinib using clonogenic assays. Representative Images are shown in Figure 4 – 8. Four of the cell lines (HCC1937, HCC1143, MDA-MB-468, and HDQ-P1) showed significant reduction in % area covered (p= 0.006, 0.007, 0.02 and 0.03 respectively relative to untreated controls) following treatment with 1 µM CpdA for 14 or 21 days. HCC1143

and HDQ-P1 also showed a significant reduction in average intensity of colonies (p= 0.03 and 0.008 respectively relative to untreated control) indicating a reduction in cell number in the individual colonies (Figure 4 - 9). HCC1937 were the most sensitive cell line with an 80.3 ± 9.7 % reduction in area covered.

Three of the five cell lines; HCC1937, HCC1143 and MDA-MB-231 tested showed a statistically significant decrease (p = 0.02, 0.002 and 0.001 respectively) in % area covered following neratinib treatment. MDA-MB-231 was the most sensitive cell line with an 85. 4 ± 5.5 % reduction in area covered relative to the untreated control. The HCC1143 and MDA-MB-231 cell lines also showed a statistically significant (p= 0.005 and 0.003 respectively) decrease in average intensity of colonies. The HCC1937 showed a slight decrease however this was not significant and the HDQ-P1 (p=0.04) cell which did not show a decrease in % area covered showed a decrease in average intensity of the colonies measured (Figure 4 - 10). Combination of treatment with CpdA and neratinib showed no significant change in % area covered or in colony intensity in any of the cell lines tested (Figure 4 - 11).

Four of the five cell lines (HCC1937, HCC1143 MDA-MB-468 and MDA-MB-231) tested showed a statistically significant decrease (p= 0.002, 0.02, 0.02 and 0.0006 respectively) in % area covered following saracatinib treatment. The cell line HDQ-P1 showed a decrease in % area covered however failed to reach significance with p-value of 0.06. HCC1143 was the most sensitive cell line with an 80.8 ± 0.1 % reduction in area covered relative to the untreated control. All of the cell lines tested also showed a statistically significant decrease in average intensity of colonies except the HCC1937 (Figure 4 - 12). Combined treatment with CpdA and saracatinib showed no significant change in % area covered or in colony intensity in any of the cell lines tested. However MDA-MB-231 shows a decrease in % area covered which is approaching significance (p=0.06) (Figure 4 - 13).

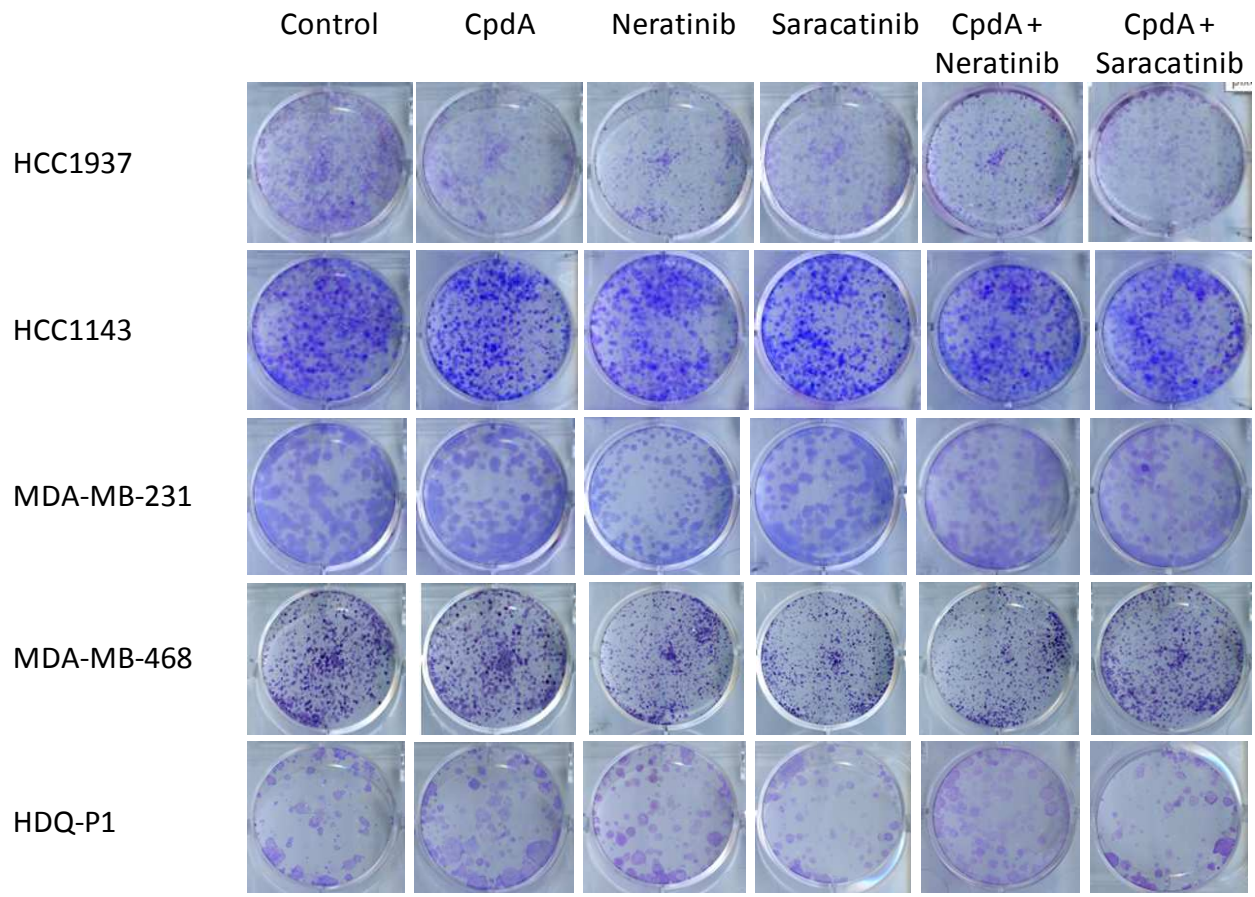

Figure 4 - 8 Representative images of clonogenic assays untreated or treatment as described. Cells were fixed with methacare fixative and stained with 1% Crystal Violet. Images are representative of triplicate experiments.

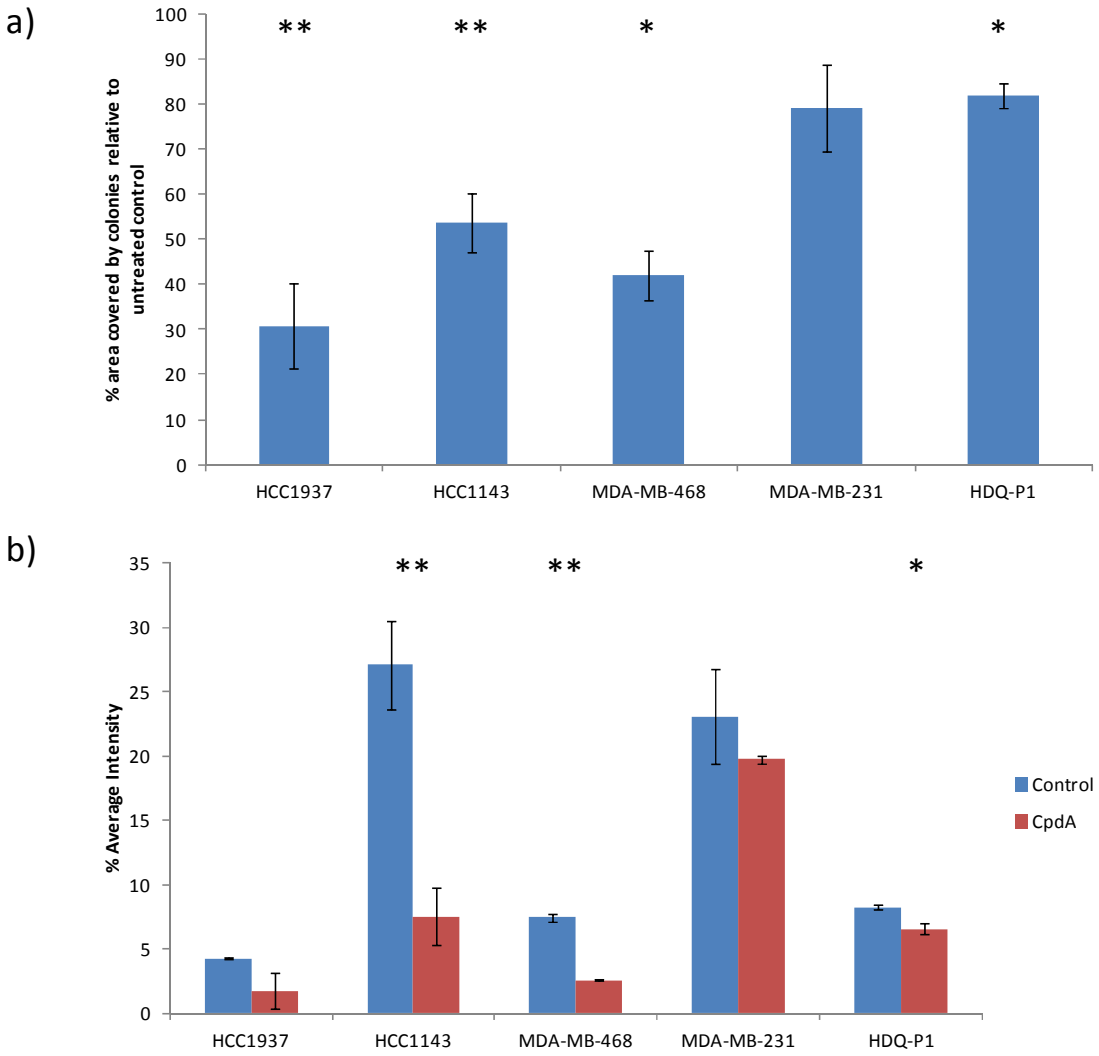

Figure 4 - 9 a) Clonogenic assays showing % area covered by colonies relative to untreated control 14-21 days post treatment with 1 µM CpdA and b) average intensity of colonies analysed after 14/21 days post treatment. Error bars represent the standard deviations of triplicate independent experiments. *= $p<0.05$, **= $p<0.01$ of CpdA compared to control values.

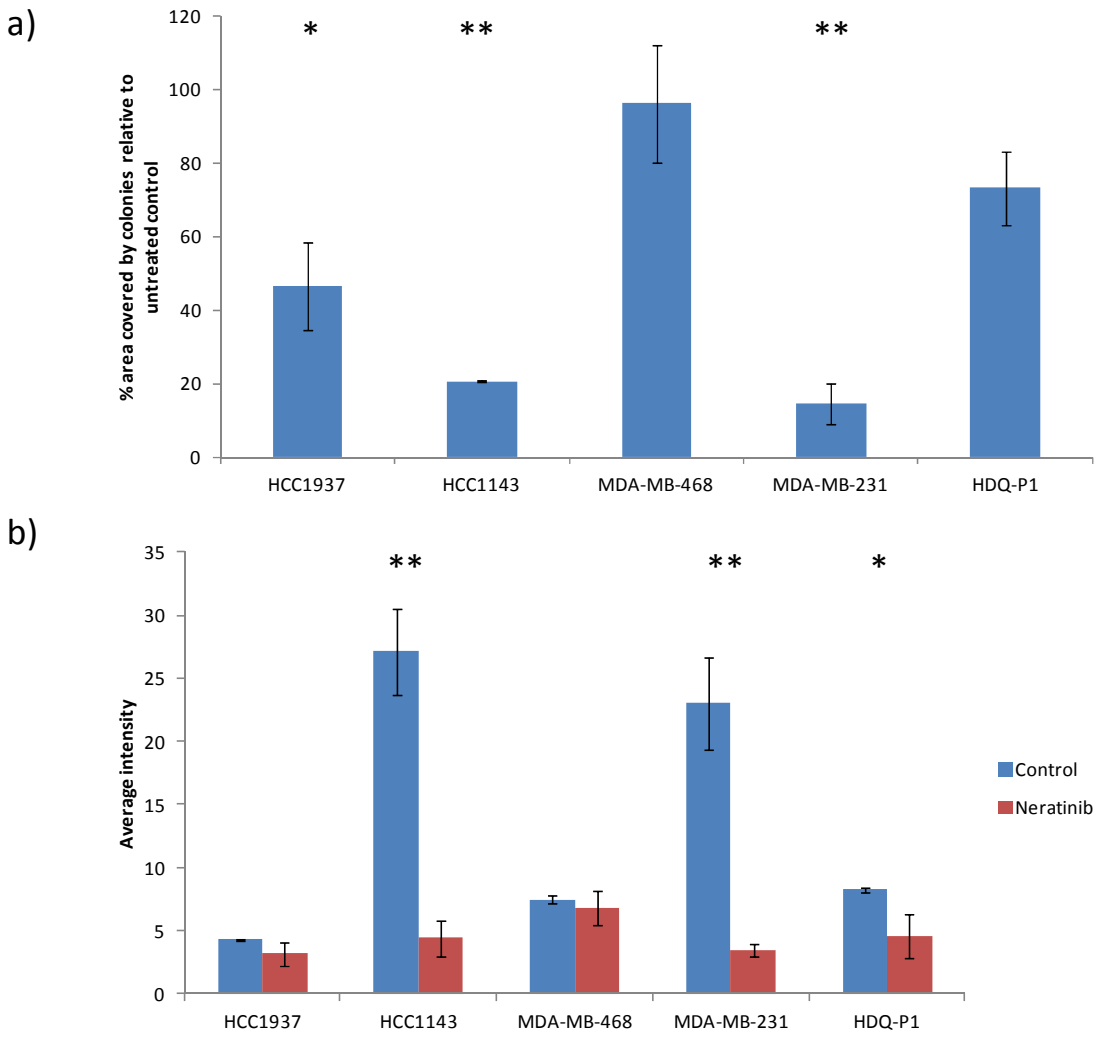

Figure 4 - 10 Clonogenic assays showing % area covered by colonies relative to untreated control 14-21 days post treatment with respective concentrations of neratinib and b) average intensity of colonies analysed after 14/21 days post treatment. Error bars represent the standard deviation of triplicate independent experiments. *= p<0.05, **= p<0.01 of neratinib treated values compared to control values.

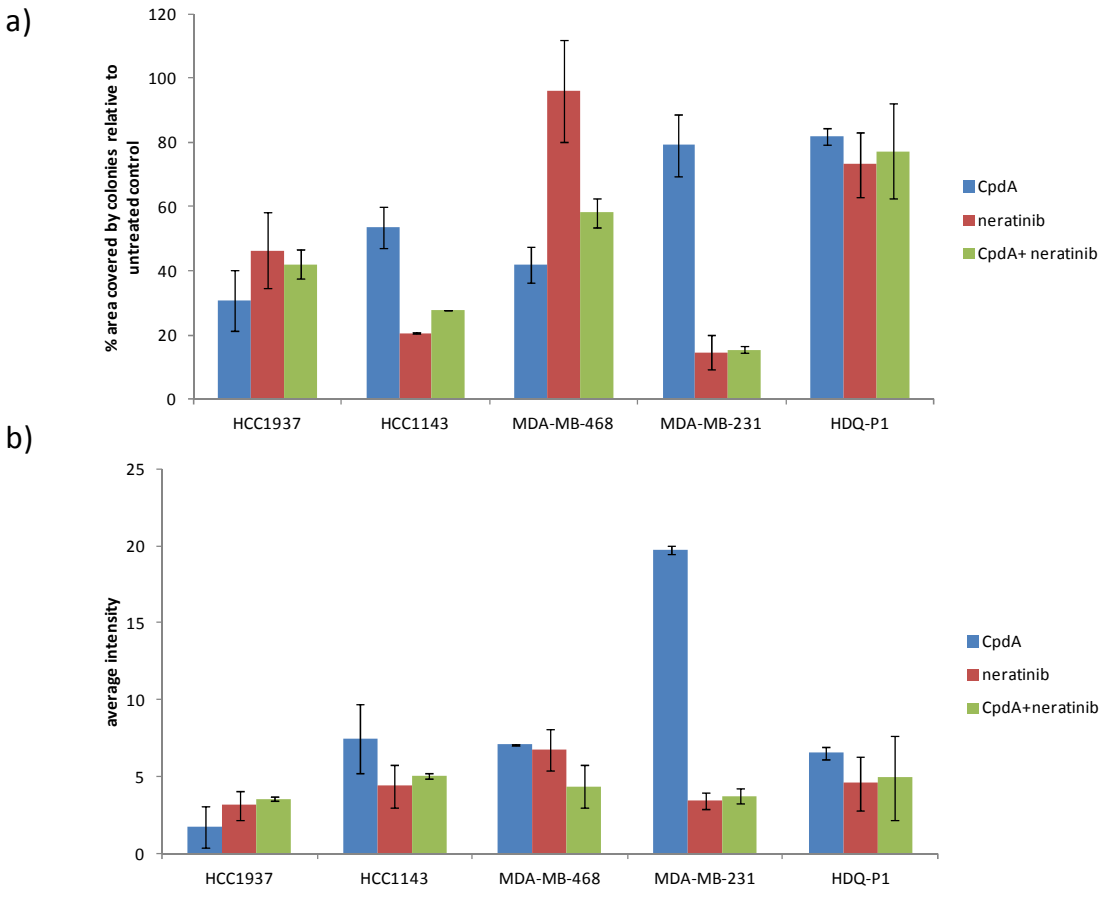

Figure 4 - 11 Clonogenic assays showing % area covered by colonies treated with CpdA and neratinib or in combination b) average intensity of colonies analysed after 14/21 days post treatment. Error bars represent the standard deviations of triplicate independent experiments.

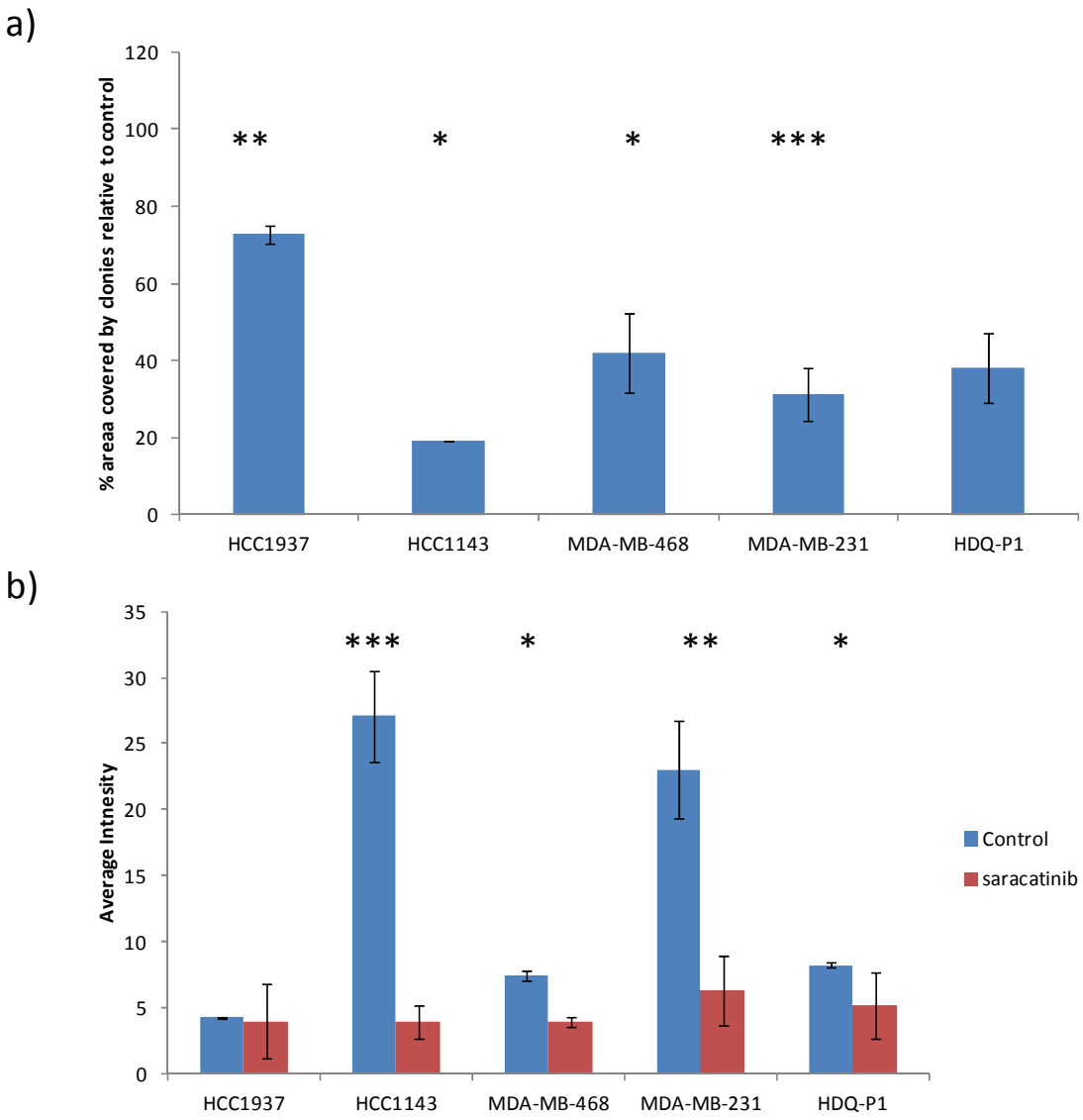

Figure 4 - 12 Clonogenic assays showing a) % area covered by colonies relative to untreated control 14-21 days post treatment with respective concentrations of neratinib and b) average intensity of colonies analysed after 14/21 days post treatment. Error bars represent the standard deviations of triplicate independent experiments * = p<0.05, **=p<0.01, *** = p<0.001of saracatinib treated values compared to control values.

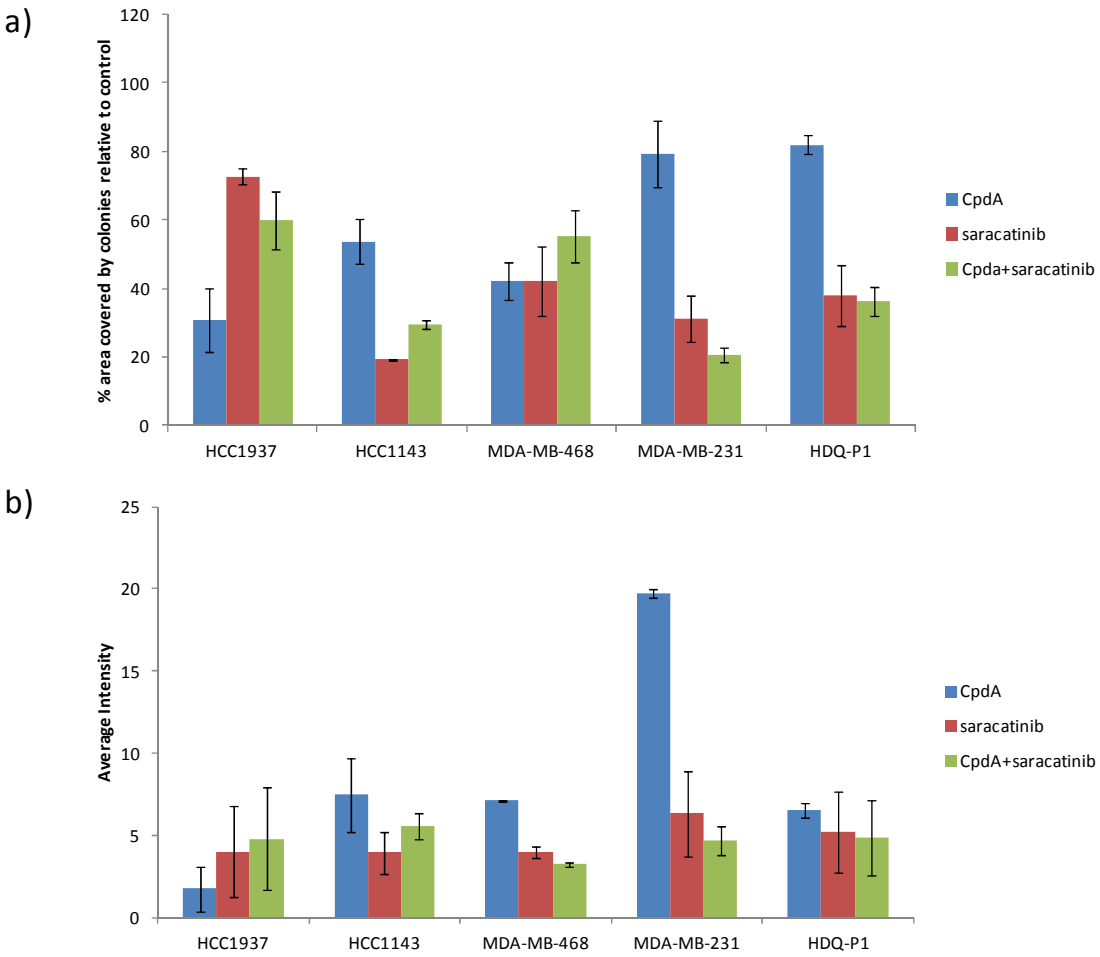

Figure 4 - 13 Clonogenic assays showing % area covered by colonies treated with CpdA and neratinib and in combination b) average intensity of colonies analysed after 14/21 days post treatment. Error bars represent the standard deviations of triplicate independent experiments.

4.3 Sensitivity to CpdA in 3D growth assays

BT20, HCC1937, HCC1143, MDA-MB-468, MDA-MB-231, HDQ-P1 and BT549 cell lines all showed the ability to form colonies when culture in 3D environment with matrigel as the support matrix. CAL-85-1 was the only cell line tested which did not form colonies and lysis of >90% of cells seeded occurred within 5 days. Representative images of colonies formed are shown with and without treatment of CpdA (10 μM) after 5/7 days growth (Figure 4 - 14). MDA-MB-468 and MDA-MB-231 were the most sensitive cell lines to CpdA in 3D assays. MDA-MB-468 showed a statistically significant 30.1 ± 10.6 % reduction in cell viability (p= 0.01) followed by MDA-MB-231 showing statistically significant 11.8 ± 0.5 % reduction (p=0.01) (Figure 4 - 15) at 10 μM. Overall the nine cell lines showed limited response in 3D culture to CpdA and were less sensitive to inhibition by CpdA than 2D cell culture (Table 4 – 2).

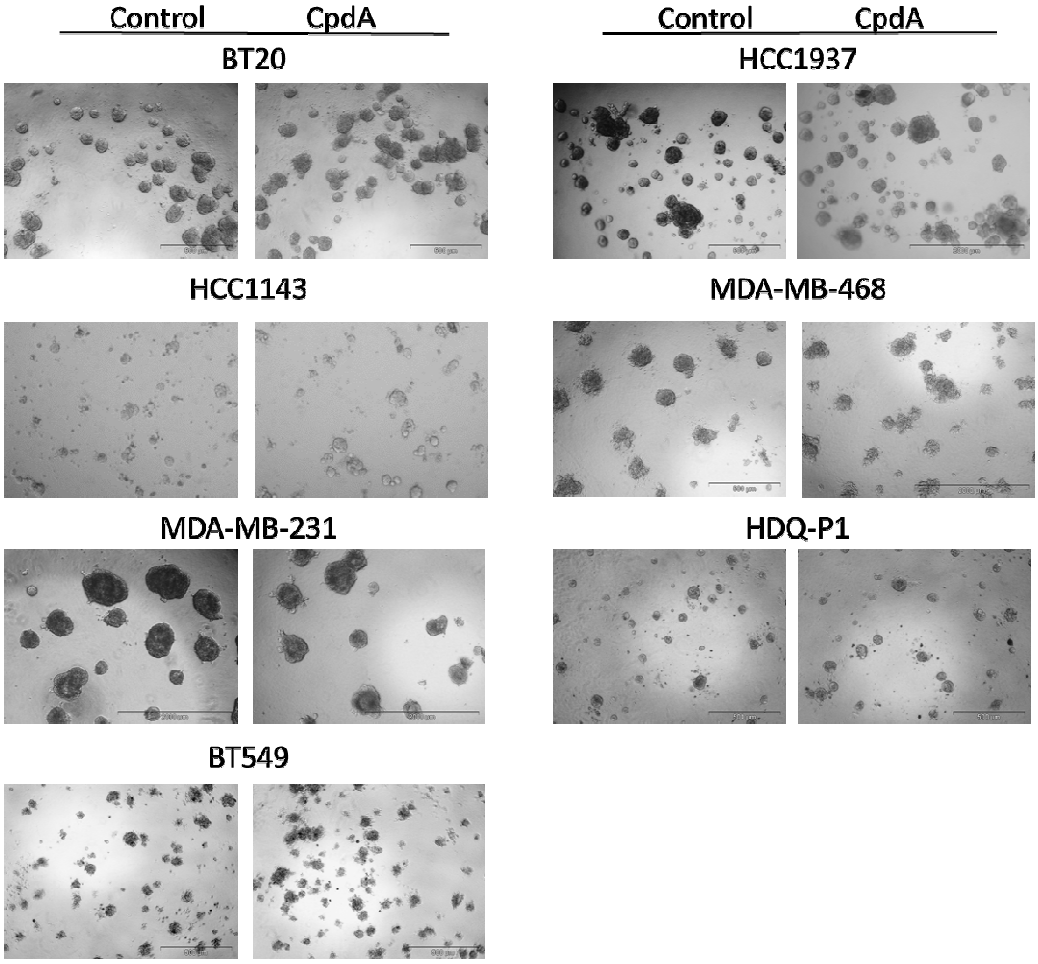

Figure 4 - 14 3D colonies formed after 5/7 days growth in 2-4% matrigel with/without CpdA treatment (10 μM).

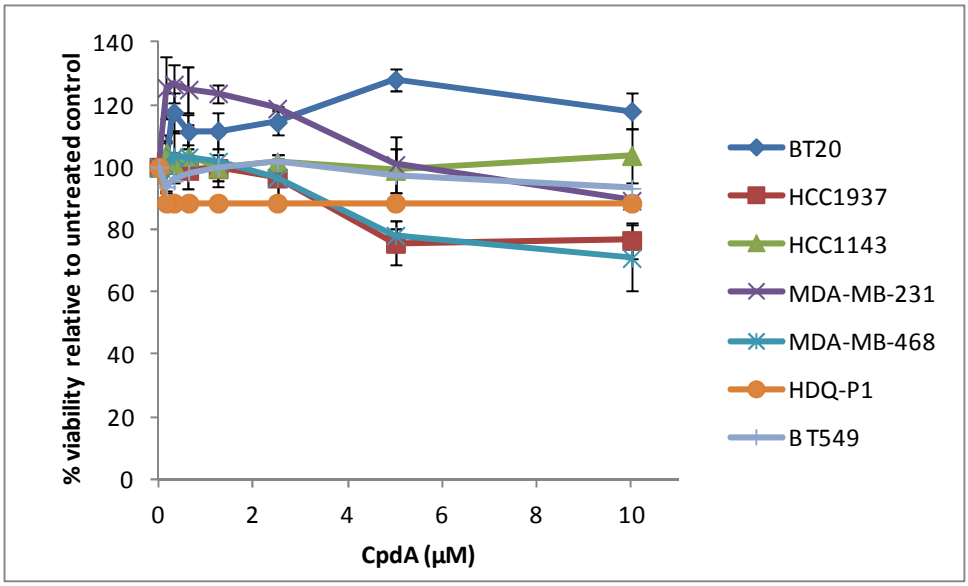

Figure 4 - 15 % viability of cells after 5/7 day treatments with serially decreasing concentrations of CpdA from 10 µM. Error bars represent standard deviations of triplicate independent experiments.

Table 4 - 2 Comparison of growth in 2D v 3D growth assays at 10 µM CpdA ± standard deviations which represent triplicate independent experiments.

Cell Line	% growth @ 10 µM-2D	% growth @ 10 µM-3D
BT20	73.7 ± 4.9	107.2 ± 5.6
HCC1937	11.4 ± 1.9	98.5 ± 5.8
HCC1143	89.9 ± 8.5	103.6 ± 8.6
MDA-MB-468	11.6 ± 1.9	89.3 ± 10.6
MDA-MB-231	9.0 ± 2.2	70.9 ± 0.6
HDQ-P1	36.7 ± 3.6	88.5 ± 10.9
BT549	41.3 ± 4.3	93.2 ± 9.7

4.4 Sensitivity of TNBC in invasion assays

We conducted invasion assays on our panel of TNBC cell lines. Representative images of cell invading after 24hrs are shown in Figure 4 – 16. MDA-MB-231 show the highest level of invasion with 190 ± 3 cells invading per 1000 cells seeded. BT20, HCC1937, HCC1143, CAL-85-1 and BT549 all show moderate levels of invasion and MDA-MB-

468, CAL-120 and HDQ-P1 show the lowest levels of invasion with 40 ± 2, 30 ± 2 and 10 ± 1 cells invading per 1000 cell seeded (Figure 4 - 17). None of the cell lines tested showed a significant response in invasion post treatment with 1 μM CpdA (Table 4 – 3, Figure 4 – 18). None of the cell lines tested showed a significant response to neratinib post treatment with 1 μM neratinib (Table 4 – 3). The addition of neratinib did not enhance the cell lines response to CpdA (Figure 4 - 19). Similarly to neratinib, saracatinib showed no significant effect on the invasion of TNBC cell lines and no significant increase in response to CpdA was noted in the combination (Table 4 – 3, Figure 4 – 20).

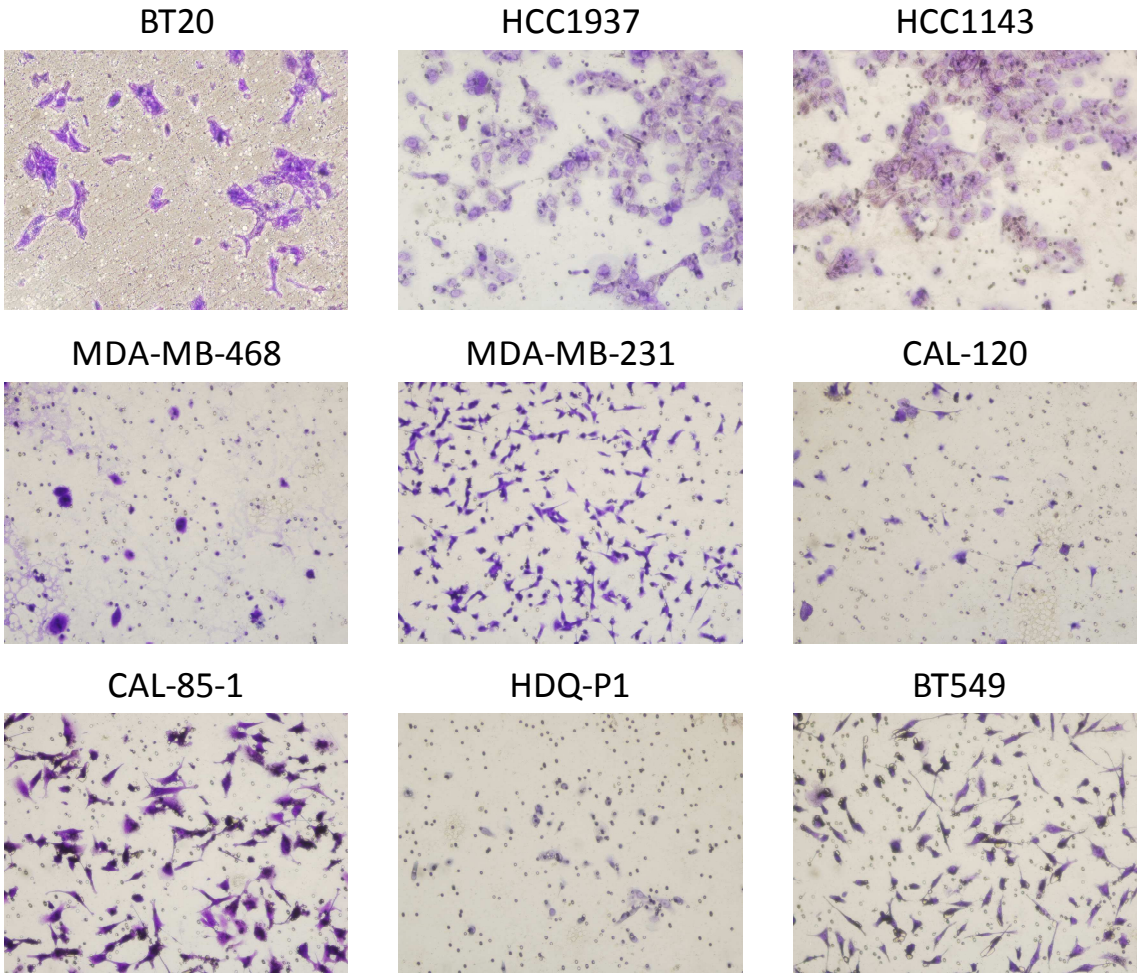

Figure 4 - 16 Representative images of invading cells (through 1 mg/mL matrigel) of nine TNBC cell lines after 24hrs.

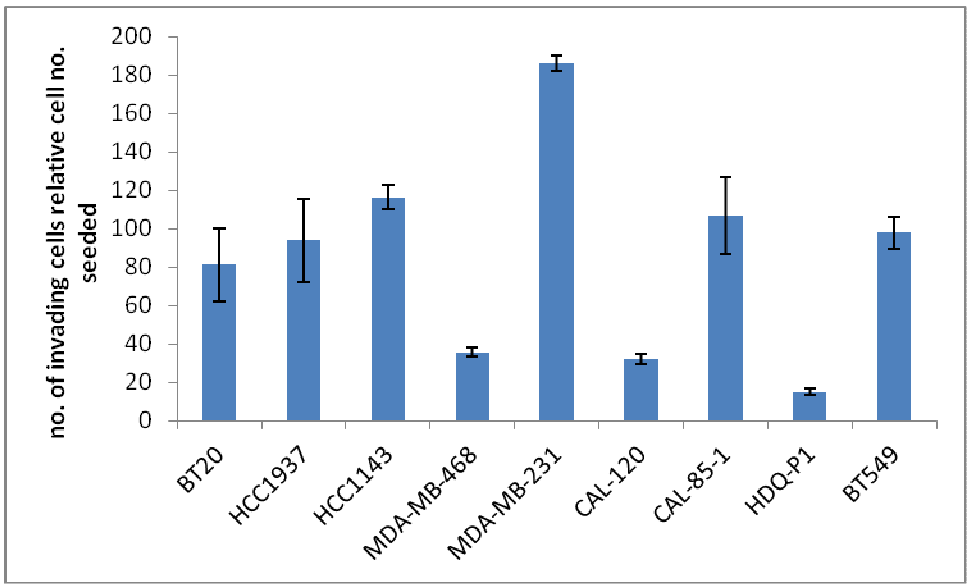

Figure 4 - 17 No. of invading cells relative to number of cells seeded (1x 10^5 or 5 x 10^4) of TNBC cell lines. Error bars represent standard deviations of independent triplicate experiments.

Table 4 - 3 shows the % invasion post treatment with 1 µM CpdA relative to untreated control

Cell lines	Subtype	No of cells invading/1000 cells seeded	% invasion @ 1 µM CpdA	% invasion @ 1 µM neratinib	% Invasion @ 1 µM saracatinib
BT20	UC	81.6 ± 18.8	88.8 ± 23.2	87.4 ± 9.3	88.0 ± 11.0
HCC1937	BL-1	93.8 ± 21.8	91.5 ± 11.9	88.3 ± 15.3	102.9 ± 8.8
HCC1143	BL-1	116.3 ± 6.4	94.2 ± 5.5	93.3 ± 6.9	101.2 ± 7.4
MDA-MB-468	BL-1	35.6 ± 2.2	114.7 ± 6.2	108.3 ± 10.5	91.9 ± 21.6
MDA-MB-231	MSL	185.9 ± 4.0	105.5 ± 2.1	84.2 ± 16.4	104.9 ± 19.4
CAL-120	M	32.1 ± 2.7	92.5 ± 12.3	97.8 ± 9.9	97.9 ± 5.3
CAL-85-1	BL-2	106.5 ± 19.9	93.6 ± 18.6	88.4 ± 15.6	76.9 ± 17.0
HDQ-P1	BL-2	15.0 ± 1.7	96.3 ± 11.4	94.5 ± 9.9	108.3 ± 10.5
BT549	M	98.0 ± 8.3	91.8 ± 8.5	87.4 ± 11.3	88.0 ± 21.6

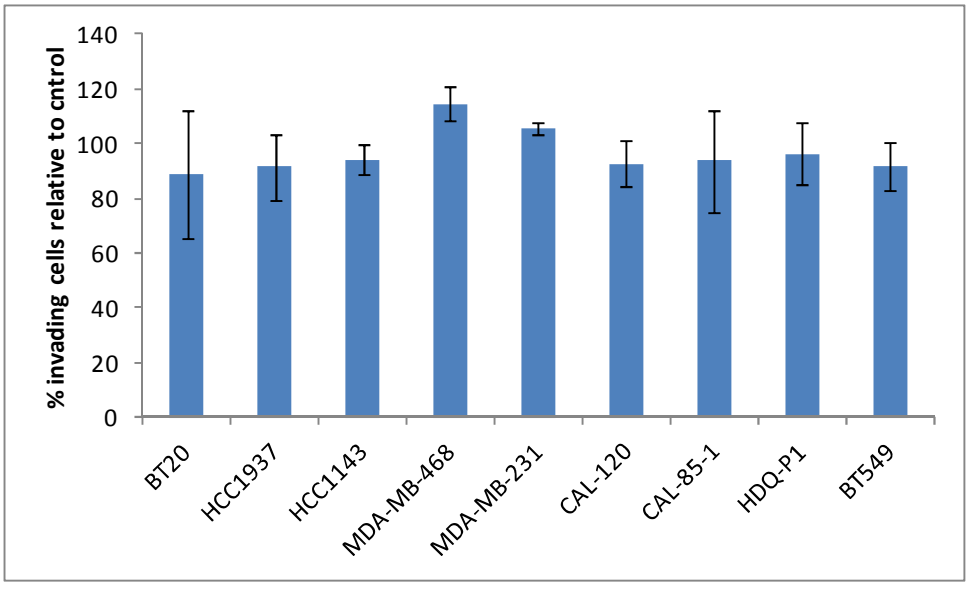

Figure 4 - 18 Invasion assays of TNBC cell lines treated with 1 µM CpdA. Error bars represent standard deviation of triplicate independent experiments.

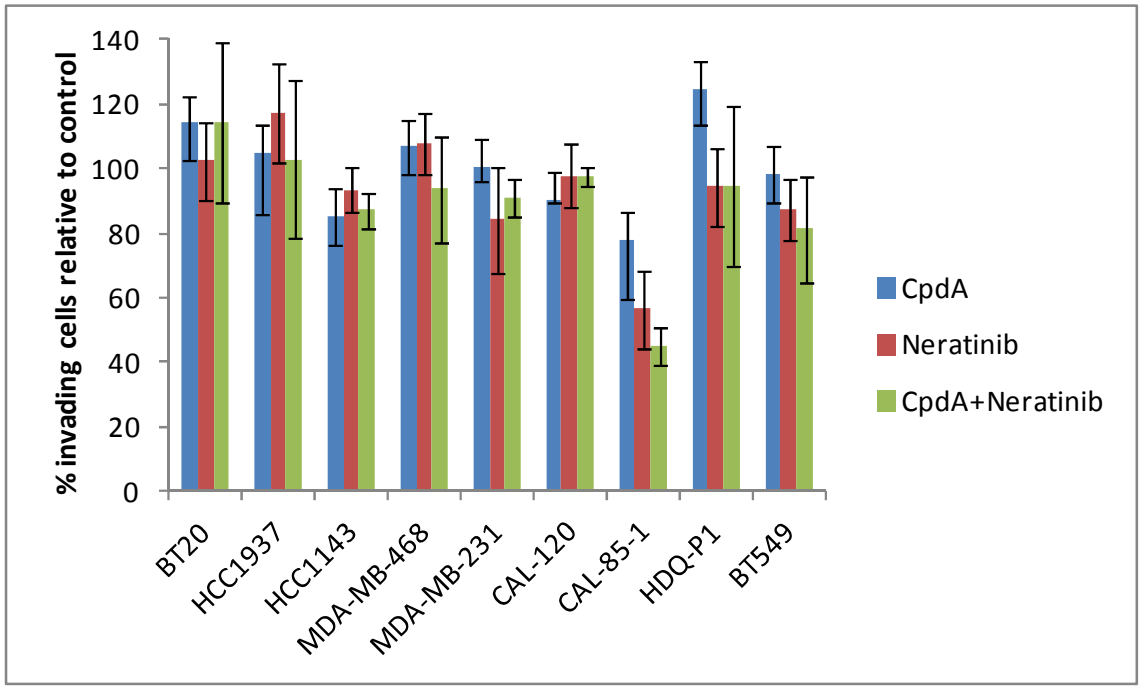

Figure 4 - 19 Invasion assays of TNBC cell lines with CpdA and neratinib at fixed concentrations of 1 µM respectively. Error bars represent standard deviation of triplicate independent experiments.

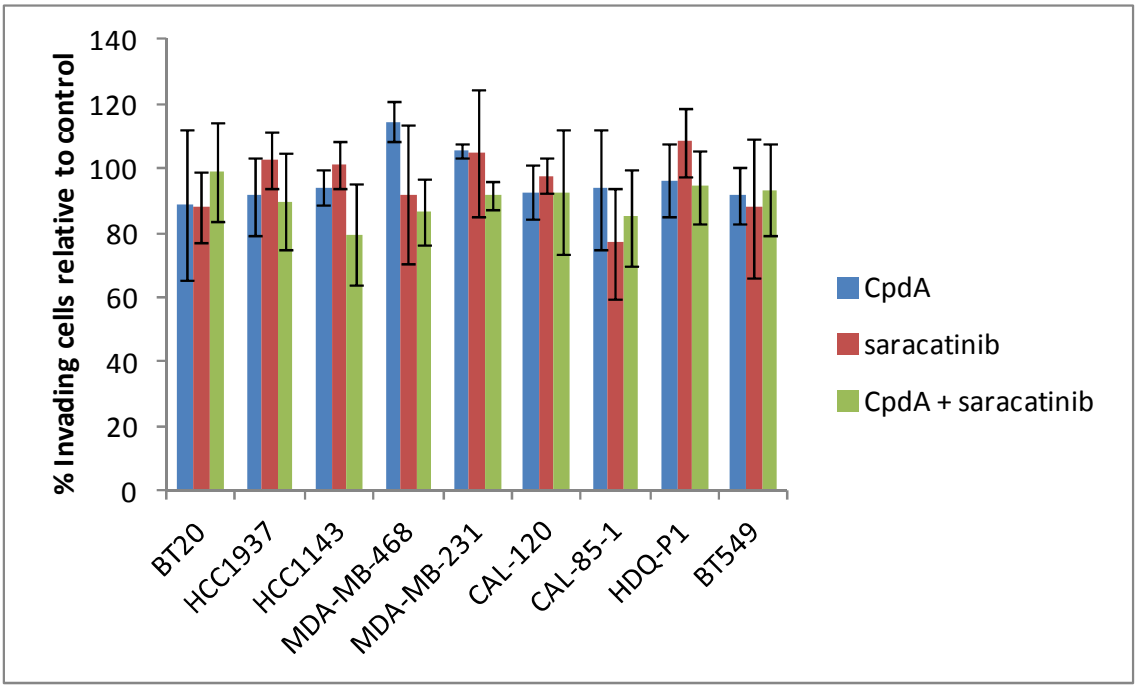

Figure 4 - 20 Invasion assays of TNBC cell lines with CpdA and saracatinib, or the combination at fixed concentrations of 1 µM respectively. Error bars represent standard deviation of triplicate independent experiments.

4.5 Sensitivity to CpdA in migration assays

We assessed the effect of HGF on the levels of migration in MDA-MB-468. HGF stimulated a significant increase in migration after 48 hrs (p=0.02) however had no significant effect at 24 hrs. Representative images of wound scratches at T0, T24 and T48 are shown in Figure 4 - 21. Rilotumumab and CpdA both inhibited the migration stimulated by HGF (p= 0.008 and 0.004 respectively) however did not significantly decrease migration below untreated control levels (Figure 4 - 22). We examined whether CpdA could inhibit basal levels of migration at 24 and 48 hrs in 5 cell lines (HCC1937, HCC1143, MDA-MB-231 and HDQ-P1 and whether the response to CpdA could be enhanced by combination with neratinib and saracatinib. The MDA-MB-231 and HDQ-P1 were not suitable for evaluation at 48 hrs. The cell lines show varying basal levels of migration with the MDA-MB-231 showing the highest level of migration with 96.4 ± 3.8 % wound closure after 24 hrs. MDA-MB-468 showed the lowest level of migration with 16.4 ± 2.9 % after 24 hrs. No significant response was seen to CpdA treatment at 24 or 48 hrs in any of the cell lines tested (Figure 4 - 24). No significant reduction was seen after 24 or 48 hrs in response to neratinib treatment at 1 µM and no

enhancement was observed with combined CpdA and neratinib treatment (Figure 4 - 25). Similarly to neratinib, no significant response was seen to saracatinib as a single agent at either 24 or 48 hrs and no enhancement of response was observed for CpdA when used in combination with saracatinib (Figure 4 - 26).

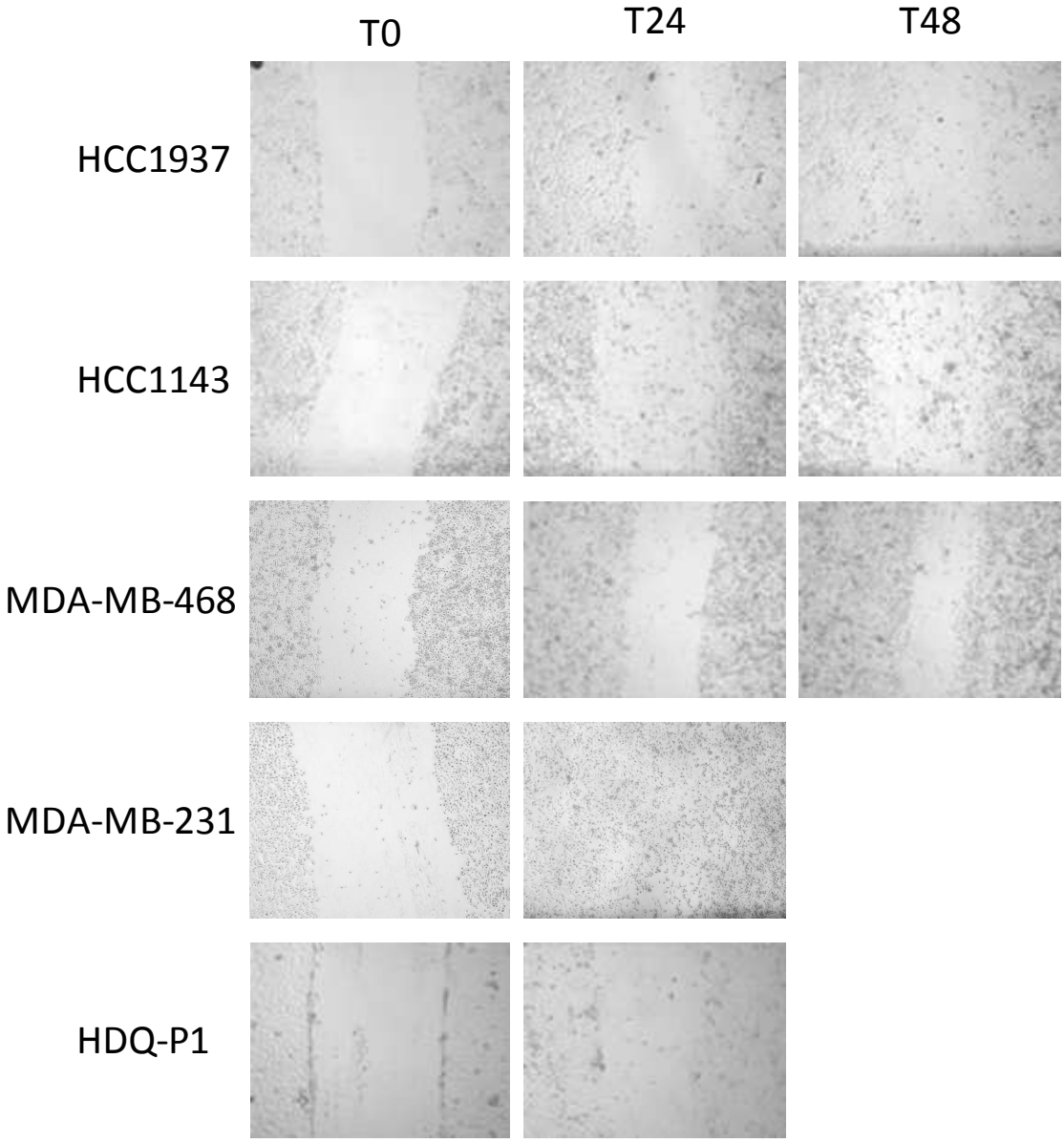

Figure 4 - 21 Wound scratch photographs of control wells taken at T0, T24 and T48 where applicable.

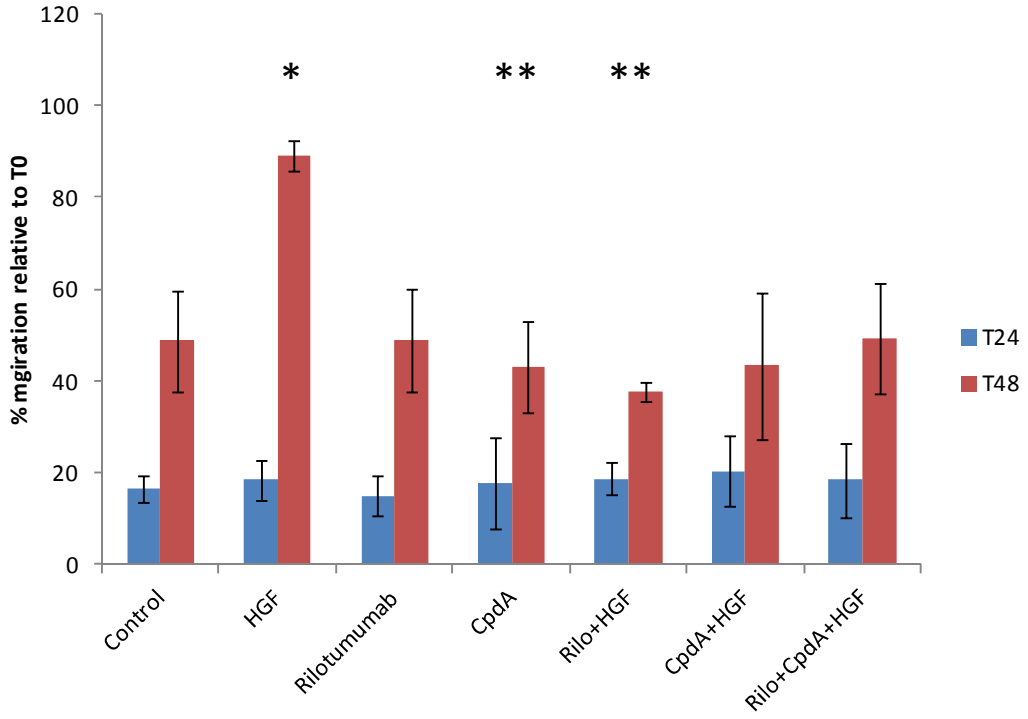

Figure 4 - 22 MDA-MB-468 levels of migration relative to T0 and T24 and T48 hrs. Cells were treated with HGF (50 µg/mL), Rilotumumab (10 µg/mL) and CpdA (1 µM). Error bars represent the standard deviation of triplicate independent experiments. * = p<0.05, **= p<0.01 relative to HGF treated values

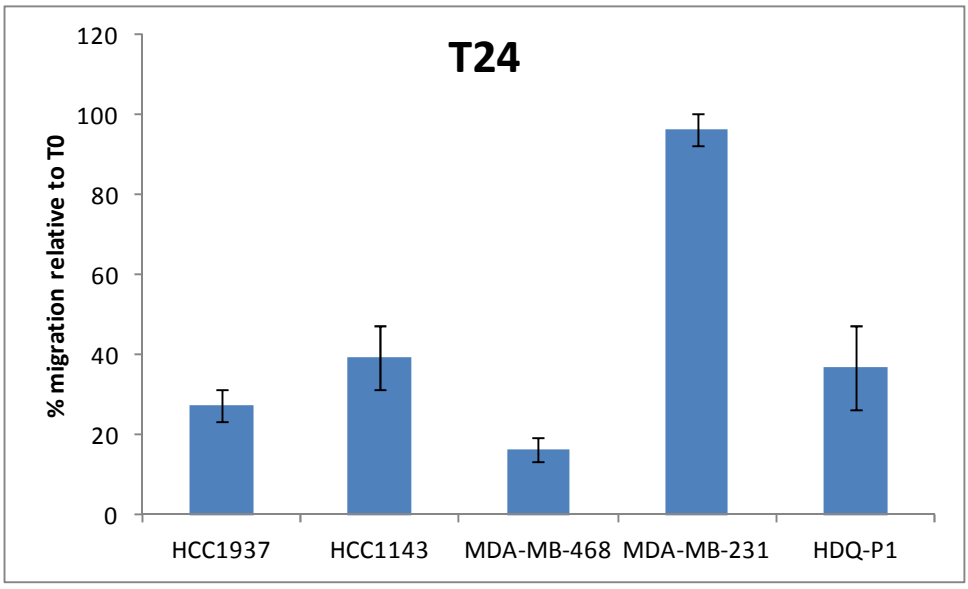

Figure 4 - 23 Basal migration levels of five TNBC cell lines as determined by wound scratch assays after 24hrs migration. Error bars represent standard deviations of triplicate independent experiments.

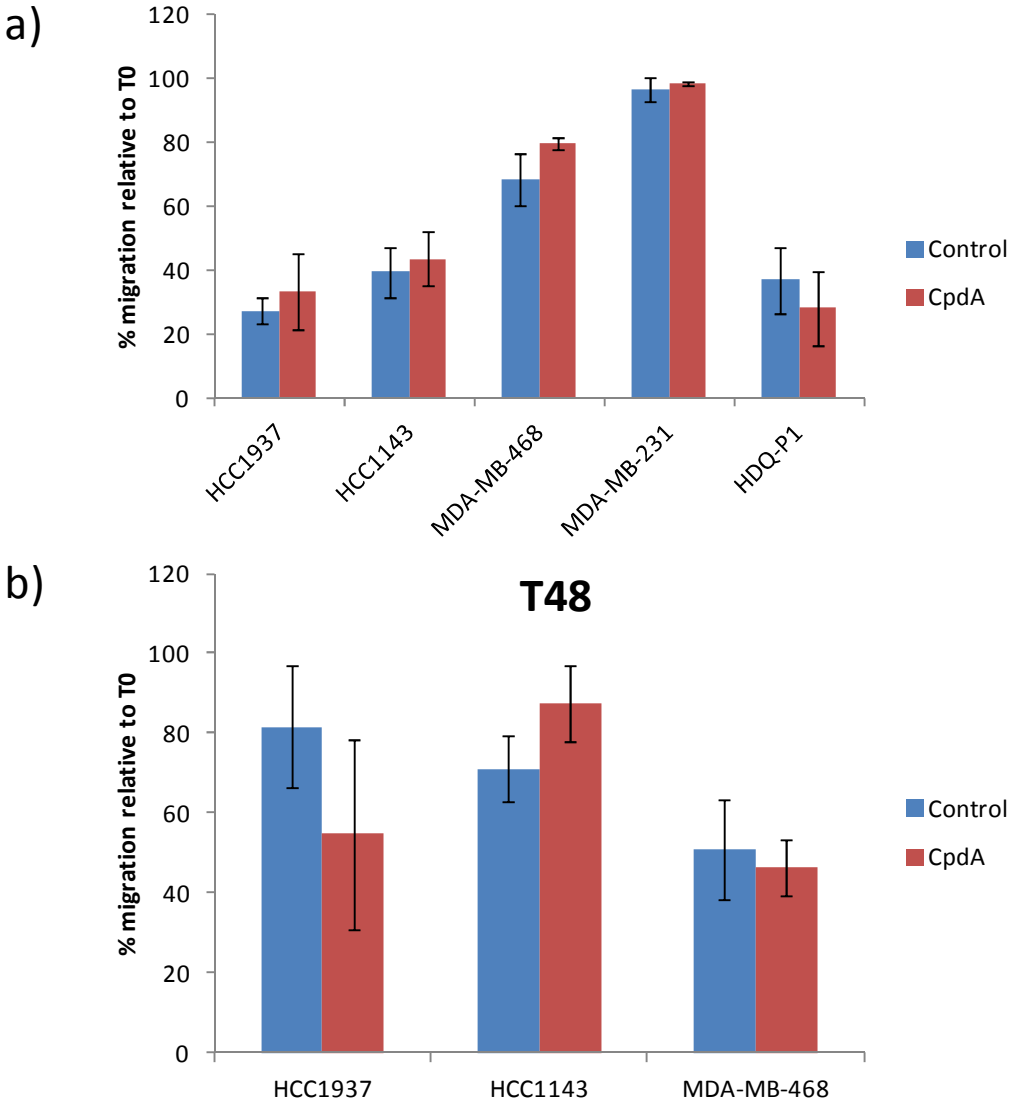

Figure 4 - 24 Migration levels relative to T0 of five TNBC cells lines treated with/without CpdA (1 µM) for a) 24hrs and b) 48 hrs. Errors bars represent standard deviations of independent triplicate experiments.

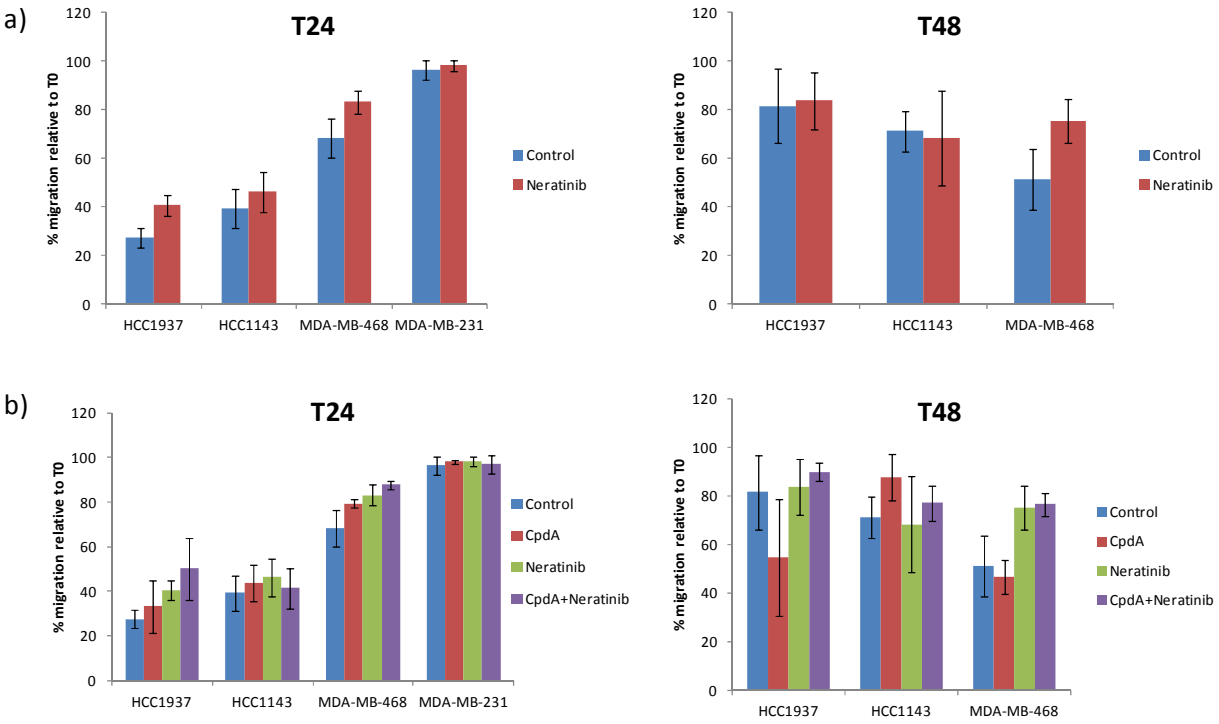

Figure 4 - 25 Migration levels relative to T0 of four TNBC cells lines treated with/without a) neratinib (1 µM) for 24 hrs (LHS) and 48 hrs(RHS) and b) migration levels relative to T0 with/without treatment of CpdA (1 µM), neratinib (1 µM) or in combination. Errors bars represent standard deviations of independent triplicate experiments.

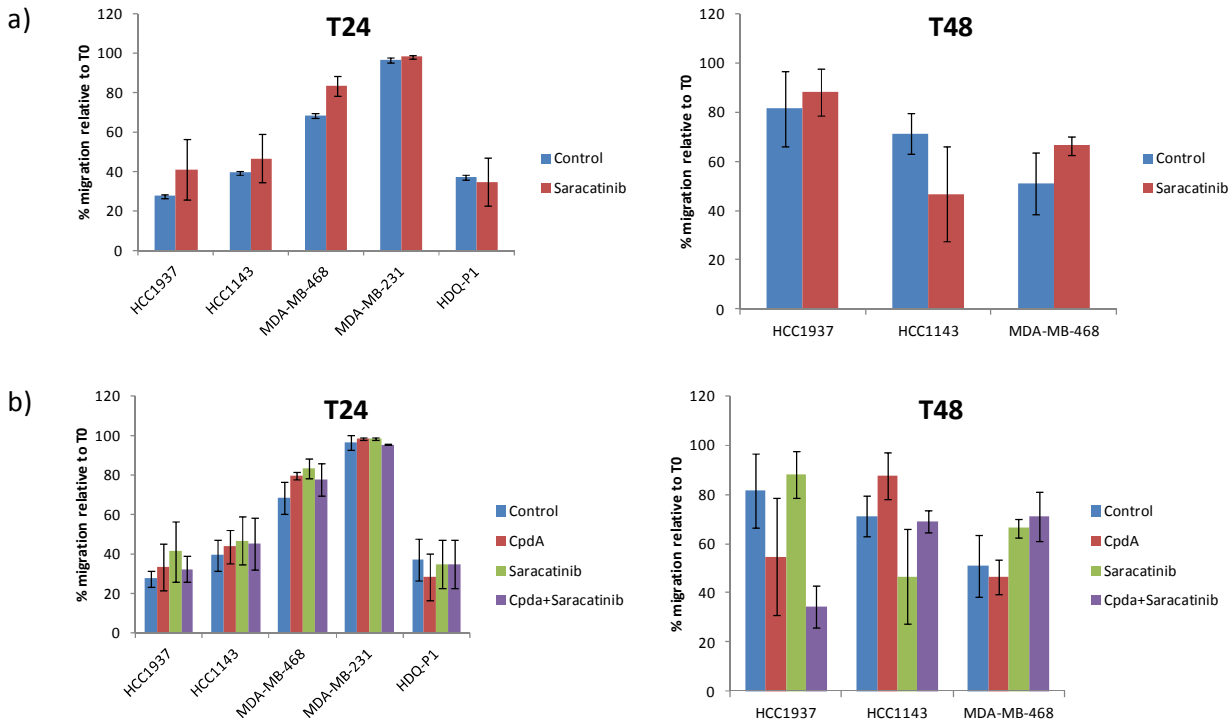

Figure 4 - 26 Migration levels relative to T0 of five TNBC cells lines treated with/without a) saracatinib (1 µM) for 24 hrs (LHS) and 48 hrs(RHS) and b) migration levels relative to T0 with/without treatment of CpdA (1 µM), saracatinib (1µM) or in combination. Errors bars represent standard deviations of independent triplicate experiments.

4.6 Summary

CpdA achieved greater than 50% growth inhibition at concentrations less than 10 µM in six of nine cell lines tested. MDA-MB-231 was the most sensitive. Combinations of CpdA and rilotumumab resulted in significantly decreased growth in three cell lines, HCC1937, MDA-MB-468 and MDA-MB-231. Neratinib only enhanced response to CpdA in one EGFR amplified cell line MDA-MB-468. Saracatinib also enhanced response to CpdA in 2D proliferation assays in four cell lines, HCC1937, MDA-MB-468, MDA-MB-231 and HDQ-P1.

Clonogenic assays showed much higher sensitivities to 1 µM CpdA than 2D assays. Four of five cell lines tested showed a response including one which did not demonstrate any response in 2D assays. The addition of neratinib or saracatinb in this case did not enhance sensitivity to CpdA in any of the cell lines.

Two cell lines showed sensitivity to CpdA treatment in 3D assays. MDA-MB-231 and MDA-MB-468 were the most sensitive in agreement with the 2D assays.

Invasion assays showed no significant response to treatment with any inhibitors. MDA-MB-231 was the most invasive cell line and HDQ-P1 was the least invasive.

In migration assays, CpdA and rilotumumab have the ability to inhibit HGF induced migration however show no significant effect on basal levels of migration.

In summary c-Met inhibition showed limited anti-cancer actively in the panel of TNBC cell lines (Table 4 – 4). Having combined treatment with neratinib or sarcatinib enhanced response is seen in a small number of cell lines (Table 4 – 5).

Table 4 - 4 Summary of responses to TNBC in 2D proliferation, clonogenic, 3D, invasion and migration assays.

Cell Line	Sub-type	2D IC_{50}	Clonogenic % inhibition @ 1 µM	3D % inhibition @ 10 µM	Invasion % inhibition at 1 µM	Migration % inhibition at 1 µM
BT20	UC	>10	NT	107.2 ± 5.6	88.8 ± 23.2	NT
HCC1937	BL1	4.1 ± 0.5	69.2 ± 9.4	98.5 ± 5.8	91.5 ± 11.9	72.6 ± 4.1
HCC1143	BL1	>10	46.3 ± 3.4	103.6 ± 8.6	94.2 ± 5.5	60.7 ± 7.9
MDA-MB-468	BL1	3.1 ± 0.4	57.9 ± 5.5	89.3 ± 10.6	114.7 ± 6.2	83.6 ± 2.9
MDA-MB-231	MSL	2.5 ± 0.3	20.7 ± 9.6	70.9 ± 0.6	105.5 ± 2.1	3.6 ± 3.83
CAL-120	M	3.8 ± 0.3	NT	NT	92.5 ± 12.3	NT
CAL-85-1	BL2	>10	NT	NT	93.6 ± 18.6	NT
HDQ-P1	BL2	5.1 ± 0.4	18.11 ± 2.8	88.5 ± 10.9	96.3 ± 11.4	63.0 ± 10.4
BT549	M	>10	NT	93.2 ± 9.7	91.8 ± 8.5	NT

Table 4 - 5 Cell lines which show enhanced response to combination. UK - Unknown

Cell Line	Sub-type	Basal A/B	2D growth	Key features
HCC1937	BL-1	A	CpdA + rilotumumab CpdA + saracatinib	BRCA PI3K WT PTEN+ P53 mutated
MDA-MDA-231	MSL	B	CpdA + rilotumumab CpdA + saracatinib	PI3K WT PTEN+ P53 mutated
MDA-MB-468	BL-1	A	CpdA + rilotumumab CpdA + neratinib CpdA+ saracatinib	PI3K WT PTEN null EGFR amplified P53 mutated
HDQ-P1	BL-2	UK	CpdA+ Sarcatinib	P53 mutated

Chapter 5

Preclinical Evaluation of PRS110 in TNBC Cell Lines

5.1 Introduction

PRS110 is a monovalent antagonist of c-Met in pre-clinical development by Pieris Ag. PRS110 is unique in its structure which is named an anticalin. The anticalins are engineered from endogenous lipocalins [228]. The lipocalins are a family of proteins which transport small hydrophobic molecules and are involved in inflammation and detoxification processes. PRS110 essentially functions as a monoclonal antibody binding to the extracellular portion of c-Met, however lacks the large fragment crystallisable (Fc) domain of monoclonal antibodies which are known to stimulate activation of receptors through cross linking and may function as a potential resistance mechanisms in monoclonal antibody therapies [254]. Anticalin molecules are suggested to overcome this. Additionally PRS110 is capable of blocking both ligand dependent and ligand-independent mechanisms of activation of c-Met. Several other monoclonal antibodies against c-Met are in development, the most promising of which was onartuzumab [233] . After initial success in Phase I and II trials in NSCLC, a Phase III trial was launched. This trial evaluated the role of onartuzumab in combination with erlotinib; however it was halted early due to lack of meaningful activity of the combination [220].

5.2 Sensitivity of TNBC cell lines to PRS110 in 2D proliferation assays

5.2.1 2D Proliferation Assays

PRS110 had no observable effect as a single agent on the proliferation of any of the 9 TNBC cell lines tested, using serially diluted concentrations from 10 μg/mL (Figure 5 - 1). The CAL-85-1 cell line while not significant (p=0.477) showed the greatest decrease with 14.4 ± 10.3 % inhibition of growth. To confirm activity and efficacy of PRS110 we tested the ovarian cancer cell line EBC-1 as a positive control. PRS110 had an IC_{50} of 1.1 ±0.08 μg/mL in the EBC-1 cell line (Figure 5 - 1). We then tested whether PRS110 at 10μg/mL could enhance response of neratinib and saracatinib at their respective IC50 concentrations (see Table 4 - 1). No significant increase in response relative to the single agents of neratinib or saracatinib was observed (Figure 5 - 2).

a

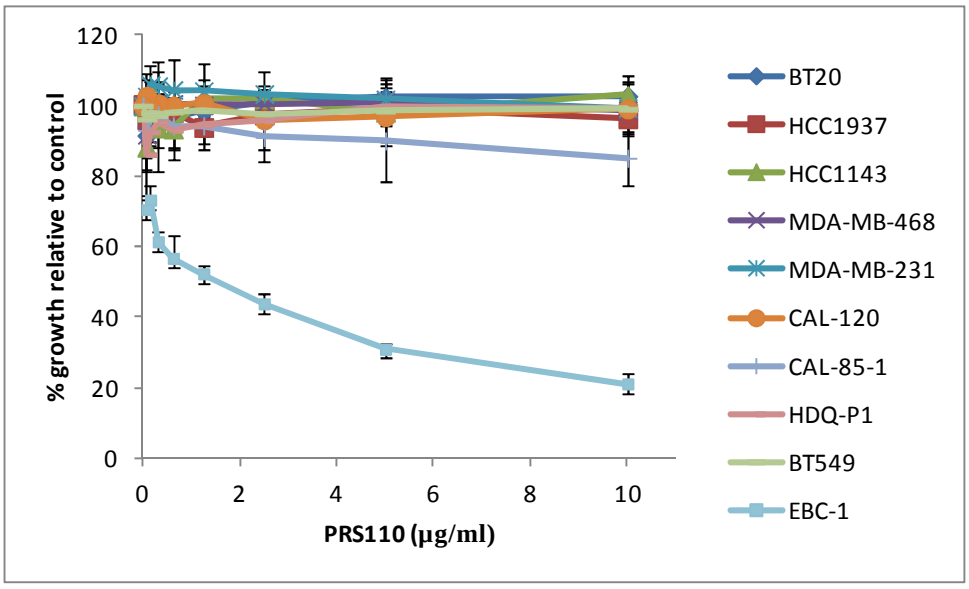

b

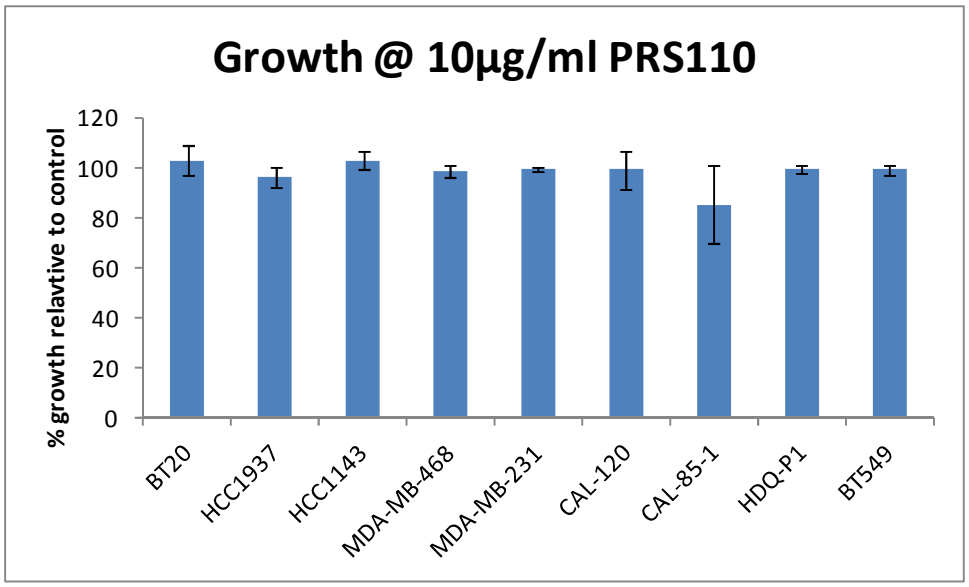

Figure 5 - 1 Proliferation assays of TNBC cell lines treated with PRS110 at serially decreasing concentrations from 10 µg/mL relative to vehicle control in 2D proliferation. Error bars represent the standard deviations of triplicate independent experiments.

a

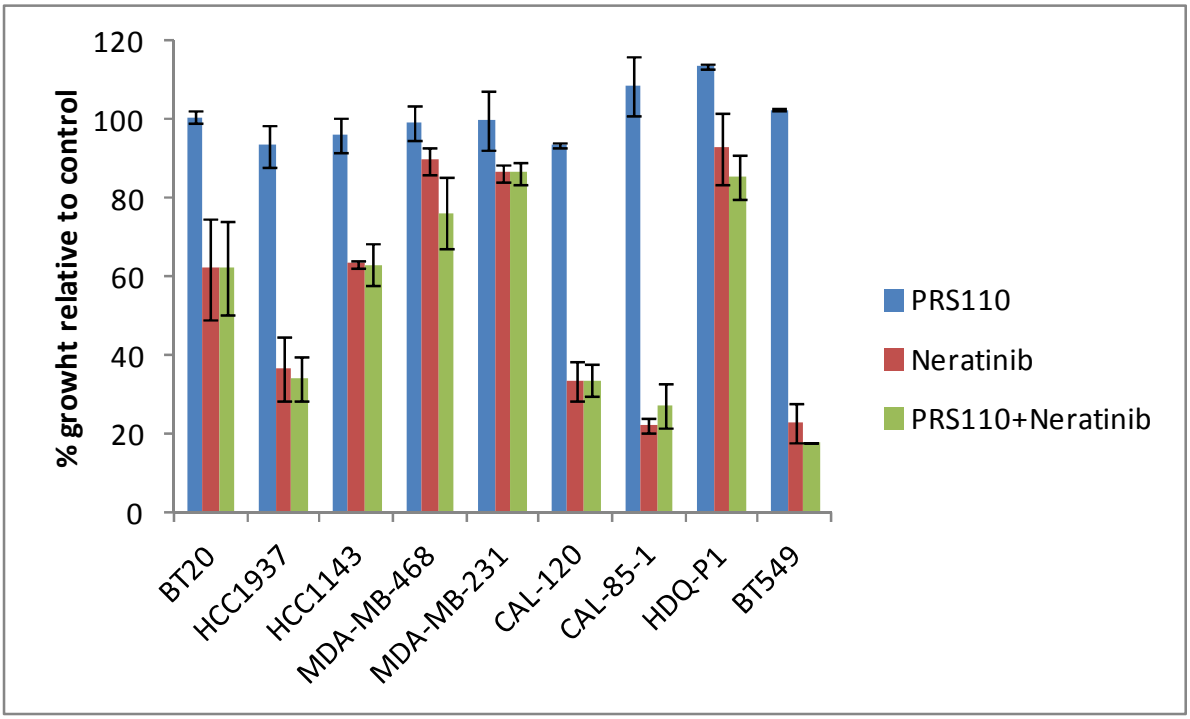

b

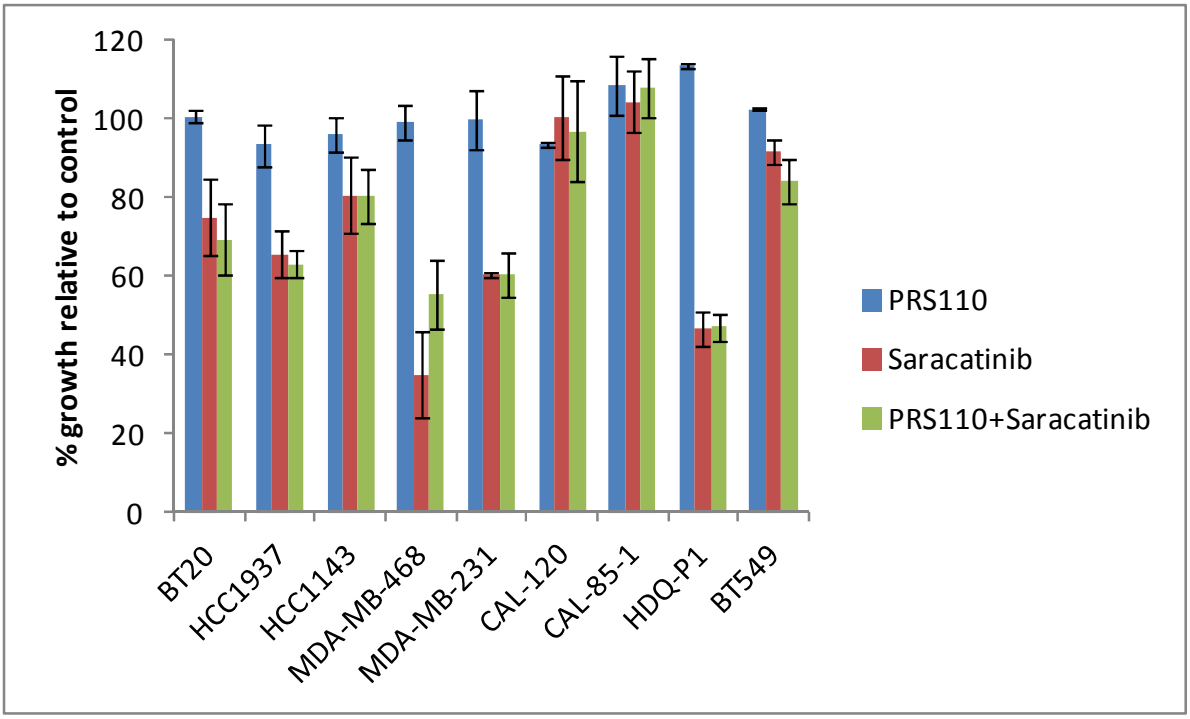

Figure 5 - 2 Proliferation assays in TNBC cells treated with PRS110 (10 µg/mL) and a) neratinib and b) saracatinib. Error bars represent the standard deviation of triplicate independent experiments.

5.2.2 Clonogenic assays

Additionally we tested the cell lines using the 2D clonogenic assay as described in Chapter 4. Briefly, clonogenic assays measure a cells ability to self-propagate

indefinitely by forming colonies from single cells. This assay is supposed to artificially represent this hallmark of cancer cells. We treated five cell lines (minimum 1 selected from each subtype of TNBC available to us) with 10 μg/mL PRS110. Representative Images are shown in Figure 5 – 3. HCC1937, HCC1143 and MDA-MB-231 cell lines all showed a significant reduction in the percentage area covered following treatment with PRS110 (p= 0.002, 0.01 and 0.02 respectively). HCC1143 was the most sensitive cell line with 56.4 ± 5.3 % reduction in area covered relative to untreated control. The HCC1143 was also the only cell to show a significant reduction in intensity of colonies relative to an untreated control (p=0.02) (Figure 5 - 4). I have previously described the response to neratinib and saracatinib in clonogenic assays in chapter 4. Briefly, HCC1937, HCC1143 and MDA-MB-231 tested showed a statistically significant decrease (p = 0.02, 0.02 and 0.001 respectively) in the percentage area cover with neratinib treatment. The HCC1143 and MDA-MB-231 cell lines also showed a statistically significant (p= 0.05 and 0.003 respectively) decrease in average intensity of colonies. Similarly, HCC1937, HCC1143 and MDA-MB-231 showed a statistically significant decrease (p= 0.002, 0.02 and 0.0006 respectively) in percentage area cover with saracatinib treatment and every cell line except HCC1937 showed a statistically significant decrease in colony intensity. Combining PRS110 and neratinib resulted in a significant decrease in percentage intensity and average intensity (p= 0.02 and 0.03 respectively) in MDA-MB-468 cells (Figure 5 - 5). The combination of PRS110 and saracatinib resulted in no significant increase in response to PRS110 alone either percentage area covered or in intensity of colonies although the MDA-MB-231 showed a trend towards decreased colony formation with the combination (Figure 5 - 6).

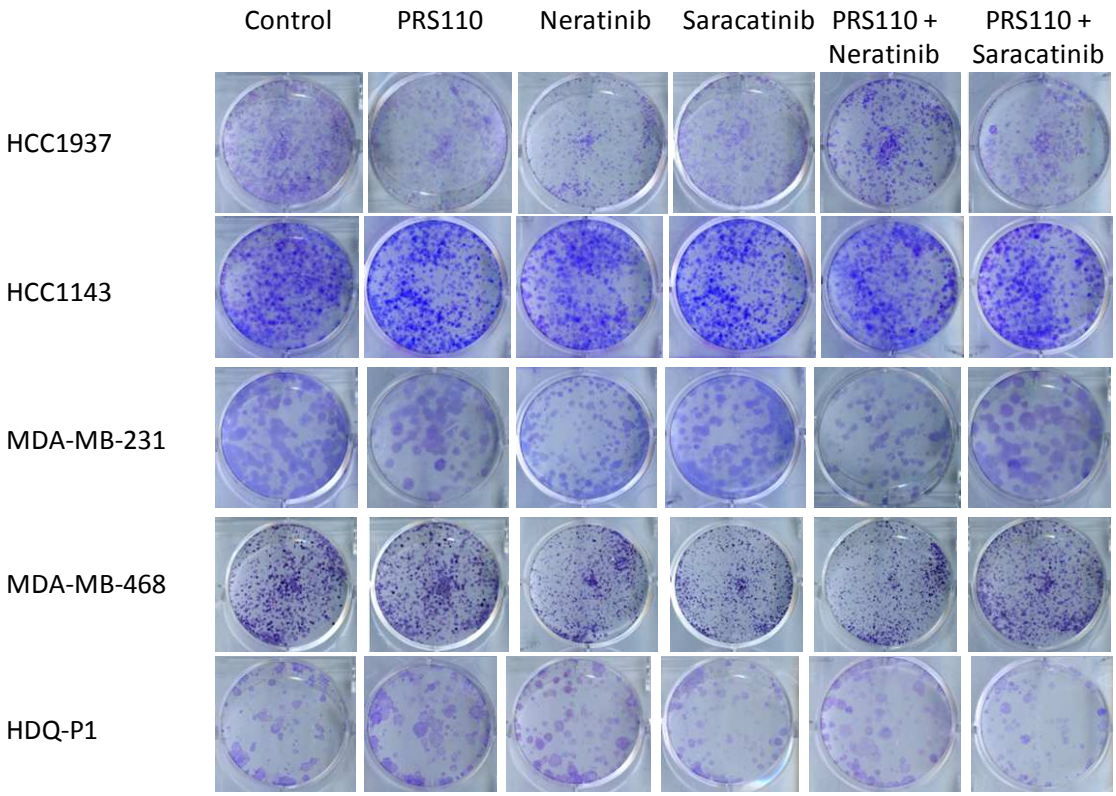

Figure 5 - 3 Representative images of colonies from clonogenic assays untreated or with PRS110, neratinib or saracatinib as single agents or with PRS110 in combination neratinib or saracatinib.

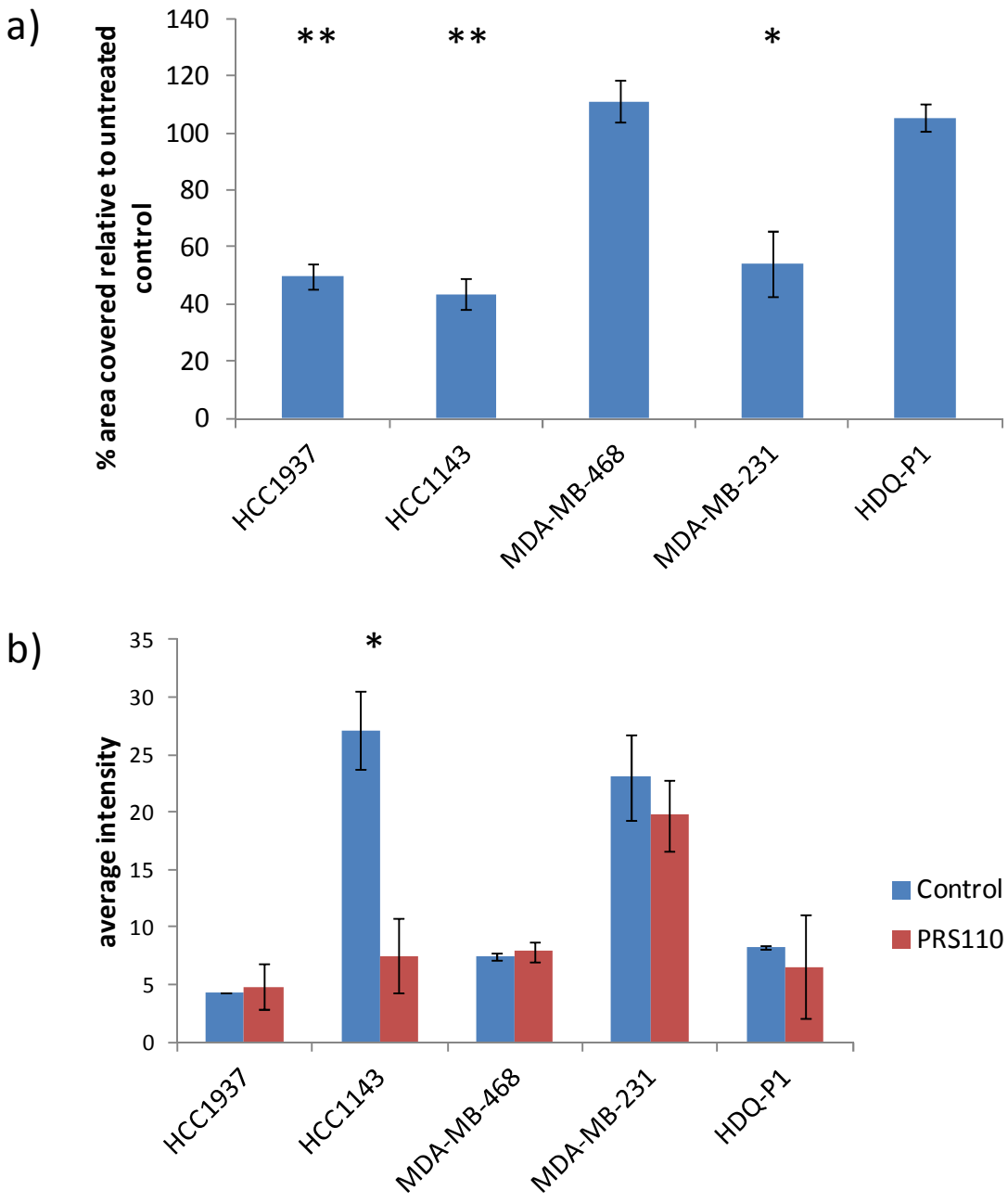

Figure 5 - 4 Clonogenic assays showing % area covered by colonies relative to untreated control 14-21 days post treatment with a) 10 µg/mL PRS110 and b) average intensity of colonies analysed after 14/21 days post treatment. *= $p < 0.05$, **= $p<0.01$ Error bars represent the standard deviations of triplicate independent experiments.

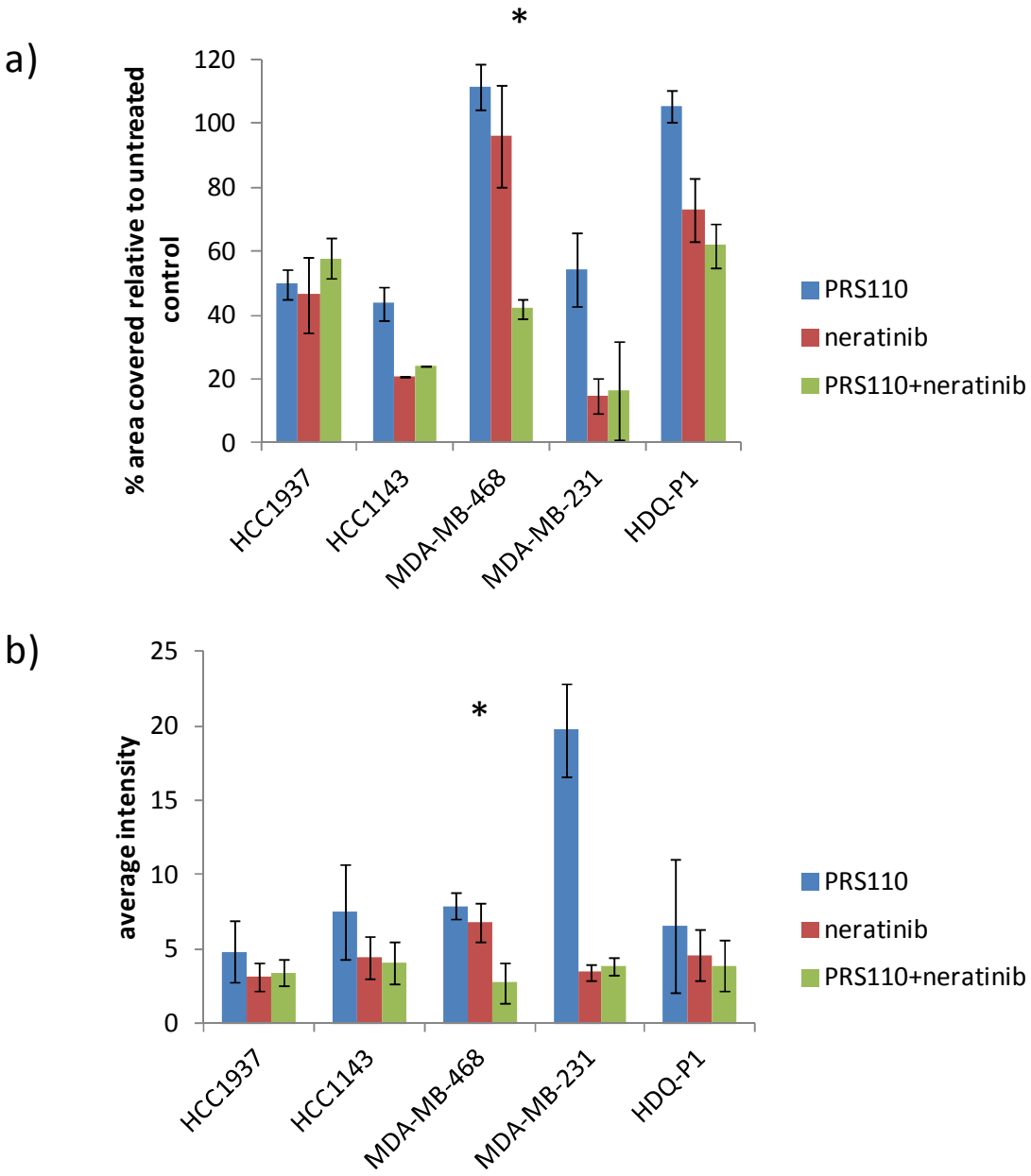

Figure 5 - 5 Clonogenic assays showing % area covered by colonies treated with PRS110 and neratinib in combination b) average intensity of colonies analysed after 14/21 days post treatment at 10 µg/mL PRS110 and IC_{20} concentrations as determined by 2D proliferation assays in 5.2.1. *= p< 0.05. Error bars represent the standard deviation of independent triplicate experiments.

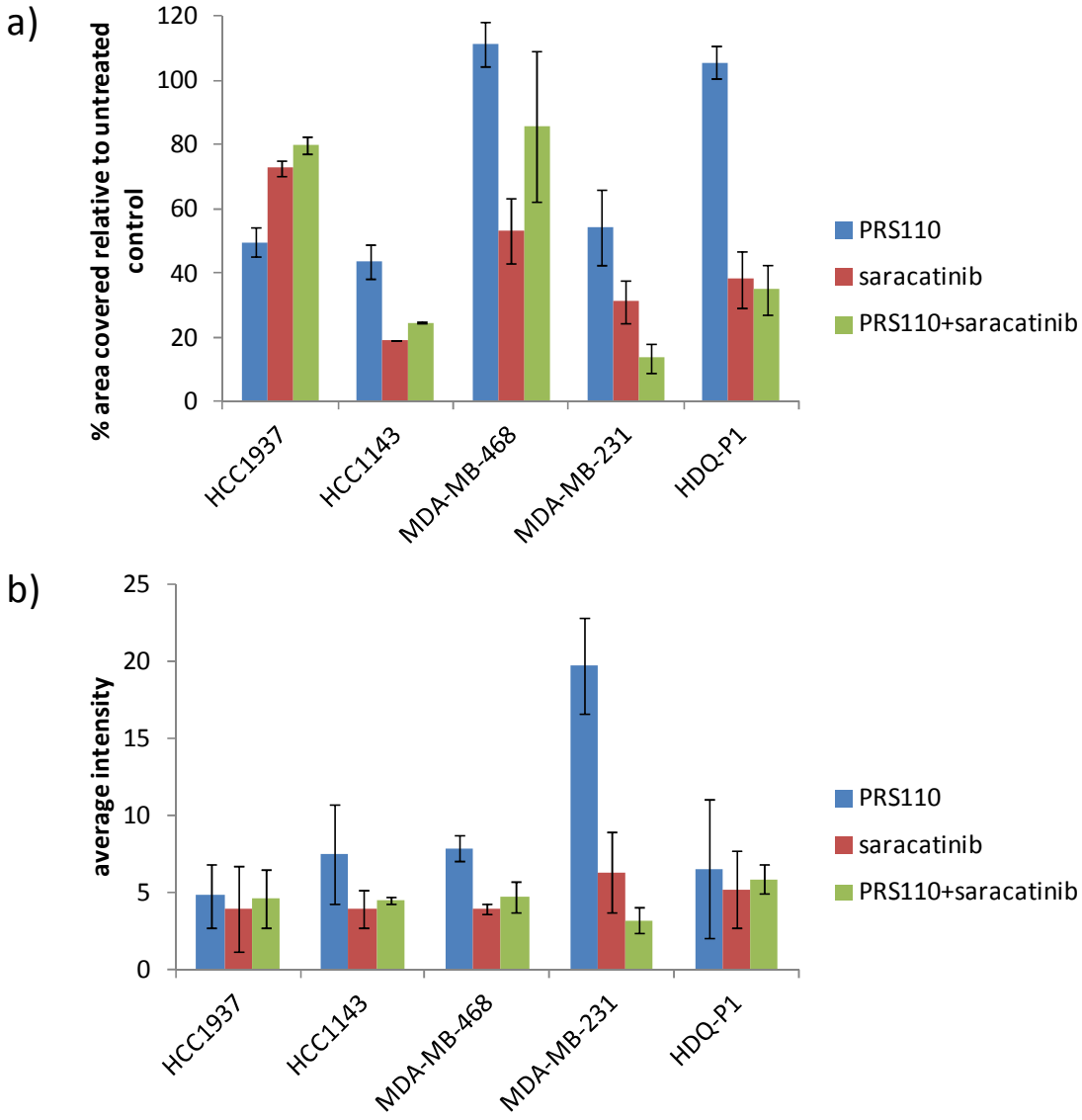

Figure 5 - 6 Clonogenic assays showing % area covered by colonies treated with PRS110 and saracatinib in combination b) average intensity of colonies analysed after 14/21 days post treatment at 10 µg/mL PRS110 and IC_{20} concentrations as determined by 2D proliferation assays in 5.2.1. Error bars represent the standard deviation of independent triplicate experiments.

5.3 Sensitivity to PRS110 in 3D assays

We tested our panel of cell lines for sensitivity to PRS110 using a 3D matrigel based assay and viability was determined using PrestoBlue® reagent. The cell lines were tested in a similar experimental set up as that of the 2D acid phosphatase assays. The cells were seeded and drugged the following day with serially decreasing concentrations of PRS110 from 10 μg/mL. Representative images of colonies are displayed in Figure 5 – 7 . No significant response was seen to treatment at the highest concentration (10 μg/mL) as described in Figure 5 – 8. When compared to 2D assays no significant difference is observed between the 2D and 3D proliferation assays. (Table 5 - 1).It is of note however that at lowest concentrations tested, PRS110 demonstrated an agonistic effect on three of the seven cell lines tested, the highest increase being the MDA-MB-231 with a % viability of 125.4 ± 8.9 when treated with 0.16 μg/mL PRS110 (Figure 5 - 8).

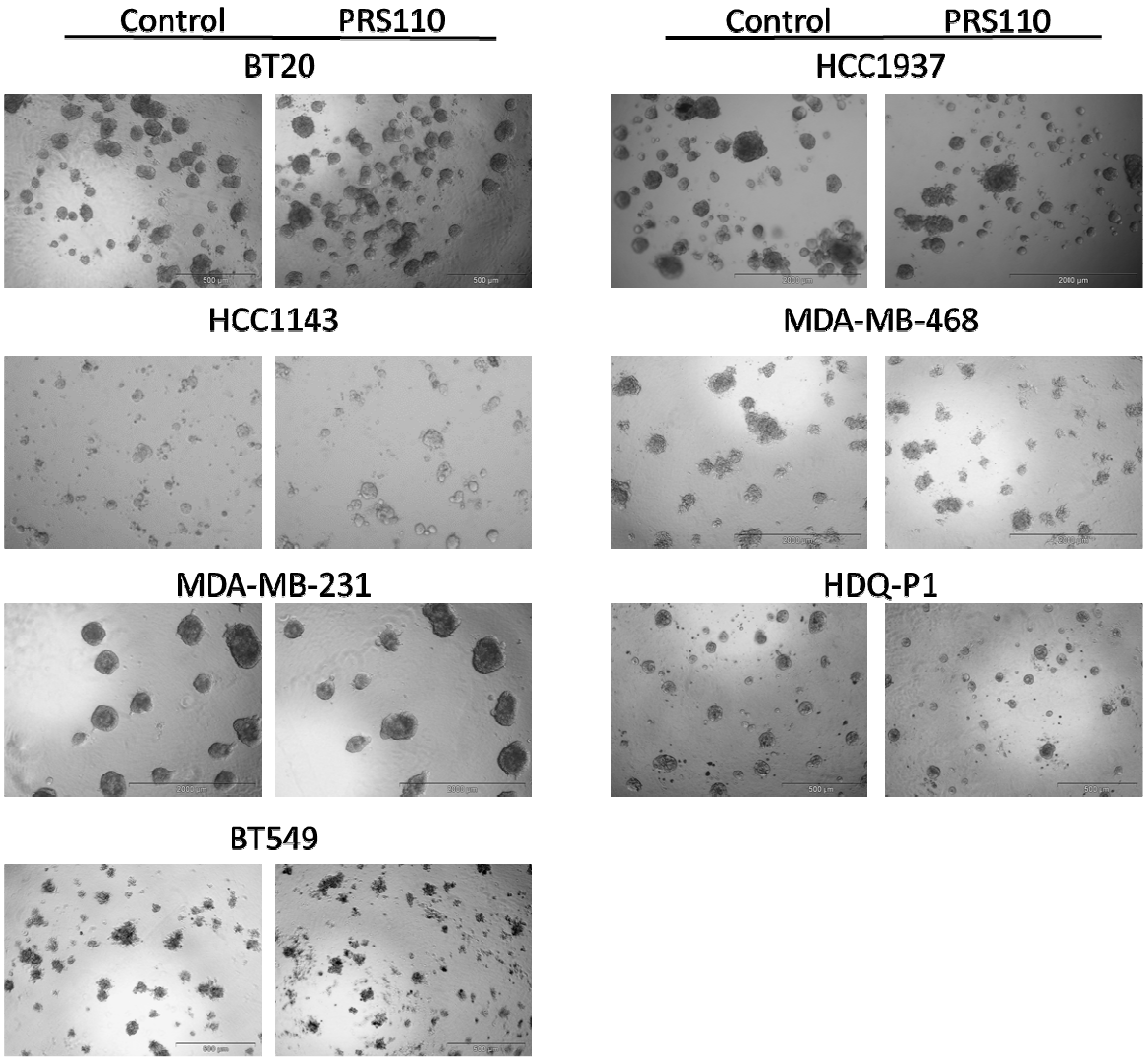

Figure 5 - 7 3D colonies formed after 5/7 days growth in 2-4% matrigel with/without PRS110 treatment (10 µg/mL).

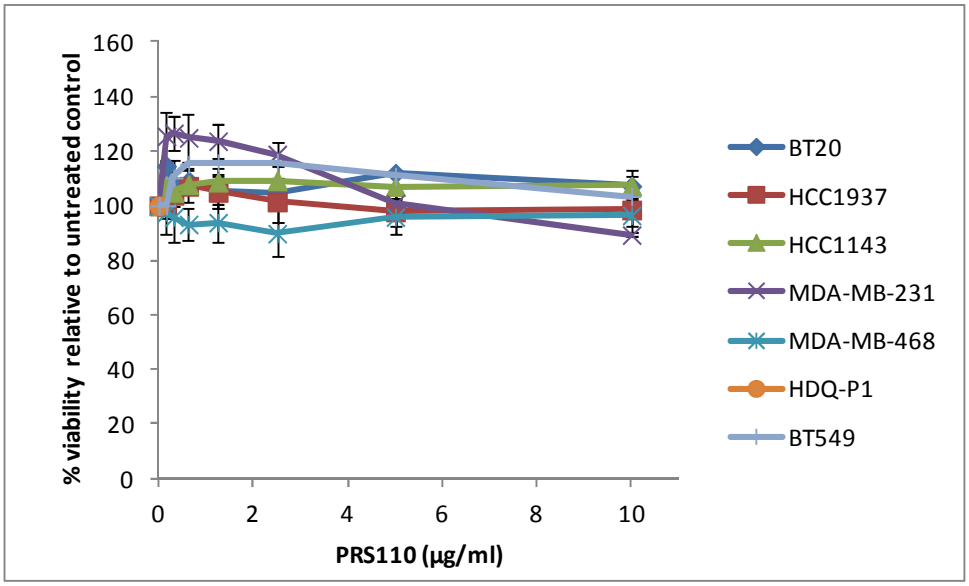

Figure 5 - 8 Percentage viability of cells in colony formation assay after 5/7 day treatments with serially decreasing concentrations of PRS110 from 10 µg/mL. Error bars represent standard deviations of independent triplicate experiments.

Table 5 - 1 Comparison of growth in 2D v 3D growth assays at 10 µg/mL PRS110 ± standard deviations which represent independent triplicate experiments.

Cell Line	% growth @ 10 µg/mL-2D	% growth @ 10 µg/mL-3D
BT20	102.7 ± 6.1	107.2 ± 5.6
HCC1937	96.4 ± 4.2	98.5 ± 6.2
HCC1143	102.9 ± 3.4	107.2 ± 3.8
MDA-MB-231	99.4 ± 0.7	89.3 ± 0.8
MDA-MB-468	98.8 ± 2.3	96.5 ± 6.3
HDQ-P1	99.1 ± 1.5	101.2 ± 5.7
BT549	99.0 ± 2.1	103.4 ± 2.1

5.4 Sensitivity to PRS110 in invasion assays

Coinciding with the 2D and 3D proliferation assays no significant response was seen to single agent treatment with 10 µg/mL PRS110 (Table 5 - 2, Figure 5 - 9). For representative images of invasion assays see Chapter 4. No significant enhancement of response to PRS110 was seen with the combination of neratinib or saracatinib however

the combination of PRS110 and neratinib in CAL-85-1 cells showed a non-significant decrease in invasion (Figure 5 - 10).

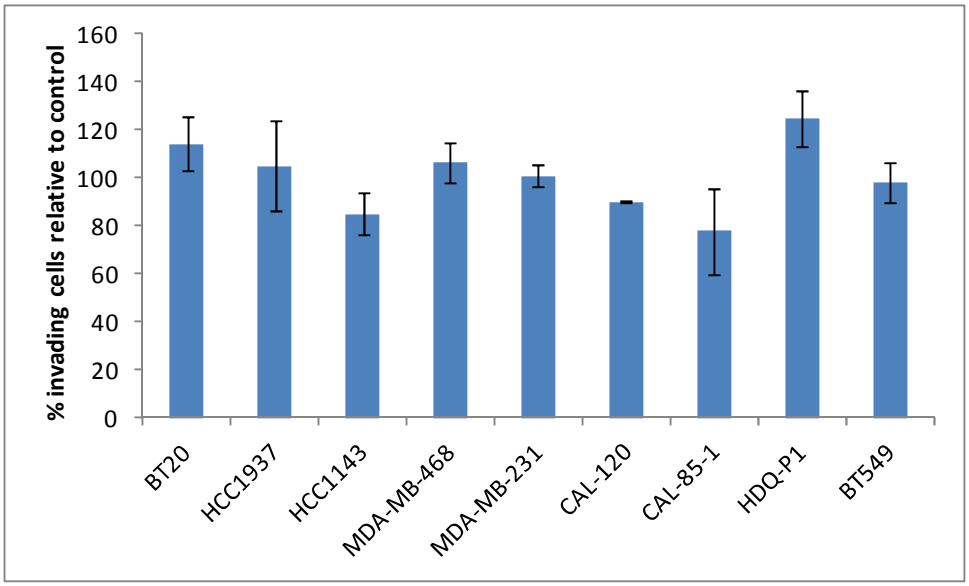

Figure 5 - 9 Sensitivity of TNBC cell lines to PRS110, in invasion assays, at a fixed concentration of 10 µg/mL. Error bars represent standard deviation of three independent biological replicates.

Table 5 - 2 shows the % invasion post treatment with 10 µg/mL PRS110 relative to untreated control.

Cell Line	% Invasion
BT20	114.1 ± 11.4
HCC1937	105.0 ± 18.8
HCC1143	85.2 ± 8.8
MDA-MB-468	106.7 ± 8.5
MDA-MB-231	100.8 ± 4.7
CAL-120	90.2 ± 0.4
CAL-85-1	77.8 ± 18.2
HDQ-P1	124.8 ± 11.4
BT549	98.4 ± 8.5

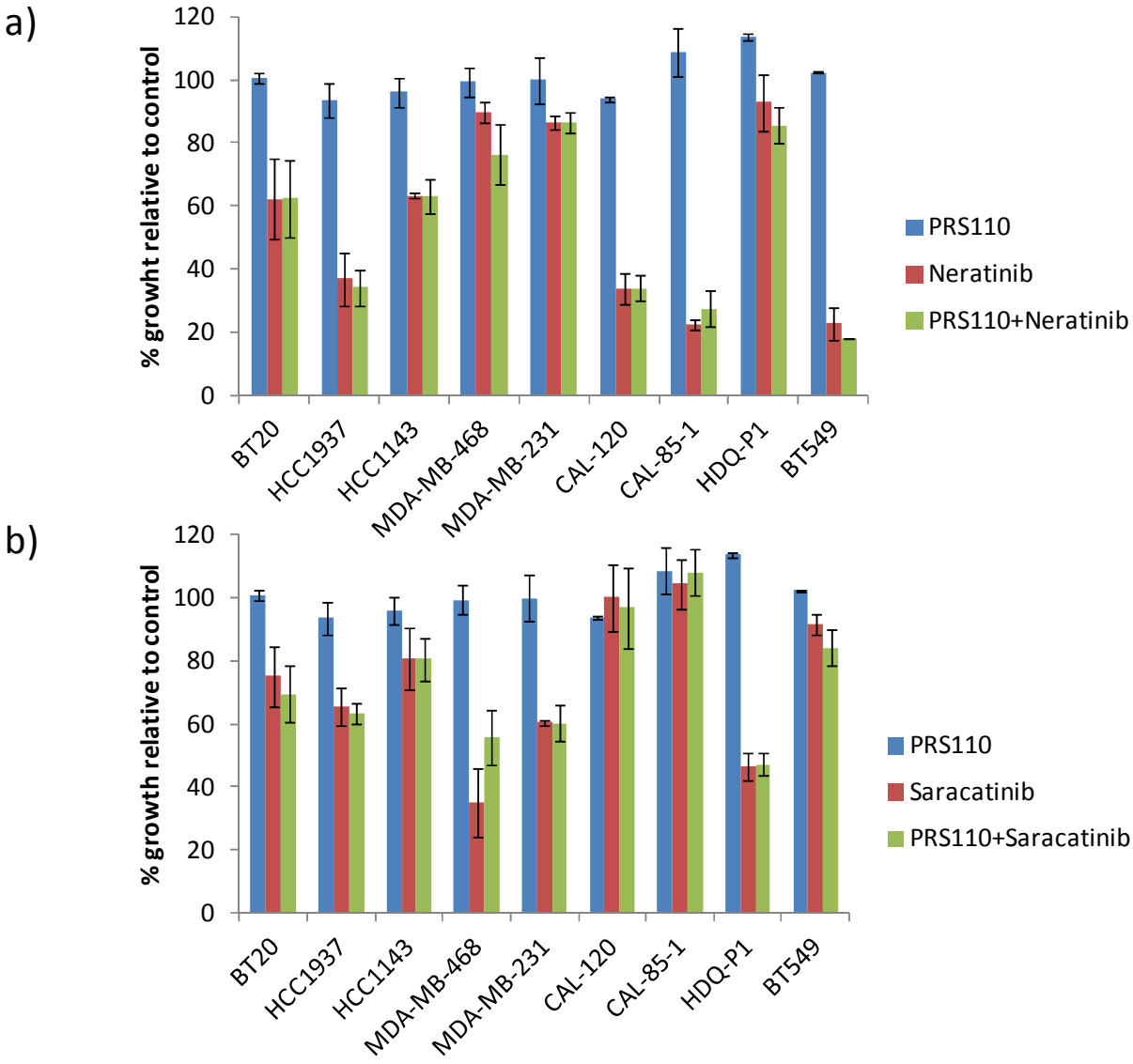

Figure 5 - 10 Sensitivity of TNBC cell lines in invasion assays a) treated with PRS110 and neratinib in combination at 1 µM and b) with PRS110 and saracatinib in combinations at 1 µM. Error bars represent standard deviation of triplicate independent experiments.

5.5 RTK signalling post PRS110 and neratinib treatment

PRS110 has showed a limited response in each of the assays tested in all of the TNBC cell lines. The CAL-85-1 cell line showed the best response, showing the highest level of inhibition in 2D proliferation assays and invasion assays. Additionally the combination of the PRS110 and neratinib in CAL-85-1 cell line resulted in a significantly decreased level of invasion. For these reasons we chose the CAL-85-1 cell line for further evaluation. To investigate the interaction of PRS110 in TNBC cells with neratinib, we used a multiplex magnetic bead assay to examine the phosphorylation of seven commonly expressed RTKs in TNBC. The CAL-85-1 cell line was treated with 0.625 µg/mL of PRS110 and 5 nM of neratinib as either single agents or in combination for 6 hrs prior to protein extraction. PRS110 decreased phosphorylation of c-Met by 71.6 ± 19.8%. Neratinib also decreased phosphorylation of EGFR and HER2 as expected however interestingly it also significantly reduced phosphorylation of c-Met. No other RTK showed significant changes in phosphorylation and the combination of PRS110 and neratinib did not significantly reduce phosphorylation compared to either agent alone (Figure 5 -11).

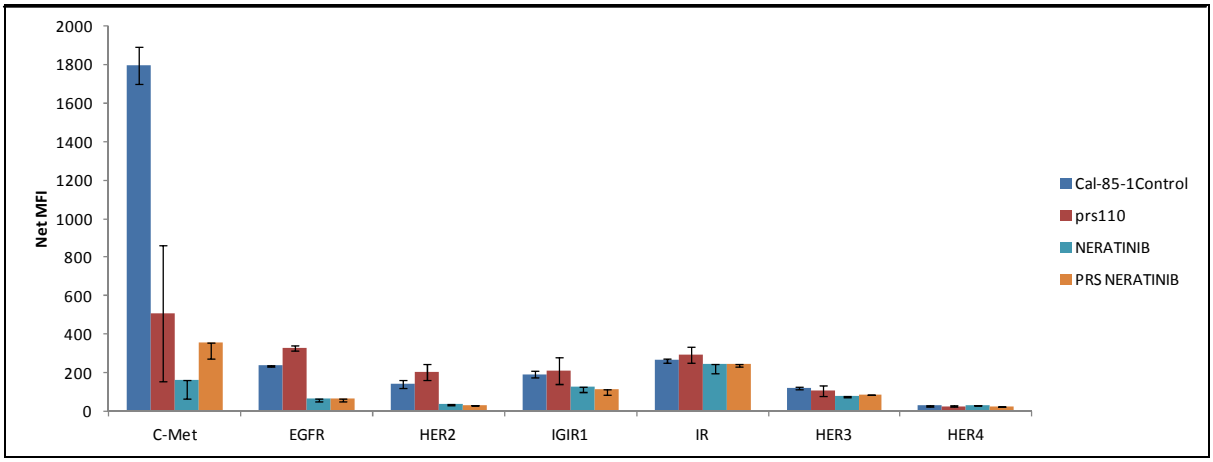

Figure 5 - 11 Phosphorylation levels of seven RTKS as determined via multiplex magnetic bead assays on CAL-85-1 cell line treated with PRS110 and neratinib, as single agents or in combination. Net MFI is median fluorescence intensity. Error bars represent the standard deviations of triplicate independent experiments.

5.6 Combined inhibition of c-Met with ALK, Axl and RON

BMS777607 is a small molecule TKI for c-Met, Axl, Ron and Tyro3 with IC_{50} of 3.9 nM, 1.1 nM, 1.8 nM and 4.3 nM respectively. Axl has been implicated in TNBC

through interaction with EGFR stimulating diverse downstream signalling pathways not activated by EGFR alone. Although not as thoroughly investigated it has been shown that Axl associates with c-Met in a similar fashion and may therefore activate c-Met independently of HGF which may not be targetable by extracellular inhibitors such as PRS110. RON is a family member of RTKs of which c-Met is the prototypic member. RON and c-Met share approximately 60% sequence homology and are thought to signal in similar fashions. Because of this duplicity it has been suggested that dual inhibition of c-Met and RON may be advantageous. We also dually inhibited c-Met and ALK using the small molecule inhibitor crizotinib. Crizotinib targets c-Met and ALK with IC_{50} of 11 and 24 nM respectively [255]. The M subtype of TNBC has shown upregulation of ALK pathway suggesting that a subset of patients may benefit from dual inhibition. We tested our panel of TNBC cell lines for sensitivity to BMS777607 and tested four cell lines for sensitivity to crizotinib.

5.6.1 BMS777607

Only two the cell lines tested with BMS777607 showed a percentage inhibition above 50%. These were BT20 and BT549, reached greater than 50% inhibition at 10 µM. The HCC1937 and the HDQ-P1 also showed a moderate inhibition of growth (33.8 ± 4.5 % and 34.6 ± 5.3% respectively) and while the other cell lines did not show any sensitivity (Figure 5 - 12).

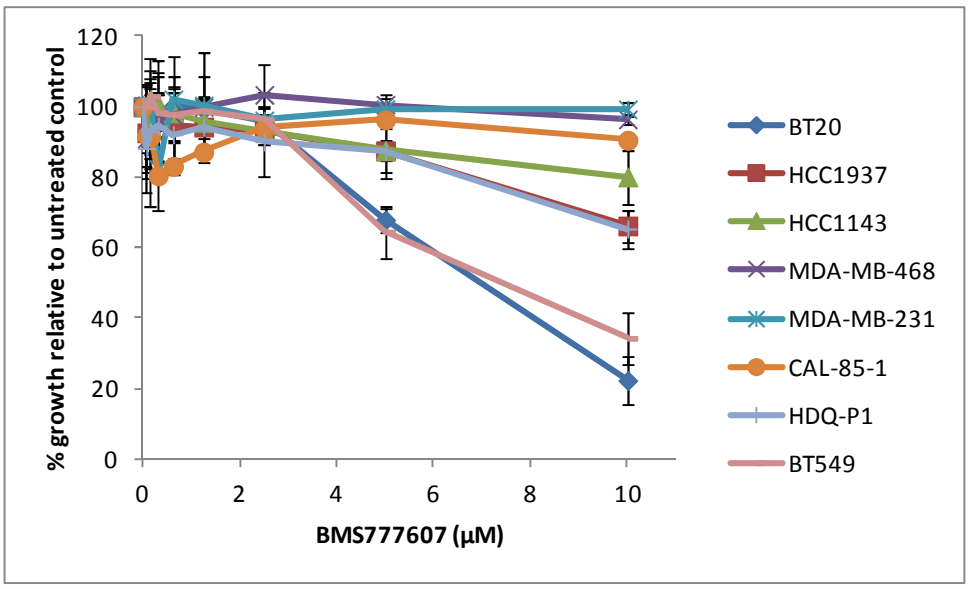

Figure 5 - 12 Sensitivity of TNBC cell lines to BMS777607 at serially decreasing concentrations from 10 µM. Error bars represent standard deviations in of independent biological triplicates.

5.7 Crizotinib

We initially tested crizotinib in four cell lines, BT20, HCC1143, MDA-MB-231 and MDA-MB-468. Only the HCC1143 showed modest effect to crizotinib. Due to the lack of efficacy of crizotinib in the TNBC cell lines it was not tested in remainder of the panel (Figure 5 - 13).

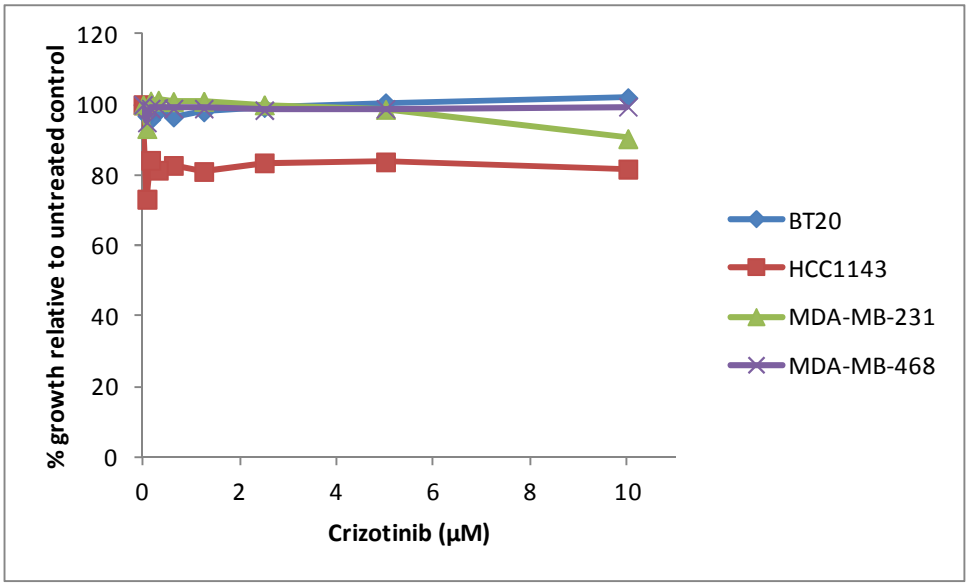

Figure 5 - 13 Sensitivity of four TNBC cell lines to crizotinib at serially decreasing concentrations from 10 µM. Error bars are indicative of independent biological replicates

5.8 Summary

PRS110 showed very little effect in proliferation assays despite varying levels of activation of c-Met in the TNBC cell lines. To confirm the activity of PRS110 in our experimental setup we tested an ovarian cancer cell line EBC-1 which we knew to be sensitive to c-Met inhibition. The EBC-1 cell line was tested at identical concentrations to the TNBC cell lines and showed a high level of sensitivity with 78.8 ± 2.9 % PRS110 has the ability to inhibit both ligand dependent and ligand independent activation. Ligand independent activation typically occurs through activation of adjacent RTKs by their respective ligands, the most likely candidate being EGFR, additionally the literature suggests a ligand independent mechanism of activation through a positive feedback loop involving c-Src. Based on these assumption we tested the combination of

EGFR inhibitor neratinib and c-Src inhibitor saracatinib. The combinations yielded no significant enhancement of response in proliferation assays.

Interestingly despite a lack of response to the acid phosphatase assays, 3 of 5 cell lines tested show significant inhibition of clonogenic growth in response to PRS110. This was accompanied by a significant decrease in intensity for two of these cell lines suggestive of a reduction in the number of cells per colony. Combining PRS110 with neratinib and saracatinib did not enhance the effects of PRS110. Anchorage independent growth, invasion and migration were also tested but no significant sensitivity was observed in majority of the cell lines. The CAL-85-1 cell lines showed some sensitivity in both proliferation and invasion assays, although the effects did not achieve statistical significance. In invasion assays the combination of PRS110 and neratinib showed a trend towards significance with a p value of 0.07 in the CAL-85-1 cell line.

Unfortunately, the CAL-85-1 did not form colonies in either 3D anchorage independent growth and the no. of colonies formed in clonogenic assays was too low to be interpreted accurately in response to treatment so we could not interpret results from these assays. We examined phosphorylation levels of seven RTKs in the CAL-85-1 treated with PRS110 and neratinib. This once again confirmed the efficacy of PRS110 which caused a reduction in p-Met levels. Interestingly neratinib not only caused a decrease in the HER family members as well as a marked reduction in c-Met.

Finally despite disappointing results from c-Met inhibition as a single agent and in combination with EGFR and c-Src we tried inhibitors which combine inhibition of other RTKs implicated in TNBC and prospective candidates suggested from the literature. BMS777607 only caused inhibition above 50% in two cell lines while crizotinib showed no response in four cell lines tested. Due to this lack of response to crizotinib we found it redundant to continue to test the rest of the panel.

Chapter 6

c-Met inhibition in a dasatinib resistant TNBC cell line

6.1 Introduction

Dasatinib is a multi-targeted tyrosine kinase inhibitor whose targets include BCR/Abl and Src family kinases. Pre-clinical work by Finn *et al.* suggested that basal-like breast cancer cell lines show higher sensitivity to dasatinib than luminal cell lines and suggest dasatinib as a potential targeted treatment for TNBC [192]. However, as a single agent in phase 2 clinical trials, dasatinib, showed limited efficacy in unselected TNBC and is currently being tested in combination with chemotherapeutics and additional targeted therapies [220, 256]. Previous work by Dr. Brendan Corkery in our laboratory led to the development and characterisation of a dasatinib resistant variant of the MDA-MB-231 cell line designated 231-DasB. The cell line was developed by constant exposure to incrementally increasing concentrations of dasatinib, from 200 nM to 500 nM over a period of 13 weeks. The 231-DasB cells show constitutive activation of c-Src even in the presence of dasatinib. Given the direct links between c-Src and c-Met we examined whether c-Met could potentially play a role in acquired resistance to dasatinib in TNBC.

6.2 Phosphorylated Src in MDA-MB-231 and 231-DasB cell lines

231-DasB and parental MDA-MB-231 were treated with 100 nM Dasatinib for 6 hours. MDA-MB-231 cells show a significant reduction in levels of p-Src compared to 231-DasB cells ($p=0.0004$) in agreement with results previously presented by Dr. Brendan Corkery (Figure 6 - 1). The 231-DasB cells show constitutive activation of p-Src (Y418) even in the presence of dasatinib. 231-Das B cells show limited response to dasatinib at concentrations up to 10 μM, whereas the dasatinib IC_{50} is 0.005 ± 0.0004 μM in MDA-MB-231. The Src family kinases consist of 9 family members with high conservation between family members at Y418. We examined phosphorylation of seven of these proteins using magnetic multiplex. In agreement with the western blots the MDA-MB-231 showed a significant reduction in p-Src. p-FYN, p-YES and p-LYN also show reductions (although not statistically significant) in phosphorylation after treatment with dasatinib. In the 231-DasB, treatment with dasatinib resulted in no decrease in phosphorylation of any of the Src proteins examined (Figure 6 - 2).

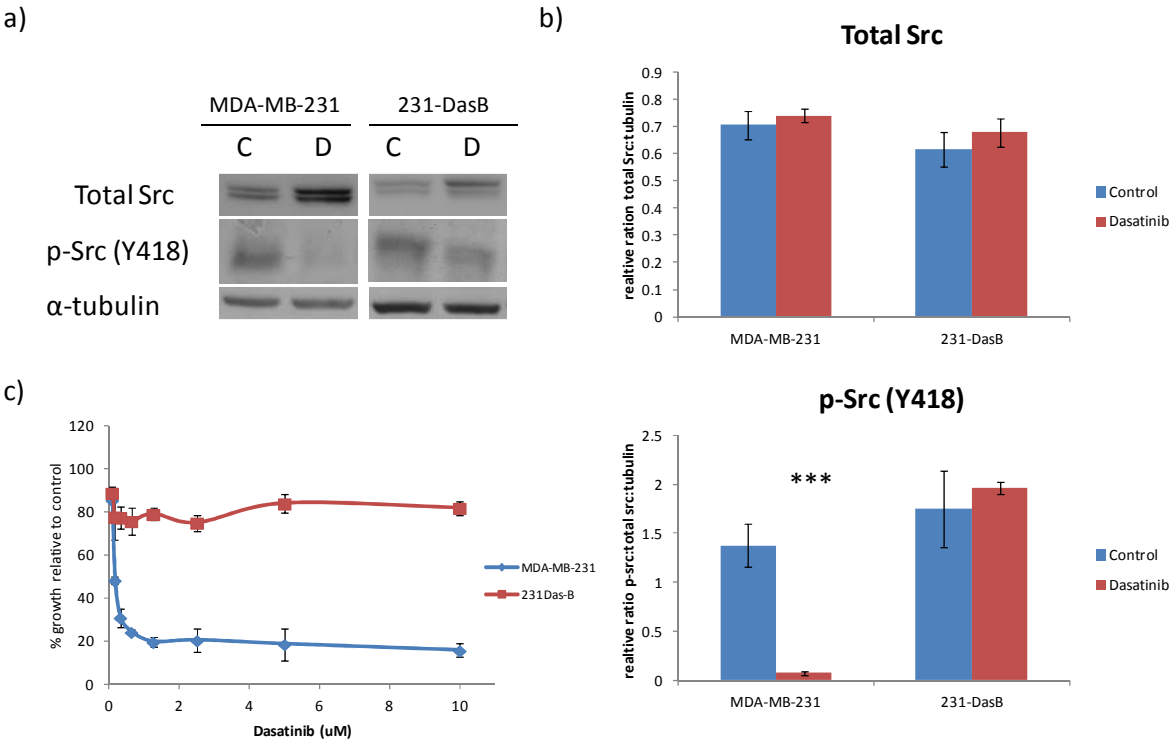

Figure 6 - 1a) Western blotting of MDA-MB-231 and 231-DasB treated with 100nM Dasatinib (D) for 6hrs b) Densitometry analysis of immunoblots of MDA-MB-231 and 231-DasB treated with 100nM Dasatinib. c) Dose response curves of MDA-MB-231 and 231-DasB treated with serially decreased concentrations of dasatinib from 10 µM. Error bars represent the standard deviations of independent biological triplicates. ***= p< 0.001

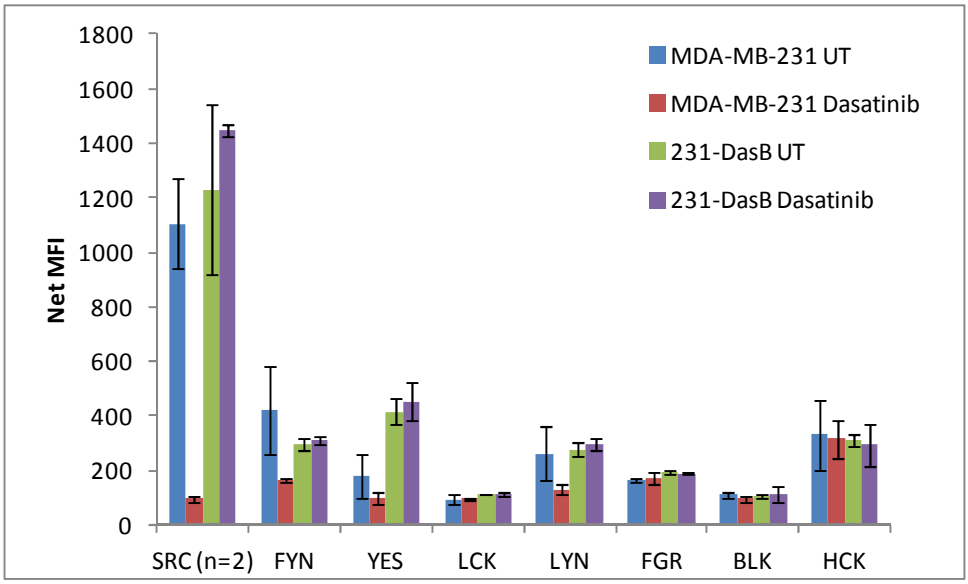

Figure 6 - 2 Phosphorylation of Src family kinases as determined by multiplex bead assay in MDA-MB-231 and 231-DasB cell lines with and without 6hr dasatinib treatment (100 nM). Error bars represent the standard deviations of triplicate independent experiments except for SRC values for MDA-MB-231, which is standard error of two independent experiments.

6.3 c-Met in 231-DasB cell line

Constitutive phosphorylation of the Src family kinases (SFKs) in the 231-DasB cell line was observed as described above. Increased activation of RTKs up-stream of SFKs may contribute to this activation. The phosphorylation status of five candidate RTKs (c-Met, EGFR, HER2, IGFIR, and IR was examined. c-Met (panTYR) was the only RTK to show any alteration in phosphorylation in the 231-DasB cells. 231-DasB cells show significantly higher levels of p-Met (p= 0.004) compared to the MDA-MB-231 (Figure 6 – 3).

Given the increased activation of p-Met in the 231-DasB cell line we hypothesised this may lead to an increased sensitivity to c-Met inhibition. 231-DasB is more sensitive to CpdA with an IC_{50} of 2.1 ± 0.1 µM compared to the MDA-MB-231 cells where CpdA has an IC_{50} of 3.5 ± 0.2 µM. The combination of CpdA and dasatinib resulted in significantly decreased growth in the MDA-MB-231 (p=0.02), however no significant effect of the combination was observed in 231-DasB cells. In a fixed ratio combination CpdA and Dasatinib show synergism with a combination index (CI) value of 0.8 ± 1.3 (Figure 6 – 4). Dr. Brendan Corkery previously described how 231-DasB showed no

significant response to dasatinib compared to MDA-MB-231 in invasion assays. We confirmed this result and examined the effect of CpdA and the combination of CpdA and dasatinib in MDA-MB-231 and 231-DasB. No significant response was seen to CpdA however the combination resulted in significantly ($p=0.002$) decreased invasion in the MDA-MB-231 cell line. No significant response was observed in the 231-DasB cell line (Figure 6 - 5). We examined the phosphorylation of the SFKs after treatment with CpdA. No significant change is observed in the parental MDA-MB-231 in response to treatment, however six of the eight p-SFKs show a significant reduction in phosphorylation in 231-DasB. FYN, YES, LCK, LYN, FGR and BLK all show significant reductions in phosphorylation ($p= 0.02, 0.02, 0.009, 0.003$ and 0.02) in response to CpdA treatment (5 µM) (Figure 6 – 6).

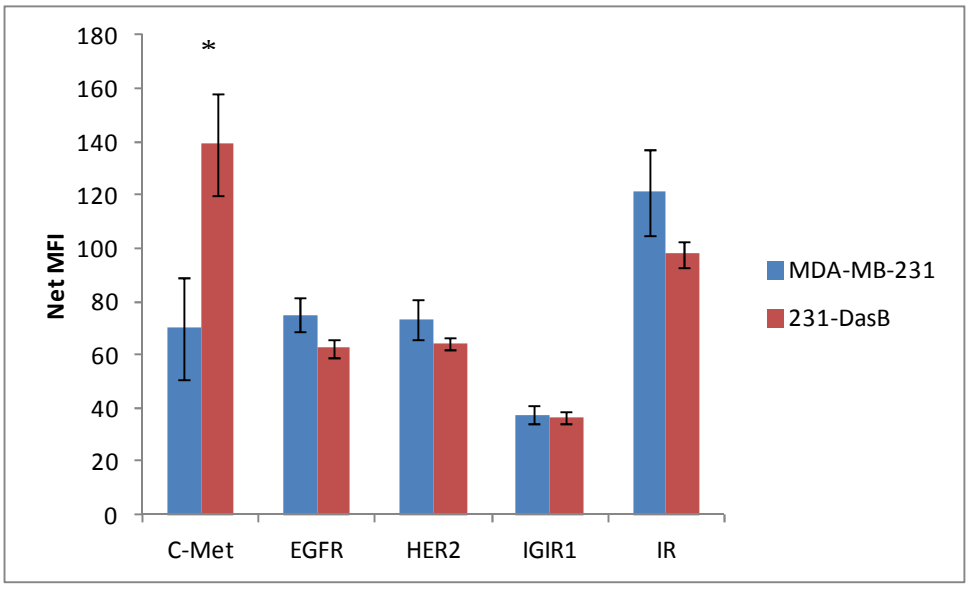

Figure 6 - 3 Phosphorylation of four RTKs in the MDA-MB-231 and 231-DasB cell lines. Error bars are standard deviations of independent biological triplicates.

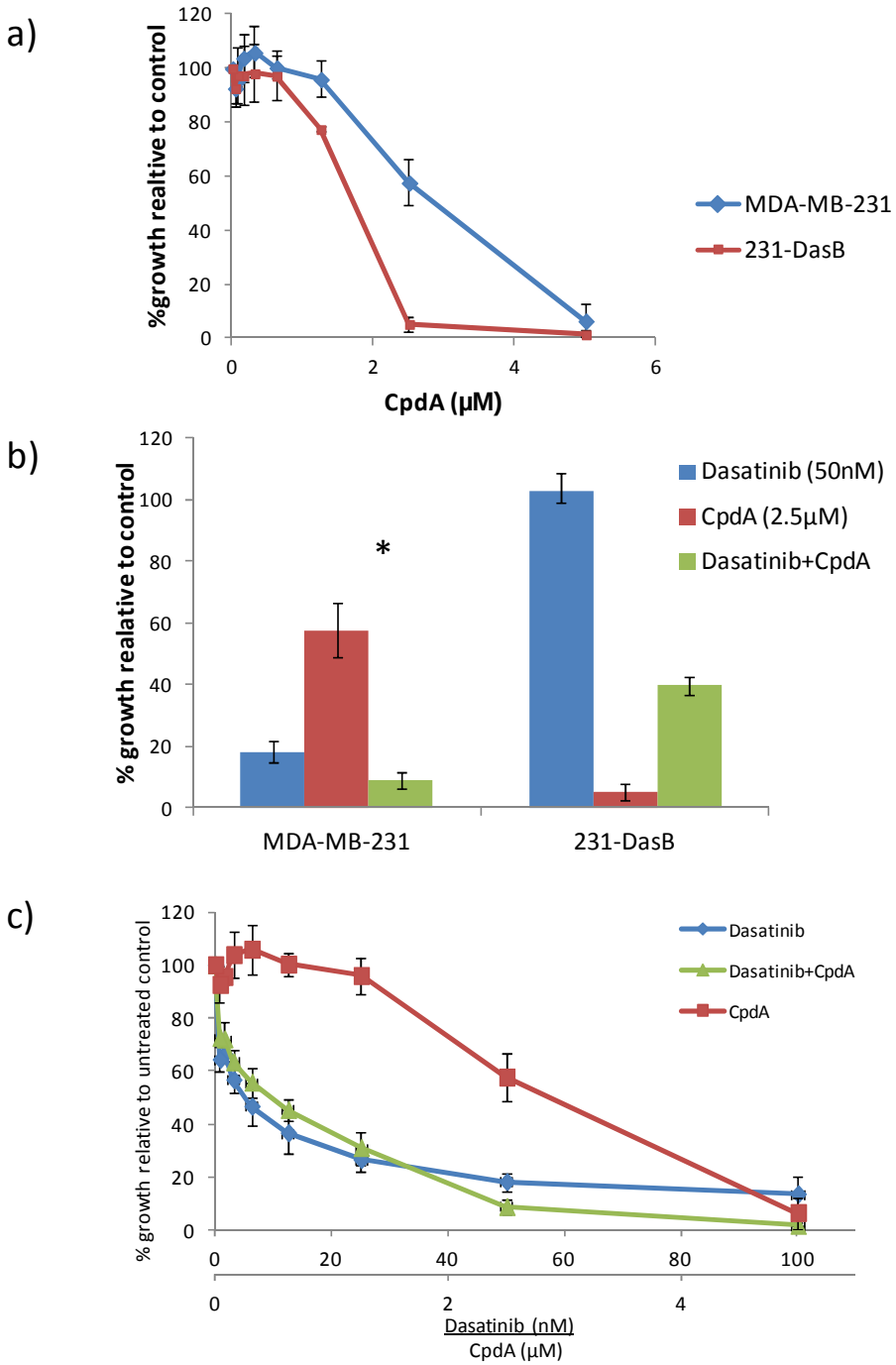

Figure 6 - 4 a) MDA-MB-231 and 231-DasB dose response curves with serially decreasing concentrations of CpdA from 5 µM. b) Fixed concentration proliferation assays at 50 nM dasatinib and 2.5 µM in MDA-MB-231 and 231-DasB cell lines. c) Fixed ratio combination of serially decreasing concentrations of dasatinib (from 100 nM) and CpdA (from 5 µM) in MDA-MB-231 cell line * = p< 0.05 Error bars represent the standard deviation of independent biological experiments.

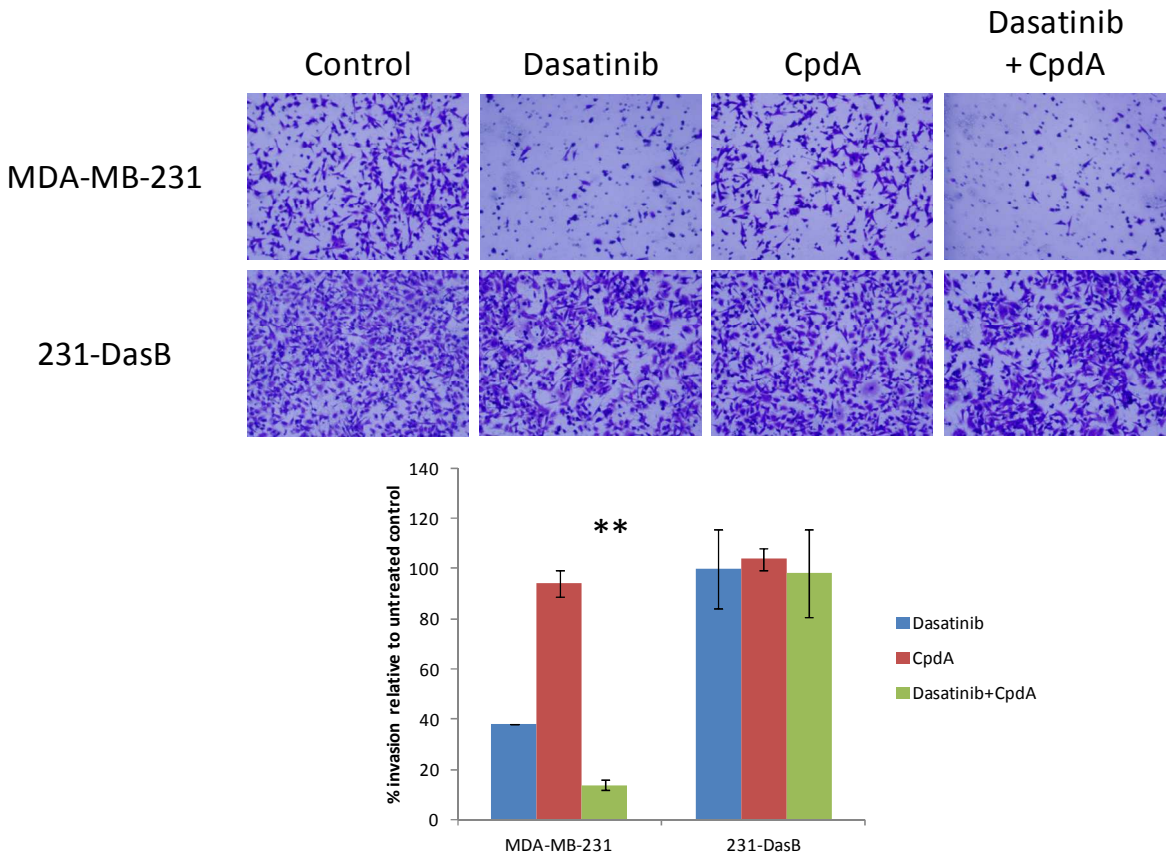

Figure 6 - 5 Representative images of invasion assays on top either untreated or with dasatinib (100 nM) or CpdA (5 µM) as described. % invasion relative to untreated control is shown below. ** = p < 0.01 Error bars represent the standard deviations of triplicate independent experiments.

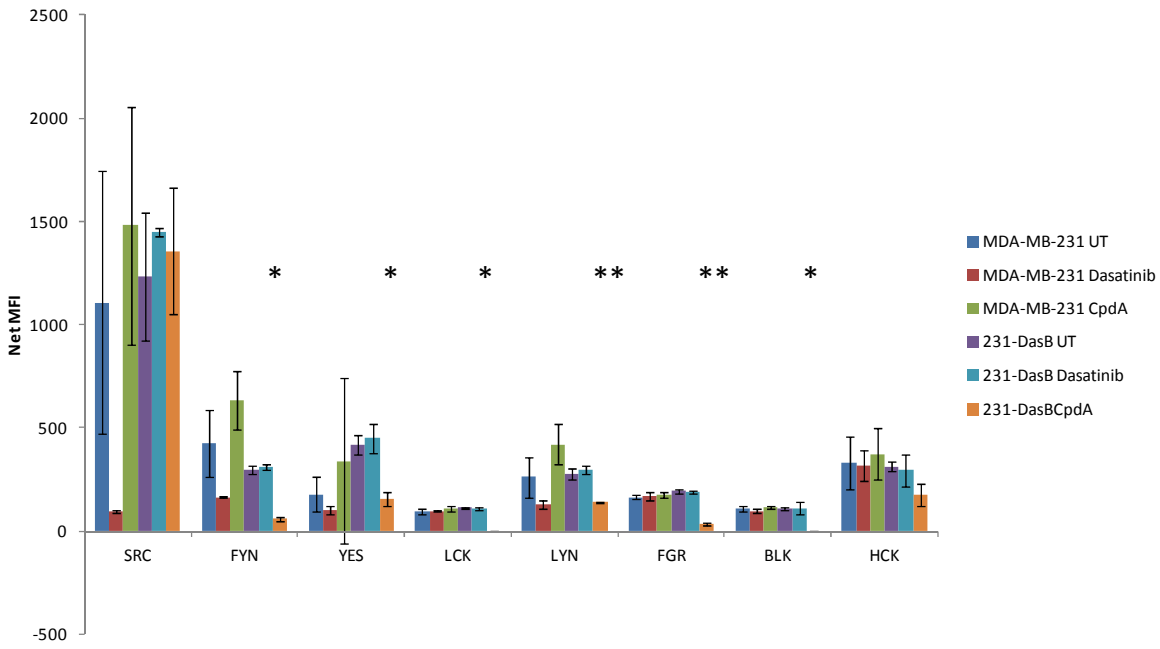

Figure 6 - 6 Phosphorylation of SFKs in MDA-MB-231 and 231-DasB in response to dasatinib 100 nM treatment and CpdA (5 µM) where NET MFI is net median fluorescence intensity. * = p<0.05, ** = p< 0.01 Error bars represent the standard deviations of triplicate independent experiments.

6.4 c-Met in MDA-MB-468 cetuximab resistant cell line MDA-MB-468CR

To examine whether the increased sensitivity to c-Met inhibition was potentially a common consequence of resistance in triple negative breast cancer, we obtained the MDA-MB-468CR and the parental MDA-MB-468 cell from the laboratory of Dr. Anthony Kong, University of Oxford. The MDA-MB-468CR cell line was developed by chronic exposure to cetuximab. At 100 µg/mL, the parental MDA-MB-468 showed a significant reduction in growth with 45.7 ± 4.2% growth inhibition compared to 0.1 ± 4.8% in the MDA-MB-468CR cell line (Figure 6 – 7). The MDA-MB-468Cr showed a higher sensitivity to CpdA with IC50 of 2.1 ± 0.2 µM compared to 3.0 ± 0.3 µM in the MDA-MB-468 parental. Combination assays of CpdA and cetuximab showed a modest but not statistically significant (p=0.18) decrease in the MDA-MB-468 cell line with 10.7 ± 6.2% decrease in growth compared CpdA as a single agent. The MDA-MB-468CR cell line also showed a decrease in the combination with 4.1 ± 2.1 % decrease in growth in the combination. The combination of cetuximab and CpdA in a fixed ratio combination in MDA-MB-468 parental cell line resulted in a synergistic combination with a CI value of 0.54 ± 0.004 (Figure 6 - 8).

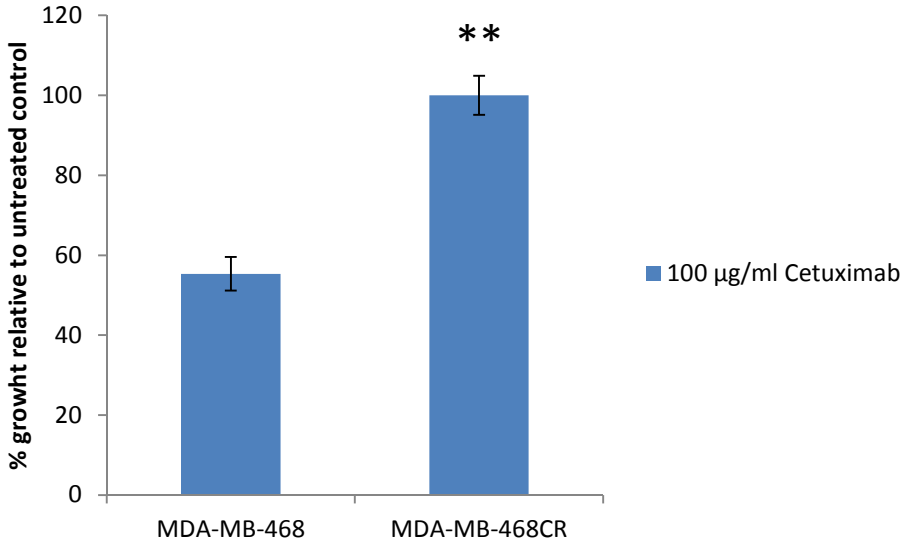

Figure 6 – 7 MDA-MB-468 and MDA-MB-468CR proliferation after 5 day treatment with 100 µg/mL cetuximab.

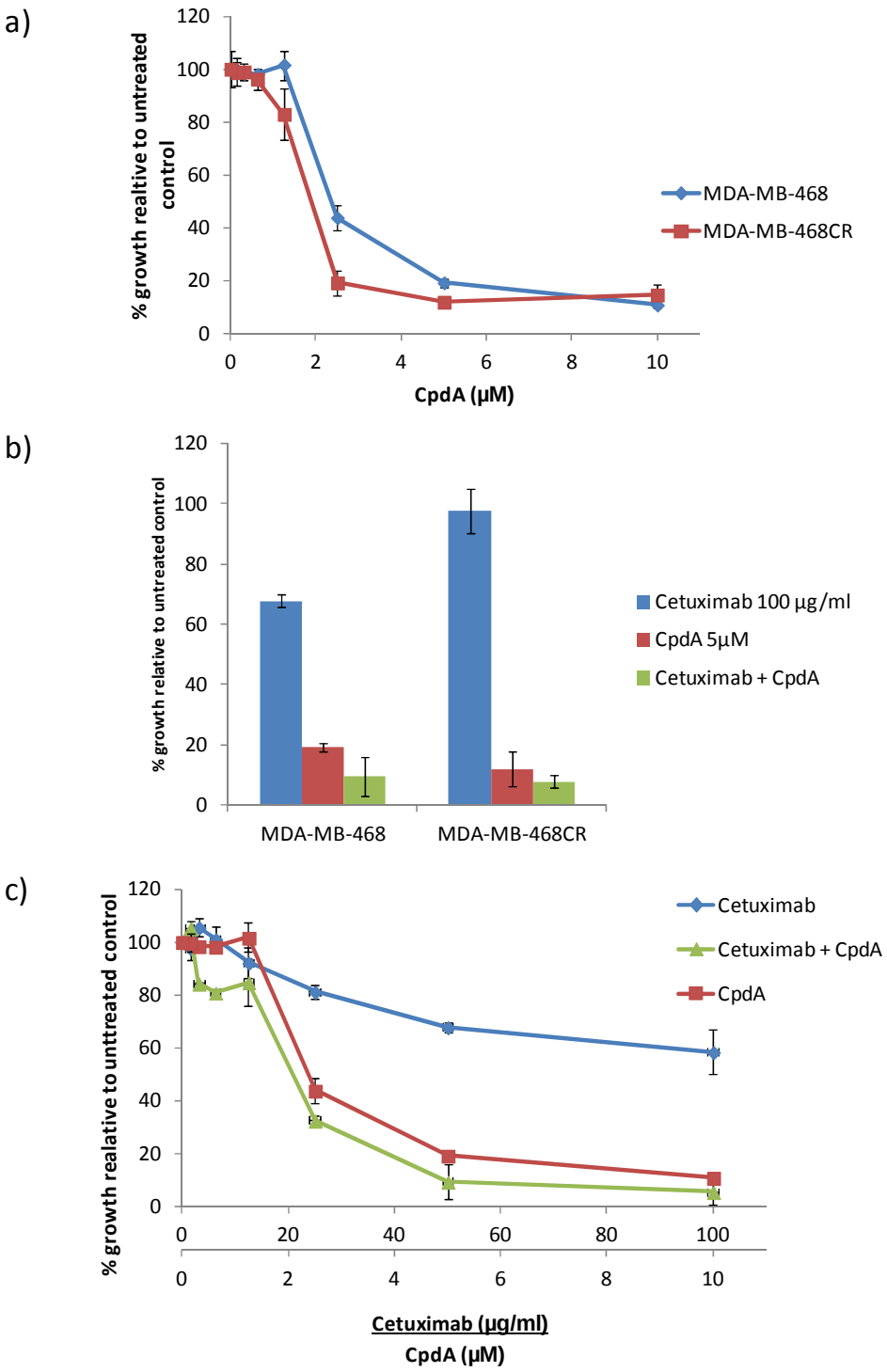

Figure 6 - 8 a) Dose response curves of MDA-MB-468 and MDA-MB-468CR treated with CpdA at serially decreasing concentrations from 10 µM b) fixed concentration combination of Cetuximab and CpdA in MDA-MB-468 and MDA-MB-468CR cell lines. c) Fixed ratio combinations of cetuximab MDA-MB-468 and MDA-MB-468CR.

6.5 Summary

231-DasB cells are resistant to dasatinib up to 10 μM and show constitutive Src phosphorylation. No significant inhibition of phosphorylation of the SFK members tested was observed. 231-DasB cells show increased p-Met and sensitivity to CpdA. Treatment with CpdA in 231-DasB cells results in significantly decreased phosphorylation of FYN, YES, LCK, LYN, FGR and BLK in contrast to the parental cell line. Combinations of CpdA and dasatinib in MDA-MB-231 results in synergistic activity of the compounds on proliferation, whereas the combination does not show activity in 231-DasB. Similarly in invasion assays the combination in MDA-MB-231 significantly reduces invasion greater than either agent alone, with no significant effect in 231-DasB cell line. The MDA-MB-468CR cell line behaves in a similar fashion with greater sensitivity to CpdA than the parental cell line and the combination in the parental cell line results in a synergistic reduction in proliferation in the parental cell line but not in the resistant variant.

Chapter 7

Novel receptor tyrosine kinases associated with TNBC

7.1 Introduction

Receptor tyrosine kinases (RTKs) are a large family of proteins involved in cell to cell signalling eliciting responses in growth, differentiation, adhesion, cell motility and death. Of the 90 tyrosine kinases identified 58 have been classified as receptor type. These 58 receptors can be sub-divided into 20 families [62]. A number of families of RTKs have been implicated in the development of many cancers including HER and IGFR families through over-expression, amplification and/or aberrant signalling of the RTKs [257]. This has led to the development of many target specific drugs in the form of monoclonal antibodies (mAbs) and small molecule inhibitors. Using an algorithm which combines gene expression data from 21 DNA microarray experiments and detailed clinical data to correlate outcome with gene expression levels we correlated the expression of each of the 58 RTKs (as described in Appendix 1) in the basal-like subtype (defined using 3 sets of classifiers (PAM50, ssp2003 and ssp2006)) in relation to the parameters disease free survival (DFS) and overall survival (OS).

Levels of RTK expression were subdivided into 3 groups; the high expression group consisting of those patients present in 75th percentile and above, the median group and the low group consisting of expression levels in the 25th percentile and below. The creation of the algorithm and survival analysis was carried out by Dr. Stephen Madden (DCU). Using a significance cut-off of $p<0.05$ in a minimum of 2/3 sets of classifiers we identified RTKs which may play a role in the development/progression of basal-like breast cancer.

7.2 RTKs associated with poor prognosis

7.2.1 Overview of RTKs implicated in basal-like/TNBC

Using the three cut-offs described above, median expression, greater than the 75th percentile referred to as the 'high' cut-off and less than the 25th percentile referred to as the 'low' cut-off, six RTKs were implicated in a poor prognosis; FGFR1, FGFR3, VEGFR1, PDGFRβ, ROS, TIE1 and EPHA5 (Table 7 - 1).

Table 7 - 1 RTKs associated with poor prognosis

RTK	DFS	OS
FGFR1	High + low	
FGFR3		Median
VEGFR1		High
PDGFRβ	High + Median	High + Median
TIE1		Median
EPHA5	Median	Median
ROS1	Median	

7.2.2 FGFR1

Using the 25th percentile (i.e. low cut-off group) for stratification, high expression of FGFR1 was associated with significantly decreased DFS using PAM50, ssp2003 and ssp2006 (p-value =0.004, 0.039 and 0.022) with hazard ratios of 1.67, 1.46 and 1.44 respectively (Figure 7 - 1). When stratified using the high group FGFR1 was also associated with a significantly decreased DFS in PAM50, ssp2003 and ssp2006 (p= 0.008, 0.009 and 0.009) with hazard ratios of 1.58, 1.53 and 1.58 respectively (Figure 7 - 2).

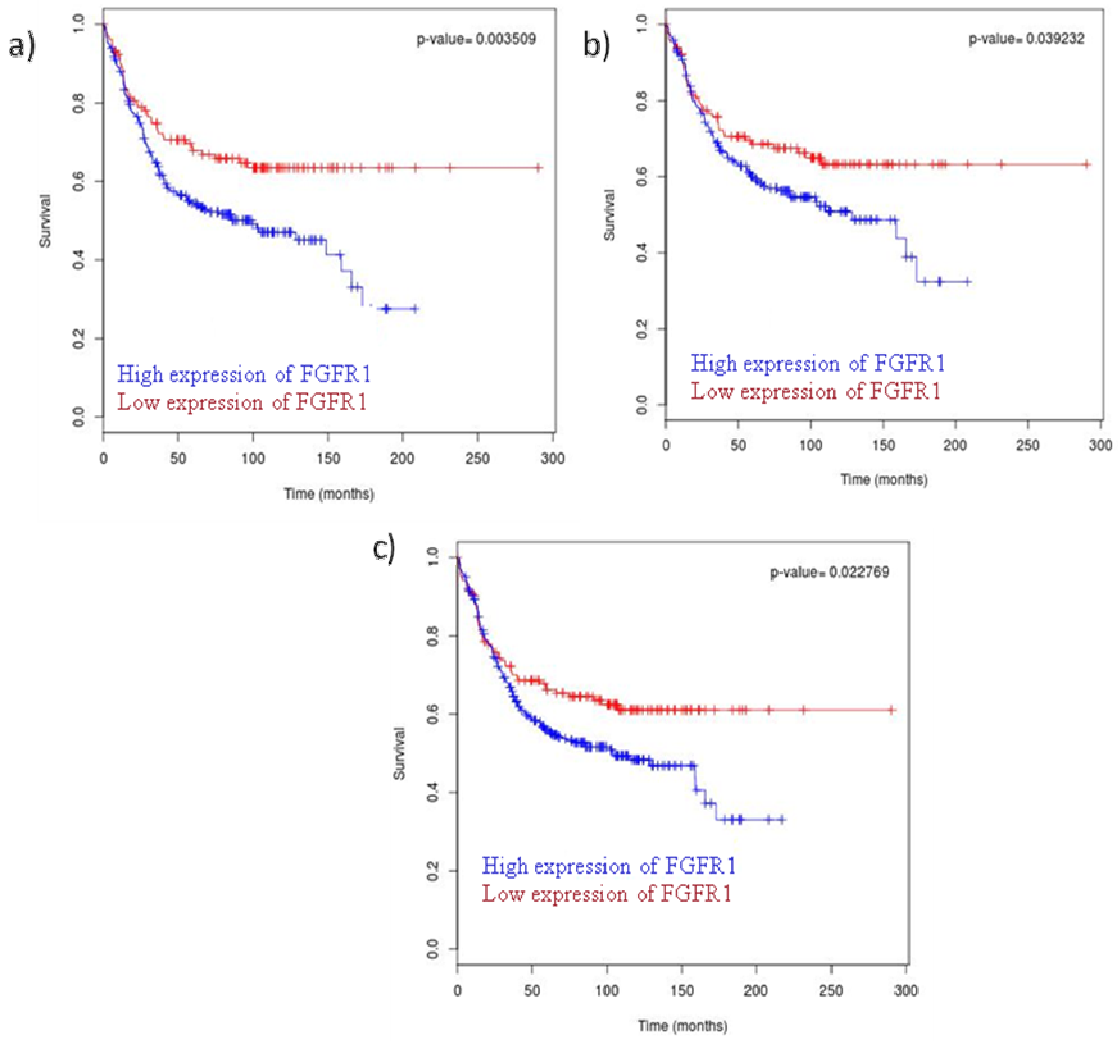

Figure 7 - 1 Kaplan Meier survival curves based on a) PAM50 classifier n= 376 high/low expression b) ssp 2003 n= 349 high/low expression c) ssp 2006 n= 456 high/low expression classifier demonstrating significant decrease in DFS with high expression of FGFR1.

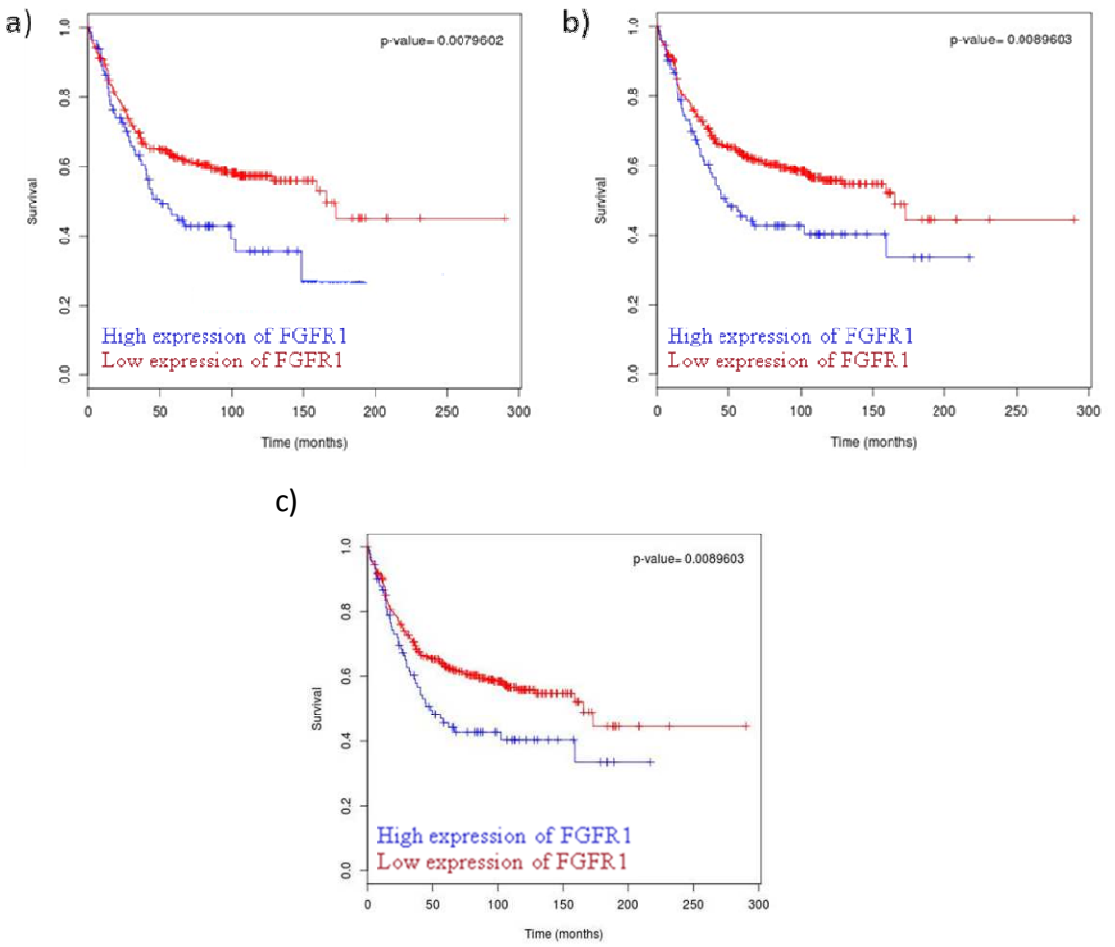

Figure 7 - 2 Kaplan Meier survival curves based on a) PAM50 classifier (n = 376) b) ssp 2003 classifier n= 349 and c) ssp2006 n= 456 demonstrating significant decrease in DFS with high expression of FGFR1.

7.2.3 FGFR3

High expression of FGFR3, using the median cut-off was associated with significantly decreased OS in PAM50 and ssp2006 (p-value = 0.041 and 0.013) with hazard ratios of 1.579 and 1.67 respectively (Figure 7 - 3).

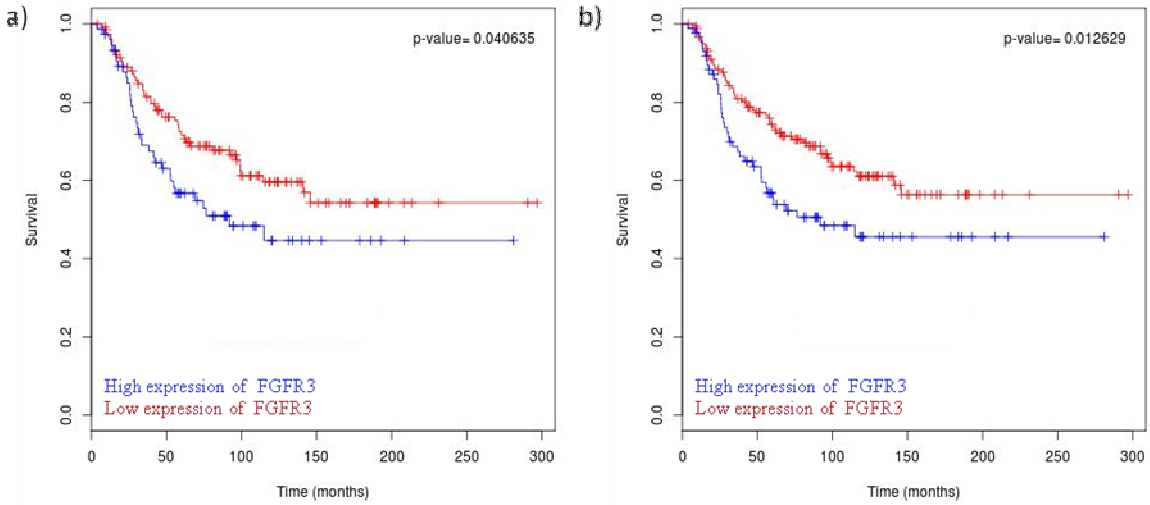

Figure 7 - 3 Kaplan Meier survival curve based on a) PAM50 classifier (n= 211) b) ssp 2006 classifier (n=250) demonstrating significant decrease in OS with high expression of FGFR3.

7.2.4 VEGFR1

High expression of VEGFR1, using the high group as a cut-off, was associated with significantly decreased OS using PAM50, ssp 2003 and ssp2006 (p-value = 0.015, 0.008 and 0.006) with hazard ratios of 1.85, 1.97 and 1.86 respectively (Figure 7 - 4).

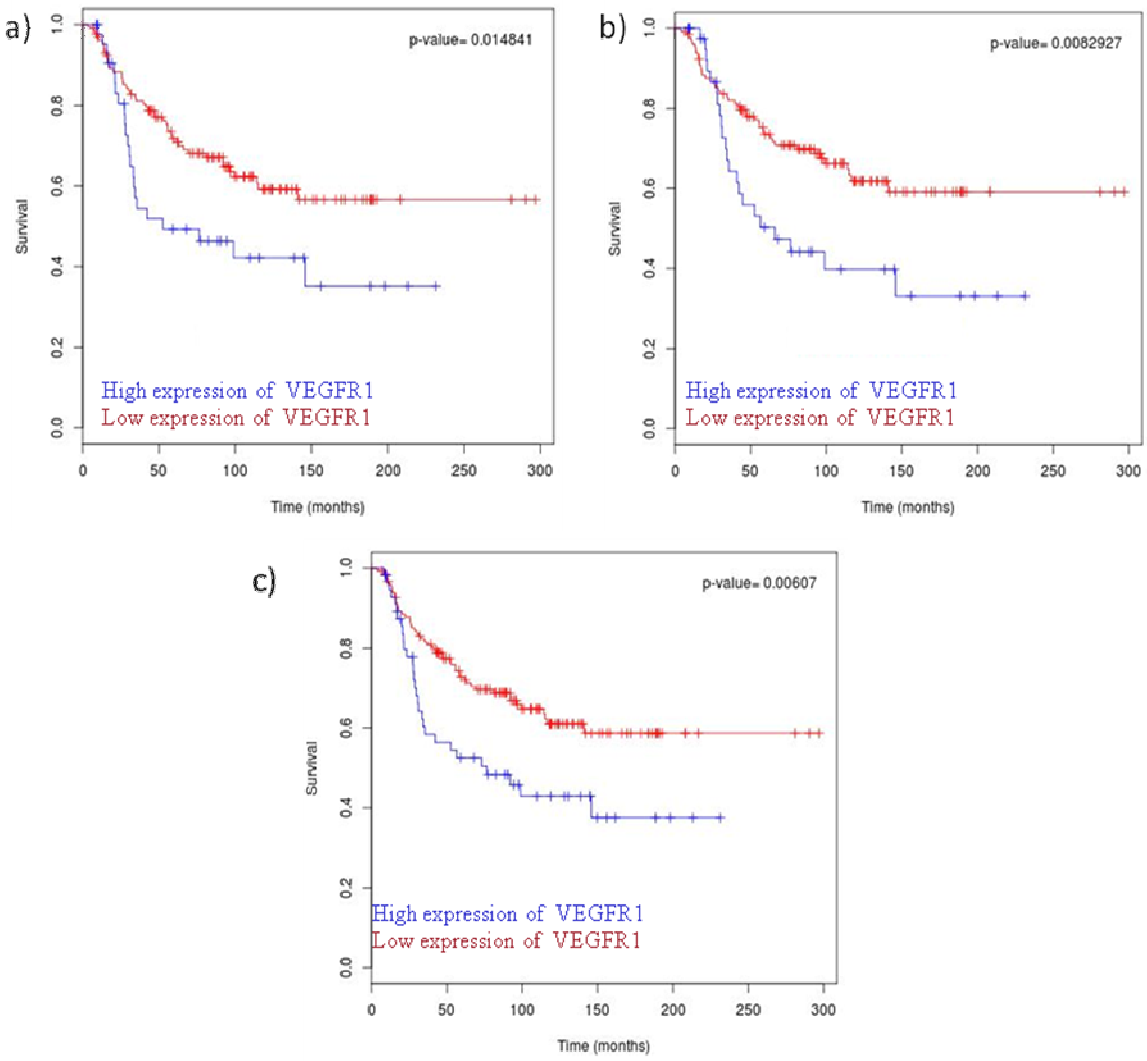

Figure 7 - 4 Kaplan Meier survival curve based on a) PAM50 classifier (n=179) b) ssp 2003 classifier (n=176) c) ssp 2003 classifier (n=211) demonstrating significant decrease in OS with high expression of VEGFR1.

7.2.5 PDGFRβ

Based on stratification using the 75th percentile, high expression of PDGFRβ was associated with significantly decreased DFS using PAM50, ssp 2003 and ssp 2006 (p-value = 0.00005, 0.001 and 0.005) with hazard ratios of 2.07, 1.87, and 1.80 respectively (Figure 7 - 5). Using the median for stratification, high expression of PDGFRβ was also associated with significantly decreased DFS using PAM50, ssp 2003 and ssp 2006 (p-value = 0.001, 0.032 and 0.001) with hazard ratios of 1.66, 1.45 and 1.59 respectively (Figure 7 - 6). Finally high expression of PDGFRβ using the median cut-off was associated with significantly decreased OS using PAM50, ssp 2003 and ssp

2006 (p-value = 0.005, 0.013 and 0.005) with hazard ratios of 2.17, 2.47 and 2.04 respectively (Figure 7 - 7).

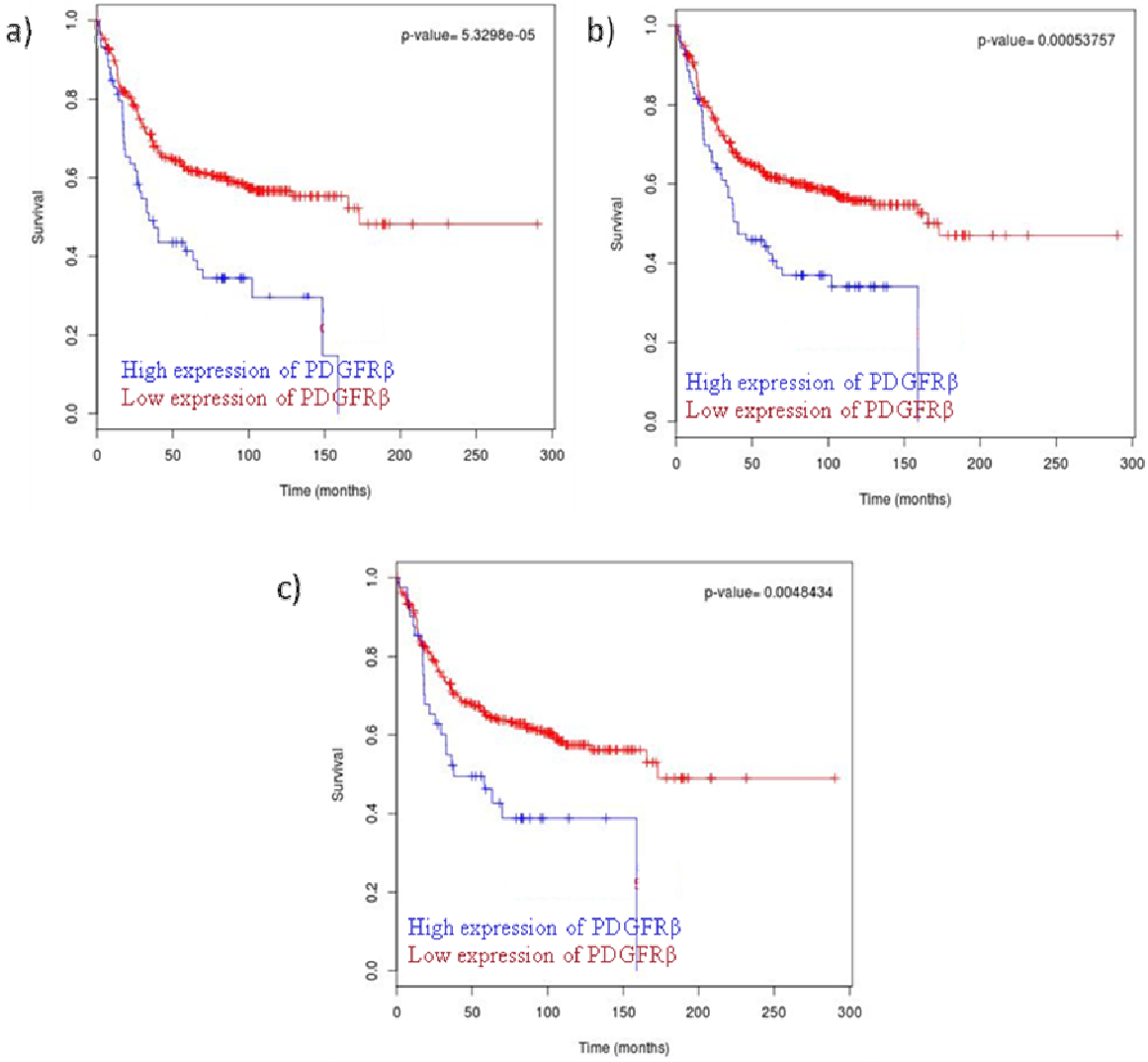

Figure 7 - 5 Kaplan Meier survival curves based on a) PAM50 classifier (n= 387) b) ssp 2003 classifier (n=361) c) ssp 2006 classifier (n=465) demonstrating significant decrease in DFS with high expression of PDGFRβ.

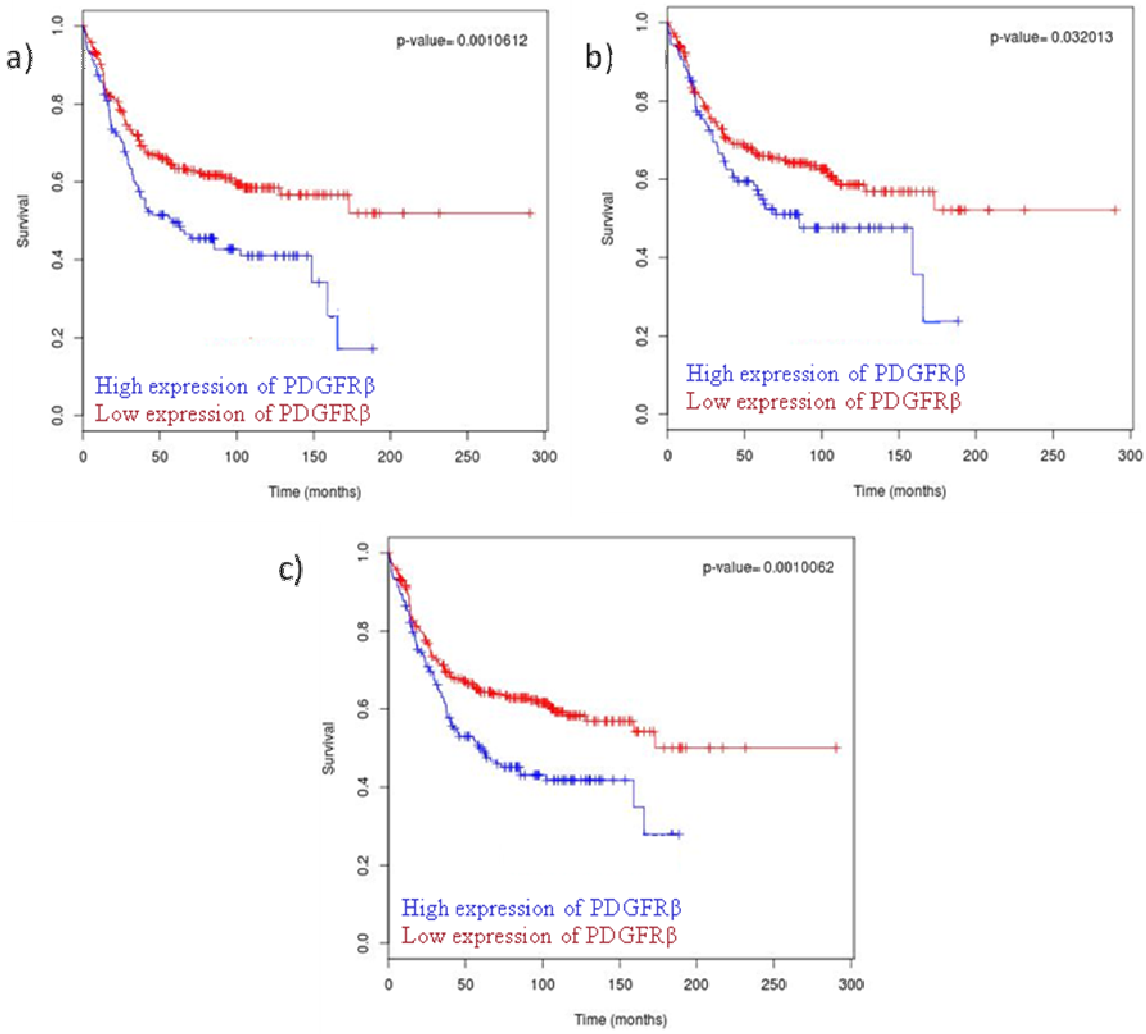

Figure 7 - 6 Kaplan Meier survival curves based on a) PAM50 classifier (n=387) b) ssp 2003 classifier (n=361) c) ssp 2006 classifier (n=465) demonstrating significant decrease in DFS with high expression of PDGFRβ.

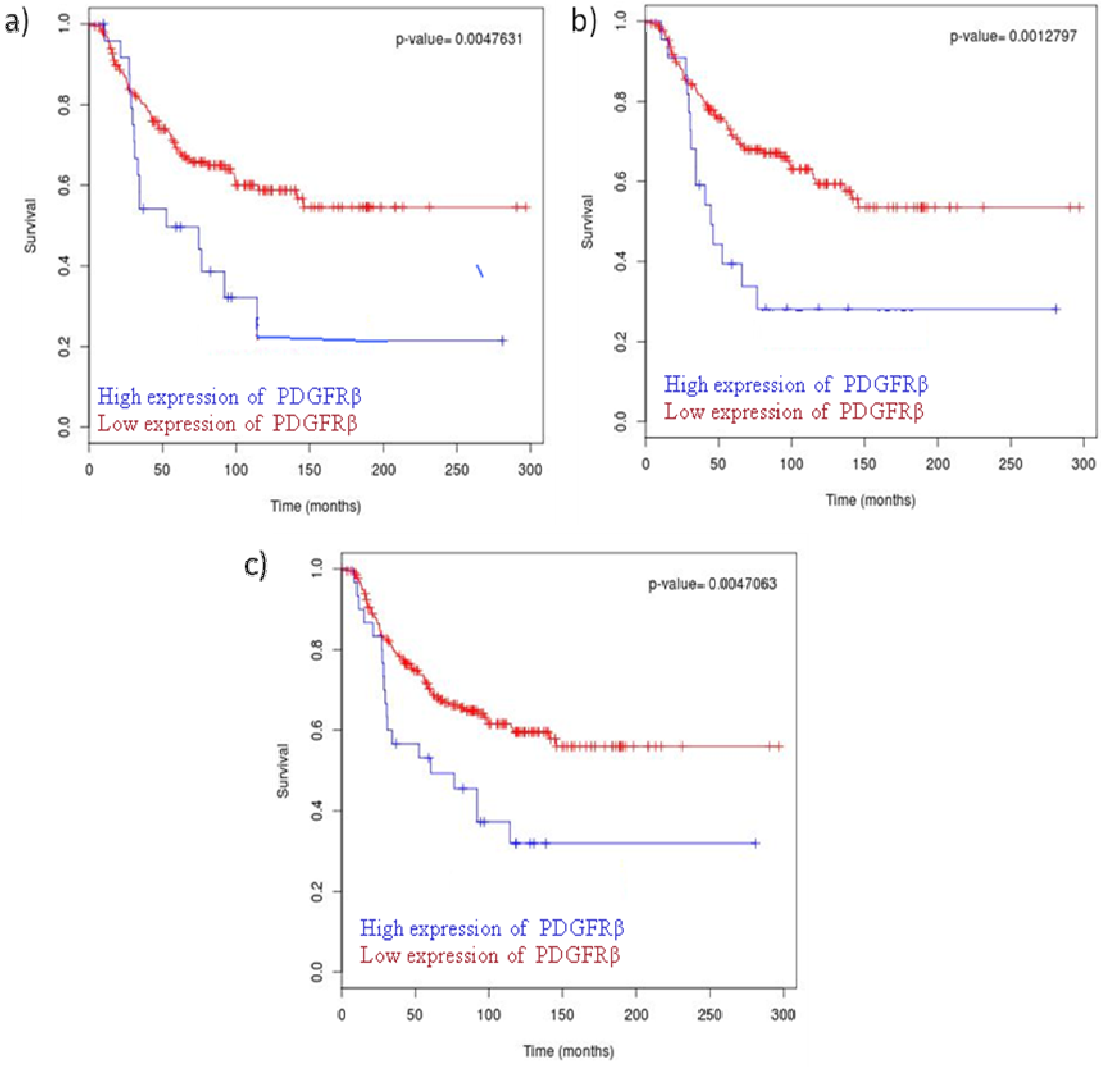

Figure 7 - 7 Kaplan Meier survival curve based on a) PAM50 classifier (n=211) b) ssp 2003 classifier (n=129) c) ssp 2006 classifier demonstrating significant decrease in OS with high expression of PDGFRβ.

7.2.6 TIE1

High expression of TIE1 using the median cut-off, was associated with significantly decreased OS in PAM50, ssp 2003 and ssp 2006 (p-value = 0.013, 0.013 and 0.008) with hazard ratios of 1.73, 1.76 and 1.72 respectively (Figure 7 - 8).

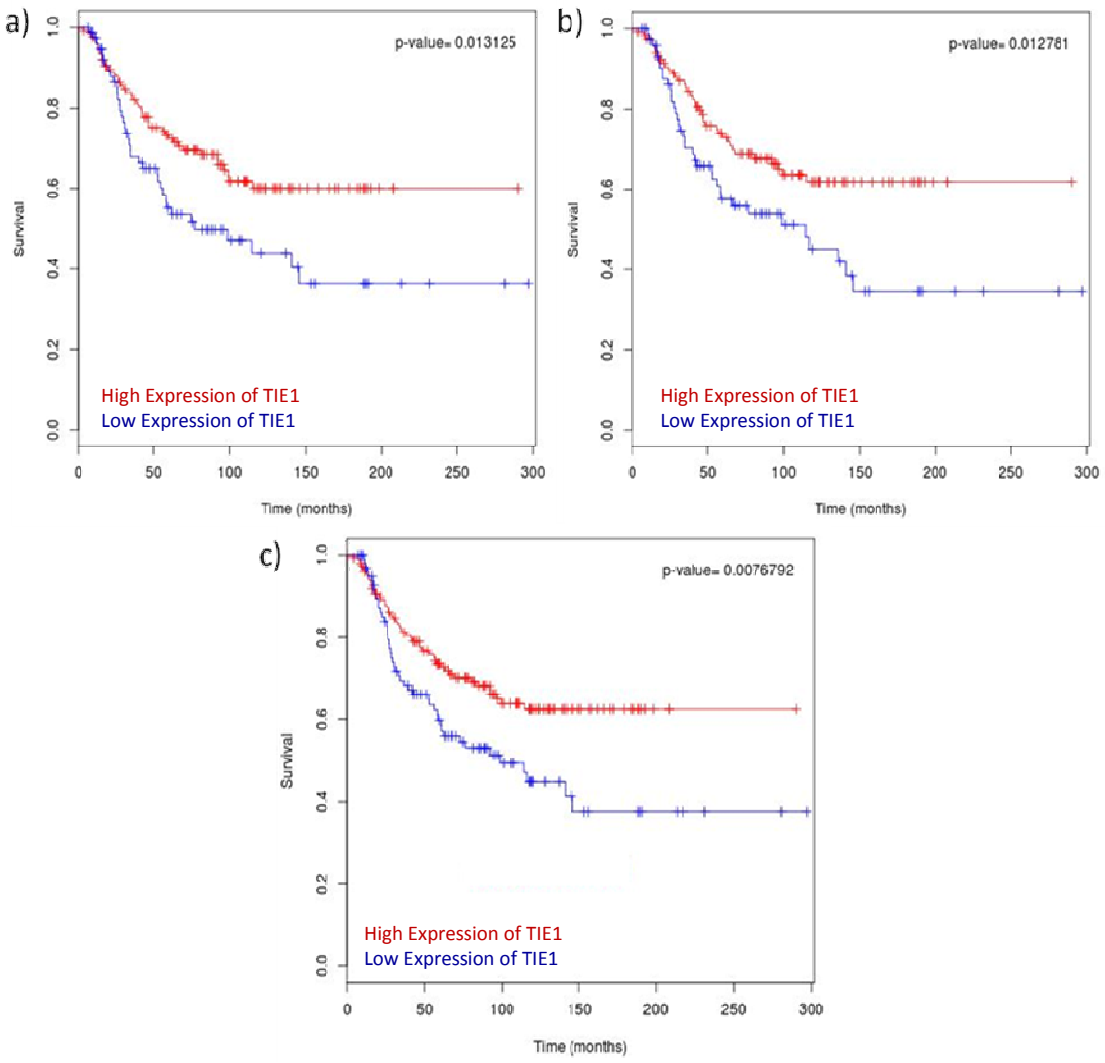

Figure 7 - 8 Kaplan Meier survival curves based on a) PAM50 classifier (n=211) b) ssp 2003 classifier (n=199) high/low expression c) ssp 2003 classifier (n=250) high/low expression demonstrating significant decrease in OS with high expression of TIE1.

7.2.7 EPHA5

EPHA5 was associated with a significantly decreased DFS in PAM50, ssp2003 and ssp2006 (p-value =0.0003, 0.020 and 0.001) with hazard ratios of 1.87, 1.59 and 1.44 respectively (Figure 7 - 9), using the median point for stratification. EPHA5 was additionally associated with significantly decreased OS using the median point in PAM50, ssp 2003 and ssp 2006 (p-value = 0.042, 0.011 and 0.007) with hazard ratios of 1.77, 2.41 and 1.98 respectively (Figure 7 - 10).

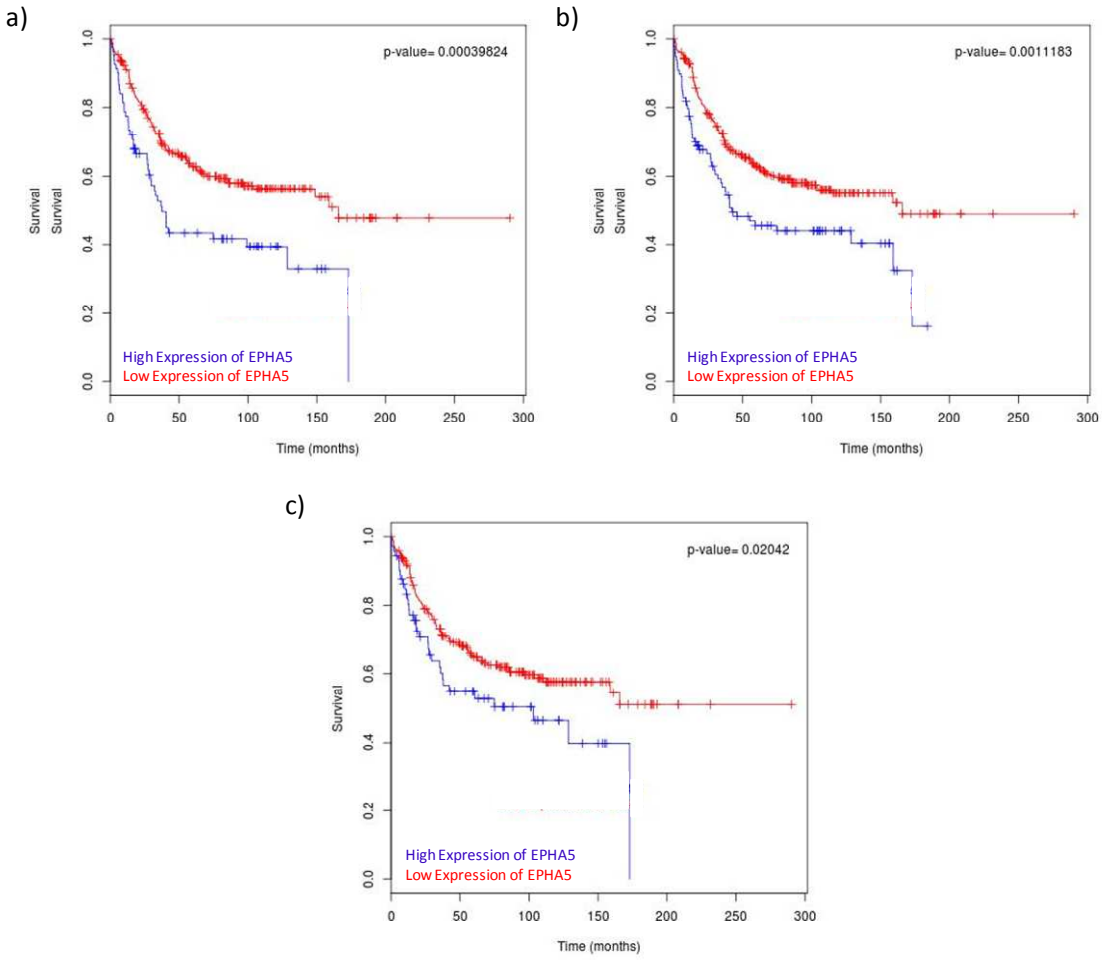

Figure 7 - 9 Kaplan Meier survival curve based on a) PAM50 classifier (n=312) b) ssp 2003 classifier (n=321) c) ssp 2006 classifier (n=413) demonstrating significant decrease in DFS with high expression of EPHA5.

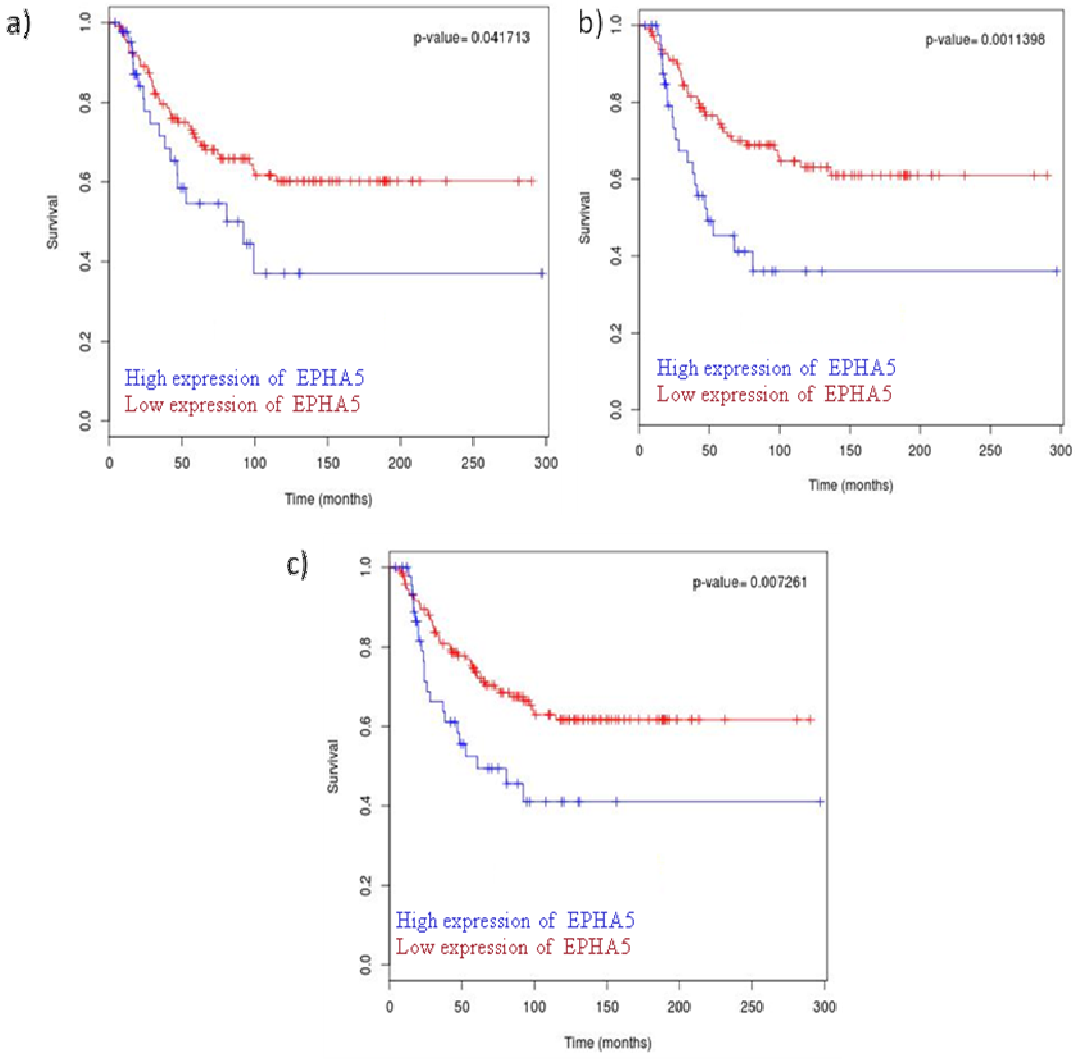

Figure 7 - 10 Kaplan Meier survival curve based on a) PAM50 classifier (n=312) b) ssp 2003 classifier n= 321 c) ssp 2006 classifier (n=413) demonstrating significant decrease in DFS with high expression of EPHA5.

7.2.8 ROS1

ROS1 was associated with significantly decreased DFS in ssp2003 and ssp2006 (p-value =0.047 and 0.015) with hazard ratios of 1.42 and 1.41 respectively, using the median point for stratification (Figure 7 - 11).

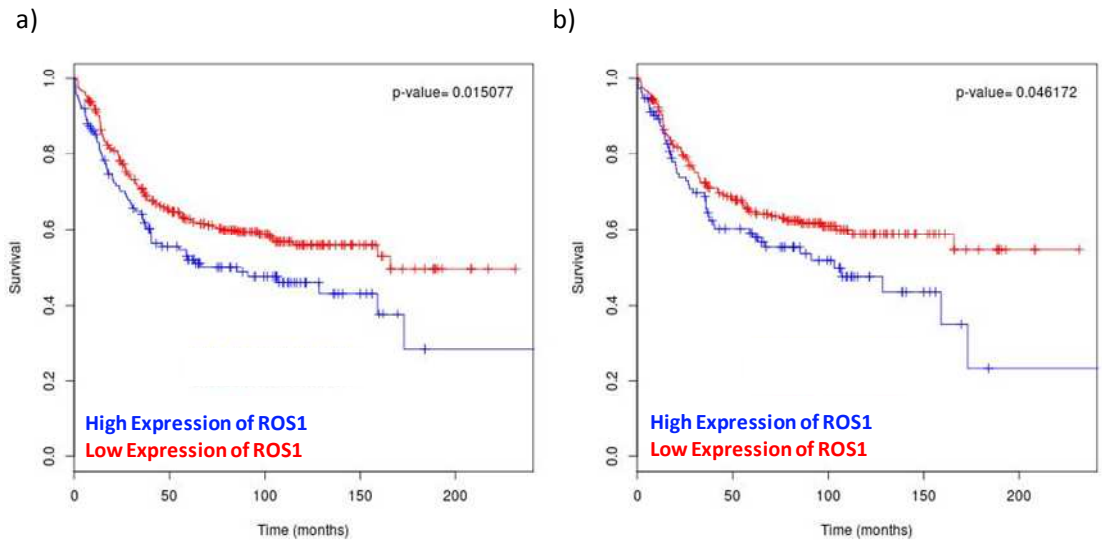

Figure 7 - 11 Kaplan Meier survival curve based on a) ssp 2003 classifier (n=368) b) ssp 2006 classifier (n=476) classifier demonstrating significant decrease in DFS with high expression of ROS1.

7.3 Selection of RTKs for further study

We selected 3 RTKs for further evaluation following a literature survey of the novelty of the proteins in breast cancer and their function. FGFR1 is well established in the development and progression of breast cancer and amplification has been observed in approximately 10% of all breast carcinomas [258]. VEGFR1 PDGFRβ and TIE1 are implicated in angiogenic processes. This would suggest that anti-angiogenic therapies may be of benefit in TNBC however clinical trials with bevacizumab have proved disappointing despite initial success [259]. The FDA has withdrawn its' approval of bevacizumab as a treatment for metastatic breast cancer due to no significant increase in survival post treatment. For these reasons, we selected EPHA5, FGFR3 and ROS1 for further evaluation. Combining the expression of these RTKs, using the median point of FGFR3, expression results in an increased hazard ratio of 3.08 (p=0.0008) in overall survival compared to the individual survival curves. The combination does not seem to have an effect on DFS relative to the individual RTKs with a hazard ratio of 1.55 (p=0.06) (Figure 7 - 12).

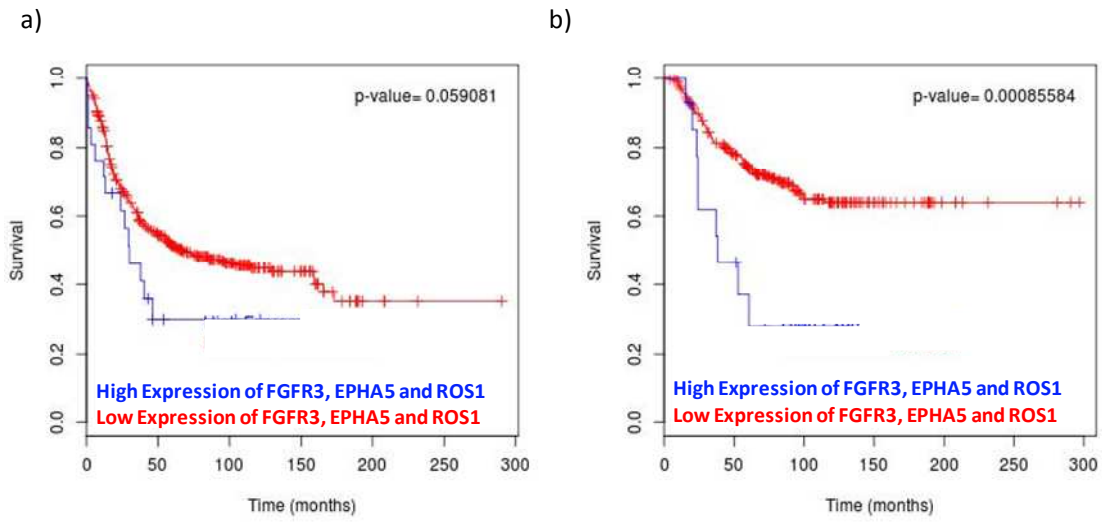

Figure 7 - 12 Kaplan Meier survival curve based on a) ssp 2006 classifier (n=422) b) ssp 2006 classifier (n=271) demonstrating significant decrease in OS with high expression of FGFR3, EPHA5 and ROS1 .

7.4 QRT-PCR in TNBC cell lines and tumour samples

We used qRT-PCR to determine mRNA expression in TNBC cell lines and a small number of tumour samples. We examined thirteen triple negative cell lines for mRNA expression of ROS1, EPHA5 and FGFR3 compared to an immortalised normal breast cell line MCF10a. RNA from 7/13 cell lines and MCF10a cell line was obtained from Mr. Bo Li, Conway Institute, UCD. ROS1 showed decreased mRNA expression in all TNBC cell lines relative to MCF10a, EPHA5 showed higher expression in 6/13 TNBC cell lines and FGFR3 showed higher expression 10/13 cell lines (Table 7 - 2).

We analysed RNA extracted from breast tumours from 7 patients for expression of FGFR3 and EPHA5 (including 3 paired tumours). The CT values were compared against the pooled CT values of 3 normal adjacent tissue samples (Table 7 - 3). EPHA5 was undetectable in all 7 tissue samples. FGFR3 expression was higher in 5/7 cases (or 8/10 individual specimens). The CT values for FGFR3 in both the cell lines and tumour samples were relatively high suggesting that it may be a low abundance mRNA.

Table 7 - 2 Results from qRT-PCR analysis of RNA from TNBC cell lines showing the Ct values and fold change relative to MCF10a. UD = Undetected

	ROS1		EPHA5		FGFR3	
Cell Line	**CT value**	**Fold Change**	**CT value**	**Fold Change**	**CT Value**	**Fold Change**
MCF10a	23.7		33.8		35.9	
BT20	32.5	-540.7	UD		28.1	186.6
HCC1143	33.00	-214.6	33.6	3.4	30.6	116.6
MDA-MB-468	26.2	-2.5	UD		34.5	6.0
HCC38	32.5	-129.4	UD		39.3	-3.1
CAL-85-1	36.3	-3323.9	UD		UD	
HDQ-P1	32.6	-249.3	34.3	1.4	31.6	37.9
BT549	31.8	-194.8	31.6	6.8	31.6	28.9
HCC70	31.4	-145.3	UD		32.8	12.1
HCC1187	31.8	-64.9	UD		34.2	14.1
MDA-MB-231	37.2	-3358.9	33.1	5.8	31.9	51.8
CAL120	37.5	-8102.5	28.6	64.4	31.8	31.5
CAL51	UD	UD	UD		38.2	1.7
MDA-MB-436	33.2	-1281.7	35.8	7.1	35.4	-1.2

Table 7 - 3 Results from QRT-PCR analysis of RNA from TNBC powdered tumour samples showing the Ct values and expression values relative to normal adjacent tissue. UD= undetected

	EPHA5	FGFR3	
Tumour	**CT value**	**CT Value**	**Fold Change**
161T A1	UD	UD	
151T A1	UD	UD	
151T A2	UD	UD	
159T A1	UD	UD	
204T A1	UD	36.7	5.5
204T A2	UD	34.5	1.6
171T A1	UD	UD	
223T A1	UD	35.6	2.6
223T A2	UD	33.3	1.5
154T A2	UD	UD	

7.5 Ephrin-A4 and FGF9 effect on proliferation

We examined whether ligands of FGFR3 and EPHA5 could potentially stimulate growth in TNBC cell lines through activation of their respective receptors. We selected two cell lines (BT20 and MDA-MB-231) on the basis of the mRNA relative levels (see Table 7 - 2) and treated with appropriate concentrations as suggested by the literature. Both FGFR3 and EPHA5 bind multiple ligands. We chose ephrin-A4 based on survival data generated from BreastMark of the ephrin ligands. Ephrin-A4 was the only ephrin to show any significant effect on DFS (p= 0.005, 0.0006 and 0.018) with hazard ratios of 1.47,1.52 and 1.40 in each of the classifiers using the median point for separation into high and low expressers (Figure 7 - 13). No significant effect was observed in OS however the combination of EPHA5 and ephrin-A4 using the median point for stratification in ssp2006 showed a significant effect on DFS (p=0.046) and OS (p= 0.016) with hazard ratios of 1.37 and 1.93 respectively (Figure 7 - 14).

No significant effect on growth was observed after 72 hrs in the BT20 treated with FGF9 or MDA-MB-231 treated with Ephrin-A4 however the MDA-MB-231 showed a trend towards increased growth with a p value of 0.059 (Figure 7 - 15)

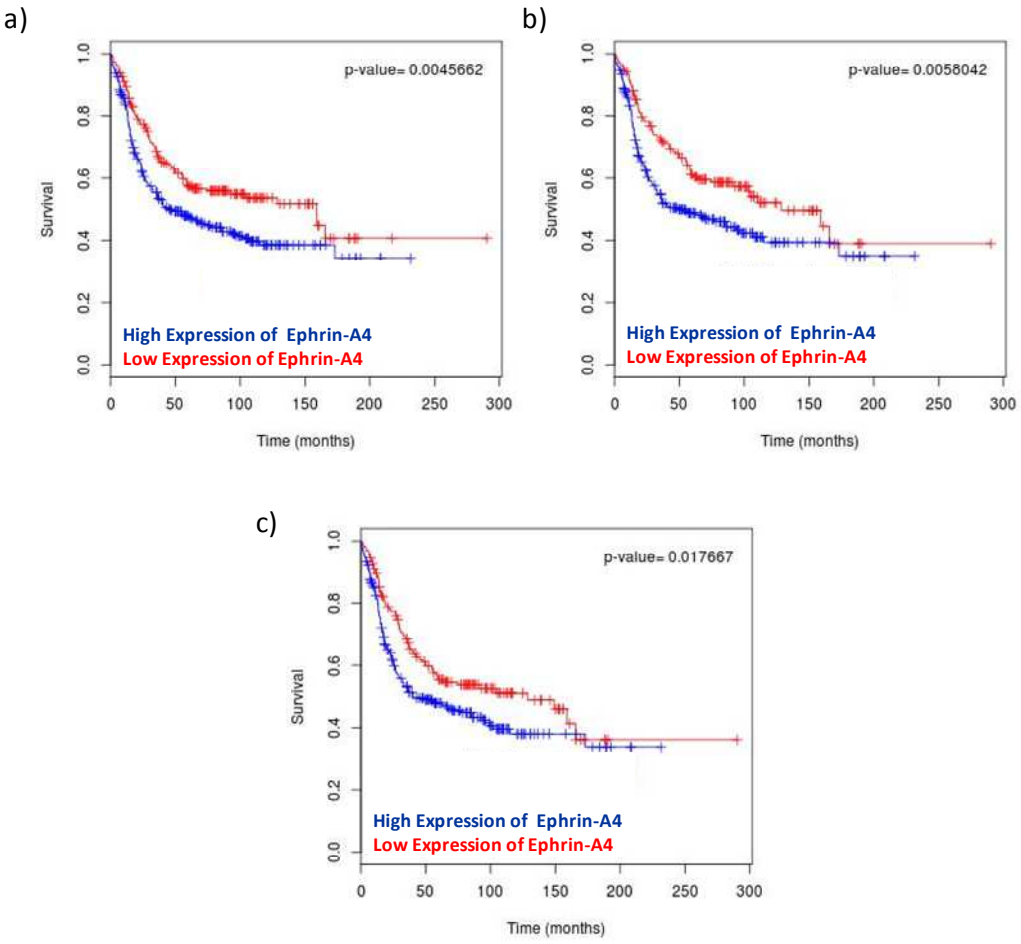

Figure 7 - 13 Kaplan Meier survival curve based on a) PAM50 classifier (n=293) b) ssp 2003 classifier (n=273) c) ssp 2006 classifier demonstrating significant decrease in DFS with high expression of ephrin-A4 (n=323).

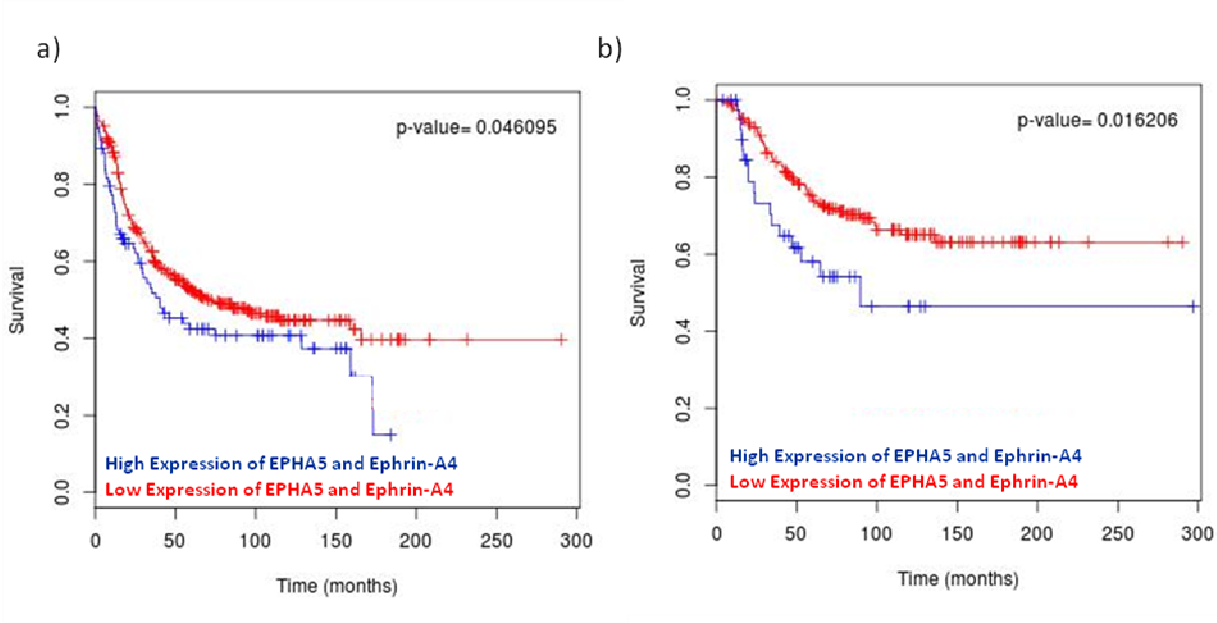

Figure 7 - 14 Kaplan Meier survival curve based on a) ssp2006 classifier b) ssp 2006 classifier demonstrating significant decrease in OS with high expression of EPHA5 and ephrin-A4.

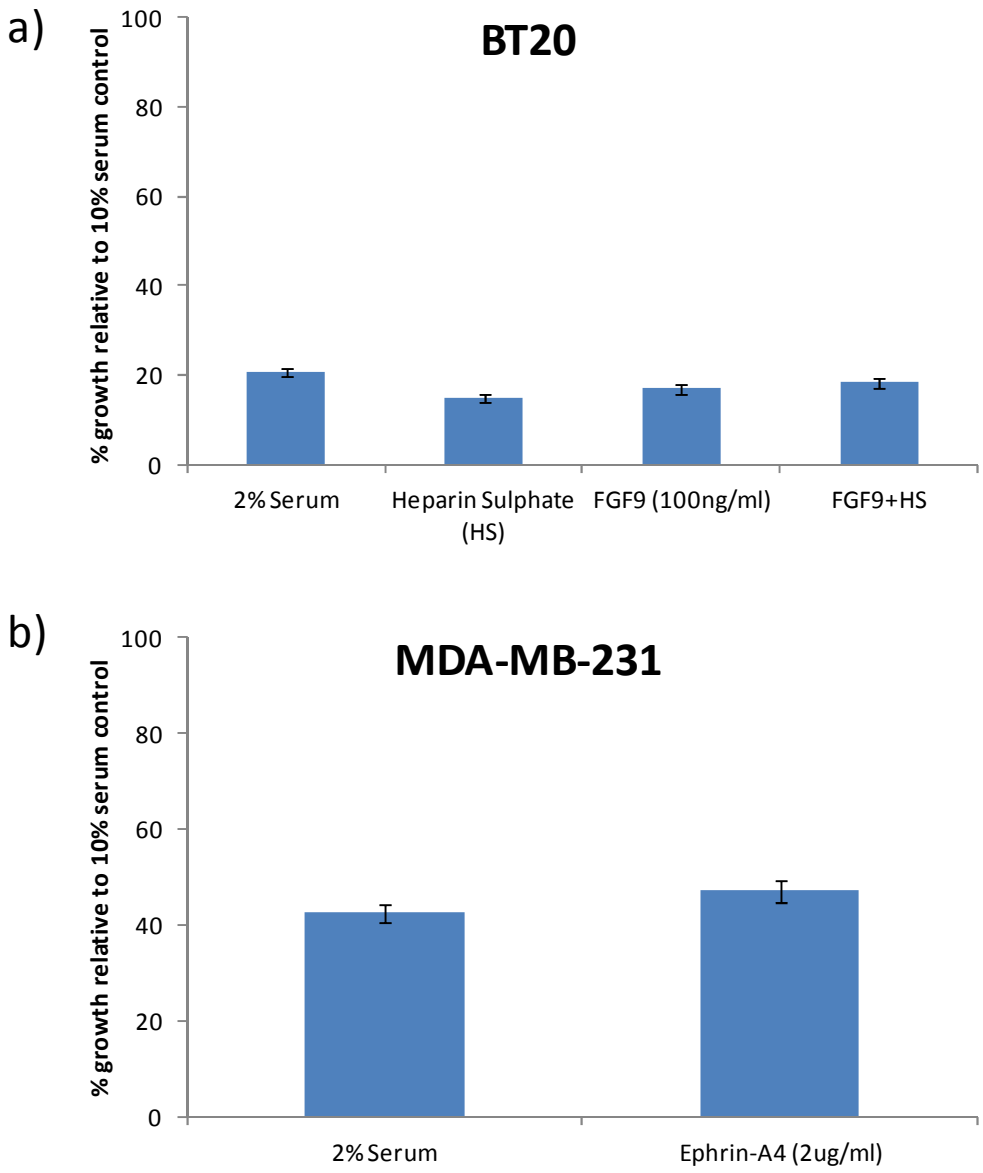

Figure 7 - 15 Proliferation assay in a) BT20 cell line treated with 100 ng/mL FGF9 for 72hrs b) MDA-MB-231 cell line treated with 2 µg/mL Ephrin-A4 for 72hrs.

7.6 Protein expression of EPHA5 and FGFR3 in TNBC

We have shown above that EPHA5 and FGFR3 mRNA levels are higher in TNBC cell lines and tumour samples than normal breast. We examined whether EPHA5 and FGFR3 protein was expressed in TNBC tumour samples using two monoclonal antibodies against FGFR3 and EPHA5 in formalin fixed paraffin embedded tumour samples in tissue-microarray format (TMA). The TMA consisted of 89 TNBC tumours selected randomly from St. Vincent's University Hospital Database.

7.6.1 TNBC tumour samples

Little literature or guidelines exist for the immunohistochemical staining of FGFR3 or EPHA5. We assessed the staining using an intensity and % positivity scoring system. Briefly a negative score was recorded in the absence of specific staining within the tumour, tumours with positive staining were scored as 1+ (weak intensity), 2+ (moderate intensity) and 3+ (strong intensity) and % positivity was divided as follows; 1-10%, 11-25%, 26-50%, 50-75% and >75% of cells stained.

7.6.2 Patient characteristics

Of the 89 tumours, 80 were suitable for examination due to lack of tumour tissue/lifting of cores. The patient characteristics are described in Table 7 - 4. The patients are predominantly older (61% >50years) with Grade 3 (85%) tumours < 2cm (54%). The majority of the tumours were ductal (93%) and negative for lymph node spread (56%).

Table 7 - 4 Patient characteristics of TNBC patients analysed (n=89)

Patient age at diagnosis	**n**	**%**
Age		
< 50	35	39
> 50	54	61
Grade		
Grade 1/2	13	15
Grade 3	76	85.0
Histological subtype		
Ductal	83	93
Lobular	5	5.6
Other	0	0
Unknown	1	1
Size		
<2cm	48	54
>2cm	40	44
Unknown	1	1
LN Status		
Negative	50	56
Positive	38	43
Unknown	1	1
LVI		
Negative	44	50
Positive	44	50
Unknown	1	1

7.6.3 FGFR3 and EPHA5 expression in TNBC patients

TMAs containing 89 TNBC tumours were obtained from St. Vincent's University Hospital and stained for FGFR3 and EPHA5. For staining 80 and 81 tumours were suitable for analysis in FGFR3 and EPHA5 stained sections respectively. The samples were unsuitable due to lack of tumour tissue or lifting of cores from slides. Each patient sample consisted of four cores/case however it must be noted that 25 of the 80 (for FGFR3) and 37 of the 81 (for EPHA5) cases analysed were either missing at least one core or no tumour tissue remained within one or more of the cores. This is due to the lack of material left on the TMA blocks after numerous cuttings.

For FGFR3 staining we observed cytoplasmic and nuclear staining in 66% and 43% of tumours respectively. Representative images of the staining observed are shown in Figure 7 - 16. No significant association is seen with any of the prognostic indicators with % positivity or intensity in the tumours positive for cytoplasmic FGFR3 (Table 7 – 5, Table 7 – 6). A significant association with was seen with nuclear staining and histological subtype in both % positivity and intensity ($p= 0.0453$ and <0.0001) however after adjusting the p value for multiple testing using the Bonferroni Correction Method, the association between % positivity and histological subtype no longer achieved significance levels ($p= 0.2718$) (Table 7 – 7, Table 7 – 8). There is a statistically significant association between intensity of nuclear FGFR3 staining and histological subtype ($p <0.0006$). For survival curves any positive staining either cytoplasmic or nuclear was given a score of one. When we examined five year recurrence and 5 year survival between the FGFR3 positive and FGFR3 negative groups no significant difference was observed between the groups (Figure 7 - 18).

For EPHA5 staining we observed both cytoplasmic (43%) and membrane staining (17%). Focal nuclear staining was also noted in 6 of 81 cases examined. Representative images of staining observed can been seen in Figure 7 - 17. No significant association is seen with any of the prognostic indicators with % positivity or intensity in the tumours positive for cytoplasmic EPHA5 (Table 7 – 9, Table 7 – 10). There is a significant association between membrane staining and age with both levels of positivity and intensity (adj $p= 0.0126$ and 0.0204) (Table 7 – 11, Table 7 – 12). Similarly to FGFR3, tumours were given a score of one for the presence of specific staining in survival studies. The resultant survival curves generated for EPHA5 positive and negative tumours show no significant differences in either 5 year recurrence or survival (Figure 7 - 19)

Finally we compared the cases which stained positive for both FGFR3 and EPHA5. Any positive staining of either marker was recorded as a positive tumour. No significant association was seen between co-staining of FGFR3 and EPHA5 and the patient prognostic indicators (Table 7 – 13). Additionally co-positivity of FGFR3 and EPHA5 did not have a significant effect on either 5 year recurrence or 5 year survival (Figure 7 - 20).

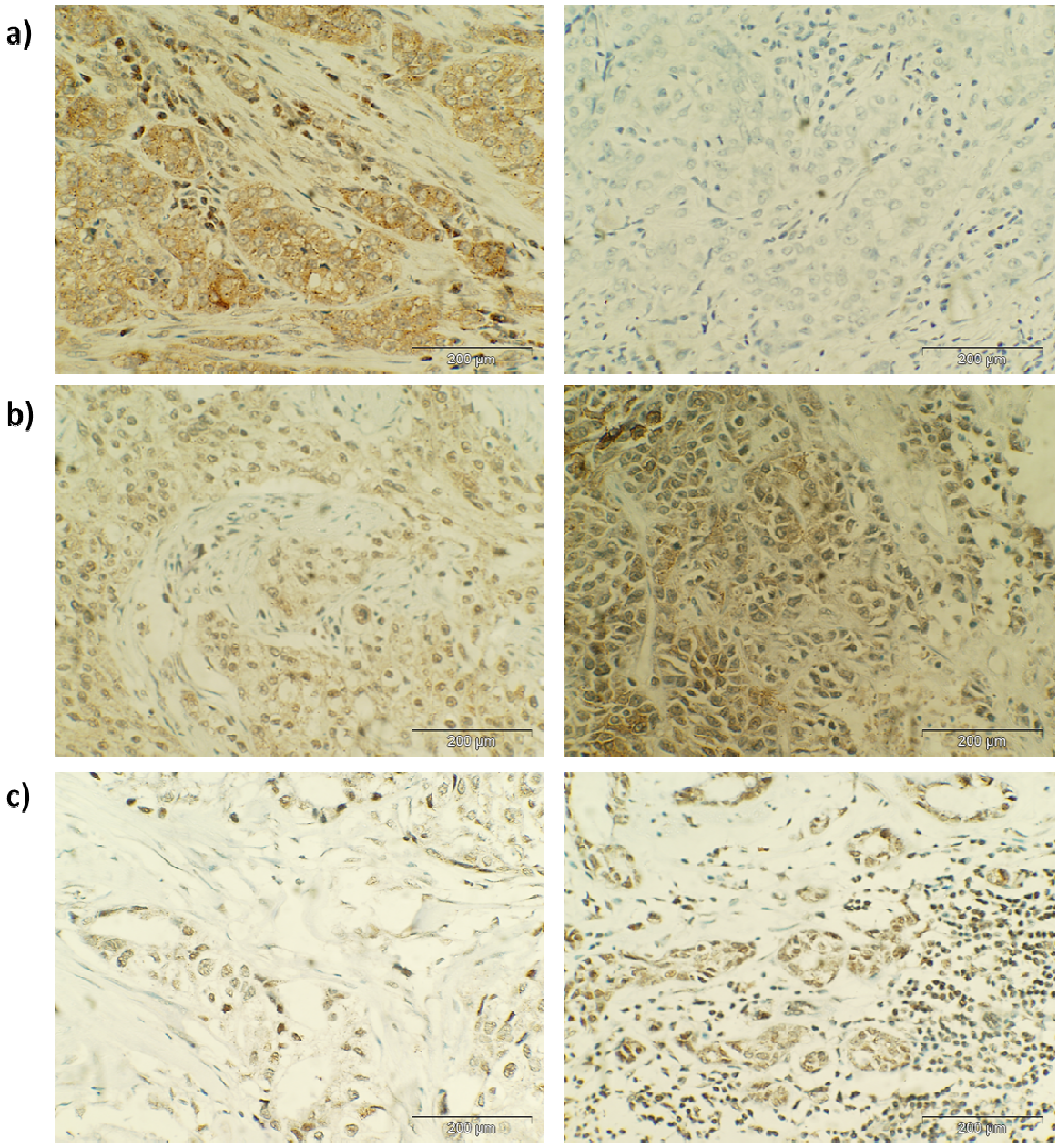

Figure 7 - 16 Representative Pictures of FGFR3 with a) TNBC positive control (LHS) and TNBC with blocking peptide (RHS) b) weak cytoplasmic staining in 50-75% of cells (RHS) and moderate cytoplasmic staining in >75% cells and c) weak nuclear staining in <10% cells (RHS) and moderate nuclear staining >10% of cells.

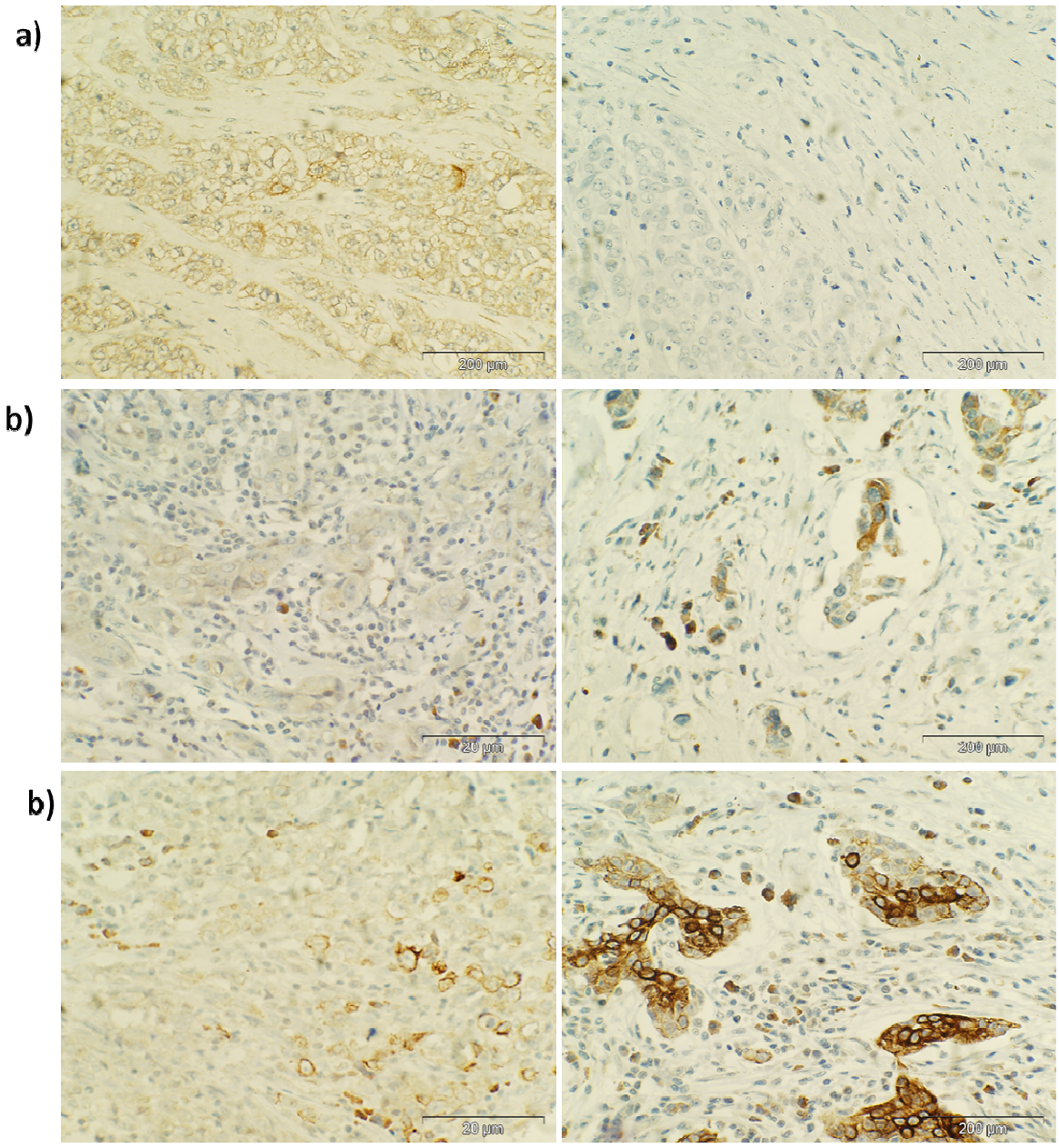

Figure 7 - 17 Representative Pictures of EPHA5 with a) TNBC positive control (LHS) and TNBC with blocking peptide (RHS) b) weak cytoplasmic staining in 25-50% of cells (RHS) and moderate cytoplasmic staining in 10-25% cells and c) moderate membrane staining in <10% cells (RHS) and strong membrane staining in >10% cells.

Table 7 - 5 Cytoplasmic FGFR3 positivity and patient prognostic indicators. P values were calculated using Chi square test

	Neg	0-10%	10-25%	26-50%	51-75%	>75%	P value
Patient age at diagnosis							
< 50	10	0	3	6	9	1	
> 50	17	2	9	11	9	3	0.6234
Grade							
Grade1/2	3	1	3	0	3	1	
Grade 3	24	1	9	17	15	3	0.2022
Histological subtype							
Ductal	24	2	11	16	19	3	
Lobular	2	0	1	0	0	1	0.3139
Unknown	1	0	0	0	0	0	
Size							
<2cm	12	2	7	5	12	1	
>2cm	15	0	4	11	7	3	0.1732
Unknown	0	0	1	0	0	0	
LN Status							
Negative	16	0	3	8	8	2	
Positive	11	2	8	8	11	2	0.3716
Unknown	0	0	1	0	0	0	
LVI							
Negative	19	2	7	6	7	3	
Positive	8	0	5	9	12	1	0.1159
Unknown	0	0	0	1	0	0	

Table 7 - 6 Cytoplasmic FGFR3 intensity and patient prognostic indicators. P values were calculated using Chi Square test. No tumour had a score of greater than 2+ (i.e. 3+)

	Neg	1+	2+	P value
Patient age at diagnosis				
< 50	10	8	12	
> 50	17	23	10	0.1034
Grade				
Grade 1/2	3	5	3	
Grade 3	24	25	19	0.8319
Unknown	0	1	0	
Histological subtype				
Ductal	24	29	22	
Lobular	2	2	0	0.4336
Unknown	1	0	0	
Size				
<2cm	12	13	15	
>2cm	15	17	7	0.1523
Unknown	0	1	0	
LN Status				
Negative	16	17	9	
Positive	11	13	13	0.3911
Unknown	0	1	0	
LVI				
Negative	19	19	11	
Positive	8	11	11	0.4399
Unknown	0	1	0	

Table 7 - 7 Nuclear FGFR3 positivity and patient prognostic indicators. P values were calculated using Chi Square test. Adjusted P values are calculated using Bonferroni Calculation

	Neg	0-10%	>10%	p value	adj P
Patient age at diagnosis					
< 50	17	9	2		
> 50	29	18	5	0.9663	
Grade					
Grade 1/2	6	3	2		
Grade 3	40	23	5	0.9431	
Unknown	0	1	0		
Histological subtype					
Ductal	45	24	5		
Lobular	0	3	2	**0.0453**	0.2718
Unknown	1	0	0		
Size					
<2cm	24	13	2		
>2cm	22	13	5	0.6552	
Unknown	0	1	0		
LN Status					
Negative	20	12	5		
Positive	26	14	2	0.5346	
Unknown	0	1	0		
LVI					
Negative	25	12	4		
Positive	20	15	3	0.6652	
Unknown	1	0	0		

Table 7 - 8 Nuclear FGFR3 intensity and patient prognostic indicators. P values were calculated using Chi Square test. Adjusted P values are calculated using Bonferroni Calculation.

	Neg	1+	2+	3+	p value	adj P
Patient age at diagnosis						
< 50	17	6	7	0		
> 50	29	11	8	1	0.8414	
Grade						
Grade 1/2	6	2	2	0		
Grade 3	40	14	13	1	0.9849	
Unknown	0	1	0	0		
Histological subtype						
Ductal	45	14	15	0		
Lobular	0	3	0	1	**<0.0001**	**<0.0006**
Unknown	1	0	0	0		
Size						
<2cm	24	9	7	0		
>2cm	22	7	8	1	0.7064	
Unknown	0	1	0	0		
LN Status						
Negative	20	9	7	1		
Positive	26	7	8	0	0.5619	
Unknown	0	1	0	0		
LVI						
Negative	25	8	8	1		
Positive	20	9	7	0	0.7939	
Unknown	1	0	0	0		

a)

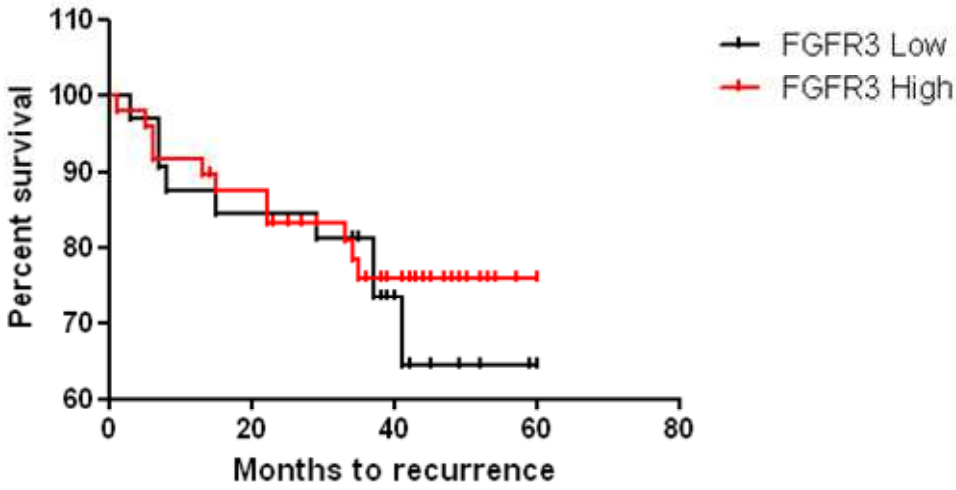

b)

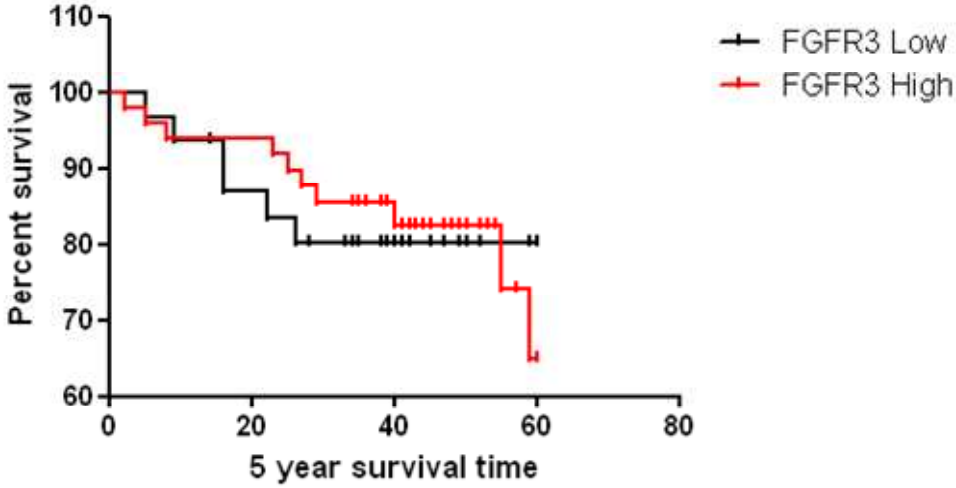

Figure 7 - 18 Kaplan Meier analysis of TNBC tumours with high (red) and low (black) expression for FGFR3 staining by immunohistochemistry in relation to a) months to recurrence b) five year survival.

Table 7 - 9 Cytoplasmic EPHA5 positivity and patient prognostic indicators. P values are calculated using Chi Square Test.

	Neg	0-10%	10-25%	26-50%	51-75%	>75%	P
Patient age at diagnosis							
< 50	18	1	4	3	3	2	0.3738
> 50	28	3	1	8	8	2	
Grade							
Grade1/2	7	0	0	3	1	0	0.5365
Grade 3	38	4	5	8	10	4	
Unknown	1	0	0	0	0	0	
Histological subtype							
Ductal	44	3	5	10	10	4	0.3749
Lobular	1	1	0	1	1	0	
Unknown	1	0	0	0	0	0	
Size							
<2cm	24	1	3	3	5	3	0.4514
>2cm	21	3	2	8	6	1	
Unknown	1	0	0	0	0	0	
LN Status							
Negative	26	2	0	5	6	0	0.0691
Positive	19	2	5	6	5	4	
Unknown	1	0	0	0	0	0	
LVI							
Negative	29	2	0	6	7	2	0.1519
Positive	16	2	5	5	4	2	
Unknown	1	0	0	0	0	0	

Table 7 - 10 Cytoplasmic EPHA5 intensity and patient prognostic indicators. P values are calculated using Chi Square Test.

	0	1+	2+	3+	P
Patient age at diagnosis					
< 50	18	10	2	1	
> 50	28	20	2	0	0.5379
Grade					
Grade 1/2	7	3	1	0	
Grade 3	38	27	3	1	0.7854
Unknown	1	0	0	0	
Histological subtype					
Ductal	44	28	3	1	
Lobular	1	2	1	0	0.2282
Unknown	1	0	0	0	
Size					
<2cm	24	12	3	0	
>2cm	21	18	1	1	0.3405
Unknown	1	0	0	0	
LN Status					
Negative	26	14	1	1	
Positive	19	16	3	0	0.3871
Unknown	1	0	0	0	
LVI					
Negative	29	15	2	1	
Positive	16	15	2	0	0.4977
Unknown	1	0	0	0	

Table 7 - 11 Membrane EPHA5 positivity and patient prognostic indicators. P values were calculated using Chi Square test. Adj P was calculated using the Bonferroni Method.

	Neg	<10%	>10%	P	adj P
Patient age at diagnosis					
< 50	20	8	3		
> 50	47	3	0	**0.0021**	**0.0126**
Grade					
Grade 1/2	10	1	0		
Grade 3	56	10	3	0.674	
Unknown	1				
Histological subtype					
Ductal	62	10	4		
Lobular	3	1	0	0.7341	
Unknown	1	0	0		
Size					
<2cm	31	7	1		
>2cm	35	4	2	0.5105	
Unknown	1	0	0		
LN Status					
Negative	34	7	1		
Positive	32	4	2	0.6021	
Unknown	1	0	0		
LVI					
Negative	40	6	1		
Positive	26	5	2	0.5509	
Unknown	1	0	0		

Table 7 - 12 Membrane EPHA5 intensity and patient prognostic indicators. P values were calculated using Chi Square test. Adj P was calculated using the Bonferroni Method.

	Neg	1+	2+	3+	P	adj P
Patient age at diagnosis						
< 50	20	3	5	3		
> 50	47	0	3	0	**0.0034**	**0.0204**
Grade						
Grade 1/2	10	0	1	0		
Grade 3	56	3	7	3	0.7828	
Unknown	1	0	0	0		
Histological subtype						
Ductal	62	3	8	3		
Lobular	3	0	1	0	0.7907	
Unknown	1	0	0	0		
Size						
<2cm	31	3	4	1		
>2cm	35	0	4	2	0.3172	
Unknown	1	0	0	0		
LN Status						
Negative	34	2	3	2		
Positive	32	1	5	1	0.7583	
Unknown	1	0	0	0		
LVI						
Negative	40	1	3	2		
Positive	24	2	5	1	0.4331	
Unknown	3	0	0	0		

a)

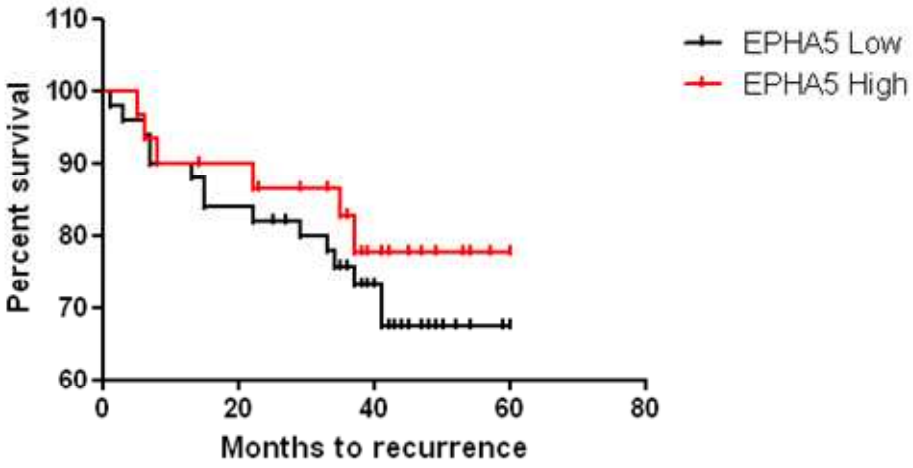

b)

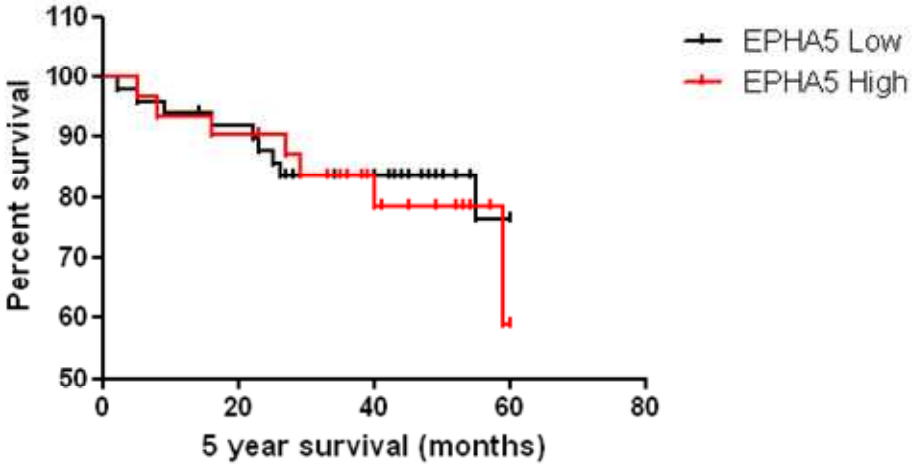

Figure 7 - 19 Kaplan Meier analysis of TNBC tumours with high (red) and low (black) expression of EPHA5 staining by immunohistochemistry in relation to a) months to recurrence b) five year survival.

Table 7 - 13 Co-positivity for FGFR3 and EPHA5 and patient prognostic indicators. P values were calculated using Fishers Exact Test.

	Neg	Pos	P
Patient age at diagnosis			
< 50	14	16	
> 50	30	20	0.2579
Grade			
Grade 1/2	7	4	
Grade 3	36	32	0.7457
Unknown	1	0	
Histological subtype			
Ductal	42	33	
Lobular	1	3	0.3257
Unknown	1	0	
Size			
<2cm	21	17	
>2cm	22	19	1
Unknown	1	0	
LN Status			
Negative	28	19	
Positive	15	17	0.3578
Unknown	1	0	
LVI			
Negative	25	16	
Positive	18	20	0.2631
Unknown	1	0	

a)

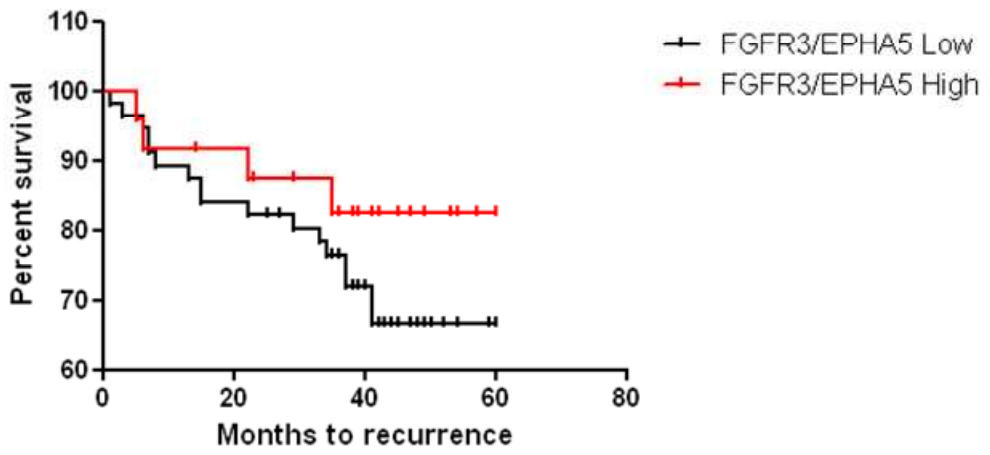

b)

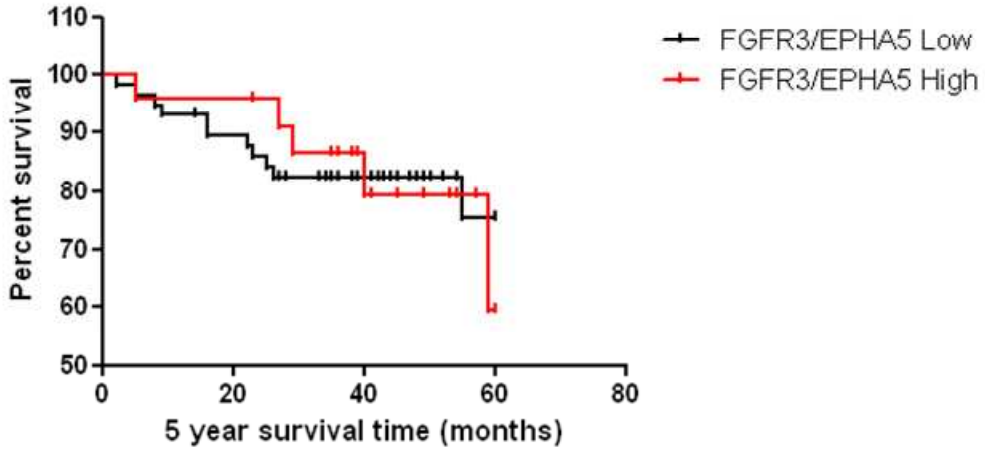

Figure 7 - 20 Kaplan Meier analysis of TNBC tumours with high (red) and low (black) expression of FGFR3 and EPHA5 by immunohistochemistry in relation to a) months to recurrence b) five year survival.

7.7 Summary

The RTKs associated with decreased DFS included EPHA5, FGFR1 and PDGFRβ. EPHA5 was significant in 3 classifiers. FGFR1 was significant using both the 75th and 25th percentile for stratification in 2/3 and 3/3 classifiers respectively. PDGFRβ was significant at the 75th and median percentile in 3 classifiers. RET was significant in 2/3 classifiers. Of the 58 RTKs examined in the Basal-like subtype expression of EPHA5, FGFR3, VEGFR1, PDGFRβ and TIE1 showed significance associated with decreased

OS. EPHA5, VEGFR1, PDGFRβ and TIE1 were significant in all 3 classifiers and FGFR3 was significant in 2/3.

After selection of RTKs for follow-up, mRNA expression of FGFR3 was upregulated in 10/13 TNBC cells lines relative to a normal immortalised breast epithelial cell line. EPHA5 mRNA was significantly up-regulated in 6/13 cell lines. Ligands of FGFR3 and EPHA5 also had no significant effect on the growth on the BT20 and MDA-MB-231 cell lines respectively.

FGFR3 also showed mRNA upregulation in 5/7 tumour samples relative to pooled adjacent normal tissue. EPHA5 mRNA was not detectable in the TN tumours tested.

Using immunohistochemistry we detected the mature proteins of FGFR3 and EPHA5 in TNBC tumour tissue. In agreement with the RNA results FGFR3 was detected in the majority of TNBC tumours. FGFR3 was localised to the cytoplasm and nucleus with positive staining in 66% and 43% respectively. FGFR3 nuclear staining was significantly associated with histological subtype with an adj p value of <0.0006. Cytoplasmic and membrane EPHA5 were detected in 43% and 17% of TNBC tumours. Membrane staining of EPHA5 was significantly associated with age (adj p= 0.0126 and 0.0204). Neither protein had a significant effect on 5 year recurrence or 5 year survival in this cohort of patients.

The combined expression of FGFR3 and EPHA5 has no significant association with the patient prognostic indicators, or 5 year recurrence and 5 year survival examined in this study.

Chapter 8

Discussion

8.1 Introduction

Triple negative breast cancer (TNBC) represents approximately 15% of all breast cancers. It is a subtype of a heterogeneous disease which not only carries a poorer prognosis than other subtypes, but patients are significantly younger, with more advanced disease when diagnosed [16]. TBNC is defined as tumours lacking expression of ER, PR and without over-expression of HER2, rendering current targeted therapies (e.g. tamoxifen and trastuzumab) redundant. Although c-Met expression has been associated with TNBC and been implicated in the development of BL tumours in mouse models, it has not been extensively evaluated as a therapeutic target for TNBC [81]. Crosstalk between EGFR and c-Met mediated through Src has been reported in numerous cancer types [251, 260, 261]. This cross-talk between c-Met, EGFR and Src has been implicated in cancer progression and drug resistance in TNBC. Therefore we examined c-Met expression in TNBC cell lines and tumour samples, and tested c-Met inhibition alone and in combination with EGFR and Src inhibition in TNBC cell lines.

8.2 c-Met/HGF expression in TNBC

8.2.1 Tumour samples

Reports of c-Met expression levels in breast tumour samples have varied widely ranging from 36 -100% positivity [138, 140, 149, 152-154, 161, 162]. In our cohort was c-Met expression was detected in 44% of TNBC compared to 26% of non-TNBC. The varying levels of positivity reported may stem from different methods of detection and differing cut-off points for determination of positivity. Tuck *et al.* determined 100% positivity with ISH and an immunoperoxidase technique [140]. Raghav *et al.* demonstrated 100% positivity of both total Met and p-Met in the triple negative subtype using a RPPA technique which involved snap freezing of fine needle aspirates [152].

Despite being a membrane bound protein no membrane staining was observed in our study. Specificity of the antibody was confirmed using a blocking peptide. It may have been beneficial to test the tumour samples with the companion diagnostic antibody (Ventana) currently used in conjunction with c-Met monoclonal antibody MetMab. Membrane staining has been noted in cases of DCIS on the apical cell membrane and was also demonstrated in breast carcinomas tested using the same antibody and similar

conditions [138, 154]. In a large cohort of Korean women, the staining identified via immunohistochemistry was predominately membrane staining with only weak cytoplasmic staining [185].The antibody used in the study described above was the companion diagnostic for MetMab mentioned above and is targeted at a C-terminal site in the c-Met protein. Cytoplasmic staining has been observed in multiple studies but only three report cytoplasmic staining separately [153, 161, 162, 167, 168]. Cytoplasmic c-Met has shown a significant association with HER2 expression and tumour metastases in node negative breast cancer patients [153, 168]. Contradicting results exist for the evaluation of membrane staining and cytoplasmic staining. *Lengyel et al.* states that cytoplasmic staining for c-Met can be used as a prognostic indicator; however the combination of c-Met membrane and cytoplasmic staining is the strongest prognostic indicator for survival over either staining pattern alone in this study. *Kang et al.* noted that antibodies targeting intracellular c-Met were significantly more prognostic than those directed against extracellular c-Met, suggesting that the cytoplasmic c-Met tail may play a more significant role in breast cancer progression than the extracellular domain [162]. Discordance between c-Met antibodies of the C- and N- terminal has also been reported previously in a separate study in gastric cancer [232]. Potentially discordance between C- and N- terminal antibodies may be due to sMet described below in Section 8.5

Over-expression of c-Met was not significantly associated with overall survival in our study. High over-expression of both c-Met and HGF has been previously associated with poorer overall survival in breast cancer [152, 153, 161]. Two studies have also examined expression of c-Met in primary breast tumours and lymph nodes. Both these studies conclude that c-Met expression is higher in lymph node metastases than primary tumours and this correlates with poor survival outcome. Both also note highly heterogeneous patterns of expression which may be related to higher intensity noted in leading edge of the tumour in DCIS and in breast carcinomas [140, 153, 154, 161]. In studies where the data is available, tumours with higher expression of c-Met relative to adjacent normal tissue tend to have a poorer prognosis than those with similar staining patterns. This is a limitation of using the TMA format as we did not have sufficient representation of normal tissue in cores to compare expression in tumour and normal tissue. The TMA format also does not allow examination of specific staining at the leading edge of the tumour.

While expression of the total protein has proved to be an invaluable marker for certain disease types e.g. HER2 overexpression significantly associates with decreased survival and is a biomarker for sensitivity to trastuzumab in breast cancer, expression of certain total proteins e.g. EGFR in NSCLC does not show any prognostic significance. A theory evolved that more important information could be derived from the activation state of the protein and not expression alone. The advent of phospho-specific antibodies in the 1980s allowed people to examine phosphorylation in FFPE, however the results were discordant. Using EGFR as an example, EGFR and p-EGFR were examined in a cohort of glioma patients. Despite high EGFR expression, p-EGFR was only observed in 1/3 of tumours and had no prognostic significance [262]. Additionally in a breast cancer cohort 54% of patients showed phosphorylation of EGFR with no association between prognostic indicators or survival. Interestingly here p-EGFR did not have an association with the EGFR expression [263].

The lack of prognostic significance of examining phospho-proteins in FFPE may be related to the stability of the phosphorylation group. Fixation and embedding is a relatively slow process allowing the continued action of endogenous phosphatases [264]. For phospho-proteins in tissue the preferential method seems to be snap freezing of tissue [152]. High p-Met has been associated with recurrence in breast cancer [249]. We had access to fresh frozen tissue from nine patients with 3 paired normal adjacent tissue samples and assessed phosphorylation using a magnetic bead multiplex assay. In 8/9 (88.8%) of the tumours we measured detectable levels of c-Met phosphorylation. Where paired samples were available, higher levels of phosphorylated c-Met were detected in the tumour tissue compared to the normal adjacent tissue in 2 of the 3 (66.6%) matched pairs. We do not currently have survival data for these patients; however given the high incidence of phosphorylation in this small sample set it would be interesting to expand this analysis to a larger cohort of patients with associated survival data to determine the prognostic significance of phospho-Met levels in TNBC. . The multiplex ELISA format is attractive as it facilitates analysis of multiple RTKs in relatively small quantities of tumour tissue.

We observed a significant association between the TNBC subtype and c-Met expression in our cohort of patients. This is in agreement with previous studies. A previous study of 168 tumours by immunohistochemistry found that c-Met expression correlated with the

absence of PR [149]. c-Met has also been independently associated with BL status, defined by ER/PR/HER2 negativity and positive for either CK 5/6, CK14 or EGFR [169]. In a study of Korean woman, c-Met significantly associated with ER and PR negativity, larger tumour size, and positive lymph nodes [169].

We found no significant association between c-Met expression and other prognostic indicators. Previous studies have demonstrated associations between clinico-pathological variables including grade, node negativity and smaller tumour size however these studies examine expression in general breast cancer and not specifically TNBC. [138, 149, 161, 167, 169].

We noted a weak association between c-Met expression levels and KI-67 percentage positivity (p= 0.051). KI-67 is a proliferation marker and has been shown to be an independent prognostic indicator for DFS in invasive breast cancers and high KI-67 indices are seen more frequently in TNBC [265, 266]. KI-67 has previously been linked with c-Met expression in hepatocellular, gastric carcinomas and NSCLC [267-269].

8.2.2 c-Met/HGF expression in TNBC cell lines

In our panel of TNBC cell lines both expression levels and activation of Met were higher in TNBC than in non-TNBC. This has been reported in panels of mixed breast cancer subtypes previously including 5 TNBC, 4 ER positive and 3 HER2 amplified [154, 185]. However to our knowledge this is the first study to report expression of c-Met in a panel of 9 TNBC cell lines. All nine TNBC cell lines showed expression of total c-Met and four (BT20, HCC1937, HCC1143 and CAL-85-1) showed phosphorylation at the activation site Y1234/Y1235. Pan-phosphorylation was also detected in all nine TNBC cell lines using magnetic bead assays. As HGF is a known ligand of c-Met, we examined HGF expression using a human HGF ELISA and qRT-PCR; based on the lack of detectable HGF protein or mRNA we can conclude that the cell lines do not produce endogenous HGF. Given the low incidence of c-Met amplification in TNBC we can assume that activation could be occurring through two potential mechanisms; ligand dependent through bovine HGF or ligand independently through receptor cross talk and feedback loops. The amino acid sequences in bovine HGF and bovine c-Met show an average of 87% consensus to the human HGF and c-Met sequences therefore, it is probable that bovine HGF is capable of inducing activation of human c-Met however no information exists on the binding affinity or

strength of activation induced [270]. Another potential mechanism of activation is through cross-talk with EGFR and Src. This is discussed fully below; however EGFR can activate c-Met through Src causing constitutive activation. It is most likely a combination of both of these mechanisms which results in activation of c-Met in the TNBC cell lines.

8.2.3 HGF in TNBC

As described above we were unable to detect mature human HGF in CM via ELISA in two TNBC cell lines (HCC1937 and MDA-MB-231) and no HGF mRNA was detected in 13 TNBC cell lines tested which indicates that the cancer cells do not produce autocrine HGF. The relationship between HGF and its role in breast cancer has been examined in both cell lines and tumour samples which support our results. Co-culture of fibroblasts and an immortalised normal breast cell line demonstrated that fibroblasts are exclusively responsible for HGF production [175]. Two non-TNBC cell lines (MCF-7 and ZR-75-1) assessed for HGF production in conditioned media were also negative for HGF [271].

High HGF levels in breast cancer tissue extracts has been shown to be a prognostic indicator associated with recurrence and survival. These studies do not take into account the location of the HGF or if the HGF is produced by malignant cells or produced by normal cells such as fibroblasts or endothelial cells [159, 160, 271]. Co-expression of c-Met and HGF mRNA has been seen in breast carcinoma cells but with most intense regions of HGF staining at the leading edge of the tumour [140]. The authors suggest this may be indicative of an autocrine loop however it may be as a result of internalisation from surrounding stroma explaining the gradient of expression [175].

The results presented in this thesis in conjunction with the literature, present a scenario where the ideal assessment of c-Met/HGF axis *in vivo* would require the determination of c-Met/HGF expression and activation ideally in snap frozen tumour samples and adjacent normal tissue in a large cohort of TNBC patients.

Many studies show that the addition of HGF stimulates proliferation, invasion and migration in 2D cell culture models; however only two of five TNBC cell lines tested (BT20 and HCC1937) showed increased growth in response to a saturating concentration of recombinant huHGF. Additionally we observed a HGF mediated increase in migration in the MDA-MB-468 which was blocked using c-Met inhibitor CpdA. CpdA however had no effect on basal levels of migration. The addition of exogenous HGF may mimic the production of HGF by stromal cells in a tumour and

thus may reflect the *in vivo* situation more closely. However, the concentrations of HGF used should reflect the concentrations that are present in the tumour microenvironment, rather than high saturating concentrations which may produce false positive results. Measurement of HGF levels in fresh frozen TN tumour specimens would be required to accurately determine the appropriate concentrations to use.

8.3 c-Met and EGFR

Reported EGFR expression levels in breast cancer range from 18% to 60% [69]}. The frequency of EGFR expression is significantly higher in TNBC and correlates adversely with chemosensitivity [20, 272, 273]. TNBC is inherently insensitive to EGFR inhibition and a mechanism suggested for this resistance is through interaction with c-Met through c-Src. c-Met expression significantly correlates with EGFR expression in breast cancer [169].

Only six tumours in our TNBC TMA were positive for EGFR. Of these six, three showed co-expression of EGFR and c-Met. All patients who showed co-expression were >50 years of age. A significant association between EGFR and age at diagnosis has been previously reported i.e. older patients have significantly lower levels of intratumoral EGFR [70].

8.4 c-Met and Src

Src is the most widely characterised member of a family of non-receptor tyrosine kinases known as the Src family. Src can be activated either by cytoplasmic proteins or through ligand dependent activation of cell surface receptors e.g. HGF binding to c-Met [96, 274].

In our cohort of patients 15/44 (34.1%) showed co-expression for c-Met and Src. Of those that showed co-expression of c-Met and Src, 7/15 (53.3%) also had detectable phospho-Src (Y418). No significant association between co-expression and clinico-pathological indicators was observed. However co-expression of c-Met and total Src and higher grade showed a trend towards significance with a p value of 0.07. Tumour grade is prognostically significant and is used to assess patients who do not show axillary lymph node involvement [275]. No significant association between DFS and OS was seen in this small cohort. Both membrane and cytoplasmic Src are detected at significantly higher levels in TNBC making it an attractive target for TNBC [193].

However, one study reported that in patients with ER positive/HER2 negative phosphorylated cytoplasmic Src was associated with increased disease-free survival indicating Src inhibition may require a predictive biomarker to determine which patients will respond well to inhibition and those in which it may have a detrimental effect [193, 194, 276, 277].

8.5 sMet and its potential role in TNBC as a biomarker or predictor of response

sMet is a truncated extracellular portion of the mature c-Met molecule which is cleaved from the cell membrane by metalloproteinases ADAM 10/17 or induced by HGF binding [278, 279]. Shedding induced by HGF is a proteolytic process reliant on signalling through protein kinase C (PKC) [278-280]. Our results demonstrate that all of the TNBC cell lines release detectable sMet into conditioned media at varying levels. The CAL-85-1 cell line showed the highest levels of sMet release and while no significant correlation was determined between Met levels and sMet in conditioned media from the TNBC cell lines, CAL-85-1 also show the highest detectable levels of total Met by western blotting. No significant correlation was seen between sMet levels and response to c-Met inhibitors (using IC_{50} values). Homo- and hetero-dimerisation of c-Met is crucial in c-Met signalling. Soluble receptors (sMet included) retain their ability to bind to membrane bound receptors however soluble receptors do not elicit a propagating signal due to lack of intracellular domain and may function as decoy receptors similarly to the mechanism of action of monoclonal antibodies e.g. anti-APO-1 as described in Section 1.6.2. sMet has been investigated in a small number of cancers as a potential biomarker and as it is expressed in all of the TNBC cell lines, it could potentially be used as a diagnostic biomarker or as a biomarker to monitor disease progression. Two studies examined sMet in serum and both found a negative correlation between levels of sMet and disease stage/burden in the individuals. These studies were carried out on multiple myeloma and gastric cancer and levels appear to be lower in disease states and drop as the disease progresses. The study on multiple myeloma did not find a significant difference in sMet levels despite a 3 ng/mL deficit in healthy individuals (similar reduction observed in gastric cancer) between the two groups however this is potentially due to low numbers within the study (n= 49/16 cancer/normal samples) in comparison to the gastric cancer study (n = 290/290 cancer/normal samples) [281, 282]. In contrast, in bladder cancer sMet levels in urine

were significantly higher than control groups, however no significant correlation was observed between sMet levels and stage of disease [283].

8.6 Cell line sensitivity to inhibitors of c-Met, HGF, EGFR and Src in TNBC cell lines

8.6.1 Characterisation of TNBC cell lines

We characterised the TNBC cell lines using three experimental approaches; invasion, migration and 3D colony formation. MDA-MB-231 were the most invasive cell line while HDQ-P1, CAL-120 and MDA-MB-468 showed the lowest levels of invasion. No association was observed between TNBC subtypes and invasion status. MDA-MB-231 have been characterised as a highly invasive cell line in the literature and therefore served as a positive control for our invasion experiments. Due to lack of response to c-Met inhibition in the invasion assays we assessed only a limited selection of the cell lines in migration assays. Again, MDA-MB-231 displaed the highest migration (fully closing the 'wound' within 24 hrs). MDA-MB-468 showed the lowest level of migration. The HCC1937 and HCC1143 also showed concordance between the invasion assays with moderate levels of migration. A discrepancy was seen within the HDQ-P1, which show moderate levels of migration compared to low levels of invasion. This may be due to the assay format. Cells are placed in serum free medium for the duration of the migration assay to minimise artificial positive results occurring due to continued proliferation. The HDQ-P1 is exquisitely sensitive to serum starvation, meaning the assays could not be interpreted at the 48 hr timepoint. The sensitivity may have resulted in a falsely elevated migration rate due to the presence of debris. This would suggest that the HDQ-P1 cells are not suitable for analysis by this method and it may be more appropriate to use a Boyden chamber approach.

Throughout the literature a number of TNBC cell lines have demonstrated the ability to form 3D colonies using a variety of techniques. These include BT20, HCC1937, MDA-MB-231, MDA-MB-468 and BT549 [284-287]. In addition to the previous studies, we have shown that the HCC1143 and HDQ-P1 produce colonies in 3D assays. Where available, images of colonies from published studies showed similar morphology to those determined in our experiments.

8.6.2 Subtypes of TNBC in the cell lines

Lehmann *et al.* identified 6 subtypes within TNBC cell lines and tumour samples, two of which were enriched in gene expression for growth factors. The BL-2 subtype is

enriched in growth factor gene expression including c-Met, EGF, NGF Wnt and IGF1R pathways [31]. Our panel of TNBC cell lines consisted of 3 BL-1 (HCC1937, HCC1143, MDA-MB-468), 2 BL-2 (CAL-85-1 and HDQ-P1), 2- M (CAL-120 and BT549) and 1 MSL (MDA-MB-231) cell lines. Burstein *et al.* recently identified gene signatures which subtyped TNBC into four groups; LAR and MSL which overlap with the Lehmann subtypes, and basal-like immunoactivated (BLIA) and basal-like immune-suppressed (BLIS) groups which consist of a mixture of the other four Lehmann subtypes [34]. The authors of this study did not apply their gene signatures to TNBC cell lines so we cannot interpret whether these subtypes impact responsiveness to the inhibitors we have tested, however we can look at the subtypes established by Lehmann *et.al.*

c-Met inhibitor responsiveness did not correlate with Lehmann subtype (BL-2 shows enrichment for c-Met), however responses to the other inhibitors were more characteristic of the subtypes, e.g. the IC_{50} of neratinib was significantly lower in the two BL2 cell lines (CAL-85-1 and HDQ-P1) than the other TNBC cell lines. MDA-MB-468 is also sensitive to neratinib and BL1 cell line. However the MDA-MB-468 cells are EGFR amplified and showed high levels of p-EGFR according to magnetic bead analysis, which may explain the neratinib sensitivity. MDA-MB-231, which belongs to the MSL subtype, was the most sensitive cell line to Src inhibition using both saracatinib and dasatinib [31, 80, 192]. In contrast, the cell lines which belong to the M subtype (CAL-120 and BT549) showed no response to saracatinib at concentrations up to 10 µM and decreased sensitivity to dasatinib when compared with MSL cell lines [31]. Dasatinib is a much more potent inhibitor of Src with an IC_{50} of 0.8 nM versus an IC_{50} of 2.7 nM for saracatinib [192, 288]. The subtypes share many gene ontologies however the major difference is the enrichment in MSL for growth factor related genes including inositol phosphate metabolism, EGFR, PDGF, calcium signalling, G-protein coupled receptor, and ERK1/2 signalling as well as ABC transporter and adipocytokine signalling.

8.7 2D Proliferation Assays

In proliferation assays we saw mixed responses to CpdA and limited responses to PRS110. The MDA-MB-231 and MDA-MB-468 cells showed the greatest response in 2D proliferation (IC_{50} 2.5 ± 0.3 and 3.1 ± 0.4 µM respectively), and in 3D assays with

11.8 ±0.5 % and 30.1 ± 10.6% reduction in cell viability after 5 days treatment with 10 μM CpdA. Sensitivity to PHA-665752, a c-Met selective inhibitor in a panel of TNBC differs dramatically to our results. Five TNBC and the HER2 over-expressing HCC1954 (which the authors Kim, Yu Jin *et al.* classified as TNBC in this study) were evaluated. BT20 and BT549 showed the highest level of sensitivity to PHA-665752, and MDA-MB-231 and MDA-MB-468 were the least sensitive cell lines [185]. In response to CpdA, BT20 and BT549 showed no significant reduction in proliferation. CpdA is a proprietary agent provided from Amgen Inc. We did not possess information on the pharmacokinetics of CpdA or the c-Met kinase IC_{50}. The IC_{50} of CpdA in the TNBC cell lines are relatively high in concentration and we did not have information as to whether this is reflective of pure c-Met inhibition or if CpdA may inhibit other kinases at concentrations greater than 2 μM. As discussed in *Section 8.6.2* the panel of TNBC cell lines did not show a correlation with the Lehmann subtypes nor did we see a correlation between activation of c-Met (via western blotting) and response to CpdA. From the literature we classified the basal subtype, the PI3K or the PTEN status of the cell lines used in relation to prediction of response to CpdA. No correlation can be seen between the IC_{50} and with PI3k status, PTEN status or basal subtype indicating these have no effect on response (Table 8 - 1).

We also tested two non-selective c-Met inhibitors, BMS-777607 (inhibits c-Met, Axl, Ron and Tyro3) and crizotinib (inhibits c-Met and ALK). Only two cell lines of eight tested with BMS-777607 achieved greater than 50% growth inhibition (BT20 and BT549). HCC1937 and HDQ-P1 achieved moderate inhibition of growth at 10 μM BMS-777607. The IC_{50} of BMS-777607 for c-Met is 3.9 nM so it seems unlikely with no effect at lower concentrations that the inhibition of growth observed is due solely to c-Met inhibition. BMS-777607 has been implicated in the induction of breast cancer cell polyploidy which decreased sensitivity to chemotherapy agents [289, 290].
Crizotinib, the ALK inhibitor, was tested in four cell lines however none achieved greater than 50% growth inhibition. HCC1143 showed the highest level of sensitivity with 27.6 ± 8.9% inhibition at 0.3 μM. ALK expression has been noted in 25% of TNBC and is associated with M and MSL subtypes [31, 237].

Considering all of the inhibitor results presented, it seems that TNBC cells are not inherently sensitive to c-Met inhibition and clinical trials of c-Met inhibitors alone would not be recommended for TNBC, on this *in vitro* analysis.

Table 8 - 1 Basal subtype, PI3K and PTEN status of TNBC cell lines [244, 291-293] **UK = unknown**

Cell Line	IC_{50}	Basal A/B	PI3K status	PTEN Status
BT20	>10	A	Mutated	Positive
HCC1937	4.1 ± 0.5	A	WT	Positive
HCC1143	>10	A	WT	Positive
MDA-MB-468	3.1 ± 0.4	A	WT	PTEN null
MDA-MB-231	2.5 ± 0.3	B	WT	Positive
CAL-120	3.8 ± 0.3	UK	WT	WT
CAL-85-1	>10	UK	WT	WT
HDQ-P1	5.1 ± 0.4	UK	WT	WT
BT549	>10	B	WT	PTEN null

8.8 Dual Inhibition of c-Met

8.8.1 c-Met receptor (CpdA) and ligand (rilotumumab)

We found increased growth inhibition in three cell lines (HCC1937, MDA-MB-468 and MDA-MB-231) when we targeted both the c-Met receptor via small molecule (CpdA) and its ligand HGF via rilotumumab. Dual targeting of the receptor c-Met and ligand HGF has not been previously tested. No response to rilotumumab was seen in the cell lines as a single agent which makes the enhancement of response intriguing. CpdA inhibits both ligand dependent and independent methods of activation of c-Met by binding intracellularly, however it would seem that some HGF dependent signalling through c-Met is occurring in the presence of CpdA. We do not know the exact mechanism of action or the specific binding site of CpdA. Potentially, CpdA may be unable bind the activated receptor due to the structural changes upon HGF binding or if CpdA is an ATP competitive molecule, it may be unable to outcompete ATP in a receptor with bound HGF.

There is an overlap of the cell lines which showed enhancement of response to CpdA in combinations with rilotumumab and saracatinib. Four cell lines (described below in

Section 8.8.3) showed enhanced response to CpdA with saracatinib (HCC1937, MDA-MB-468, MDA-MB-231 and HDQ-P1). Three of these cell lines also showed enhanced response to CpdA in combination with rilotumumab which suggests that HGF mediated signalling in TNBC cell lines may primarily signal downstream through Src. This result is novel and requires further investigation to characterise the mechanism. This combination warrants further testing in an appropriate *in vivo* model expressing recombinant huHGF [81] to determine its anti-tumour activity.

8.8.2 c-Met (CpdA) and EGFR (neratinib)

Previous data from our laboratory has shown that the first generation EGFR inhibitor, gefitinib has some activity in TNBC cell lines, particularly in combination with chemotherapy [74]. We evaluated neratinib, an irreversible and highly potent pan-erbB family receptor tyrosine kinase inhibitor. Although neratinib targets the erbB family, due to high levels of EGFR in TNBC the expected predominant effect would be as a result of EGFR inhibition. All nine cell lines tested showed sensitivity to neratinib with IC_{50} values ranging from 0.03 to 6.6 µM. The most sensitive cell lines were CAL-85-1 and HDQ-P1 (as described in *Section 8.6.2*). Cell lines of basal A subtype demonstrate greater sensitivity to neratinib which is in agreement with our IC_{50} results [294]. The two basal B cell lines used in this study, MDA-MB-231 and BT549 have IC_{50} values of 2.8 ± 0.2 µM and 6.6 ± 0.5 µM compared to IC_{50} <1 µM for all basal A cell lines tested. The M (including MSL) subtype of the TNBC cells showed the lowest sensitivity to neratinib with the IC_{50} greater than 1 µM in each of the cell lines. Neratinib has been determined to be effective at a dose of 240 mg given orally. Doses above this resulted in adverse grade 3 events [295, 296]. This dose results in peak plasma concentrations of approximately 100 nM implying that only three cell lines (CAL-85-1, MDA-MB-468 and HDQ-P1) would be classed as sensitive.

As mentioned above there is significant cross-talk between c-Met and EGFR and the reciprocal relationship between EGFR, c-Met and Src has been described in detail in Chapter 1. Many studies have shown that c-Met is implicated in resistance to EGFR inhibitors. We evaluated combined targeting of c-Met and EGFR in our 2D proliferation assays. The only cell line that showed a significant decrease in proliferation with the combination is MDA-MB-468. The MDA-MB-468 cells are among the most responsive to CpdA and are sensitive to neratinib. The only other cell line which showed sensitivity to neratinib and respond to CpdA is the HDQ-P1 although with a much higher IC_{50} and a trend toward significance, suggesting sensitivity to both agents is essential for

synergy. The MDA-MB-468 are EGFR amplified with mutated PTEN [244, 297]. Given the lack of synergism in our other EGFR amplified cell line BT20 we can conclude that EGFR amplification alone is not sufficient to cause a synergistic response. Synergy has been observed in the EGFR amplified breast cancer cell line SUM229 cells and SU11274 (selective c-Met inhibitor) [181]. It is also possible that HGF activation of c-Met may be necessary for synergy in response to dual targeting of c-Met and EGFR. In a xenograft model, human HGF production was required for synergy in a variety of cell types including breast [190]. Neratinib is additionally capable of inhibiting phosphorylation of c-Met, as observed in the multiplex luminex assay in the CAL-85-1 cell line. In agreement with the 2D proliferation results no significant decrease in phosphorylation was observed in the combination of PRS110 and neratinib. Neratinib as a single agent inhibited the phosphorylation of c-Met. This result suggests that there may be an interaction between c-Met and EGFR in this TNBC cell line. Previous studies have shown that c-Met inhibitors are capable of overcoming EGFR inhibitor resistance. [181, 187, 213]. HGF and EGF synergy in activating both c-Met and EGFR have also been observed in NSCLC [298] therefore it is likely than neratinib may exert its effect on c-Met through downstream feedback loops. A potential candidate for this interaction is Src which has been previously implicated in crosstalk between c-Met and EGFR [213].

8.8.3 c-Met (CpdA) and Src (saracatinib)

Saracatinib is a selective small molecule inhibitor of Src and Abl kinases. *In vitro* saracatinib has the ability to block Src phosphorylation leading to reduced Src kinase activity; it inhibits anchorage dependent and independent growth in ER positive cell lines [299]. TNBC cell lines were markedly less responsive to growth inhibition by saracatinb when compared to dasatinib (dasatinib is a much more potent inhibitor of Src with an IC_{50} <0.8 nM compared to 2.7 nM for saracatinib). The MDA-MB-231 cells were among the most responsive when treated with either compound. HDQ-P1 showed the highest sensitivity to saracatinib. The maximum tolerated dose of saracatinib in patients was 175 mg daily which produces serum concentrations of approximately 1 µM [288]. Using this as a guideline for sensitivity four cell lines would be classed as sensitive (HCC1937, MDA-MB-231, CAL-85-1 and HDQ-P1). Development of saracatinib has been discontinued due to lack of efficacy in reducing primary tumour burden in multiple cancers including primary breast, however this does not negate its possibility for use in combination regimens [253].

The combination of CpdA and saracatinib significantly enhanced response in four cell lines, HCC1937, MDA-MB-231, MDA-MB-468 and HDQ-P1. As described above for neratinib, these cell lines all show sensitivity to both saracatinib and CpdA as single agents prior to combination. Interactions between c-Src and c-Met have been implicated in mediating resistance to c-Src inhibitors in head and neck cancers where dual inhibition produced a synergistic effect [251].

The enhanced response to the combination regimens warrants further investigation, for example to determine if these combinations could enhance response to chemotherapy in TNBC.

8.8.4 Clonogenic Assays

Clonogenic assays test the ability of cells to propagate indefinitely from a single cell to large colonies. Not every cell will have the ability to form these colonies. This technique was initially described in the 1950s and used to assess cell response to radiation therapies [300]. We used automated software (ImageJ) to analyse the colonies formed using two parameters: (i) percentage area covered to represent the size of the colonies and (ii) average intensity of colonies to represent the number of cells. The thresholds for each of these can be adjusted to eliminate cells which have only undergone 2-3 divisions and growth arrested or cells which do not proliferate after seeding. ImageJ has been shown to be comparable to manual counting and minimises time required for analysis of clonogenic assays [301]. All five cell lines showed a decrease in clonogenic growth in response to 1 µM CpdA treatment, however only four achieved statistical significance. If we compare the effect 1 µM CpdA has on the cells in 2D proliferation assays, the cells were inherently more sensitive to Met inhibition in clonogenic assays. A similar trend is observed with treatment with PRS110. One possible explanation for the increased sensitivity may be the presence of luminal progenitors, from which basal breast cancer is derived, which show enhanced clonogenic growth properties *in vitro*. These luminal progenitors express high levels of c-Met relative to other epithelial cell populations and therefore may be more responsive to c-Met inhibition [174, 302]. If the progenitor cells are responsible for the increased sensitivity, a more differentiated cell line which correspondingly would have lower levels of progenitors would be less sensitive. This may explain why the MDA-MB-231(post-EMT), which shows the highest sensitivity to CpdA in 2D proliferation assays, show no significant response in clonogenic assays. In contrast, HCC1143 cells, which are a poorly differentiated cell line showed high levels of sensitivity to CpdA in

clonogenic assays despite showing no significant response to CpdA in 2D proliferation assays. Three of the five cell lines showed a statistically significant decrease in area covered after treatment with PRS110, however two cell lines showed an increase in clonogenic growth post treatment. PRS110 is highly selective for c-Met, however, CpdA like other small molecules inhibitors may inhibit other kinases explaining the different response to the two inhibitors. It is interesting to note the similarities between the profile of neratinib sensitivities and response to PRS110 in the clonogenic assays. HCC1937, HCC1143 and MDA-MB-231 all showed significant decreases in area covered in response to neratinib and PRS110. This raises the issue of cross talk between EGFR and c-Met in mediating resistance in the clonogenic assays. If PRS110 is not at a saturating concentration, selective pressure may exist to form heterodimers with EGFR. The same situation may occur in reverse for EGFR inhibitor neratinib. The two cell lines (MDA-MB-468 and HDQ-P1) which showed little response in clonogenic assays were treated with substantially lower concentrations of neratinib than other cell lines, leaving free EGFR to bind to c-Met and elicit resistance. This hypothesis is supported by the statistically significant decreased clonogenic activity in MDA-MB-468 when combining PRS110 with neratinib. The HDQ-P1 cell line also showed a decrease in clonogenic growth with the combination.

Similarly to CpdA when the cell lines that are more sensitive to neratinib in 2D proliferation assays (MDA-MB-468 and HDQ-P1) are treated with neratinib as a single agent in a clonogenic assay, they show a limited response. The cell lines HCC1937, MDA-MB-231 and HCC1143 were significantly more sensitive to neratinib in clonogenic assays than 2D proliferation assays. In contrast, when treated with saracatinib the clonogenic assays showed little deviations in response between the cell lines, similarly to the 2D proliferation results. Again the cell lines were inherently more sensitive to saracatinib in the clonogenic assays than 2D proliferation. However, no significant enhancement of response to CpdA or PRS110 was seen in combination with saracatinib.

Little literature exists about the signalling that occurs in the cells to stimulate colony formation and further investigation is warranted. Examination of c-Met and EGFR signalling pathways in cells isolated from clonogenic assays compared to cells grown in 2D assays may help to elucidate the differences in the pathways activated in 2D or clonogenic assays.

8.8.5 3D Assays

The cell lines which showed a response at 10 μM in 2D proliferation assays did not show similar responses in the 3D assays. The 3D assay used in this thesis is a modified version of an embedded matrigel 3D protocol carried out in 96 well plates to minimise cell number therefore allowing the more rapid quantification of the cells ability to form colonies [303]. 3D cell culture is thought to possess the ability to recapitulate the natural tumour environment. It has been shown that 3D culture is more representative of a tumours responsiveness to an agent and will often show higher resistance to cytotoxic agents [304]. Alternative signalling pathways may also be activated in 3D cell culture; one example includes EGFR and beta1-integrin. The signalling relationship between these two receptors is not fully functioning in 2D breast tumour cells however in 3D cell culture interaction it becomes one of the integral signalling pathways for these two receptors [305, 306]. This also accompanies an increased dependence on MAPK downstream signals and renders TNBC cells more sensitive to MAPK kinase inhibitors [305, 307]. Our results show marked less sensitivity to CpdA in 3D assays than 2D potentially for the reasons described above. A selective c-Met inhibitor EMD1214063 has previously shown the ability to decrease 3D colony formation in the MDA-MB-468 but not the MDA-MB-231 at a concentration of 5 μM. At 5 μM EMD1214063 also inhibits IRAK4, TrkA, Axl, IRAK1, and Mer suggesting that colony inhibition may not be solely due to c-Met inhibition [308, 309].

8.8.6 Invasion and Migration assays

Our invasion and migration assays showed no significant response to CpdA, PRS110, neratinib or saracatinib as single agents or in combinations in any of the TNBC cell lines tested. The efficacy of dasatinib inhibiting MDA-MD-231 invasion (see section 8.9) and the efficacy of CpdA inhibiting rhHGF-induced migration in the MDA-MB-468 served as validation for our experimental design however others have reported inhibition of invasion and migration using pre-treatment with inhibitors. c-Met inhibition by tivantinib significantly reduced migration in wound scratch assays in the MDA-MB-231 cells. In this experimental design however the cells were treated with tivantinib while still actively proliferating to reach confluence [81]. A monoclonal antibody against EGFR reduced the invasion of BT549 after 48 hrs pre-treatment [261]. In our migration assays, stimulation with HGF only had a significant effect on migration after 48 hrs. It has also been shown using a computer model in keratinocytes that transient c-Met activation and sustained EGFR signalling are imperative for

stimulating long-term cell migration [310]. All of these factors depict a time dependent role for c-Met and EGFR signalling in the regulation of invasion and migration. Thus, the invasion and migration experiments may need to be repeated using a pre-treatment for each of the inhibitors, or prolonging the experimental timepoints. If the experimental timepoints were to be extended, optimisation would be required. In migration assays, the cells are in SFM for the duration of the assay. As we have seen with HDQ-P1 (in *Section 8.6.1*) cell lines this may not be feasible for migration assays due to cell death and debris. The invasion assays would also require cell number optimisation. The cell lines are highly invasive after 24 hrs, thus to avoid saturation of the membrane cell numbers would need to be reduced.

8.9 c-Met in resistant models of TNBC

Given the numerous publications which characterise a c-Met/EGFR/SRC axis, it followed that c-Met could be implicated in resistance to these inhibitors. Dasatinib is a small molecule multi-kinase inhibitor which showed activity *in vitro* in TNBC cell lines. Previous work by Tryfonopoulos *et al.* within our group showed TNBC cell lines MDA-MB-231, MDA-MB-468 and HCC1937 had IC_{50} values of less than 1 µM when treated with dasatinib [193].

We have shown in two models of acquired resistance, increased sensitivity to c-Met inhibition via CpdA. In the 231-DasB cell line, acquired resistance to dasatinib is associated with maintenance of phosphorylation of Src at Y418. This site is highly conserved across the SFKs and as such it is possible that other members of the SFKs could be responsible for this constitutive phosphorylation. However based on a multiplex assay for several SFK family members, it appears that dasatinib does not inhibit phosphorylation of any of the SFKs tested in the resistant cells. We examined whether this constitutive activation was mediated through RTK signalling. Of the RTKs examined, only c-MET showed an increase in phosphorylation consistent with increased sensitivity to CpdA. Although we have previously shown that activated c-Met is not a predictor of response to CpdA, it seems increased p-Met following treatment may predict increased sensitivity to Met inhibition. Interestingly, the combination of CpdA and dasatinib resulted in significantly enhanced growth inhibition in only the parental cell line. This enhancement of response was also seen in invasion assays. The reason for the higher sensitivity may be related to the ability of CpdA to inhibit

phosphorylation of the SFK members, FYN, YES, LCK, LYN, FGR and BLK, despite their resistance to dasatinib inhibition, while having no effect on Src.

Results similar to those seen in the 231-DasB cell line were also seen in the cetuximab resistant cell line MDA-MB-468CR. Cetuximab is a monoclonal antibody which binds to EGFR and blocks binding of EGF thereby inhibiting downstream signalling [311]. EGFR inhibitors have shown promising pre-clinical activity in TNBC cell lines however clinical trials have been disappointing [74, 312]. Cetuximab has been tested in phase II and phase III trials with a combination of chemotherapeutic agents including docetaxel, carboplatin, ixabepilone and cisplatin [220]. Those studies with results available, report underwhelming effects of cetuximab, offering modest increases in overall response rate and progression free survival [313-315]. Cetuximab in combination with carboplatin produced responses in only 20% of metastatic TNBC with little effect on EGFR signalling. The authors suggest this is due to alternative methods of activation of EGFR. Based on our results, we would suggest this may involve enhanced c-Met signalling.

In the MDA-MB-468 cells, the resistant variant again showed increased sensitivity to c-Met inhibition by CpdA. Combined treatment with cetuximab and CpdA showed synergistic inhibition of growth in the parental cell line and no significant effect in the MDA-MB-468CR. This data may suggest a general escape mechanism for acquired resistance to therapies through a switch to dependency on c-Met signalling. The increased activation of c-Met occurs in a relatively rapid fashion after 48 hrs treatment in breast cancer cell lines, which would indicate that new protein synthesis is not required [181, 184, 213]. Blockade of EGFR encourages ligand independent activation of c-Met through a feedback loop of Src mediated activation in a number of cancer types including breast [184, 213, 298]. One limitation of this study is that we are assessing increased c-Met sensitivity in models where there is a stronger basal propensity to signal through c-Met after inhibition of EGFR or Src due to crosstalk between the receptors. c-Met has previously been implicated in other models of acquired resistance to other small molecule inhibitors, chemotherapy and radiotherapies. Cabozantinib a small molecule c-Met inhibitor was shown to overcome gemcitibine resistance in pancreatic cancer and quite encouragingly displayed only a very low level of acquired resistance despite long term treatment [316]. A similar situation was observed in two primary multiple myeloma cell lines which show increased p-Met at the development of resistance compared to the sensitive cell lines [317]. In the MDA-MB-

231 cell line, ionising radiation increases the activation of c-Met and targeting the cells with a c-Met inhibitor sensitises the cells to radiation therapy [214]. Met has also been implicated in resistance to antiangiogenic therapies in bevacizumab resistant glioblastomas. Upregulation of c-Met was noted after exposure to bevacizumab, although the authors do not evaluate a c-Met inhibitor or its response. We hope to obtain and evaluate other models of other acquired resistance in the TNBC setting to determine if increased dependence/activation of c-Met is a general escape mechanism in acquired resistance.

Our results suggest that while c-Met may be a potential target in the acquired resistance setting, it may also be appropriate to target c-Met in combination with other therapies to prevent the development of resistance, as illustrated by the response of the parental cell lines to the combinations. Both of the parental cell lines tested were initially sensitive to c-Met inhibition. We do not know if c-Met would also play a role in acquired resistance to other drugs in cells that are not innately sensitive to c-Met inhibition. Testing this hypothesis in humans would require strong predictive biomarker for c-Met sensitivity. To our knowledge currently no biomarker exists for c-Met sensitivity in TNBC. Met amplification has been shown in other cancers as a potential biomarker however amplification has not been observed in breast cancer [318]. Some studies have used expression of c-Met to identify suitable patients and the results seem to indicate that the c-Met high groups are more responsive. These studies provide more reason to identify a strong clinical biomarker for c-Met response as patients grouped within the c-Met low groups trended towards worse prognosis after treatment with Met inhibitors [319].

We are also aware of the limitations of using cell line models of resistance. Gillet *et al.* has shown that drug resistant cell lines are comparably more similar to each other than the tumour types from which they are derived. It would thus be important to evaluate changes in p-Met in TN tumours following drug treatment to determine the clinical relevance of c-Met in acquired drug resistance.

8.10 c-Met as a therapeutic target in TNBC

Our results do not support further evaluation of c-Met inhibitors alone as a first line treatment for TNBC. Similarly to EGFR, c-Met is expressed however, response to inhibition is limited. There are possible alternatives, for example using c-Met as a potential binding site for an antibody-drug conjugate (ADC), however our IHC studies in a cohort of Irish patients suggest that an ADC might not be effective as c-Met was

detected in the cytoplasm only. In search of a more effective therapy we evaluated the 58 known RTKs in search of new targets. The implications of the results of this thesis in those aspects are discussed below. Another potential target implicated for TNBC in this thesis was that of the insulin receptor.

8.10.1 Other RTKs implicated in TNBC

The sub-type of TNBC is somewhat a controversial grouping, with many arguing that lack of known target does not justify the grouping of a vast array of diverse tumours into a single group. Many studies have identified different subtypes within TNBC/BLBC which may impact a tumours responsiveness to a target agent [31, 33, 34]. Over 50% of RTKs have been implicated in proliferative disorders and as such are considered good options for targeted treatment of cancer [48, 49]. There are 58 known RTKs distributed across 20 families [62]. We examined the 58 known RTKs to identify other RTKs which may offer possible options for targeted treatment and/or the discovery of potential biomarkers in BLBC/TNBC. The RTKs which we identified as associated with a poor prognosis were EPHA5, FGFR1, FGFR3, VEGFR1, PDGFRβ and TIE1.

The FGF receptors have been implicated in the development and progression of breast cancer particularly FGFR1 and FGFR2. FGFR1 has previously been identified as an independent prognostic marker and expression of FGFR1 may serve as a biomarker of response to chemoradiotherapy while FGFR2 has been implicated as a target for inhibition in TNBC [320, 321]. Breast carcinoma cell lines MDA-MB-134 (FGFR1 amplified), SUM 52PE and MFM-2231 (FGFR2 amplified) harbouring an FGFR amplification have shown exquisite sensitivity when treated with a pan-FGFR inhibitor, ponatinib. This study also tested the T47D and TNBC cell line MDA-MB-231 which show WT FGFR expression and observed no significant sensitivity to ponantinib [322] A number of other inhibitors of FGFR are currently in clinical trials, making FGFR1 an appealing target in TNBC [220, 322].

Both VEGFR1 and PDGFRβ are involved in angiogenesis in cancer and have been associated previously with poor prognosis in breast cancer [323, 324].The VEGFR gene encodes two splice variants of VEGFR1, a full 200kDA VEGFR1 receptor and a 110 smaller protein known as soluble VEGFR1. The soluble form of VEGFR1 functions as decoy receptor for VEGF thereby acting as a negative regulator for VEGF induced angiogenesis. Three breast carcinoma cell lines (MDA-MB-231, T47D and MCF-7) were examined for expression of VEGFR1. In the ER positive cell lines soluble

VEGFR1 (T47D and MCF-7) is down-regulated by oestrogen. This would consequently allow more free VEGF to activate angiogenic pathways in ER positive tumours [325]. VEGFR1 was also significantly associated with HER2 status and response to neo-adjuvant radiotherapy. Similar to our results VEGFR1 expression (stratified using the 75th percentile) was associated with a poorer DFS and OS [326]. Schmidt *et al.* associated VEGFR1 with VEGF expression and advanced tumour stage in node negative patients [327]. The VEGF receptors have also demonstrated the propensity to encourage metastases at different sites dependent on the host organ of the tumour. In renal carcinoma VEGFR1 is implicated in metastases to the liver [328]. The study by Schmidt *et al*. has implications for potential clinical applicability of VEGFR1 inhibitors; VEGFR1 could potentially provide a viable treatment option for patients who have developed specific metastases.

PDGFRβ has been correlated with invasive behaviour in mammary carcinomas and the development of metastases. PI3K signalling is the major signalling point through which PDGFR signalling occurs, activation of this pathway seems primarily to do with autocrine activation and is required for EMT transition [329][329]. Early studies found that PDGFRβ was localised to epithelial cells in breast carcinomas and was significantly decreased in post-menopausal tissue [330].

Relatively little work has been conducted on TIE1 compared to its isoform TIE2 however it is one half of the TIE RTK family, which function to promote angiogenesis through binding of angiopoietins (ANG-1 and ANG-2) and is expressed principally by endothelial cells. TIE1 is over-expressed in breast carcinoma and undergoes activation through regulated proteolytic cleavage by a number of proteins including VEGF suggesting possible redundancy between the functions of TIE1 and VEGFR1 [331, 332].

The three RTKs described above are involved in angiogenic pathways. Many anti-angiogenic agents have been approved for other malignancies including renal cancer and colorectal cancer however the responses in breast cancer have been variable. It was initially thought that anti-angiogenics demonstrated the ability to reverse resistance and chemosensitise tumours, however other models demonstrated tumour regrowth with ongoing treatment and an increase of angiogenic activity once treatment was withdrawn [333]. One reason suggested for these variable responses is the heterogeneity of breast cancer, however our results support the hypothesis that TNBC/BLBC may respond preferentially to anti-angiogenic therapies. Angiogenesis has been shown to play a key

role in the progression of breast cancer. Increased angiogenic activity in pre-cancerous states such as fibrocystic disease and DCIS has been associated with increased risk of development of breast carcinoma [334, 335]. Microvessel density (MVD) has been established as one of the key parameters to evaluate angiogenic activity. High MVD has been associated with progression to IDC in DCIS; and with poor outcome/development of metastases in breast carcinomas [335-337]. MVD also shows an association with tumour stage and lymph node metastases [338]. In TNBC, MVD is significantly higher than other subtypes of breast cancer and was significantly associated with larger tumours of a higher grade [339]. No significant association was observed between MVD and DFS or OS [339]. MVD is a well established prognostic marker however criticism exists over its use as a method of examining angiogenic burden of a tumour. A study by Nalwoga *et al.* developed the vascular proliferative index (VPI) which is the ratio of the proliferative MVD (pMVD) (mm^2) to the MVD (mm^2) divided by 100. In this study, VPI significantly associates with angiogenesis levels, EGFR, cytokeratin 5/6, P-cadherin, high grade tumours and p53 expression in BLBC.

There are currently seven FDA approved anti-angiogenic TKIs which target the VEGFR, PDGFR, EGF and FGF receptors; sunitinib, sorafenib, pazopanib, axitinib, vandetanib, cabozantinib, and regorafenib. On the whole, trials of anti-angiogenic TKIs as single agents or in combinations with other therapeutics have been disappointing, with many not achieving primary endpoints, no increase in overall/progression free survival or showing serious adverse affects [340-345]. Clinical trials evaluating sorafenib in combination with cisplatin in early stage TNBC and cabozantinib in metastatic TNBC are currently underway and hopefully will yield more promising results [220].

Despite the disappointing results, potential remains for TKIs targeting these angiogenic RTKs. A number of the RTKs described above have been implicated in metastases formation; therefore anti-angiogenics could potentially be used to lessen the metastatic burden of cancer. Combined inhibition of VEGF and VEGFR in BO2 cells abrogated its ability to metastasise to bone [346]. C-Met inhibitors have also previously shown the ability to inhibit bone metastases in mouse models [81]. Anti-angiogenic agent sunitinib, induced metastases through c-Met signalling, which was subsequently inhibited using crizotinib suggesting a potential role for combination therapy of c-Met and anti-angiogenic inhibitors in 4T1 (breast), H460 (lung) and Colo205 (colorectal)

cells [347]. Cabozantinib a dual c-Met/VEGFR inhibitor has shown activity in the treatment of metastatic patients with bone metastases in reducing cancer burden [348].

We initially chose three RTKs for follow up from the results generated by analysis of the BreastMark dataset [239]. These were ROS1, FGFR3 and EPHA5. Aside from novelty of these receptors in TNBC, these receptors showed a significant association with decreased DFS and OS.

ROS1 belongs to the sevenless subfamily of tyrosine kinase insulin receptors. It has been associated with a high KI-67 index in invasive breast carcinomas although seems to have a positive relationship with other poor prognostic indicators. Activation of ROS1 in lung cancer is primarily through ROS fusion proteins and signalling in breast cancer cells is mediated through PI3K [349, 350]. Low ROS1 expression is associated with higher grade, increased mitotic count and low oestrogen receptor [351]. In our results ROS1 mRNA was down-regulated in all of the cell lines relative to normal immortalised epithelial cells, therefore high expression may be due to detection of ROS1 mRNA from other cell types e.g. endothelial cells or tumour infiltrating immune cells. Expression in these cell types has not been previously reported and suggests a need for further examination. ROS1 expression may also be up-regulated in adjacent normal tissue. In this case the possibility exists that ROS1 may act as stimulator of tumour growth/angiogenesis from the normal tissue through cell/cell interaction supported by the association of ROS1 with KI-67 proliferative index [351].

We examined FGFR3 and EPHA5 in further detail using an mRNA screen of 13 TNBC cell lines and 7 TNBC patient samples (3 with paired tumour and normal samples). In the cell lines the fold change was calculated by comparing CT values against those of immortalised mammary epithelial cell line MCF10a. The CT values of the tumour samples were normalised to pooled values of normal adjacent tissue. Normal adjacent tissue has limitations as a comparison as it is likely to show some artefactual changes relative to normal tissue of a healthy person. The ideal situation would be to compare mRNA levels from a pooled collection of healthy tissues isolated from reduction mammaplasty [352] but this was not available for this analysis. FGFR3 showed higher levels of mRNA in both the cell lines and the tumours and EPHA5 showed higher levels in tumour samples compared to the non-cancerous samples. Initially, our intention was to functionally validate knockdown of these proteins in TNBC cell lines by siRNA to determine whether they were suitable targets to pursue. The CT values of the cell lines,

were high suggesting that mRNA levels are quite low. In an attempt to examine the role of FGFR3 and EPHA5 in the cell lines we tested the effects of ligands on proliferation of the cell lines with the highest mRNA levels. We chose FGF9 and as FGFR3 binds FGF1and FGF9 [353, 354]However FGF18 has recently been reported as potential ligand may function as a FGFR3 ligand [355]. FGF9 was selected from the FGFR ligands as it does not bind to FGFR1. FGF9 additionally requires the presence of heparin sulphate to bind to FGFR3 [356]. The ephrin family of receptors are promiscuous receptors. The ephrin-A receptors have the ability to bind all of the ephrin-A ligands. Ephrin-A4 was the only ephrin to show any significant association with DFS obtained from the BreastMark database. High levels of Ephrin-A4 significantly decreased DFS in basal-like breast cancer. Neither ligand showed any significant effects on the growth of the TNBC cells. Due to the difficulties encountered with functional validation of FGFR3 and EPHA5 *in vitro*, we chose to evaluate their expression in TN tumours to determine their clinical relevance.

In our cohort of TNBC we detected expression of both FGFR3 and EPHA5. FGFR3 was expressed cytoplasmically in 66% of tumours and 44% were positive for nuclear staining. The nuclear staining was statistical significant, with an association seen between intensity/expression levels and histological subtype. Cytoplasmic and nuclear staining of FGFR3 in breast cancer has been noted before [357]. FGFR3 consists of two splice variants FGFR3 IIIb and FGFR3 IIIc [358]. FGFR3 IIIb is predominantly expressed in epithelial cells while FGFR3 IIIc features more predominantly in cells of mesenchymal origin. The location of FGFR3 expression activates distinct pathways in pancreatic cancer. Epithelial cells signal through STAT kinases where FGFR3 signalling in mesenchymal cells is through the MAPK pathway; however they also report that FGFR3 has tumour suppressive properties in epithelial cells [359]. Early studies detected the two isoforms of FGFR3 of which one predominately localises within the nucleus. FGFR IIIb, which has a lower molecular weight, is the form of FGFR3 localised in the nucleus [357]. FGFR3 has also been implicated in the development of bone metastases in breast cancer [360]. Currently, there are at least five clinical trials with inhibitors capable of inhibiting FGFR3; however no agent specifically targeting FGFR3 exists. Most are pan-FGFR or FGFR/VEGFR inhibitors which are being tested in metastatic or ER positive breast cancer. Most are early stage, proof of concept or efficacy trials [220]. Based on the frequent expression of FGFR3 in

the TN tumours, preclinical evaluation of inhibitors which target FGFR3 may be worth further pursuing.

EPHA5 staining was detected in the cytoplasm and cell membrane of the tumour cells in our study and had a significant association with a younger age at diagnosis. Age is one of the strongest poor prognostic indicators used [275]. The Eph family of receptors are the largest subfamily of RTKs. Different Eph receptors have been shown to play a role in modulating the transition from non-invasive to invasive tumours through up-regulation of genes involved in angiogenesis [361]. The role of EPHA5 has been explored somewhat in breast cancers; EPHA5 in cell lines has been found to be frequently epigenetically silenced by promoter methylation which corresponded to decreased protein expression in both primary breast tumours and breast cancer cell lines including the TNBC cell line MDA-MB-231. Silencing of EPHA5 was detected in only 64% of primary breast tumours which may suggest that a subset of breast cancer may express EPHA5 as a poor prognostic indicator [362]. EPHA5 has been associated with tumour dormancy pathways. Tumour dormancy is one of the currently accepted theories for breast cancer recurrence and dormant tumour cells are known to be resistant to standard chemotherapies including doxorubicin [363]. It is possible that through its role in tumour dormancy EPHA5 participates significantly in progression of TNBC. This may suggest that introducing an EPHA5 inhibitor in combination with primary chemotherapy may delay recurrences and improve overall survival, however much further study and examination would be required prior to implementing this strategy. Inhibitors targeting EPHA2 and EPHA3 are currently in clinical trials and the University of Texas have a patent on a peptide that inhibits EPHA5 making studies of EPHA5 inhibition an exciting future prospect [220, 364].

Although the Kaplan Meier survival curves for FGFR3 and EPHA5 did not achieve statistical significance (most likely due to small number of events occurring), the trends matched those observed in the BreastMark database. The combination of expression of FGFR3, EPHA5 and ROS1 mRNA results in a highly statistically significant survival curve with a hazard ratio of 3.08. Co-expression of FGFR3, EPHA5 and ROS1 mRNA may represent a biomarker panel to identify TNBC who have a poorer prognosis and require more aggressive treatment to improve survival. The Kaplan Meier survival curves for FGFR3 and EPHA5 combined expression from our cohort of TNBC did not reach statistical significance, however again the trend for both DFS and OS is worse for high expression of both.

8.10.2 Insulin Receptor in TNBC

Another potentially interesting target for TNBC which we identified in the 9 TNBC tumours examined for phosphorylation of RTKs is the insulin receptor (IR). The phosphorylation levels of the IR were significantly higher than the other RTKs. The cell line panel when assessed did not show such significant differences between the phosphorylation of the IR and other RTKs. While this is potentially an accurate reflection of IR phosphorylation status in the tumours caution must be exercised when interpreting the results. The phospho proteome can show significant fluctuations even in the process of tissue procurement. IRS-1 (an insulin receptor related protein) has shown the ability to increase its phosphorylation levels >20% post-excision [365]. While every care is taken to freeze the tissues immediately, time to freezing can vary significantly and as such IR phosphorylation levels may be falsely elevated.

However this does not negate the potential for the IR to be a target for therapies in TNBC. Early studies showed the overexpression of the IR in breast cancers compared to normal tissue and a significant association with age of the patient, tumour grade and ER positivity [366]. Insulin expression has also been confirmed in a number of ER positive cell lines which show increased responsiveness to insulin binding and activation of the IR via IGF-1 [367]. Additionally women with high levels of insulin have an increased risk factor in the development of breast cancer [368]. The phosphorylated IR has also been shown to be expressed in all subtypes of invasive breast cancer. In this study phosphorylated IR and total IR were shown to correlate with poorer overall survival [369]. IR is alternatively spliced to form two isoforms α and β. Examination of the mRNA levels of each isoform suggest the IRα may be the more dominant isoform in breast cancer. mRNA levels of IRβ are decreased relative to normal adjacent tissue while IRα was relatively similar [370].

8.11 Conclusions/Limitations and Future Work

c-Met is expressed at high levels in TNBC and at significantly higher levels than other breast cancer subtypes. We observed no significant association with progression or survival. c-Met/HGF inhibitors (CpdA, rilotumumab, PRS110, Crizotinib and BMS-777607) show limited responses in *in vitro* assays. While activity of CpdA, PRS110 and crizotinib were confirmed by responses in 2D proliferation assays a positive control was

not tested for rilotumumab. The U87-MG-LUC2 would be an appropriate positive control cell line as evidenced by the results of the HGF ELISA and qRT-PCR. Clonogenic assays for c-Met inhibitors (CpdA and PRS110) showed the highest level of sensitivity to growth inhibition. These results suggest that c-Met signalling may have an active role in tumour initiation. This combined with the evidence supporting a role for c-Met in the initiation of BLBC in mouse models might suggest a potential role in cancer prevention in high risk cases.

Targeting of c-Met and HGF through CpdA and rilotumumab showed a significant reduction in proliferation of three TNBC cell lines, however this result must be evaluated with caution as a positive control HGF expressing cell line was not included. We suggested the enhancement of response is due to interaction between human c-Met and bovine HGF. This hypothesis could be tested by examining phosphorylation levels of c-Met after rilotumumab treatment or co-immunoprecipation of human c-Met/bovine HGF to examine the presence of complexes. Thus the mechanism of the interaction between CpdA and rilotumumab requires further examination and may potentially be best evaluated in a recombinant huHGF expressing mouse model.

Targeting EGFR/Src in combination with c-Met showed a significant decrease in proliferation in TNBC cell lines. However the concentrations of CpdA tested may not be therapeutically relevant as they were in the micromolar range. Further evaluation of the combinations in fixed ratio combination assays over a range of concentrations of CpdA may provide more insight into the therapeutic relevance of these combinations. Furthermore, drug scheduling assays could potentially enhance response as evidenced by Mueller *et al.* In this study resistance to EGFR inhibitor gefitinib in TNBC SUM229 occurred in a time dependent manner and was mediated through c-Met/Src re-activation of EGFR signalling [213]. Finally combinations of c-Met with chemotherapy agents could also be beneficial for TNBC and warrant testing. Any potential clinical trial would be required to meet the current standard of care which involves chemotherapy regimens. Additionally c-Met has been implicated in resistance to chemotherapy in a number of clinical situations therefore c-Met blockade consecutively or in a scheduled manner as described above may enhance response to chemotherapy [198, 316, 317].

In tumour samples EGFR expression was too low for evaluation, however co-expression of c-Met and Src was seen in 83.3% of tumours. Phosphorylated Src was detectable in 38.8% of these tumours. No significant association was seen between any clinico-pathological variables and recurrence/OS. The trend in the Kaplan Meier curve for c-Met and phosphorylated Src suggest an increase in survival for high expressers, similar to what was previously reported. This highlights the need for selective biomarkers to identify patients who may benefit from c-Met/Src targeted therapies.

We identified c-Met as an escape mechanism for acquired resistance to two targeted agents dasatinib and cetuximab. The resistant variants were more sensitive to c-Met inhibition than their parental cell lines. We believe this may represent a common escape pathway and future work would include evaluating this is other models of resistance, including models of chemotherapy resistance.

We identified seven RTKs associated with poorer prognosis in TNBC, most of which have been previously implicated in angiogenic activity. Given the lack of success of anti-angiogenic agents in TNBC further examination is required to interrogate the possibility of combined expression of all or some of these RTKs could potentially form a protein signature to identify potential responders to antiangiogenic therapies.

FGFR3 and EPHA5 are expressed in TNBC tumour samples however protein expression in cell lines was undetectable. FGFR3 nuclear staining was significantly associated with histological subtype and membrane staining of EPHA5 was significantly associated with age. Trends in the Kaplan Meier Curves show a decreased DFS/OS with high expression of these proteins. To truly determine the potential prognostic significance of these RTKs a much larger cohort of patients should be examined. Preclinical evaluation of inhibitors of FGFR3 and EPHA5, preferably specific inhibitors, would help to determine their potential as targets for TNBC. Additionally, patient derived xenografts (PDX) may be required for *in vivo* evaluation, due to the lack of expression of these RTKs in the cell lines analysed. Lastly, combined expression of FGFR3, EPHA5 and ROS1 should be evaluated as a novel prognostic biomarker panel of TNBC.

References

1. Hennighausen L, Robinson GW. Signaling pathways in mammary gland development. *Dev Cell*. 2001;1(4):467-75.

2. Cancer in ireland 1994-2011: Annual report of the national cancer registry 2014 [Internet]. Available from: http://www.ncri.ie/sites/ncri/files/pubs/annual%20report%202014.pdf.

3. Polyak K. Breast cancer: Origins and evolution. *J Clin Invest*. 2007;117(11):3155-63.

4. Wiseman BS, Werb Z. Stromal effects on mammary gland development and breast cancer. *Science*. 2002;296(5570):1046-9.

5. Arnone P, Zurrida S, Viale G, et al. The TNM classification of breast cancer: Need for change. *Updates Surg*. 2010;62(2):75-81.

6. Weigelt B, Geyer FC, Reis-Filho JS. Histological types of breast cancer: How special are they? *Mol Oncol*. 2010;4(3):192-208.

7. Sørlie T, Perou CM, Tibshirani R, et al. Gene expression patterns of breast carcinomas distinguish tumor subclasses with clinical implications. *Proc Natl Acad Sci U S A*. 2001;98(19):10869-74.

8. Sørlie T, Tibshirani R, Parker J, et al. Repeated observation of breast tumor subtypes in independent gene expression data sets. *Proc Natl Acad Sci U S A*. 2003;100(14):8418-23.

9. Perou C, M., Sùrlie T, Eisen M, B., et al. Molecular portraits of human breast tumours. *Nature*. 2000;406(6797):747-52.

10. Osborne CK, Zhao H, Fuqua SA. Selective estrogen receptor modulators: Structure, function, and clinical use. *J Clin Oncol*. 2000;18(17):3172-86.

11. Browne BC, O'Brien N, Duffy MJ, et al. HER-2 signaling and inhibition in breast cancer. *Curr Cancer Drug Targets*. 2009;9(3):419-38.

12. O'Sullivan CC, Connolly RM. Pertuzumab and its accelerated approval: Evolving treatment paradigms and new challenges in the management of HER2-positive breast cancer. *Oncology (Williston Park)*. 2014;28(3):186,94, 196.

13. Verma S, Miles D, Gianni L, et al. Trastuzumab emtansine for HER2-positive advanced breast cancer. *N Engl J Med*. 2012;367(19):1783-91.

14. Widakowich C, de Azambuja E, Gil T, et al. Molecular targeted therapies in breast cancer: Where are we now? *Int J Biochem Cell Biol*. 2007;39(7–8):1375-87.

15. Elizabeth HM, Hammond MD, Hayes DF, et al. American society of clinical Oncology/College of american pathologists guideline recommendations for

immunohistochemical testing of estrogen and progesterone receptors in breast cancer. *Jour Onc Prac*. 2010;6(4):195-7.

16. RodrÃguez-Pinilla SM, SarriÃ³ D, Honrado E, et al. Prognostic significance of basal-like phenotype and fascin expression in node-negative invasive breast carcinomas. *Clin Cancer Res*. 2006;12(5):1533-9.

17. Dent R, Trudeau M, Pritchard KI, et al. Triple-negative breast cancer: Clinical features and patterns of recurrence. *Clin Cancer Res*. 2007;13(15 Pt 1):4429-34.

18. Livasy CA, Karaca G, Nanda R, et al. Phenotypic evaluation of the basal-like subtype of invasive breast carcinoma. *Mod Pathol*. 2005;19(2):264-71.

19. Abd El-Rehim DM, Ball G, Pinder SE, et al. High-throughput protein expression analysis using tissue microarray technology of a large well-characterised series identifies biologically distinct classes of breast cancer confirming recent cDNA expression analyses. - *International Journal of Cancer.* 2005;116(3):340-50*DOI-10.1002/ijc.21004*.

20. Nielsen TO, Hsu FD, Jensen K, et al. Immunohistochemical and clinical characterization of the basal-like subtype of invasive breast carcinoma. *Clin Cancer Res*. 2004;10(16):5367-74.

21. Korsching E, Packeisen J, Agelopoulos K, et al. Cytogenetic alterations and cytokeratin expression patterns in breast cancer: Integrating a new model of breast differentiation into cytogenetic pathways of breast carcinogenesis. *Lab Invest*. 2002;82(11):1525-33.

22. Kandoth C, McLellan MD, Vandin F, et al. Mutational landscape and significance across 12 major cancer types. *Nature*. 2013;502(7471):333-9.

23. Siziopikou KP, Ariga R, Proussaloglou KE, et al. The challenging estrogen receptor-negative/ progesterone receptor-Negative/HER-2-negative patient: A promising candidate for epidermal growth factor receptor-targeted therapy? - *The Breast Journal.* 2006;12(4):360-2*DOI- 10.1111/j.1075-122X.2006.00276.x*.

24. Wang Y, Waters J, Leung ML, et al. Clonal evolution in breast cancer revealed by single nucleus genome sequencing. *Nature*. 2014;512(7513):155-60.

25. Bergamaschi A, Kim YH, Wang P, et al. Distinct patterns of DNA copy number alteration are associated with different clinicopathological features and gene-expression subtypes of breast cancer. *Genes Chromosom Cancer*. 2006;45(11):1033-40.

26. Richard F, Pacyna-Gengelbach M, SchlÃ¼ns K, et al. Patterns of chromosomal imbalances in invasive breast cancer. *Int J Cancer*. 2000;89(3):305-10.

27. Herschkowitz JI, Simin K, Weigman VJ, et al. Identification of conserved gene expression features between murine mammary carcinoma models and human breast tumors. *Genome Biol*. 2007;8(5):R76,2007-8-5-r76.

28. Prat A, Parker J, Karginova O, et al. Phenotypic and molecular characterization of the claudin-low intrinsic subtype of breast cancer. *Breast Cancer Res*. 2010;12(5):R68.

29. Sabatier R, Finetti P, Guille A, et al. Claudin-low breast cancers: Clinical, pathological, molecular and prognostic characterization. *Mol Cancer*. 2014;13:228,4598-13-228.

30. Herschkowitz JI, Simin K, Weigman VJ, et al. Identification of conserved gene expression features between murine mammary carcinoma models and human breast tumors. *Genome Biol*. 2007;8:R76.

31. Lehmann BD, Bauer JA, Chen X, et al. Identification of human triple-negative breast cancer subtypes and preclinical models for selection of targeted therapies. *J Clin Invest*. 2011;121(7):2750-67.

32. Hoadley KA, Yau C, Wolf DM, et al. Multiplatform analysis of 12 cancer types reveals molecular classification within and across tissues of origin. *Cell*. 2014;158(4):929-44.

33. Prat A, Adamo B, Cheang MC, et al. Molecular characterization of basal-like and non-basal-like triple-negative breast cancer. *Oncologist*. 2013;18(2):123-33.

34. Burstein MD, Tsimelzon A, Poage GM, et al. Comprehensive genomic analysis identifies novel subtypes and targets of triple-negative breast cancer. *Clin Cancer Res*. 2014.

35. Lim E, Vaillant F, Wu D, et al. Aberrant luminal progenitors as the candidate target population for basal tumor development in BRCA1 mutation carriers. *Nat Med*. 2009;15(8):907-13.

36. Turner NC, Reis-Filho J. Basal-like breast cancer and the BRCA1 phenotype. *Oncogene*. 0000;25(43):5846-53.

37. Recently published ASCO guidelines [Internet].: Institute for quality; 2015 [updated 20/01/2015; cited 15/04/2015]. Available from: http://www.instituteforquality.org/recently-published-asco-guidelines.

38. Mauri D, Pavlidis N, Ioannidis JPA. Neoadjuvant versus adjuvant systemic treatment in breast cancer: A meta-analysis. *Journal of the National Cancer Institute*. 2005;97(3):188-94.

39. Fisher C, Ma C, Gillanders W, et al. Neoadjuvant chemotherapy is associated with improved survival compared with adjuvant chemotherapy in patients with triple-negative breast cancer only after complete pathologic response. *Annals of Surgical Oncology*. 2012;19(1):253-8.

40. Chemotherapy medicines [Internet].: Breastcancer.org; 2015 [updated 05.03.2015; cited 30.03.2015]. Available from: http://www.breastcancer.org/treatment/chemotherapy/medicines.

41. NCCN clinical practice guidelines in oncology, breast cancer version 2 [Internet].: National Comprehensive Cancer Network; 2015; cited 30.03.2015]. Available from: http://www.nccn.org/professionals/physician_gls/pdf/breast.pdf.

42. Effects of radiotherapy and of differences in the extent of surgery for early breast cancer on local recurrence and 15-year survival: An overview of the randomised trials. *The Lancet*;366(9503):2087-106.

43. Bartelink H, Horiot J, Poortmans P, et al. Recurrence rates after treatment of breast cancer with standard radiotherapy with or without additional radiation. *N Engl J Med*. 2001;345(19):1378-87.

44. Carey LA, Dees EC, Sawyer L, et al. The triple negative paradox: Primary tumor chemosensitivity of breast cancer subtypes. *Clin Cancer Res*. 2007;13(8):2329-34.

45. Rouzier R, Perou CM, Symmans WF, et al. Breast cancer molecular subtypes respond differently to preoperative chemotherapy. *Clin Cancer Res*. 2005;11(16):5678-85.

46. Sirohi B, Arnedos M, Popat S, et al. Platinum-based chemotherapy in triple-negative breast cancer. *Ann Oncol*. 2008;19(11):1847-52.

47. Carey LA. Directed therapy of subtypes of triple-negative breast cancer. *The Oncologist*. 2011;16(suppl 1):71-8.

48. Gschwind A, Fischer OM, Ullrich A. The discovery of receptor tyrosine kinases: Targets for cancer therapy. *Nat Rev Cancer*. 2004;4(5):361-70.

49. Duffy MJ, McGowan PM, Crown J. Targeted therapy for triple-negative breast cancer: Where are we? *Int J Can*. 2012;131(11):2471-7.

50. Gerber DE. Targeted therapies: A new generation of cancer treatments. *Am Fam Physician*. 2008;77(3):311-9.

51. Weiner LM, Borghaei H. Targeted therapies in solid tumors: Monoclonal antibodies and small molecules. *Hum Antibodies*. 2006;15(3):103-11.

52. Eisenbeis AM, Grau SJ. Monoclonal antibodies and fc fragments for treating solid tumors. *Biologics*. 2012;6:13-20.

53. Goldstein NI, Prewett M, Zuklys K, et al. Biological efficacy of a chimeric antibody to the epidermal growth factor receptor in a human tumor xenograft model. *Clinical Cancer Research*. 1995;1(11):1311-8.

54. Braghiroli MI, Sabbaga J, Hoff PM. Bevacizumab: Overview of the literature. *Expert Rev Anticancer Ther*. 2012;12(5):567-80.

55. Ludwig DL, Pereira DS, Zhu Z, et al. Monoclonal antibody therapeutics and apoptosis. *Oncogene*. 0000;22(56):9097-106.

56. Trauth BC, Klas C, Peters AM, et al. Monoclonal antibody-mediated tumor regression by induction of apoptosis. *Science*. 1989;245(4915):301-5.

57. Mehren Mv, Adams GP, Weiner LM. Monoclonal antibody therapy for cancer. *Annu Rev Med*. 2003;54(1):343-69.

58. Houghton AN, Mintzer D, Cordon-Cardo C, et al. Mouse monoclonal IgG3 antibody detecting GD3 ganglioside: A phase I trial in patients with malignant melanoma. *Proceedings of the National Academy of Sciences*. 1985;82(4):1242-6.

59. Simpson A, Caballero O. Monoclonal antibodies for the therapy of cancer. *BMC Proceedings*. 2014;8:O6.

60. Mellor J, Brown M, Irving H, et al. A critical review of the role of fc gamma receptor polymorphisms in the response to monoclonal antibodies in cancer. *Journal of Hematology & Oncology*. 2013;6(1):1.

61. Niculescu-Duvaz I. Trastuzumab emtansine, an antibody-drug conjugate for the treatment of HER2+ metastatic breast cancer. *Curr Opin Mol Ther*. 2010;12(3):350-60.

62. Robinson DR, Wu Y, Ling S. The protein tyrosine kinase family of the human genome. *Oncogene*. 2000;19(49):5548-57.

63. Cadena D, Gill G. Receptor tyrosine kinases. *FASEB J*. 1992;6(6):2332-7.

64. King C, Kraus M, Aaronson S. Amplification of a novel v-erbB-related gene in a human mammary carcinoma. *Science*. 1985;229(4717):974-6.

65. Lemmon MA, Schlessinger J. Cell signaling by receptor tyrosine kinases. *Cell*. 2010;141(7):1117-34.

66. Klijn JG, Look MP, Portengen H, et al. The prognostic value of epidermal growth factor receptor (EGF-R) in primary breast cancer: Results of a 10 year follow-up study. *Breast Cancer Res Treat*. 1994;29(1):73-83.

67. Fox SB, Smith K, Hollyer J, et al. The epidermal growth factor receptor as a prognostic marker: Results of 370 patients and review of 3009 patients. *Breast Cancer Res Treat*. 1994;29(1):41-9.

68. Sainsbury JR, Farndon JR, Needham GK, et al. Epidermal-growth-factor receptor status as predictor of early recurrence of and death from breast cancer. *Lancet*. 1987;1:1398-402.

69. Stratford A, Habibi G, Astanehe A, et al. Epidermal growth factor receptor (EGFR) is transcriptionally induced by the Y-box binding protein-1 (YB-1) and can be inhibited with iressa in basal-like breast cancer, providing a potential target for therapy. *Breast Cancer Res*. 2007;9(5):R61.

70. Sainsbury JR, Malcolm AJ, Appleton DR, et al. Presence of epidermal growth factor receptor as an indicator of poor prognosis in patients with breast cancer. *J Clin Pathol*. 1985;38(11):1225-8.

71. Brabender J, Danenberg KD, Metzger R, et al. Epidermal growth factor receptor and HER2-neu mRNA expression in non-small cell lung cancer is correlated with survival. *Clin Cancer Res*. 2001;7(7):1850-5.

72. Meyers MB, Shen WP, Spengler BA, et al. Increased epidermal growth factor receptor in multidrug-resistant human neuroblastoma cells. *J Cell Biochem*. 1988;38(2):87-97.

73. Liu D, He J, Yuan Z, et al. EGFR expression correlates with decreased disease-free survival in triple-negative breast cancer: A retrospective analysis based on a tissue microarray. *Medical Oncology*. 2012;29(2):401-5.

74. Corkery B, Crown J, Clynes M, et al. Epidermal growth factor receptor as a potential therapeutic target in triple-negative breast cancer. *Annals of Oncology*. 2009;20(5):862-7.

75. von Minckwitz G, Jonat W, Fasching P, et al. A multicentre phase II study on gefitinib in taxane- and anthracycline-pretreated metastatic breast cancer. *Breast Cancer Res Treat*. 2005;89(2):165-72.

76. Baselga J, Albanell J, Ruiz A, et al. Phase II and tumor pharmacodynamic study of gefitinib in patients with advanced breast cancer. *Journal of Clinical Oncology*. 2005;23(23):5323-33.

77. Kaur H, Silverman P, Singh D, et al. Toxicity and outcome data in a phase II study of weekly docetaxel in combination with erlotinib in recurrent and/or metastatic breast cancer (MBC). *ASCO Meeting Abstracts*. 2006;24(18_suppl):10623.

78. Ronnstrand L. Signal transduction via the stem cell factor receptor/c-kit. *Cell Mol Life Sci*. 2004;61(19):2535-48.

79. Modi S, Seidman AD, Dickler M, et al. A phase II trial of imatinib mesylate monotherapy in patients with metastatic breast cancer. *Breast Cancer Res Treat*. 2005;90(2):157-63.

80. Tryfonopoulos D, O' Donovan N, Corkery B, et al. Activity of dasatinib with chemotherapy in triple-negative breast cancer cells. *ASCO Meeting Abstracts*. 2009;27(suppl).

81. Previdi S, Abbadessa G, Dalò F, et al. Breast Cancer–Derived bone metastasis can be effectively reduced through specific c-MET inhibitor tivantinib (ARQ 197) and shRNA c-MET knockdown. *Mol Cancer Ther*. 2012;11(1):214-23.

82. Ponzo MG, Lesurf R, Petkiewicz S, et al. Met induces mammary tumors with diverse histologies and is associated with poor outcome and human basal breast cancer. *Proc Natl Acad Sci U S A*. 2009;106(31):12903-8.

83. Cooper C, S., Park M, Blair D, G., et al. Molecular cloning of a new transforming gene from a chemically transformed human cell line. *Nature*. 1984;311:29-33.

84. Park M, Dean M, Cooper CS, et al. Mechanism of met oncogene activation. *Cell*. 1986;45(6):895-904.

85. Park M, Dean M, Kaul K, et al. Sequence of MET protooncogene cDNA has features characteristic of the tyrosine kinase family of growth-factor receptors. *Proc Natl Acad Sci U S A*. 1987;84(18):6379-83.

86. Gautam M, Shrikhande A, Kijima T, et al. Role of the hepatocyte growth factor receptor, c-met, in oncogenisis and potential for therapeutic inhibition. *Cytokine Growth Factor Rev*. 2002;13(1):41-59.

87. Gherardi E, Youles M, E., Miguel R, N., et al. Functional map and domain structure of MET, the product of the c-met protooncogene and receptor for hepatocyte growth factor/scatter factor. *Proc Nat Acad Sci USA*. 2003;100(21):12039-44.

88. Tempest PR, Stratton MR, Cooper CS. Structure of the met protein and variation of the met protein kinase activity among human tumour cell lines. *Br J Cancer*. 1988;58(1):3-7.

89. Artigiani S, Comoglio PM, Tamagnone L. Plexins, semaphorins, and scatter factor receptors: A common root for cell guidance signals? *IUBMB Life*. 1999;48(5):477-82.

90. Maestrini E, Tamagnone L, Longati P, et al. A family of transmembrane proteins with homology to the MET-hepatocyte growth factor receptor. *Proc Nat Acad Sci USA*. 1996;93(2):674-8.

91. Gaudino G, Follenzi A, Naldini L, et al. Ron is a heterodimeric tyrosine kinase receptor activated by the HGF homologue MSP. *EMBO J*. 1994;13(15):3524-32.

92. Medico E, Mongiovi AM, Huff J, et al. The tyrosine kinase receptors ron and sea control 'scattering' and morphogenesis of liver progenitor cells in vitro. *Mol Biol Cell*. 1996;7(4):495-504.

93. Blumenschein GR, Mills GB, Gonzalez-Angulo AM. Targeting the hepatocyte growth Factor–cMET axis in cancer therapy. *J Clin Oncol*. 2012;30(26):3287-96.

94. Graveel CR, Tolbert D, Vande Woude GF. MET: A critical player in tumorigenesis and therapeutic target. *Cold Spring Harb Perspect Biol*. 2013;5(7):a009209.

95. Naldini L, Vigna E, Ferracini R, et al. The tyrosine kinase encoded by the MET proto-oncogene is activated by autophosphorylation. *Mol Cell Biol*. 1991;11(4):1793-803.

96. Ponzetto C, Bardelli A, Zhen Z, et al. A multifunctional docking site mediates signaling and transformation by the hepatocyte growth factor/scatter factor receptor family. *Cell*. 1994;77(2):261-71.

97. Park WS, Dong SM, Kim SY, et al. Somatic mutations in the kinase domain of the Met/Hepatocyte growth factor receptor gene in childhood hepatocellular carcinomas. *Cancer Res*. 1999;59(2):307-10.

98. Di Renzo MF, Olivero M, Martone T, et al. Somatic mutations of the MET oncogene are selected during metastatic spread of human HNSC carcinomas. *Oncogene*. 2000;19(12):1547-55.

99. Ponzetto C, Bardelli A, Maina F, et al. A novel recognition motif for phosphatidylinositol 3-kinase binding mediates its association with the hepatocyte growth factor/scatter factor receptor. *Mol Cell Biol*. 1993;13(8):4600-8.

100. Gaule PB, Crown J, O'Donovan N, et al. cMET in triple-negative breast cancer: Is it a therapeutic target for this subset of breast cancer patients? *Expert Opin Ther Targets*. 2014;18(9):999-1009.

101. Naldini L, Weidner KM, Vigna E, et al. Scatter factor and hepatocyte growth factor are indistinguishable ligands for the met receptor. *EMBO J*. 1991;10(10):2867-78.

102. Bhargava M, Joseph A, Knesel J, et al. Scatter factor and hepatocyte growth factor: Activities, properties, and mechanism. *Cell Growth Differ*. 1992;3(1):11-20.

103. Tashiro K, Hagiya M, Nishizawa T, et al. Deduced primary structure of rat hepatocyte growth factor and expression of the mRNA in rat tissues. *Proc Natl Acad Sci U S A*. 1990;87(8):3200-4.

104. Nakamura T, Nawa K, Ichihara A, et al. Purification and subunit structure of hepatocyte growth factor from rat platelets. *FEBS Lett*. 1987;224(2):311-6.

105. Nakamura T, Nishizawa T, Hagiya M, et al. Molecular cloning and expression of human hepatocyte growth factor. *Nature*. 1989;342(6248):440-3.

106. Naldini L, Tamagnone L, Vigna E, et al. Extracellular proteolytic cleavage by urokinase is required for activation of hepatocyte growth factor/scatter factor. *EMBO J*. 1992;11(13):4825-33.

107. Mars W, Zarnegar R, Michalopoulos G. Activation of hepatocyte growth factor by the plasminogen activators uPA and tPA. *Am J Pathol*. 1993;143(3):949-58.

108. Miyazawa K, Shimomura T, Naka D, et al. Proteolytic activation of hepatocyte growth factor in response to tissue injury. *J Biol Chem*. 1994;269(12):8966-70.

109. Lokker NA, Mark MR, Luis EA, et al. Structure-function analysis of hepatocyte growth factor: Identification of variants that lack mitogenic activity yet retain high affinity receptor binding. *EMBO J*. 1992;11(7):2503-10.

110. Hartmann G, Naldini L, Weidner KM, et al. A functional domain in the heavy chain of scatter factor/hepatocyte growth factor binds the c-met receptor and induces cell dissociation but not mitogenesis. *Proc Nat Acad Sci USA*. 1992;89(23):11574-8.

111. Matsumoto K, Tajima H, Okazaki H, et al. Heparin as an inducer of hepatocyte growth factor. *J Biochem*. 1993;114(6):820-6.

112. Kemp LE, Mulloy B, Gherardi E. Signalling by HGF/SF and met: The role of heparan sulphate co-receptors. *Biochemical Society Transactions*. 2006;34(3):414-7.

113. Chirgadze D, Y., Hepple J, P., Zhou H, et al. Crystal structure of the NK1 fragment of HGF/SF suggests a novel mode for growth factor dimerisation and receptor binding. *Nat Struct Biol*. 1996;6(1):72-9.

114. Tolbert WD, Daugherty-Holtrop J, Gherardi E, et al. Structural basis for agonism and antagonism of hepatocyte growth factor. *Proc Natl Acad Sci U S A*. 2010;107(30):13264-9.

115. Fruman D, Meyers R, Cantly L. Phosphoinositide kinases. *Annu Rev Biochme*. 1998;67:481--507.

116. Sarbassov DD, Guertin DA, Ali SM, et al. Phosphorylation and regulation of Akt/PKB by the rictor-mTOR complex. *Science*. 2005;307(5712):1098-101.

117. Bu R, Uddin S, Bavi P, et al. HGF/c-met pathway has a prominent role in mediating antiapoptotic signals through AKT in epithelial ovarian carcinoma. *Lab Invest*. 2011;91(1):124-37.

118. Liu Y, Shi Q, Qi M, et al. Interruption of hepatocyte growth factor signaling augmented oridonin-induced death in human non-small cell lung cancer A549 cells *via* c-met-nuclear factor-κB-cyclooxygenase-2 and c-met-bcl-2-caspase-3 pathways. *Biol Pharm Bull*. 2012;35(7):1150-8.

119. Boccaccio C, Ando M, Tamagnone L, et al. Induction of epithelial tubules by growth factor HGF depends on the STAT pathway. *Nature*. 1998;391(6664):285-8.

120. Kermorgant S, Parker PJ. Receptor trafficking controls weak signal delivery: A strategy used by c-met for STAT3 nuclear accumulation. *J Cell Biol*. 2008;182(5):855-63.

121. Silva CM. Role of STATs as downstream signal transducers in src family kinase-mediated tumorigenesis. *Oncogene*. 0000;23(48):8017-23.

122. Trusolino L, Bertotti A, Comoglio PM. MET signalling: Principles and functions in development, organ regeneration and cancer. *Nat Rev Mol Cell Biol*. 2010;11(12):834-48.

123. Jeffers M, Taylor GA, Weidner KM, et al. Degradation of the met tyrosine kinase receptor by the ubiquitin-proteasome pathway. *Mol Cell Biol*. 1997;17(2):799-808.

124. Cho K, Park JH, Park C, et al. Identification of a pivotal endocytosis motif in c-met and selective modulation of HGF-dependent aggressiveness of cancer using the 16-mer endocytic peptide. *Oncogene*. 2012.

125. Peschard P, Fournier TM, Lamorte L, et al. Mutation of the c-cbl TKB domain binding site on the met receptor tyrosine kinase converts it into a transforming protein. *Mol Cell*. 2001;8(5):995-1004.

126. Peschard P, Ishiyama N, Lin T, et al. A conserved DpYR motif in the juxtamembrane domain of the met receptor family forms an atypical c-Cbl/Cbl-b tyrosine kinase binding domain binding site required for suppression of oncogenic activation. *Journal of Biological Chemistry*. 2004;279(28):29565-71.

127. Sangwan V, Paliouras GN, Abella JV, et al. Regulation of the met receptor-tyrosine kinase by the protein-tyrosine phosphatase 1B and T-cell phosphatase. *J Biol Chem*. 2008;283(49):34374-83.

128. Abella JV, Parachoniak CA, Sangwan V, et al. Dorsal ruffle microdomains potentiate met receptor tyrosine kinase signaling and down-regulation. *J Biol Chem*. 2010;285(32):24956-67.

129. Uehara Y, Minowa O, Mori C, et al. Placental defect and embryonic lethality in mice lacking hepatocyte growth factor/scatter factor. *Nature*. 1995;373(6516):702-5.

130. Schmidt C, Bladt F, Goedecke S, et al. Scatter factor/hepatocyte growth factor is essential for liver development. *Nature*. 1995;373(6516):699-702.

131. Wang Y, Selden C, Farnaud S, et al. Hepatocyte growth factor (HGF/SF) is expressed in human epithelial cells during embryonic development; studies by in situ hybridisation and northern blot analysis. *J Anat*. 1994;185 (Pt 3)(Pt 3):543-51.

132. Bladt F, Riethmacher D, Isenmann S, et al. Essential role for the c-met receptor in the migration of myogenic precursor cells into the limb bud. *Nature*. 1995;376(6543):768-71.

133. Chmielowiec J, Borowiak M, Morkel M, et al. c-met is essential for wound healing in the skin. *J Cell Biol*. 2007;177(1):151-62.

134. Yant J, Buluwela L, Niranjan B, et al. In VivoEffects of hepatocyte growth Factor/Scatter factor on mouse mammary gland development. *Exp Cell Res*. 1998;241(2):476-81.

135. Lee S, Huang P, Roller P, et al. Matriptase/epithin participates in mammary epithelial cell growth and morphogenesis through HGF activation. *Mech Dev*. 2010;127(1-2):82-95.

136. Tatsumi R, Anderson JE, Nevoret CJ, et al. HGF/SF is present in normal adult skeletal muscle and is capable of activating satellite cells. *Dev Biol*. 1998;194(1):114-28.

137. Soriano JV, Pepper MS, Nakamura T, et al. Hepatocyte growth factor stimulates extensive development of branching duct-like structures by cloned mammary gland epithelial cells. *J Cell Sci*. 1995;108(2):413-30.

138. Lindemann K, Resau J, Nährig J, et al. Differential expression of c-met, its ligand HGF/SF and HER2/neu in DCIS and adjacent normal breast tissue. *Histopathology*. 2007;51(1):54-62.

139. Kim C-, Koh YW, Han JH, et al. c-met expression as an indicator of survival outcome in patients with oral tongue carcinoma. *Head Neck*. 2010:n/a,n/a.

140. Tuck AB, Park M, Sterns EE, et al. Coexpression of hepatocyte growth factor and receptor (met) in human breast carcinoma. *Am J Pathol*. 1996;148(1):225-32.

141. Schmidt L, Duh F, Chen F, et al. Germline and somatic mutations in the tyrosine kinase domain of the MET proto-oncogene in papillary renal carcinomas. *Nat Genet*. 1997;16:68-73.

142. Kentsis A, Reed C, Rice KL, et al. Autocrine activation of the MET receptor tyrosine kinase in acute myeloid leukemia. *Nat Med*. 2012;18(7):1118-22.

143. Toiyama Y, Yasuda H, Saigusa S, et al. Co-expression of hepatocyte growth factor and c-met predicts peritoneal dissemination established by autocrine hepatocyte growth factor/c-met signaling in gastric cancer. *Int J Cancer*. 2012;130(12):2912-21.

144. Xie Q, Bradley R, Kang L, et al. Hepatocyte growth factor (HGF) autocrine activation predicts sensitivity to MET inhibition in glioblastoma. *Proc Nat Acad Sci USA*. 2012;109(2):570-5.

145. Weidner KM, Behrens J, Vandekerckhove J, et al. Scatter factor: Molecular characteristics and effect on the invasiveness of epithelial cells. *J Cell Biol*. 1990;111(5 Pt 1):2097-108.

146. Jeffers M, Rong S, Vande Woude G. Enhanced tumorigenicity and invasion-metastasis by hepatocyte growth factor/scatter factor-met signalling in human cells concomitant with induction of the urokinase proteolysis network. *Mol Cell Biol*. 1996;16(3):1115-25.

147. Kajiya K, Hirakawa S, Ma B, et al. Hepatocyte growth factor promotes lymphatic vessel formation and function. *EMBO J*. 2005;24(16):2885-95.

148. Graveel CR, DeGroot JD, Su Y, et al. Met induces diverse mammary carcinomas in mice and is associated with human basal breast cancer. *Proc Nat Acad Sci USA*. 2009;106(31):12909-14.

149. Carracedo A, Egervari K, Salido M, et al. FISH and immunohistochemical status of the hepatocyte growth factor receptor (c-met) in 184 invasive breast tumors. *Breast Cancer Res*. 2009;11(2):402.

150. Turner N, Lambros MB, Horlings HM, et al. Integrative molecular profiling of triple negative breast cancers identifies amplicon drivers and potential therapeutic targets. *Oncogene*. 2010;29(14):2013-23.

151. de Melo Gagliato D, Jardim DLF, Falchook G, et al. Analysis of MET genetic aberrations in patients with breast cancer at MD anderson phase I unit. *Clin Breast Cancer*. 2014;14(6):468-74.

152. Raghav KP, Wang W, Liu S, et al. cMET and phospho-cMET protein levels in breast cancers and survival outcomes. *Clin Cancer Res*. 2012;18(8):2269-77.

153. Lengyel E, Prechtel D, Resau JH, et al. C-met overexpression in node-positive breast cancer identifies patients with poor clinical outcome independent of Her2/neu. *Int J Oncol*. 2005;113(4):678-82.

154. Beviglia L, Matsumoto K, Lin C, et al. Expression of the C-Met/HGF receptor in human breast carcinoma: Correlation with tumor progression. *Int J Can*. 1997;74:301-9.

155. Coleman RE. Clinical features of metastatic bone disease and risk of skeletal morbidity. *Clin Cancer Res*. 2006;12(20):6243s-9s.

156. Previdi S, Maroni P, Matteucci E, et al. Interaction between human-breast cancer metastasis and bone microenvironment through activated hepatocyte growth factor/Met and β-catenin/Wnt pathways. *Eur J Cancer*. 2010;46(9):1679-91.

157. Feng Y, Pan T, Pant DK, et al. SPSB1 promotes breast cancer recurrence by potentiating c-MET signaling. *Cancer Discov*. 2014;doi:10.1158/2159-8290.CD-13-0548.

158. Jung HY, Joo HJ, Park JK, et al. The blocking of c-met signaling induces apoptosis through the increase of p53 protein in lung cancer. *Cancer Res Treat*. 2012;44(4):251-61.

159. Yamashita J, Ogawa M, Yamashita S, et al. Immunoreactive hepatocyte growth factor is a strong and independent predictor of recurrence and survival in human breast cancer. *Cancer Res*. 1994;54(7):1630-3.

160. Yao Y, Jin L, Fuchs A, et al. Scatter factor protein levels in human breast cancers. *Am J Pathol*. 1996;149(5):1707-17.

161. Edakuni G, Sasatomi E, Satoh T, et al. Expression of the hepatocyte growth factor/c-met pathway is increased at the cancer front in breast carcinoma. *Pathol Int*. 2001;51(3):172-8.

162. Kang JY, Dolled-Filhart M, Ocal IT, et al. Tissue microarray analysis of hepatocyte growth Factor/Met pathway components reveals a role for met, matriptase, and hepatocyte growth factor activator inhibitor 1 in the progression of node-negative breast cancer. *Cancer Res*. 2003;63(5):1101-5.

163. Toi M, Taniguchi T, Ueno T, et al. Significance of circulating hepatocyte growth factor level as a prognostic indicator in primary breast cancer. *Clin Can Res*. 1998;4(3):659-64.

164. Sheen-Chen S, Liu Y, Eng H, et al. Serum levels of hepatocyte growth factor in patients with breast cancer. *Cancer Epidemiol Biomarkers Prev*. 2005;14(3):715-7.

165. Fan S, Wang JA, Yuan RQ, et al. Scatter factor protects epithelial and carcinoma cells against apoptosis induced by DNA-damaging agents. *Oncogene*. 1998;17(2):131-41.

166. Huang S, Ouyang N, Lin L, et al. HGF-induced PKCζ Activation increases functional CXCR4 expression in human breast cancer cells. *PLoS ONE*. 2012;7(1):e29124.

167. Garcia S, Dales J, Charafe-Jauffret E, et al. Overexpression of c-met and of the transducers PI3K, FAK, JAK in breast carcinomas correlates with shorter survival and neoangiogenesis. *Int J Oncol*. 2007;31:48-58.

168. S. Garcia, DalÃ¨s,JP, Charafe-Jauffret,E., et al. Poor prognosis in breast carcinomas correlates with increased expression of targetable CD146 and c-Met and with proteomic basal-like phenotype*Human pathology*386830-841.

169. Ho-Yen CM, Green AR, Rakha EA, et al. C-met in invasive breast cancer. *Cancer*. 2014;120(2):163-71.

170. Charafe-Jauffret E, Ginestier C, Monville F, et al. Gene expression profiling of breast cell lines identifies potential new basal markers. *Oncogene*. 2005;25(15):2273-84.

171. Gonçalves A, Charafe-Jauffret E, Bertucci F, et al. Protein profiling of human breast tumor cells identifies novel biomarkers associated with molecular subtypes. *Mol Cell Proteomics*. 2008;7(8):1420-33.

172. Inanc M, Ozkan M, Karaca H, et al. Cytokeratin 5/6, c-met expressions, and PTEN loss prognostic indicators in triple-negative breast cancer. *Medical Oncology*. 2013;31(1):1-8.

173. Knight JF, Lesurf R, Zhao H, et al. Met synergizes with p53 loss to induce mammary tumors that possess features of claudin-low breast cancer. *Proc Natl Acad Sci U S A*. 2013.

174. Gastaldi S, Sassi F, Accornero P, et al. Met signaling regulates growth, repopulating potential and basal cell-fate commitment of mammary luminal progenitors: Implications for basal-like breast cancer. *Oncogene*. 2013;32(11):1428-40.

175. Casbas-Hernandez P, D'Arcy M, Roman-Perez E, et al. Role of HGF in epithelial-stromal cell interactions during progression from benign breast disease to ductal carcinoma in situ. *Breast Cancer Res*. 2013;15(5):R82.

176. Sung KE, Su X, Berthier E, et al. Understanding the impact of 2D and 3D fibroblast cultures on in vitro breast cancer models. *PLoS ONE*. 2013;8(10):e76373.

177. Wu JM, Fackler MJ, Halushka MK, et al. Heterogeneity of breast cancer metastases: Comparison of therapeutic target expression and promoter methylation between primary tumors and their multifocal metastases. *Clin Can Res*. 2008;14(7):1938-46.

178. Finkbeiner MR, Astanehe A, To K, et al. Profiling YB-1 target genes uncovers a new mechanism for MET receptor regulation in normal and malignant human mammary cells. *Oncogene*. 2009;28(11):1421-31.

179. Engelman JA, Zejnullahu K, Mitsudomi T, et al. MET amplification leads to gefitinib resistance in lung cancer by activating ERBB3 signaling. *Science*. 2007;316(5827):1039-43.

180. Turke AB, Zejnullahu K, Wu Y, et al. Preexistence and clonal selection of MET amplification in EGFR mutant NSCLC. *Science*. 2010;17(1):77-88.

181. Mueller KL, Yang ZQ, Haddad R, et al. EGFR/Met association regulates EGFR TKI resistance in breast cancer. *J Mol Signal*. 2010;5:8 doi: 10.1186/1750-2187-5-8.

182. Bergstrom JD, Westermark B, Heldin NE. Epidermal growth factor receptor signaling activates met in human anaplastic thyroid carcinoma cells. *Exp Cell Res*. 2000;259:293-9.

183. Fischer OM, Giordano S, Comoglio PM, et al. Reactive oxygen species mediate met receptor transactivation by G protein-coupled receptors and the epidermal growth factor receptor in human carcinoma cells. *J Biol Chem*. 2004;279(28):28970-8.

184. Song N, Liu S, Zhang J, et al. Cetuximab-induced MET activation acts as a novel resistance mechanism in colon cancer cells. *Int J Mol Sci*. 2014;15(4):5838-51.

185. Kim YJ, Choi J, Seo J, et al. MET is a potential target for use in combination therapy with EGFR inhibition in triple-negative/basal-like breast cancer. *Int J Can*. 2014;134(10):2424-36.

186. Bonine-Summers A, Aakre ME, Brown KA, et al. Epidermal growth factor receptor plays a significant role in hepatocyte growth factor mediated biological responses in mammary epithelial cells. *Cancer Biology & Therapy*. 2007;6(4):561-70.

187. Mueller KL, Madden JM, Zoratti GL, et al. Fibroblast-secreted hepatocyte growth factor mediates epidermal growth factor receptor tyrosine kinase inhibitor resistance in triple-negative breast cancers through paracrine activation of met. *Breast Cancer Res*. 2012;14(4):R104.

188. Jo M, Stolz DB, Esplen JE, et al. Cross-talk between epidermal growth factor receptor and c-met signal pathways in transformed cells. *J Biol Chem*. 2000;275(12):8806-11.

189. Xu H, Stabile LP, Gubish CT, et al. Dual blockade of EGFR and c-met abrogates redundant signaling and proliferation in head and neck carcinoma cells. *Clin Can Res*. 2011;17(13):4425-38.

190. Zhang Y, Staal B, Essenburg C, et al. MET kinase inhibitor SGX523 synergizes with epidermal growth factor receptor inhibitor erlotinib in a hepatocyte growth Factor–Dependent fashion to suppress carcinoma growth. *Cancer Res*. 2010;70(17):6880-90.

191. Parsons SJ, Parsons JT. Src family kinases, key regulators of signal transduction. *Oncogene*. 0000;23(48):7906-9.

192. Finn R, Dering J, Ginther C, et al. Dasatinib, an orally active small molecule inhibitor of both the src and abl kinases, selectively inhibits growth of basal-type/triple-

negative breast cancer cell lines growing in vitro. *Breast Cancer Res Treat*. 2007;105(3):319-26.

193. Tryfonopoulos D, Walsh S, Collins DM, et al. Src: A potential target for the treatment of triple-negative breast cancer. *Ann Oncol*. 2011;22(10):2234-40.

194. Sánchez-Bailón MP, Calcabrini A, Gómez-Domínguez D, et al. Src kinases catalytic activity regulates proliferation, migration and invasiveness of MDA-MB-231 breast cancer cells. *Cell Signal*. 2012;24(6):1276-86.

195. Gartner E, Kim E, L Choi L, et al. Preclinial efficacy of the combination of met and src family kinase inhbitors in triple negative breast cancer. *Cancer Res (24 Suppl; abstr PD08-08)*. 2011;71((24 Suppl; abstr PD08-08)).

196. Gaule P, Collins D, Walsh N, et al. Met and HGF inhibition in triple-negative breast cancer cell lines. *J Clin Oncol*. 2011;31((Suppl; abstr 1066)).

197. Wilson TR, Fridlyand J, Yan Y, et al. Widespread potential for growth-factor-driven resistance to anticancer kinase inhibitors. *Nature*. 2012;advance online publication.

198. Chen C, Kim H, Liska D, et al. MET activation mediates resistance to lapatinib inhibition of HER2-amplified gastric cancer cells. *Molecular Cancer Therapeutics*. 2012;11(3):660-9.

199. Liu L, Shi H, Liu Y, et al. Synergistic effects of foretinib with HER-targeted agents in MET and HER1- or HER2-coactivated tumor cells. *Mol Can Ther*. 2011;10(3):518-30.

200. Paulson AK, Linklater ES, Berghuis BD, et al. MET and ERBB2 are coexpressed in ERBB2+ breast cancer and contribute to innate resistance. *Mol Can Res*. 2013;11(9):1112-21.

201. Khoury H, Naujokas MA, Zuo D, et al. HGF converts ErbB2/Neu epithelial morphogenesis to cell invasion. *Mol Biol Cell*. 2005;16(2):550-61.

202. Shattuck DL, Miller JK, Carraway KL, et al. Met receptor contributes to trastuzumab resistance of Her2-overexpressing breast cancer cells. *Cancer Res*. 2008;68(5):1471-7.

203. Minuti G, Cappuzzo F, Duchnowska R, et al. Increased MET and HGF gene copy numbers are associated with trastuzumab failure in HER2-positive metastatic breast cancer. *Br J Cancer*. 2012;107(5):793-9.

204. Trusolino L, Bertotti A, Comoglio PM. A signaling adapter function for α6β4 integrin in the control of HGF-dependent invasive growth. *Cell*. 2001;107(5):643-54.

205. Chung J, Yoon S, Lipscomb EA, et al. The met receptor and α6β4 integrin can function independently to promote carcinoma invasion. *J Biol Chem*. 2004;279(31):32287-93.

206. Chan P, Chen S, Chen C, et al. Crosstalk between hepatocyte growth factor and integrin signaling pathways. *J Biomed Sci*. 2006;13:215-25.

207. Singleton PA, Salgia R, Moreno-Vinasco L, et al. CD44 regulates hepatocyte growth factor-mediated vascular integrity. *J Biol Chem*. 2007;282(42):30643-57.

208. Orian-Rousseau V, Chen L, Sleeman JP, et al. CD44 is required for two consecutive steps in HGF/c-met signaling. *Genes Dev*. 2002;16(23):3074-86.

209. Pennacchietti S, Michieli P, Galluzzo M, et al. Hypoxia promotes invasive growth by transcriptional activation of the met protooncogene. *Cancer Cell*. 2003;3(4):347-61.

210. Comito G, Calvani M, Giannoni E, et al. HIF-1α stabilization by mitochondrial ROS promotes met-dependent invasive growth and vasculogenic mimicry in melanoma cells. *Free Radic Biol Med*. 2011;51(4):893-904.

211. Tacchini L, De Ponti C, Matteucci E, et al. Hepatocyte growth factor-activated NF-κB regulates HIF-1 activity and ODC expression, implicated in survival, differently in different carcinoma cell lines. *Carcinogenesis*. 2004;25(11):2089-100.

212. Hsu Y, Yao J, Chan L, et al. Definition of PKC-a, CDK6, and MET as therapeutic targets in triple-negative breast cancer. *Cancer Res*. 2014;74(17):4822-35.

213. Mueller KL, Hunter LA, Ethier SP, et al. Met and c-src cooperate to compensate for loss of epidermal growth factor receptor kinase activity in breast cancer cells. *Cancer Res*. 2008;68:3314-22.

214. De Bacco F, Luraghi P, Medico E, et al. Induction of MET by ionizing radiation and its role in radioresistance and invasive growth of cancer. *J Natl Cancer Inst*. 2011;103(8):645-61.

215. Sun B, Liu R, Xiao Z, et al. c-MET protects breast cancer cells from apoptosis induced by sodium butyrate. *PLoS ONE*. 2012;7(1):e30143.

216. Winer EP, Tolaney S, Nechushtan H, et al. Activity of cabozantinib (XL184) in metastatic breast cancer (MBC): Results from a phase II randomized discontinuation trial (RDT). *ASCO Meeting Abstracts*. 2012;30(15_suppl):535.

217. Tolaney SM, Guo H, Barry WT, et al. A phase II study of tivantinib (ARQ-197) for metastatic triple-negative breast cancer. *ASCO Meeting Abstracts*. 2014;32(15_suppl):1106.

218. Katayama R, Aoyama A, Yamori T, et al. Cytotoxic activity of tivantinib (ARQ 197) is not due solely to c-MET inhibition. *Cancer Res*. 2013;73(10):3087-96.

219. Munshi N, Jeay S, Li Y, et al. ARQ 197, a novel and selective inhibitor of the human c-met receptor tyrosine kinase with antitumor activity. *Mol Cancer Ther*. 2010;9(6):1544-53.

220. Http://clinicaltrials.gov/ [Internet].; 2014. Available from: http://clinicaltrials.gov/.

221. Zou HY, Li Q, Lee JH, et al. An orally available small-molecule inhibitor of c-met, PF-2341066, exhibits cytoreductive antitumor efficacy through antiproliferative and antiangiogenic mechanisms. *Cancer Res*. 2007;67(9):4408-17.

222. Liu X, Newton RC, Scherle PA. Developing c-MET pathway inhibitors for cancer therapy: Progress and challenges. *Trends Mol Med*. 2010;16(1):37-45.

223. Qian F, Engst S, Yamaguchi K, et al. Inhibition of tumor cell growth, invasion, and metastasis by EXEL-2880 (XL880, GSK1363089), a novel inhibitor of HGF and VEGF receptor tyrosine kinases. *Cancer Res*. 2009;69(20):8009-16.

224. Qi W, Cooke L, Stejskal A, et al. MP470, a novel receptor tyrosine kinase inhibitor, in combination with erlotinib inhibits the HER family/PI3K/Akt pathway and tumor growth in prostate cancer. *BMC Cancer*. 2009;9(1):142.

225. Rosen PJ, Sweeney CJ, Park DJ, et al. AMG102, an HGF/SF antagonist, in combination with anti-angiogenesis targeted therapies in adult patients with advanced solid tumours. *ASCO Annual Meeting*. 2008;26(15S):3570.

226. Gille H, Matschiner G, Hulsmeyer M, et al. Exploiting the anticalin therapeutic protein platform for the treatment of cMet ligand-independent and dependent tumors - discovery and characterization of a highly specific and potent c-met antagonist with drug-like properties. *Cancer Res*. 2012;72(8):Supplement 1.

227. [Internet].; 2012. Available from: http://www.pieris-ag.com/.

228. Olwill SA, Joffroy C, Gille H, et al. A highly potent and specific MET therapeutic protein antagonist with both ligand-dependent and ligand-independent activity. *Mol Can Ther*. 2013;12(11):2459-71.

229. Giordano S. Rilotumumab, a mAb against human hepatocyte growth factor for the treatment of cancer. *Curr Opin Mol Ther*. 2009;11(4):448-55.

230. Reardan DA, Cloughsey TF, Raizer JJ, et al. Phase II study of AMG 102, a fully human neutralizing antibody against hepatocyte growth factor/scatter factor, in patients with recurrent glioblastoma multiforme. *ASCO Meeting Abstracts*. 2008;26(15S):2051.

231. Jun HT, Sun J, Rex K, et al. AMG 102, A fully human anti-hepatocyte growth Factor/Scatter factor neutralizing antibody, enhances the efficacy of temozolomide or docetaxel in U-87 MG cells and xenografts. *Clin Can Res*. 2007;13(22):6735-42.

232. Krueger JS, Laffin B, Lange H, et al. Evaluation of immunohistochemistry assays against c-met and HGF to guide companion diagnostic decisions. *Cancer Res*. 2014;74(19 Supplement):2842-.

233. Merchant M, Ma X, Maun HR, et al. Monovalent antibody design and mechanism of action of onartuzumab, a MET antagonist with anti-tumor activity as a therapeutic agent. *Proc Natl Acad Sci U S A*. 2013;110(32):E2987-96.

234. Spigel DR, Ervin TJ, Ramlau RA, et al. Randomized phase II trial of onartuzumab in combination with erlotinib in patients with advanced Non–Small-cell lung cancer. *J Clin Oncol*. 2013;31(32):4105-14.

235. Media release [Internet].; 2014. Available from: http://www.roche.com/media/media_releases/med-cor-2014-03-03.htm.

236. Jones SF, Cohen RB, Bendell JC, et al. Safety, tolerability, and pharmacokinetics of TAK 701, a humanized anti-hepatocyte growth factor (HGF) monoclonal antibody, in patients with advanced non-hematologic malignancies: First in human phase I dose-escalation study. *ASCO Meeting Abstracts*. 2010;28(15S):3081.

237. Sachdev JC, Naini P, Arteta-Bulos R, et al. Anaplastic lymphoma kinase (ALK): A potential oncogenic driver in triple-negative breast cancer? *ASCO Meeting Abstracts*. 2013;31(15_suppl):1067.

238. Wagh PK, Peace BE, Waltz SE. Met-related receptor tyrosine kinase ron in tumor growth and metastasis. *Adv Cancer Res*. 2008;100:1-33.

239. Madden S, Clarke C, Gaule P, et al. BreastMark: An integrated approach to mining publicly available transcriptomic datasets relating to breast cancer outcome. *Breast Cancer Res*. 2013;15(4):R52.

240. Sankaranarayanan R, Swaminathan R, Lucas E. Statistical methods for cancer survival. In: Cancer survival in Africa, Asia, the Caribbean and Central America (SurvCan). IARC Scientific Publications volume 162 ed. Lyon; 2011. p. 7-13.

241. Clark TG, Bradburn MJ, Love SB, et al. Survival analysis part I: Basic concepts and first analyses. *Br J Cancer*. 0000;89(2):232-8.

242. Weigelt B, Mackay A, A'hern R, et al. Breast cancer molecular profiling with single sample predictors: A retrospective analysis. *Lancet Oncol*. 2010;11(4):339-49.

243. Elstrodt F, Hollestelle A, Nagel JHA, et al. BRCA1 mutation analysis of 41 human breast cancer cell lines reveals three new deleterious mutants. *Cancer Research*. 2006;66(1):41-5.

244. Hoeflich KP, O'Brien C, Boyd Z, et al. In vivo antitumor activity of MEK and phosphatidylinositol 3-kinase inhibitors in basal-like breast cancer models. *Clin Can Res*. 2009;15(14):4649-64.

245. Albini A, Iwamoto Y, Kleinman HK, et al. A rapid in vitro assay for quantitating the invasive potential of tumor cells. *Cancer Res*. 1987;47(12):3239-45.

246. Liang C, Park AY, Guan J. In vitro scratch assay: A convenient and inexpensive method for analysis of cell migration in vitro. *Nat Protocols*. 2007;2(2):329-33.

247. Livak KJ, Schmittgen TD. Analysis of relative gene expression data using real-time quantitative PCR and the $2^{-\Delta\Delta CT}$ method. *Methods*. 2001;25(4):402-8.

248. Chou T, Talalay P. Analysis of combined drug effects: A new look at a very old problem. *Trends Pharmacol Sci*. 1983;4(0):450-4.

249. Hochgräfe F, Zhang L, O'Toole SA, et al. Tyrosine phosphorylation profiling reveals the signaling network characteristics of basal breast cancer cells. *Cancer Res*. 2010;70(22):9391-401.

250. Ma PC, Tretiakova MS, Nallasura V, et al. Downstream signalling and specific inhibition of c-MET//HGF pathway in small cell lung cancer: Implications for tumour invasion. *Br J Cancer*. 2007;97(3):368-77.

251. Sen B, Peng S, Saigal B, et al. Distinct interactions between c-src and c-met in mediating resistance to c-src inhibition in head and neck cancer. *Clin Can Res*. 2011;17(3):514-24.

252. Garnett J, Chumbalkar V, Vaillant B, et al. Regulation of HGF expression by ΔEGFR-mediated c-met activation in glioblastoma cells. *Neoplasia*. 2013;15(1):73-84.

253. Gucalp A, Sparano JA, Caravelli J, et al. Phase II trial of saracatinib (AZD0530), an oral SRC-inhibitor for the treatment of patients with hormone receptor-negative metastatic breast cancer. *Clin Breast Cancer*. 2011;11(5):306-11.

254. Lipman NS, Jackson LR, Trudel LJ, et al. Monoclonal versus polyclonal antibodies: Distinguishing characteristics, applications, and information resources. *ILAR Journal*. 2005;46(3):258-68.

255. Ou SI. Crizotinib: A novel and first-in-class multitargeted tyrosine kinase inhibitor for the treatment of anaplastic lymphoma kinase rearranged non-small cell lung cancer and beyond. *Drug Des Dev Ther*. 2011;5:471-85.

256. Finn RS, Bengala C, Ibrahim N, et al. Dasatinib as a single agent in triple-negative breast cancer: Results of an open-label phase 2 study. *Clin Can Res*. 2011;17(21):6905-13.

257. Zwick E, Bange J, Ullrich A. Receptor tyrosine kinase signalling as a target for cancer intervention strategies. *Endocr Relat Cancer*. 2001;8(3):161-73.

258. Elbauomy Elsheikh S, Green A, Lambros M, et al. FGFR1 amplification in breast carcinomas: A chromogenic in situ hybridisation analysis. *Breast Cancer Res*. 2007;9(2):R23.

259. Cameron D, Brown J, Dent R, et al. Adjuvant bevacizumab-containing therapy in triple-negative breast cancer (BEATRICE): Primary results of a randomised, phase 3 trial. *Lancet Oncol*. 2013;14(10):933-42.

260. Acunzo M, Romano G, Palmieri D, et al. Cross-talk between MET and EGFR in non-small cell lung cancer involves miR-27a and Sprouty2. *Proceedings of the National Academy of Sciences*. 2013;110(21):8573-8.

261. Ferraro DA, Gaborit N, Maron R, et al. Inhibition of triple-negative breast cancer models by combinations of antibodies to EGFR. *Proc Natl Acad Sci U S A*. 2013;110(5):1815-20.

262. Cortas T, Eisenberg R, Fu P, et al. Activation state egfr and STAT-3 as prognostic markers in resected non-small cell lung cancer. *Lung Cancer*. 2007;55(3):349-55.

263. Nieto Y, Nawaz F, Jones RB, et al. Prognostic significance of overexpression and phosphorylation of epidermal growth factor receptor (EGFR) and the presence of truncated EGFRvIII in locoregionally advanced breast cancer. *J Clin Oncol*. 2007;25(28):4405-13.

264. Mandell J. Immunohistochemical assessment of protein phosphorylation state: The dream and the reality. *Histochem Cell Biol*. 2008;130(3):465-71.

265. Inwald EC, Klinkhammer-Schalke M, HofstÃ¤dter F, et al. Ki-67 is a prognostic parameter in breast cancer patients: Results of a large population-based cohort of a cancer registry. *Breast Cancer Res Treat*. 2013;139(2):539-52.

266. Nishiyama Y, Nishimura R, Osako T, et al. Ki-67, p53, and clinical outcomes of patients with triple-negative breast cancer. *ASCO Meeting Abstracts*. 2012;30(27_suppl):142.

267. Wu J, Yu J, Wu H, et al. Expressions and clinical significances of c-MET, p-MET and E2f-1 in human gastric carcinoma. *BMC Research Notes*. 2014;7(1):6.

268. Grigioni WF, Fiorentino M, D'Errico A, et al. Overexpression of c-met protooncogene product and raised Ki67 index in hepatocellular carcinomas with respect to benign liver conditions. *Hepatology*. 1995;21(6):1543-6.

269. Masuya ,D., Huang ,C., Liu ,D., et al. The tumour-stromal interaction between intratumoral c-met and stromal hepatocyte growth factor associated with tumour growth and prognosis in non-small-cell lung cancer patients. *Br J Cancer*. 2004;90(8):1555-62.

270. Yamaji D, Kimura K, Watanabe A, et al. Bovine hepatocyte growth factor and its receptor c-met: CDNA cloning and expression analysis in the mammary gland. *Domest Anim Endocrinol*. 2006;30(3):239-46.

271. Yamashita J, Ogawa M, Beppu T. Immunoreactive hepatocyte growth factor is present in tissue extracts from human breast cancer but not in conditioned medium of human breast cancer cell lines. *Res Commun Chem Pathol Pharmacol*. 1993;82:249-52.

272. Nogi H, Kobayashi T, Suzuki M, et al. EGFR as a paradoxical predictor of chemosensitivity and outcome among triple negative breast cancer. *Oncol Rep*. 2009;21(2):413-7.

273. Tischkowitz M, Brunet J, Begin L, et al. Use of immunohistochemical markers can refine prognosis in triple negative breast cancer. *BMC Cancer*. 2007;7(1):134.

274. Finn RS. Targeting src in breast cancer. *Annal Oncol*. 2008;19(8):1379-86.

275. Cianfrocca M, Goldstein LJ. Prognostic and predictive factors in early-stage breast cancer. *Oncologist*. 2004;9:606-16.

276. Elsberger B, Tan BA, Mitchell TJ, et al. Is expression or activation of src kinase associated with cancer-specific survival in ER-, PR- and HER2-negative breast cancer patients? *Am J Pathol*. 2009;175(4):1389-97.

277. Fan P, McDaniel RE, Kim HR, et al. Modulating therapeutic effects of the c-src inhibitor via oestrogen receptor and human epidermal growth factor receptor 2 in breast cancer cell lines. *Eur J Cancer*. 2012;48(18):3488-98.

278. Prat M, Crepaldi T, Gandino L, et al. C-terminal truncated forms of met, the hepatocyte growth factor receptor. *Mol Cell Biol*. 1991;11(12):5954-62.

279. Petrelli A, Circosta P, Granziero L, et al. Ab-induced ectodomain shedding mediates hepatocyte growth factor receptor down-regulation and hampers biological activity. *Proc Nat Acad Sci USA*. 2006;103(13):5090-5.

280. Chalupsky K, Kanchev I, Zbodakova O, et al. ADAM10/17-dependent release of soluble c-met correlates with hepatocellular damage. *Folia Biologica*. 2013;59:76-86.

281. Wader KF, Fagerli U, Holt RU, et al. Soluble c-met in serum of patients with multiple myeloma: Correlation with clinical parameters. *Eur J Haematol*. 2011;87(5):394-9.

282. Yang JJ, Yang JH, Kim J, et al. Soluble c-met protein as a susceptible biomarker for gastric cancer risk: A nested case-control study within the korean multicenter cancer cohort. *Int J Cancer*. 2013;132(9):2148-56.

283. McNeil B, Sorbellini M, Grubb R, et al. Preliminary evaluation of urinary soluble met as a biomarker for urothelial carcinoma of the bladder. *J Transl Med*. 2014;12(1):199.

284. Sultan AS, Brim H, Sherif ZA. Co-overexpression of janus kinase 2 and signal transducer and activator of transcription 5a promotes differentiation of mammary cancer cells through reversal of epithelial?mesenchymal transition. *Cancer Sci*. 2008;99(2):272-9.

285. Palafox M, Ferrer I, Pellegrini P, et al. RANK induces Epithelial–Mesenchymal transition and stemness in human mammary epithelial cells and promotes tumorigenesis and metastasis. *Cancer Research.* 2012;72(11):2879-88*DOI10.1158/0008-5472.CAN-12-0044*.

286. Walerych D, Napoli M, Collavin L, et al. The rebel angel: Mutant p53 as the driving oncogene in breast cancer. *Carcinogenesis*. 2012;33(11):2007-17.

287. Banerjee A, Wu Z, Qian P, et al. ARTEMIN synergizes with TWIST1 to promote metastasis and poor survival outcome in patients with ER negative mammary carcinoma. *Breast Cancer Res*. 2011;13(6):R112.

288. Baselga J, Cervantes A, Martinelli E, et al. Phase I safety, pharmacokinetics, and inhibition of src activity study of saracatinib in patients with solid tumors. *Clin Can Res*. 2010;16(19):4876-83.

289. Lombardo LJ, Lee FY, Chen P, et al. Discovery of N-(2-chloro-6-methyl-phenyl)-2-(6-(4-(2-hydroxyethyl)-piperazin-1-yl)-2-methylpyrimidin-4-ylamino)thiazole-5-carboxamide (BMS-354825), a dual Src/Abl kinase inhibitor with potent antitumor activity in preclinical assays. *J Med Chem*. 2004;47:6658-61.

290. Sharma S, Zeng JY, Zhuang CM, et al. Small-molecule inhibitor BMS-777607 induces breast cancer cell polyploidy with increased resistance to cytotoxic chemotherapy agents. *Mol Cancer Ther*. 2013;12(5):725-36.

291. deGraffenried LA, Fulcher L, Friedrichs WE, et al. Reduced PTEN expression in breast cancer cells confers susceptibility to inhibitors of the PI3 kinase/Akt pathway. *Annal Oncol*. 2004;15(10):1510-6.

292. Kao J, Salari K, Bocanegra M, et al. Molecular profiling of breast cancer cell lines defines relevant tumor models and provides a resource for cancer gene discovery. *PLoS ONE*. 2009;4(7):e6146.

293. Saal LH, Gruvberger-Saal S, Persson C, et al. Recurrent gross mutations of the PTEN tumor suppressor gene in breast cancers with deficient DSB repair. *Nat Genet*. 2008;40(1):102-7.

294. Mullooly M, O'Brien NA, Conklin D, et al. Preclinical studies with neratinib in triple-negative breast cancer. *ASCO Meeting Abstracts*. 2013;31(15_suppl):1054.

295. Wong K, Fracasso PM, Bukowski RM, et al. A phase I study with neratinib (HKI-272), an irreversible pan ErbB receptor tyrosine kinase inhibitor, in patients with solid tumors. *Clin Can Res*. 2009;15(7):2552-8.

296. Burstein HJ, Sun Y, Dirix LY, et al. Neratinib, an irreversible ErbB receptor tyrosine kinase inhibitor, in patients with advanced ErbB2-positive breast cancer. *J Clin Oncol*. 2010;28(8):1301-7.

297. Armstrong DK, Kaufmann SH, Ottaviano YL, et al. Epidermal growth factor-mediated apoptosis of MDA-MB-468 human breast cancer cells. *Cancer Res*. 1994;54(20):5280-3.

298. Puri N, Salgia R. Synergism of EGFR and c-met pathways, cross-talk and inhibition, in non-small cell lung cancer. *J Carcinog*. 2008;7:9.

299. Herynk MH, Beyer AR, Cui Y, et al. Cooperative action of tamoxifen and c-src inhibtion in preventing the growth of estrogen receptor-positive human breast cancer cells. *Mol Cancer Ther*. 2006;5:3023-31.

300. Franken NAP, Rodermond HM, Stap J, et al. Clonogenic assay of cells in vitro. *Nat Protocols*. 2006;1(5):2315-9.

301. Cai Z, Chattopadhyay N, Liu WJ, et al. Optimized digital counting colonies of clonogenic assays using ImageJ software and customized macros: Comparison with manual counting. *Int J Radiat Biol*. 2011;87(11):1135-46.

302. Molyneux G, Geyer FC, Magnay F, et al. BRCA1 basal-like breast cancers originate from luminal epithelial progenitors and not from basal stem cells. *Cell Stem Cell*. 2010;7(3):403-17.

303. Lee GY, Kenny PA, Lee EH, et al. Three-dimensional culture models of normal and malignant breast epithelial cells. *Nat Meth*. 2007;4(4):359-65.

304. Desoize B, Jardillier J. Multicellular resistance: A paradigm for clinical resistance? *Crit Rev Oncol*. 2000;36(2–3):193-207.

305. Wang F, Weaver VM, Petersen OW, et al. Reciprocal interactions between ß1-integrin and epidermal growth factor receptor in three-dimensional basement membrane breast cultures: A different perspective in epithelial biology. *Proc Nat Acad Sci USA*. 1998;95(25):14821-6.

306. Bisell MJ, Weaver VM, Lelievre SA, et al. Tissue structure, nucleur organisation and gene expression in normal and malignant breast. *Cancer Res*. 1999;59:1757-64.

307. Li Q, Chow AB, Mattingly RR. Three-dimensional overlay culture models of human breast cancer reveal a critical sensitivity to mitogen-activated protein kinase kinase inhibitors. *J Pharmacol Exp Ther*. 2010;332(3):821-8.

308. Bladt F, Faden B, Friese-Hamim M, et al. EMD 1214063 and EMD 1204831 constitute a new class of potent and highly selective c-met inhibitors. *Clin Can Res*. 2013;19(11):2941-51.

309. Sohn J, Liu S, Parinyanitikul N, et al. cMET activation and EGFR-directed therapy resistance in triple-negative breast cancer. *Journal of Cancer*. 2014;5(9):745-53.

310. Singh A, Nascimento JM, Kowar S, et al. Boolean approach to signalling pathway modelling in HGF-induced keratinocyte migration. *Bioinformatics*. 2012;28(18):i495-501.

311. Kirkpatrick P, Graham J, Muhsin M. Cetuximab. *Nat Rev Drug Discov*. 2004;3(7):549-50.

312. Oliveras-Ferraros C, Vazquez-Martin A, Lopez-Bonet E, et al. Growth and molecular interactions of the anti-EGFR antivody cetuximab and the DNA cross-linkin gaent cisplatin in gefitinib-resistant MDA-MB-468 cells: New porpsects in the treatment of triple-negative/basal-like breast cancer. *Int J Oncol*. 2008;33:1165-76.

313. TrÃ©dan O, Campone M, Jassem J, et al. Ixabepilone alone or with cetuximab as first-line treatment for Advanced/Metastatic triple-negative breast cancer. *Clinical Breast Cancer*.

314. Baselga J, Gomez P, Greil R, et al. Randomized phase II study of the anti-epidermal growth factor receptor monoclonal antibody cetuximab with cisplatin versus

cisplatin alone in patients with metastatic triple-negative breast cancer. *J Clin Oncol*. 2013;31(20):2586-92.

315. Carey LA, Rugo HS, Marcom PK, et al. TBCRC 001: Randomized phase II study of cetuximab in combination with carboplatin in stage IV triple-negative breast cancer. *J Clin Oncol*. 2012;30(21):2615-23.

316. Hage C, Rausch V, Giese N, et al. The novel c-met inhibitor cabozantinib overcomes gemcitabine resistance and stem cell signaling in pancreatic cancer. *Cell Death Dis*. 2013;4(5):e627.

317. Moschetta M, Basile A, Ferrucci A, et al. Novel targeting of phospho-cMET overcomes drug resistance and induces anti-tumor activity in multiple myeloma. *Clin Can Res*. 2013;doi :10.1158/1078-0432.CCR-13-0039.

318. Zeng Z, Weiser MR, Kuntz E, et al. c-met gene amplification is associated with advanced stage colorectal cancer and liver metastases. *Cancer Lett*. 2008;265(2):258-69.

319. Koeppen H, Rost S, Yauch RL. Developing biomarkers to predict benefit from HGF/MET pathway inhibitors. *J Pathol*. 2014;232(2):210-8.

320. Sharpe R, Pearson A, Herrera-Abreu MT, et al. FGFR signaling promotes the growth of triple-negative and basal-like breast cancer cell lines both in vitro and in vivo. *Clin Can Res*. 2011;17(16):5275-86.

321. Massabeau C, Sigal-Zafrani B, Belin L, et al. The fibroblast growth factor receptor 1 (FGFR1), a marker of response to chemoradiotherapy in breast cancer? *Breast Cancer Res Treat*. 2012;134(1):259-66.

322. Gozgit JM, Wong MJ, Moran L, et al. Ponatinib (AP24534), a multitargeted pan-FGFR inhibitor with activity in multiple FGFR-amplified or mutated cancer models. *Mol Can Ther*. 2012;11(3):690-9.

323. Dhakal HP, Naume B, Synnestvedt M, et al. Expression of vascular endothelial growth factor and vascular endothelial growth factor receptors 1 and 2 in invasive breast carcinoma: Prognostic significance and relationship with markers for aggressiveness. *Histopathology*. 2012;61(3):350-64.

324. Paulsson J, Sjöblom T, Micke P, et al. Prognostic significance of stromal platelet-derived growth factor β-receptor expression in human breast cancer. *Am J Pathol*. 2009;175(1):334-41.

325. Elkin M, Orgel A, Kleinman HK. An angiogenic switch in breast cancer involves estrogen and soluble vascular endothelial growth factor receptor 1. *J Natl Cancer Inst*. 2004;96(11):875-8.

326. Linardou H, Kalogeras K, Kronenwett R, et al. The prognostic and predictive value of mRNA expression of vascular endothelial growth factor family members in breast cancer: A study in primary tumors of high-risk early breast cancer patients participating

in a randomized hellenic cooperative oncology group trial. *Breast Cancer Res*. 2012;14(6):R145.

327. Schmidt M, Voelker H, Kapp M, et al. Expression of VEGFR-1 (flt-1) in breast cancer is associated with VEGF expression and with node-negative tumour stage. *Anticancer Research*. 2008;28(3A):1719-24.

328. Lee Y, Karl DL, Maduekwe UN, et al. Differential effects of VEGFR-1 and VEGFR-2 inhibition on tumor metastases based on host organ environment. *Cancer Res*. 2010;70(21):8357-67.

329. Jechlinger M, Sommer A, Moriggl R, et al. Autocrine PDGFR signaling promotes mammary cancer metastasis. *J Clin Invest*. 2006;116(6):1561-70.

330. Coltrera MD, Wang J, Porter PL, et al. Expression of platelet-derived growth factor B-chain and the platelet-derived growth factor receptor ß subunit in human breast tissue and breast carcinoma. *Cancer Res*. 1995;55(12):2703-8.

331. Singh H, Milner CS, Aguilar Hernandez MM, et al. Vascular endothelial growth factor activates the tie family of receptor tyrosine kinases. *Cell Signal*. 2009;21(8):1346-50.

332. Yang XH, Hand RA, Livasy CA, et al. Overexpression of the receptor tyrosine kinase tie-1 intracellular domain in breast cancer. *Tumour Biol*. 2003;24(2):61-9.

333. Marta Pàez-Ribes, Allen,Elizabeth, Hudock,James, et al. Antiangiogenic Therapy Elicits Malignant Progression of Tumors to Increased Local Invasion and Distant Metastasis*Cancer cell*153220-231.

334. Guinebretiere J, Monique GL, Gaviolle A, et al. Angiogenesis and risk of breast cancer in women with fibrocystic disease. *Journal of the National Cancer Institute*. 1994;86(8):635-6.

335. Guidi AJ, Schnitt SJ, Fischer L, et al. Vascular permeability factor (vascular endothelial growth factor) expression and angiogenesis in patients with ductal carcinoma in situ of the breast. *Cancer*. 1997;80(10):1945-53.

336. Weidner N, Semple JP, Welch WR, et al. Tumor angiogenesis and metastasis — correlation in invasive breast carcinoma. *N Engl J Med*. 1991;324(1):1-8.

337. Weidner N, Folkman J, Pozza F, et al. Tumor angiogenesis: A new significant and independent prognostic indicator in early-stage breast carcinoma. *Journal of the National Cancer Institute.* 1992;84(24):1875-87*DOI10.1093/jnci/84.24.1875*.

338. Choi WW, Lewis MM, Lawson D, et al. Angiogenic and lymphangiogenic microvessel density in breast carcinoma: Correlation with clinicopathologic parameters and VEGF-family gene expression. *Mod Pathol*. 2005;18(1):143-52.

339. Mohammed RA, Ellis IO, Mahmmod AM, et al. Lymphatic and blood vessels in basal and triple-negative breast cancers: Characteristics and prognostic significance. *Mod Pathol*. 2011;24(6):774-85.

340. Curigliano G, Pivot X, CortÃ©s J, et al. Randomized phase II study of sunitinib versus standard of care forÂ patients with previously treated advanced triple-negative breastÂ cancer. *The Breast*;22(5):650-6.

341. Bergh J, Bondarenko IM, Lichinitser MR, et al. First-line treatment of advanced breast cancer with sunitinib in combination with docetaxel versus docetaxel alone: Results of a prospective, randomized phase III study. *J Clin Oncol*. 2012.

342. Baselga J, Segalla JGM, Roché H, et al. Sorafenib in combination with capecitabine: An oral regimen for patients with HER2-negative locally advanced or metastatic breast cancer. *J Clin Oncol*. 2012;30(13):1484-91.

343. Taylor SK, Chia S, Dent S, et al. A phase II study of pazopanib in patients with recurrent or metastatic invasive breast carcinoma: A trial of the princess margaret hospital phase II consortium. *Oncologist*. 2010;15(8):810-8.

344. Rugo HS, Stopeck AT, Joy AA, et al. Randomized, placebo-controlled, double-blind, phase II study of axitinib plus docetaxel versus docetaxel plus placebo in patients with metastatic breast cancer. *J Clin Oncol*. 2011;29(18):2459-65.

345. Boer K, Lang I, Llombart-Cussac A, et al. Vandetanib with docetaxel as second-line treatment for advanced breast cancer: A double-blind, placebo-controlled, randomized phase II study. *Invest New Drugs*. 2012;30(2):681-7.

346. Bachelier R, Confavreux CB, Peyruchaud O, et al. Combination of anti-angiogenic therapies reduces osteolysis and tumor burden in experimental breast cancer bone metastasis. *Int J Cancer*. 2014;135(6):1319-29.

347. Shojaei F, Simmons BH, Lee JH, et al. HGF/c-met pathway is one of the mediators of sunitinib-induced tumor cell type-dependent metastasis. *Cancer Lett*. 2012;320(1):48-55.

348. Exelixis' cabozantinib shows encouraging clinical activity in patients with metastatic breast cancer [Internet]. SOUTH SAN FRANCISCO: Exelixis; 2011 [updated 07/12/11; cited 04/12/14]. Available from: http://ir.exelixis.com/phoenix.zhtml?c=120923&p=irol-newsArticle_print&ID=1637629.

349. LEE HT, KIM SK, CHOI MR, et al. Effects of the activated mitogen-activated protein kinase pathway via the c-ros receptor tyrosine kinase on the T47D breast cancer cell line following alcohol exposure. *Oncol Rep*. 2013;29(3):868-74.

350. Takeuchi K, Soda M, Togashi Y, et al. RET, ROS1 and ALK fusions in lung cancer. *Nat Med*. 2012;18(3):378-81.

351. Eom M, Lkhagvadorj S, Oh SS, et al. ROS1 expression in invasive ductal carcinoma of the breast related to proliferation activity. *Yonsei Med J*. 2013;54(3):650-7.

352. Schummer M, Green A, Beatty JD, et al. Comparison of breast cancer to healthy control tissue discovers novel markers with potential for prognosis and early detection. *PLoS ONE*. 2010;5(2):e9122.

353. Henriksson ML, Edin S, Dahlin AM, et al. Colorectal cancer cells activate adjacent fibroblasts resulting in FGF1/FGFR3 signaling and increased invasion. *Am J Pathol*. 2011;178(3):1387-94.

354. Yin Y, Betsuyaku T, Garbow JR, et al. Rapid induction of lung adenocarcinoma by fibroblast growth factor 9 signaling through FGF receptor 3. *Cancer Res*. 2013;73(18):5730-41.

355. Davidson D, Blanc A, Filion D, et al. Fibroblast growth factor (FGF) 18 signals through FGF receptor 3 to promote chondrogenesis. *Journal of Biological Chemistry*. 2005;280(21):20509-15.

356. Hecht D, Zimmerman N, Bedford M, et al. Identification of fibroblast growth factor 9 (FGF9) as a high affinity, heparin dependent ligand for FGF receptors 3 and 2 but not for FGF receptors 1 and 4. *Growth Factors*. 1995;12(3):223-33.

357. Zammit C, Barnard R, Gomm J, et al. Altered intracellular localization of fibroblast growth factor receptor 3 in human breast cancer. *J Pathol*. 2001;194(1):27-34.

358. Avivi A, Yayon A, Givol D. A novel form of FGF receptor-3 using an alternative exon in the immunoglobulin domain III. *FEBS Lett*;330(3):249-52.

359. Lafitte M, Moranvillier I, Garcia S, et al. FGFR3 has tumor suppressor properties in cells with epithelial phenotype. *Mol Cancer*. 2013;12(1):83.

360. Smid M, Wang Y, Klijn JGM, et al. Genes associated with breast cancer metastatic to bone. *J Clin Oncol*. May 20, 2006;24(15):2261-7.

361. Fox BP, Kandpal RP. Invasiveness of breast carcinoma cells and transcript profile: Eph receptors and ephrin ligands as molecular markers of potential diagnostic and prognostic application. *Biochem Biophys Res Commun*. 2004;318(4):882-92.

362. Fu D, Wang Z, Wang B, et al. Frequent epigenetic inactivation of the receptor tyrosine kinase EphA5 by promoter methylation in human breast cancer. *Hum Pathol*. 2010;41(1):48-58.

363. Naumov G, Townson J, MacDonald I, et al. Ineffectiveness of doxorubicin treatment on solitary dormant mammary carcinoma cells or late-developing metastases. *Breast Cancer Res Treat*. 2003;82(3):199-206.

364. Harrison C. Patents related to EPH receptors and ligands. *Nat Rev Drug Discov*. 2014;13(1):13-.

365. Espina V, Edmiston KH, Heiby M, et al. A portrait of tissue phosphoprotein stability in the clinical tissue procurement process. *Mol Cell Proteomics*. 2008;7(10):1998-2018.

366. Papa V, Pezzino V, Costantino A, et al. Elevated insulin receptor content in human breast cancer. *J Clin Invest*. 1990;86(5):1503-10.

367. Milazzo G, Giorgino F, Damante G, et al. Insulin receptor expression and function in human breast cancer cell lines. *Cancer Res*. 1992;52(14):3924-30.

368. Goodwin PJ. Insulin in the adjuvant breast cancer setting: A novel therapeutic target for lifestyle and pharmacologic interventions? *J Clin Oncol*. 2008;26(6):833-4.

369. Law JH, Habibi G, Hu K, et al. Phosphorylated insulin-like growth factor-I/Insulin receptor is present in all breast cancer subtypes and is related to poor survival. *Cancer Res*. 2008;68(24):10238-46.

370. Huang J, Morehouse C, Streicher K, et al. Altered expression of insulin receptor isoforms in breast cancer. *PLoS ONE*. 2011;6(10):e26177.

Appendix 1

Table A1 - 1 Entrez Gene I.D.s and Probe I.D.s used for survival analsis in BreastMark Database

RTK	Entrez Gene	Probe I.D
ALK	238	208211_s_at
ALK	238	208212_s_at
LTK	4058	217184_s_at
LTK	4058	207106_s_at
AXL	558	202685_s_at
AXL	558	202686_s_at
MER	10461	211913_s_at
MER	10461	206028_s_at
MER	10461	211912_at*
TYRO3	7301	211432_s_at
TYRO3	7301	211431_s_at
DDR1	780	1007_s_at
DDR1	780	208779_x_at
DDR1	780	207169_x_at
DDR1	780	210749_x_at
DDR2	4921	205168_at
DDR2	4921	225442_at
DDR2	4921	227561_at
DDR2	4921	205168_at
EGFR	1956	210984_x_at
EGFR	1956	211607_x_at
EGFR	1956	201984_s_at
EGFR	1956	201983_s_at
EGFR	1956	211551_at
EGFR	1956	211550_at
EGFR	1956	224999_at
EGFR	1956	1565484_x_at

RTK	Entrez Gene	Probe I.D
EGFR	1956	1565483_at
ERBB2	2064	210930_s_at
ERBB2	2064	216836_s_at
ERBB2	2064	234354_x_at
ERBB3	2065	202454_s_at
ERBB3	2065	226213_at
ERBB3	2065	215638_at
ERBB3	2065	1563253_s_at
ERBB3	2065	1563252_at
ERBB4	2066	206794_at
ERBB4	2066	214053_at
ERBB4	2066	233498_at
ERBB4	2066	233494_at*
EPHA1	2041	205977_s_at
EPHA2	1969	203499_at
EPHA3	2042	206070_s_at
EPHA3	2042	211164_at
EPHA3	2042	206071_s_at
EPHA3	2042	206070_s_at
EPHA4	2043	206114_at
EPHA4	2043	227449_at
EPHA4	2043	229374_at
EPHA4	2043	228948_at
EPHA5	2044	215664_s_at
EPHA5	2044	215664_s_at
EPHA5	2044	237939_at
EPHA6	285220	233184_at
EPHA6	285220	1561396_at
EPHA7	2045	206852_at
EPHA7	2045	238533_at
EPHA7	2045	1554629_at
EPHA7	2045	229288_at

RTK	Entrez Gene	Probe I.D
EPHA7	2045	229288_at
EPHA8	2046	1554069_at
EPHA8	2046	231796_at
EPHB1	2047	210753_s_at
EPHB1	2047	211898_s_at
EPHB1	2047	230425_at
EPHB1	2047	211898_s_at
EPHB2	2048	209589_s_at
EPHB2	2048	211165_x_at
EPHB2	2048	210651_s_at
EPHB2	2048	209588_at
EPHB3	2049	1438_at
EPHB3	2049	204600_at
EPHB4	2050	202894_at
EPHB4	2050	216680_s_at
EPHB6	2051	204718_at
FGFR1	2260	211535_s_at
FGFR1	2260	210973_s_at
FGFR1	2260	207937_x_at
FGFR1	2260	215404_x_at
FGFR1	2260	207822_at*
FGFR1	2260	226705_at
FGFR2	2263	211401_s_at
FGFR2	2263	203639_s_at
FGFR2	2263	208234_x_at
FGFR2	2263	208228_s_at
FGFR2	2263	203638_s_at
FGFR2	2263	208225_at
FGFR2	2263	211399_at
FGFR2	2263	211400_at
FGFR2	2263	208229_at*
FGFR3	2261	204380_s_at

RTK	Entrez Gene	Probe I.D
FGFR3	2261	204379_s_at
FGFR4	2264	211237_s_at
FGFR4	2264	204579_at
FGFR4	2264	1554962_a_at
IGF1R	3480	203627_at
IGF1R	3480	203628_at
IGF1R	3480	208441_at*
IGF1R	3480	225330_at
INSR	3643	213792_s_at
INSR	3643	207851_s_at
INSR	3643	226450_at
INSR	3643	226212_s_at
INSRR	3645	215776_at
MET	4233	211599_x_at
MET	4233	203510_at
MET	4233	213816_s_at
MET	4233	213807_x_at
MET	4233	211599_x_at
RON	4486	205455_at
MUSK	4593	207633_s_at
MUSK	4593	207632_at
MUSK	4593	241122_s_at
CSF1R	1436	203104_at
FLT3	2322	206674_at
KIT	3815	205051_s_at
PDGFRA	5156	203131_at
PDGFRA	5156	215305_at
PDGFRA	5156	211533_at
PDGFRA	5156	1554828_at
PDGFRB	5159	202273_at
PTK7	5754	207011_s_at
PTK7	5754	1555324_at

RTK	Entrez Gene	Probe I.D
RET	5979	205879_x_at
RET	5979	215771_x_at
RET	5979	211421_s_at
ROR1	4919	205805_s_at
ROR1	4919	211057_at
ROR1	4919	232060_at
ROR2	4920	205578_at
ROS1	6098	207569_at
RYK	6259	214172_x_at
RYK	6259	202853_s_at
RYK	6259	216976_s_at
TEK	7010	217711_at
TEK	7010	206702_at
TIE	7075	204468_s_at
TIE	7075	1560657_at
NTRK1	4914	208605_s_at
NTRK2	4915	207152_at
NTRK2	4915	221796_at
NTRK2	4915	221795_at
NTRK2	4915	214680_at
NTRK2	4915	236095_at
NTRK2	4915	229463_at
NTRK3	4916	217033_x_at
NTRK3	4916	217377_x_at
NTRK3	4916	206462_s_at
NTRK3	4916	215115_x_at
NTRK3	4916	215025_at
NTRK3	4916	213960_at
NTRK3	4916	215311_at
NTRK3	4916	217033_x_at
NTRK3	4916	1557795_s_at
VEGFR1	2321	210287_s_at

RTK	Entrez Gene	Probe I.D
VEGFR1	2321	204406_at*
VEGFR1	2321	226498_at
VEGFR1	2321	226497_s_at
VEGFR1	2321	232809_s_at*
VEGFR2	3791	203934_at
VEGFR3	2324	210316_at
VEGFR3	2324	234379_at
VEGFR3	2324	229902_at
AATYK	9625	205986_at
AATYK2	22853	206223_at
AATYK2	22853	226375_at
AATYK3	114783	1557103_a_at
STYK1	55359	221696_s_at
STYK1	55359	220030_at